Biologically-Aware Algorithms for Connectomics

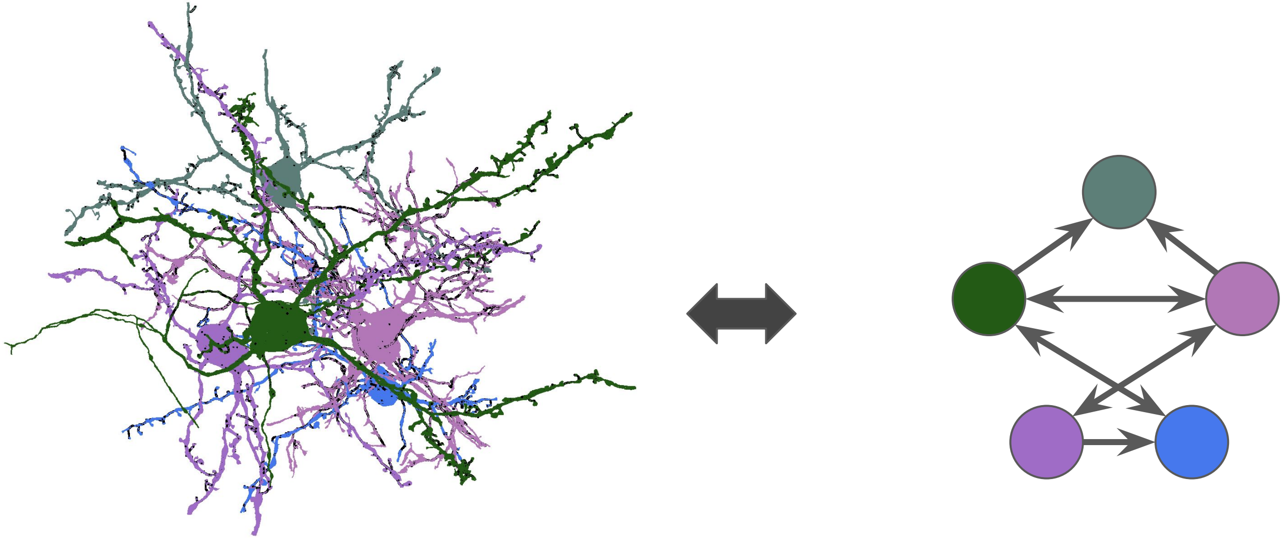

Brian Matejek

Advisor: Hanspeter Pfister
Committee: Michael Mitzenmacher, Todd Zickler

Connectomics

Goal: Extract the wiring diagram from a brain

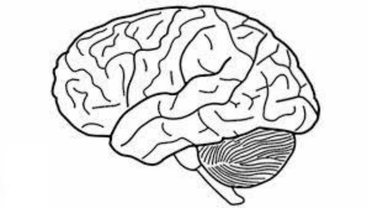

Connectomics

Goal: Extract the wiring diagram from a brain

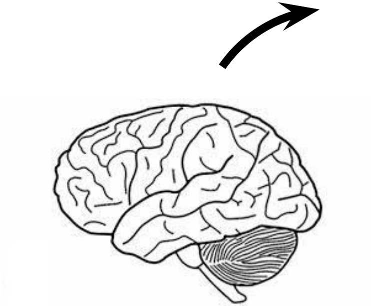

Nanometer-Resolution Imaging

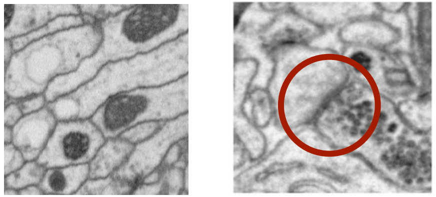

Connectomics

Goal: Extract the wiring diagram from a brain

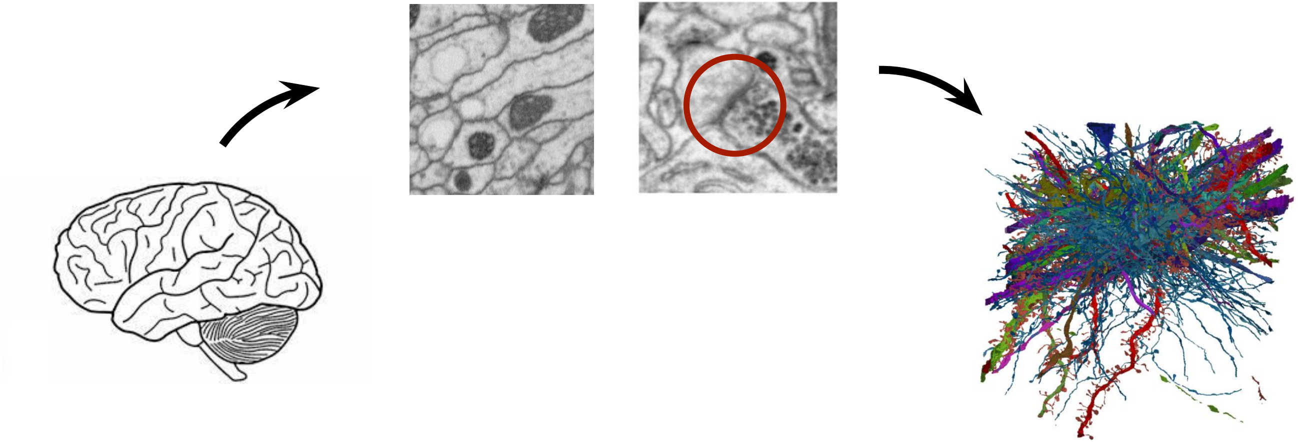

Nanometer-Resolution Imaging

Circuit Reconstruction

Connectomics

Goal: Extract the wiring diagram from a brain

Nanometer-Resolution Imaging

Circuit Reconstruction

Improved Neural Networks, Medicine, Models

Connectomics

Goal: Extract the wiring diagram from a brain

Nanometer-Resolution Imaging

Circuit Reconstruction

Improved Neural Networks, Medicine, Models

Better Understanding

Connectomics

Goal: Extract the wiring diagram from a brain

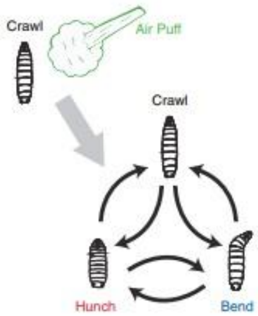

Behavior

Jovanic *et al.*, Competitive Disinhibition Mediates Behavioral Choice and Sequences in Drosophila, Cell 2016

Connectomics

Goal: Extract the wiring diagram from a brain

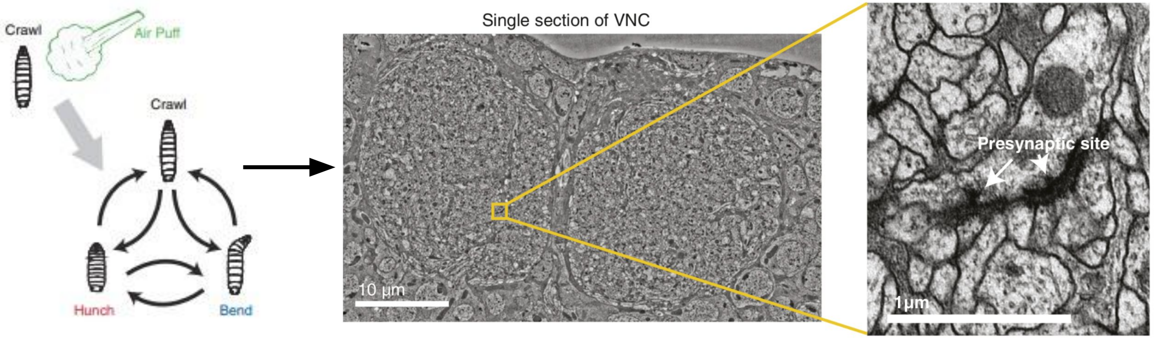

Behavior

Structure

Jovanic *et al.*, Competitive Disinhibition Mediates Behavioral Choice and Sequences in Drosophila, Cell 2016

Connectomics

Goal: Extract the wiring diagram from a brain

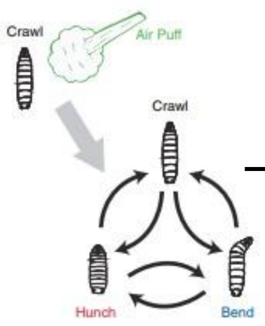

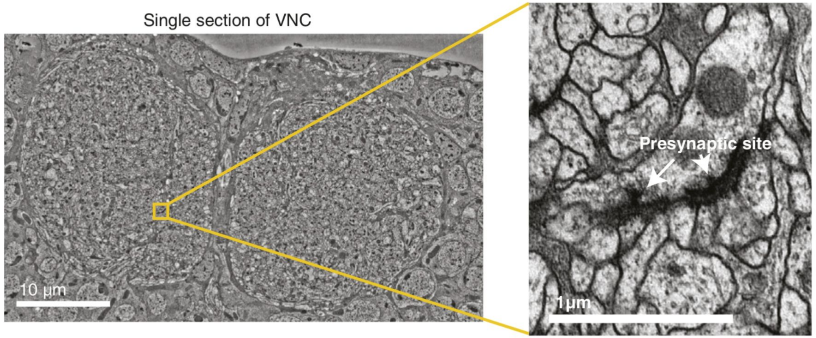

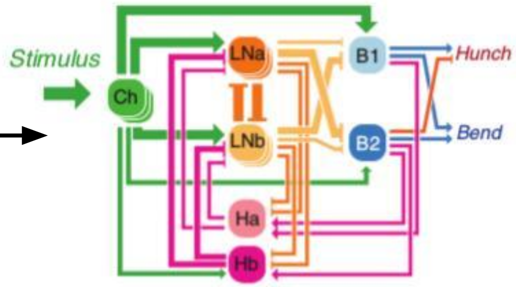

Behavior

Structure

Function

Jovanic *et al.*, Competitive Disinhibition Mediates Behavioral Choice and Sequences in Drosophila, Cell 2016

Connectomics

Goal: Extract the wiring diagram from a brain

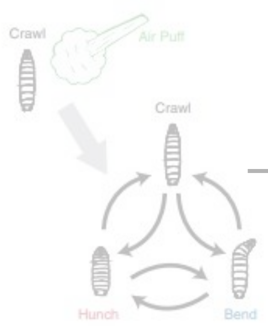

Behavior

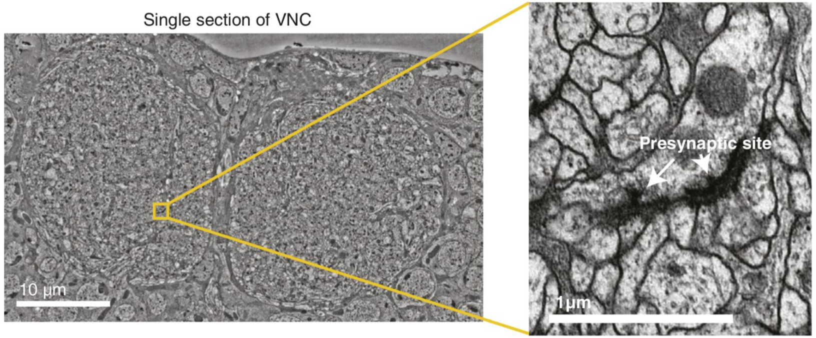

Structure

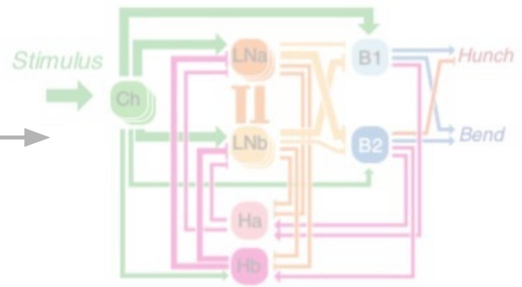

Function

Jovanic *et al.*, Competitive Disinhibition Mediates Behavioral Choice and Sequences in Drosophila, Cell 2016

Connectomics Pipeline

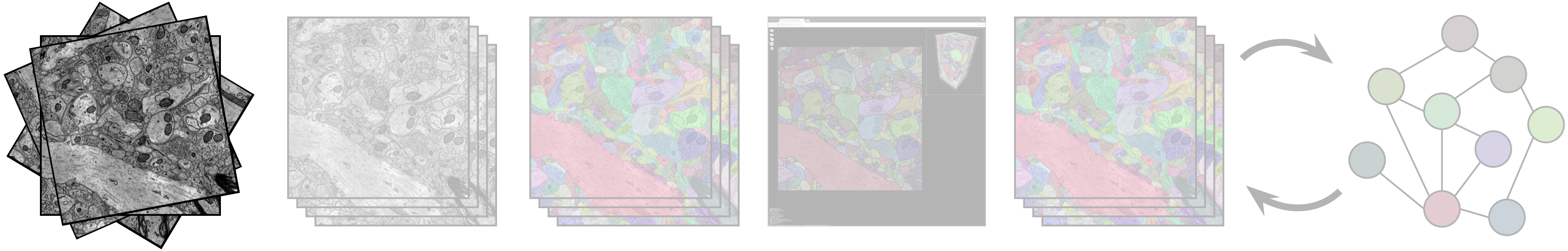

Acquisition

Registration

Segmentation

Proofreading

Network Analysis

Suissa-Peleg *et al.*, Automatic Neural Reconstruction from Petavoxel of Electron Microscopy, Microscopy and Microanalysis 2016
Schalek *et al.*, Imaging a 1 mm^3 Volume of Rat Cortex Using a MultiBeam SEM, Microscopy and Microanalysis 2016
Xu *et al.*, Enhanced FIB-SEM Systems for Large-Volume 3D Imaging, biorxiv 2020
Yin *et al.*, A Petascale Automated Imaging Pipeline for Mapping Neuronal Circuits with High-Throughput Transmission Electron Microscopy, Nature Communications 2020

Image Acquisition

Multi-beam electron microscopes collect 1 TB of raw image data every hour

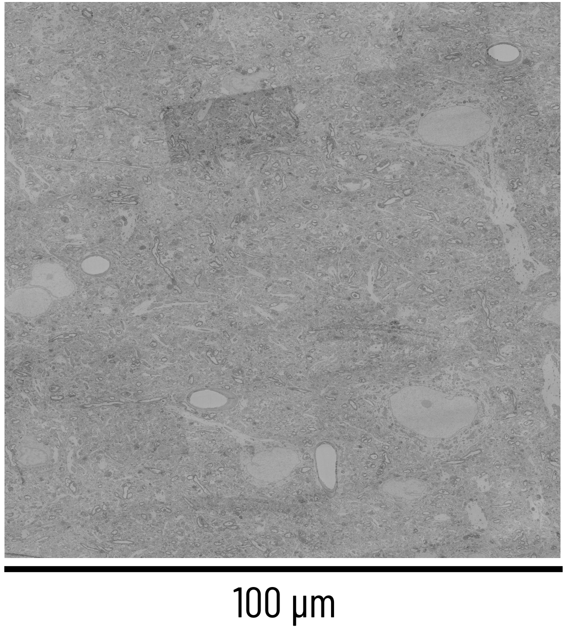

Image Acquisition

Multi-beam electron microscopes collect 1 TB of raw image data every hour

Can image 1 mm^3 of image data (2 PB) in 6 months

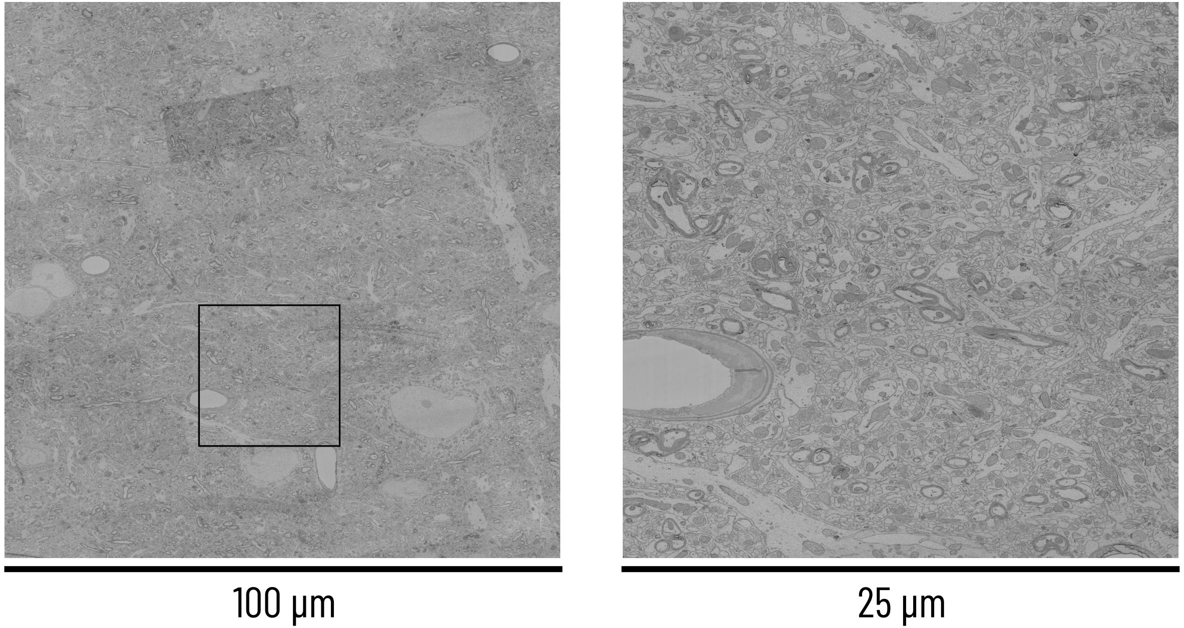

Image Acquisition

Multi-beam electron microscopes collect 1 TB of raw image data every hour

Can image 1 mm^3 of image data (2 PB) in 6 months

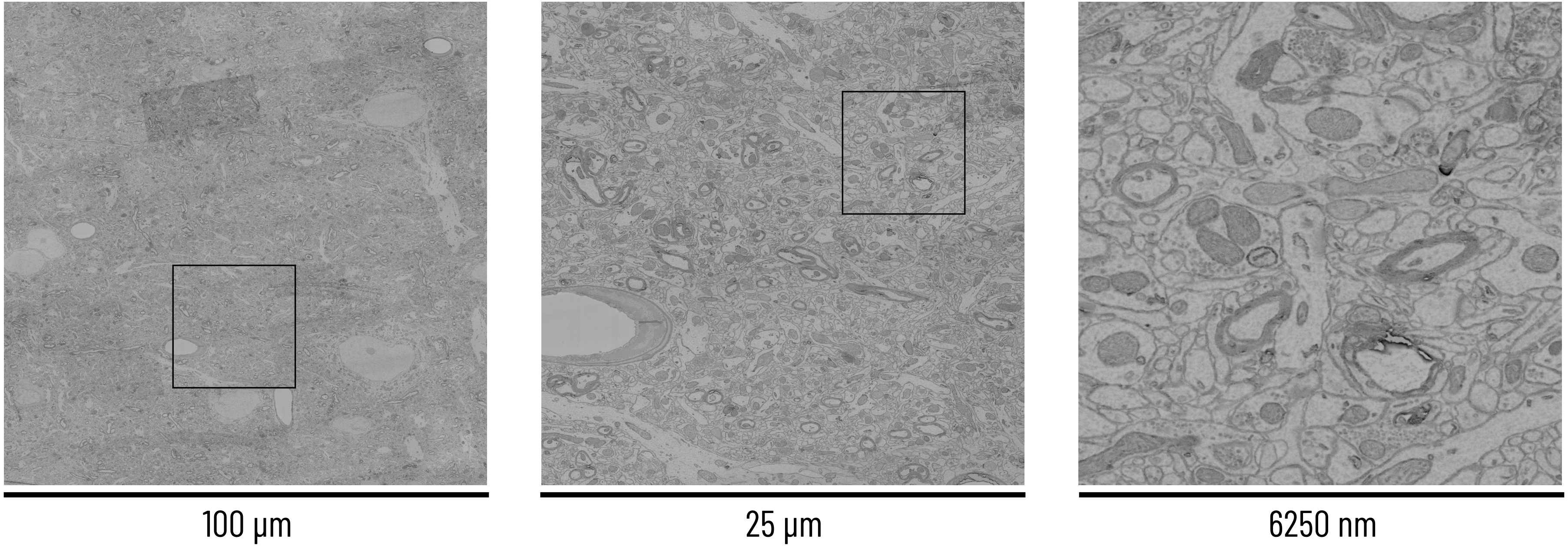

Connectomics Pipeline

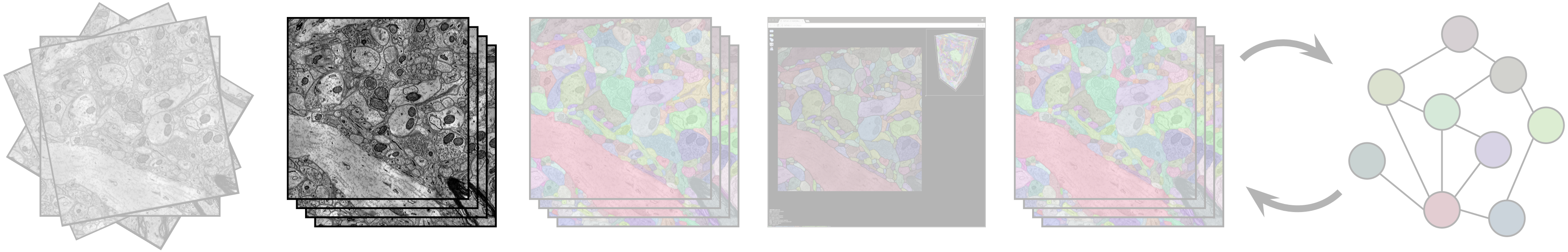

Acquisition

Registration

Segmentation

Proofreading

Network Analysis

Saalfield *et al.*, Elastic Volume Reconstruction from Series of Ultra-thin Microscopy Sections, Nature 2012
Khairy *et al.*, Joint Deformable Registration of Large EM Image Volumes: A Matrix Solver Approach, arxiv 2018

Registration

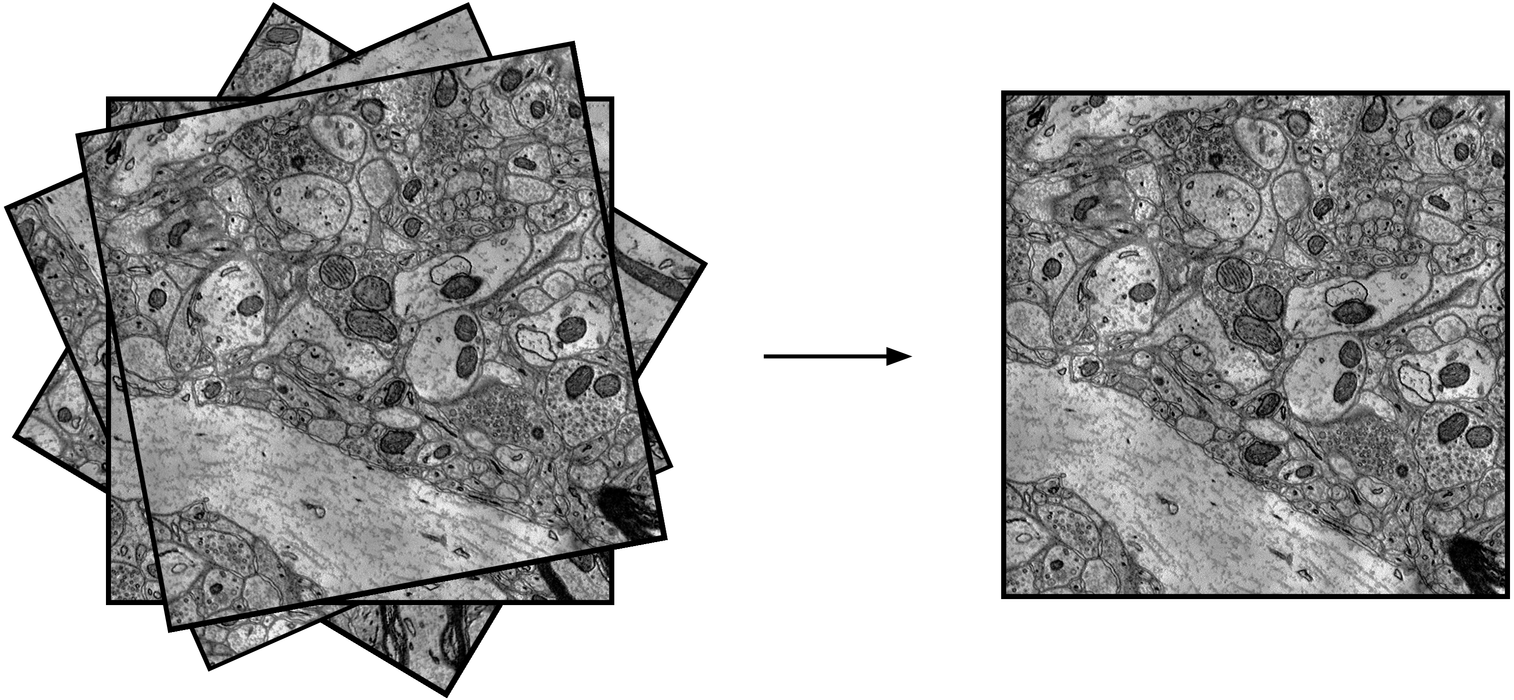

Connectomics Pipeline

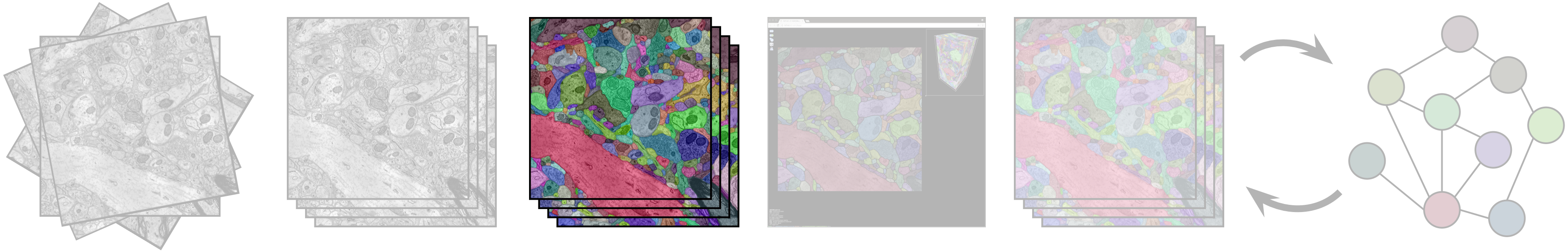

Acquisition

Registration

Segmentation

Proofreading

Network Analysis

Nunez-Iglesias *et al.*, Machine Learning of Hierarchical Clustering to Segment 2D and 3D Images, PLoS ONE 2014
Cicek *et al.*, 3D U-Net: Learning Dense Volumetric Segmentation from Sparse Annotation, MICCAI 2016
Zeng *et al.*, DeepEM3D: Approaching Human-Level Performance on 3D Anisotropic EM Image Segmentation, Bioinformatics 2017
Pape *et al.*, Solving Large Multicut Problems for Connectomics via Domain Decomposition, ICCV 2017
Lee *et al.*, Superhuman Accuracy on the SNEMI3D Connectomics Challenge, arxiv 2017
Januszewski et al., High-Precision Automated Reconstruction of Neurons with Flood-Filling Networks, Nature Methods 2018

Label Volumes

Two voxels have the same label only if they belong to the same neuron

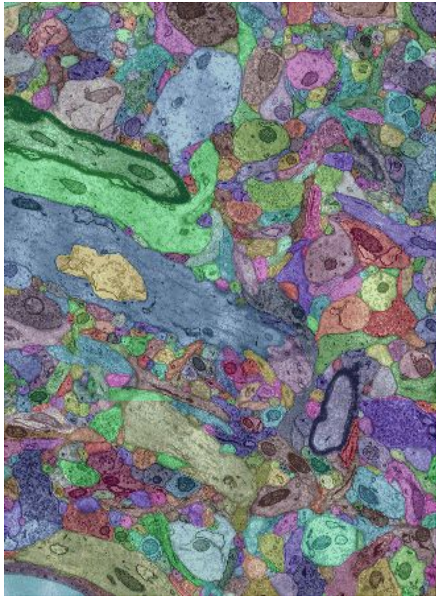

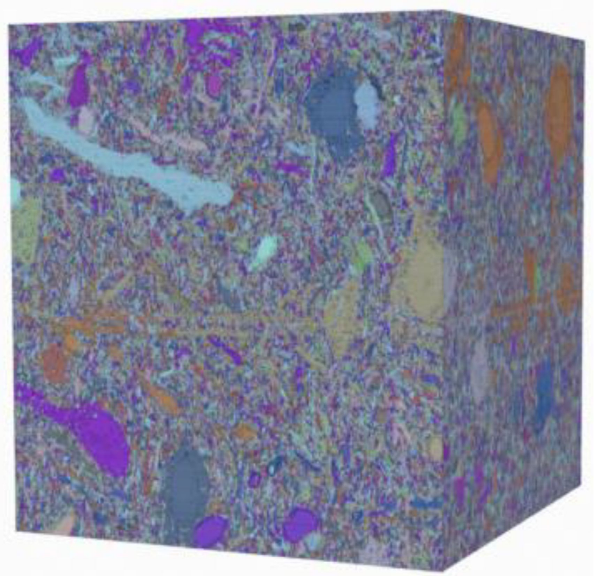

Label Volumes

Two voxels have the same label only if they belong to the same neuron

Typically use 64 bits per voxel to label each segment uniquely

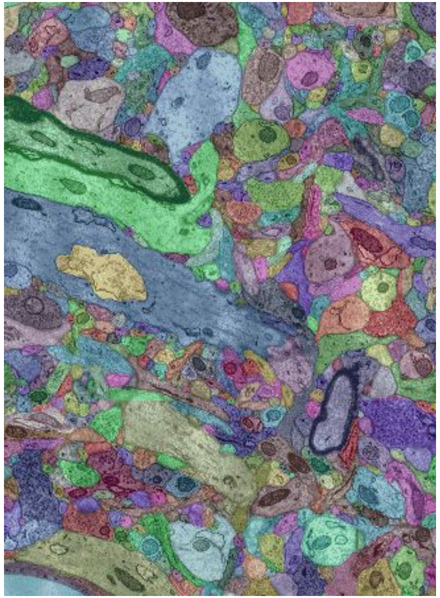

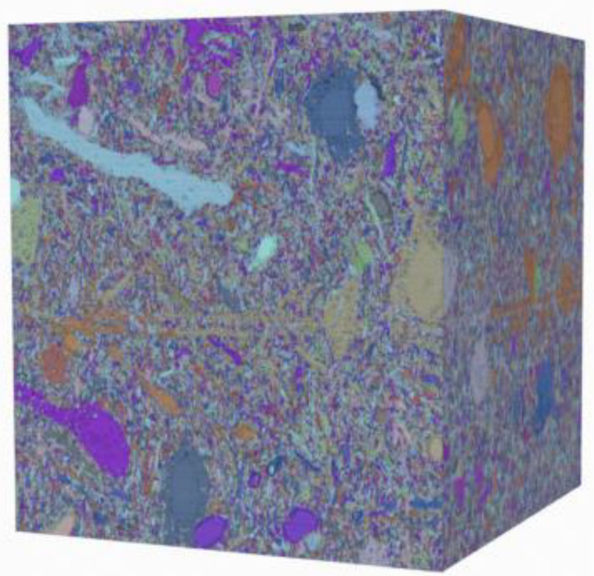

Connectomics Pipeline

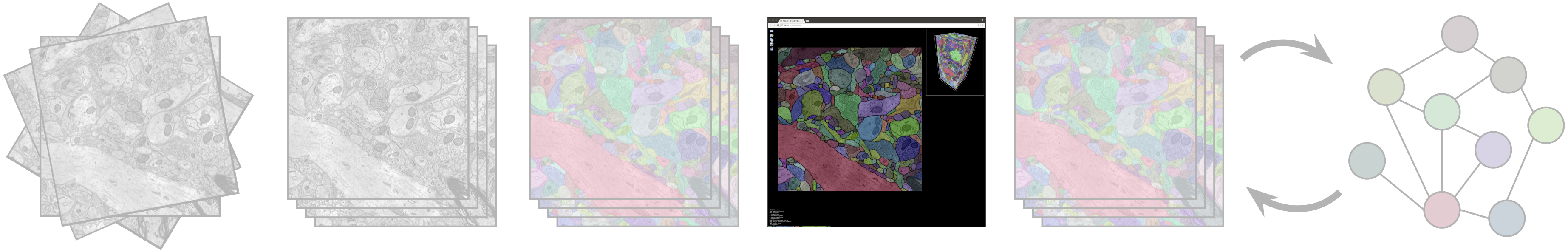

Acquisition

Registration

Segmentation

Proofreading

Network Analysis

Haehn *et al.*, Design and Evaluation of Interactive Proofreading Tools for Connectomics, IEEE VIS 2014
Zung *et al.*, An Error Detection and Correction Framework for Connectomics, NIPS 2017
Haehn *et al.*, Guided Proofreading of Automatic Segmentations for Connectomics, CVPR 2018
Dmitriev *et al.*, Efficient Correction for EM Connectomics with Skeletal Representation, BMVC 2018
Matejek *et al.*, Biologically-Constrained Graphs for Global Connectomics Reconstruction, CVPR 2019

Merge Errors

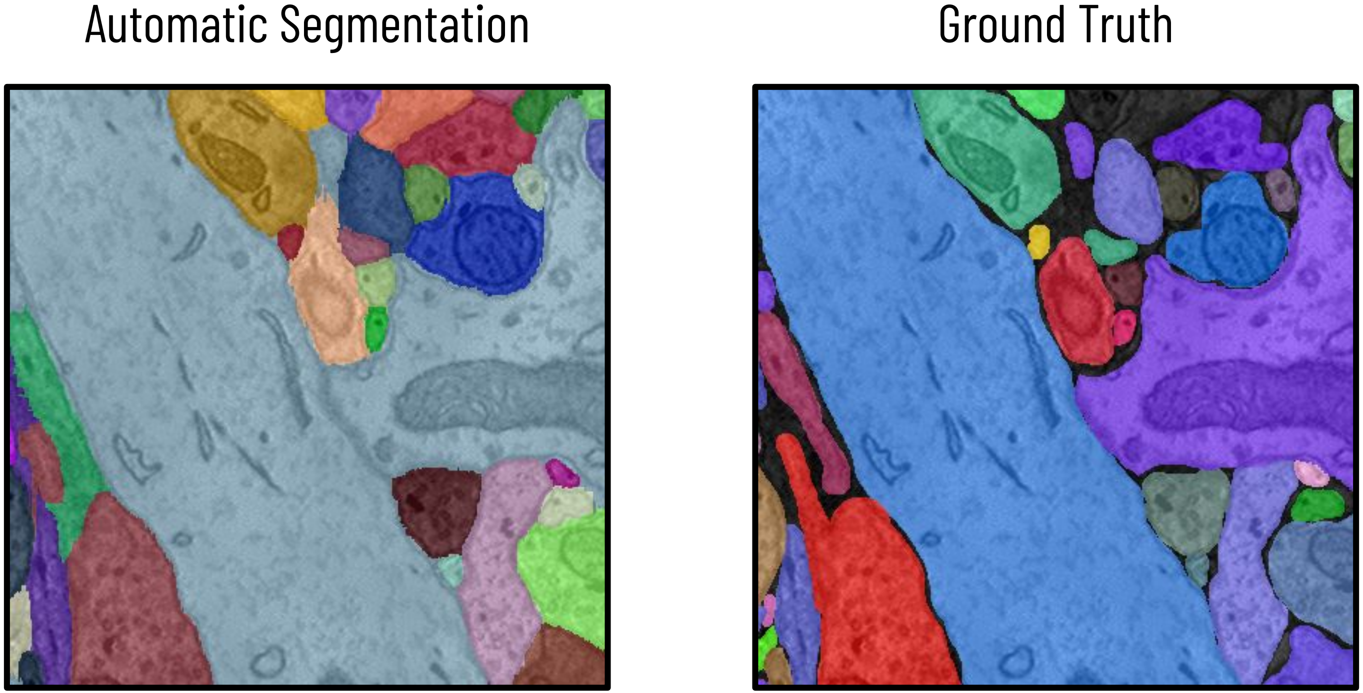

Automatic Segmentation

Ground Truth

Merge Errors

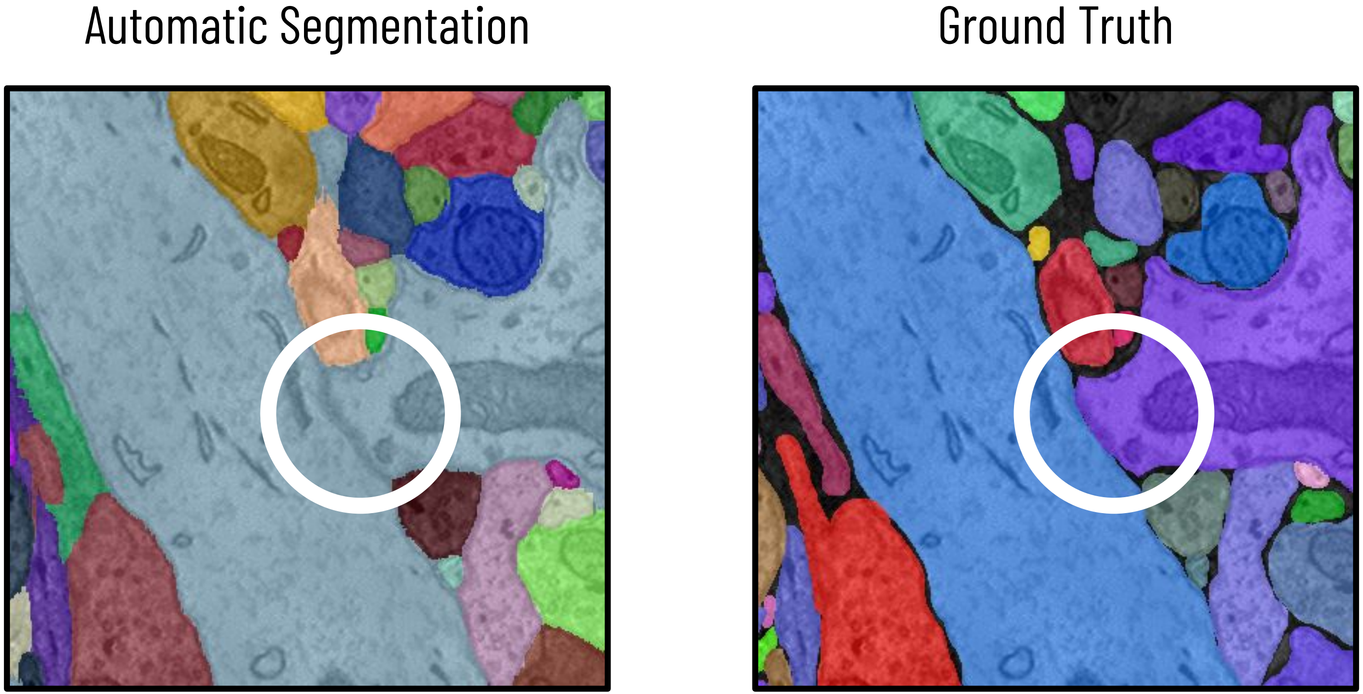
Automatic Segmentation

Ground Truth

Split Errors

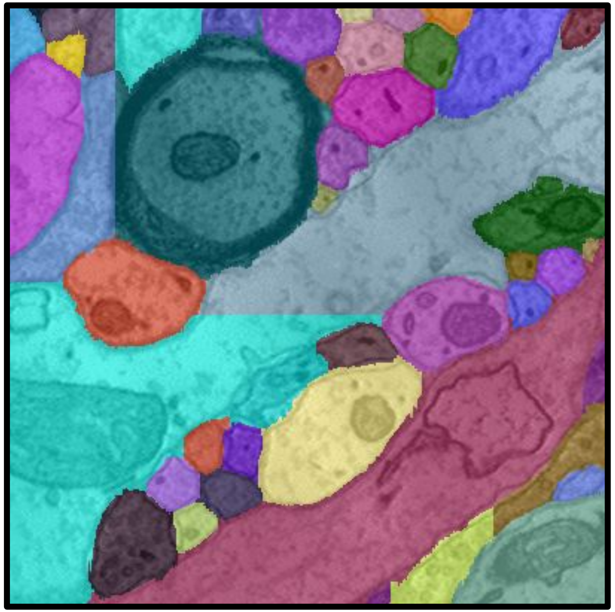

Automatic Segmentation

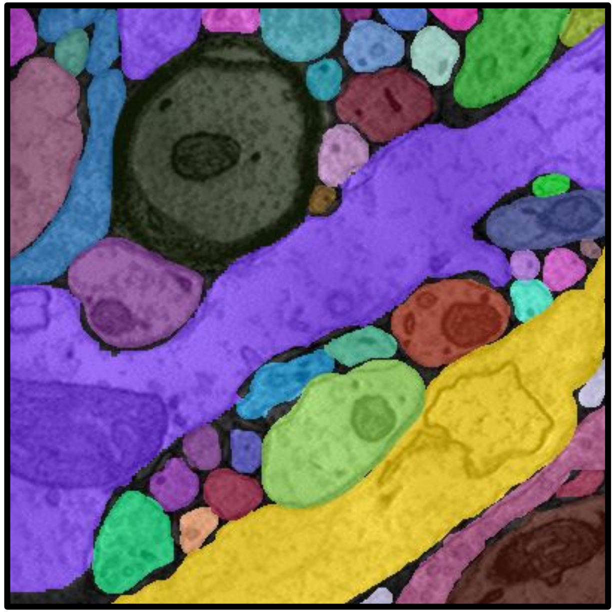

Ground Truth

Split Errors

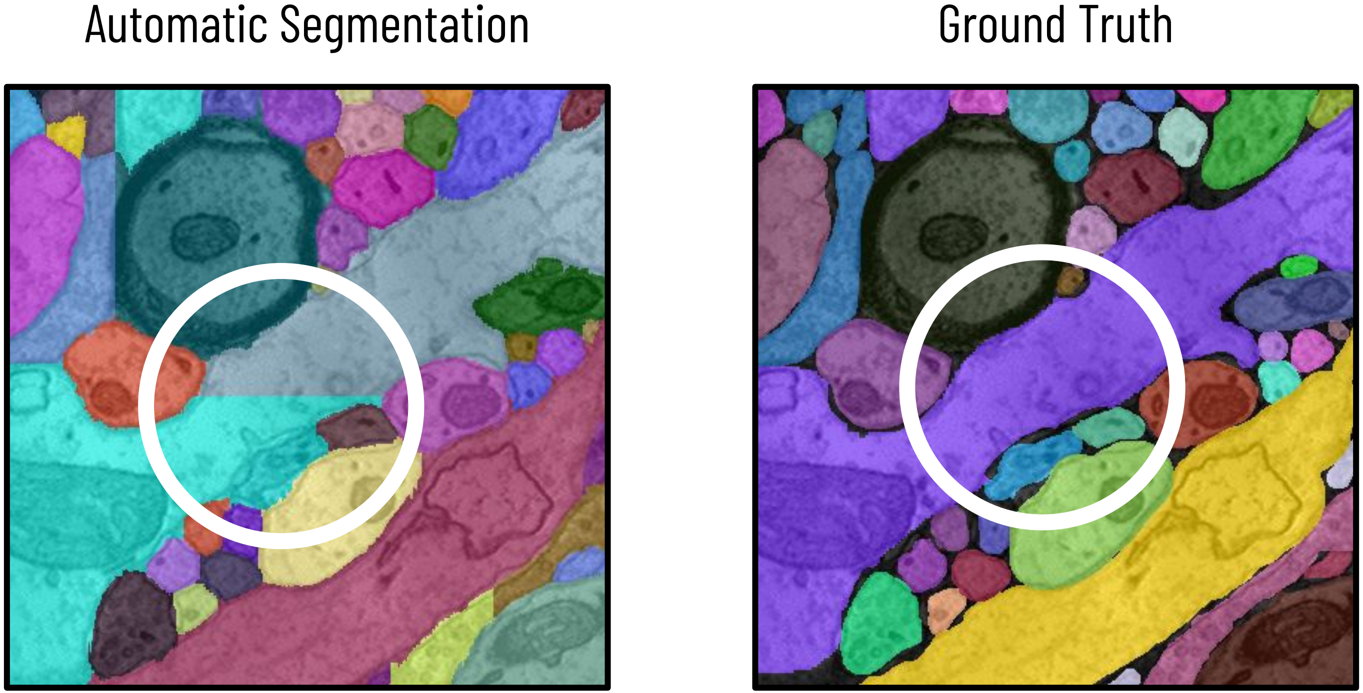

Connectomics Pipeline

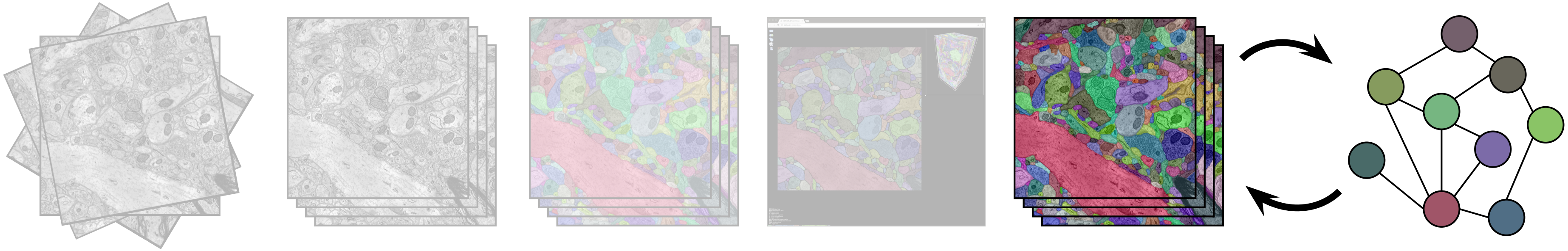

Acquisition Registration Segmentation Proofreading Network Analysis

Sorger *et al.*, neuroMAP - Interactive Graph-Visualization of the Fruit Fly's Neural Circuit, BioVIS 2013
Al-Awami *et al.*, NeuroLines: A Subway Map Metaphor for Visualizing Nanoscale Neuronal Connectivity, IEEE VIS 2014
Haehn *et al.*, Scalable Interactive Visualization for Connectomics, MDPI Informatics 2017
Cook *et al.*, Whole-Animal Connectomes of Both *Caenorhabditis elegans* Sexes, Nature 2019
Scheffer *et al.*, A Connectome and Analysis of the Adult *Drosophila* Central Brain, eLife 2020

Network Analysis

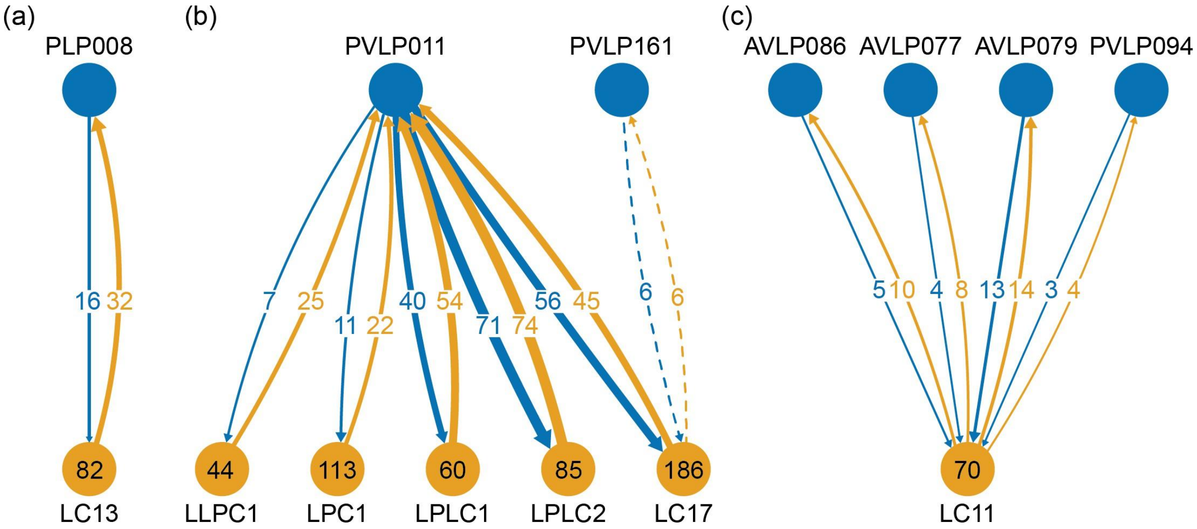

Scheffer *et al.*, A Connectome and Analysis of the Adult *Drosophila* Central Brain, eLife 2020

Image to Analysis Pipeline

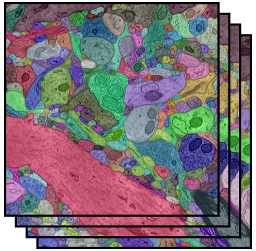

Segmentation

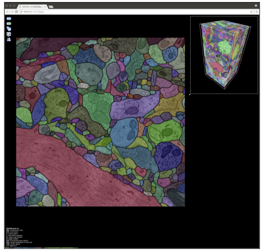

Proofreading

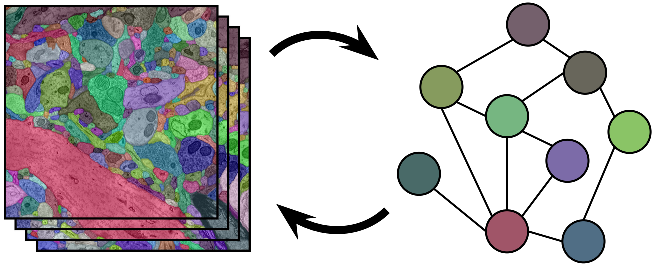

Network Analysis

Scale Challenges of Connectomics

Reconstructing wiring diagrams requires extreme differences in scale

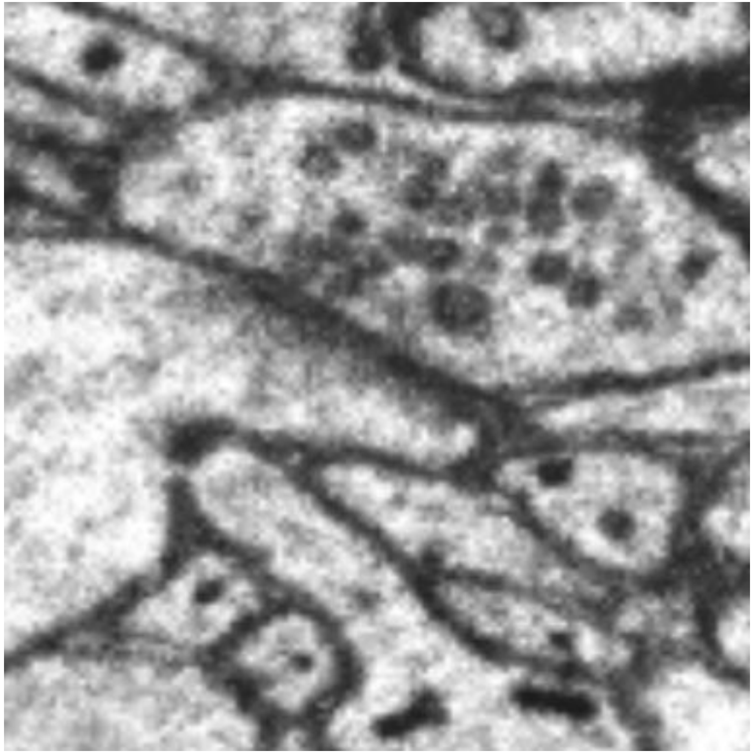

4-10 nanometer resolution

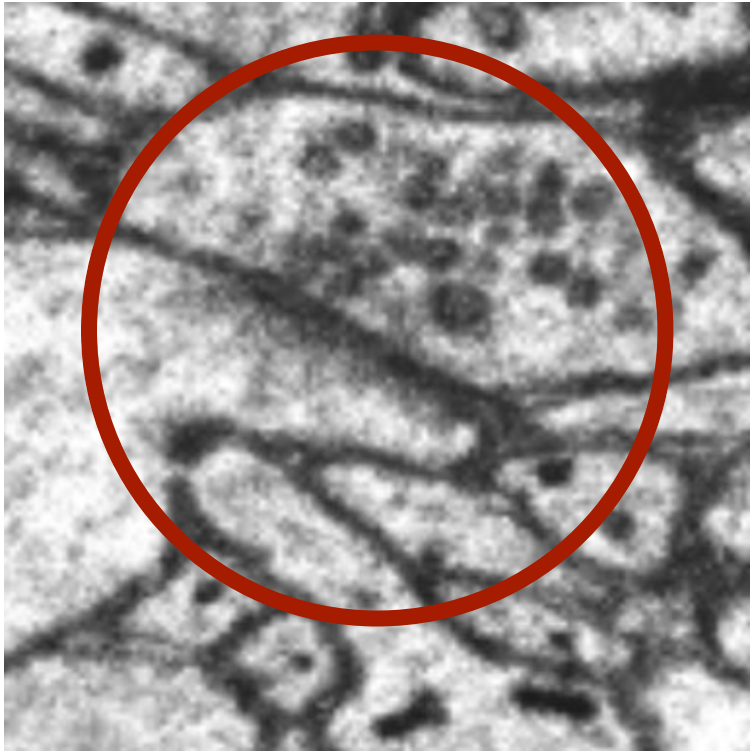

4-10 nanometer resolution

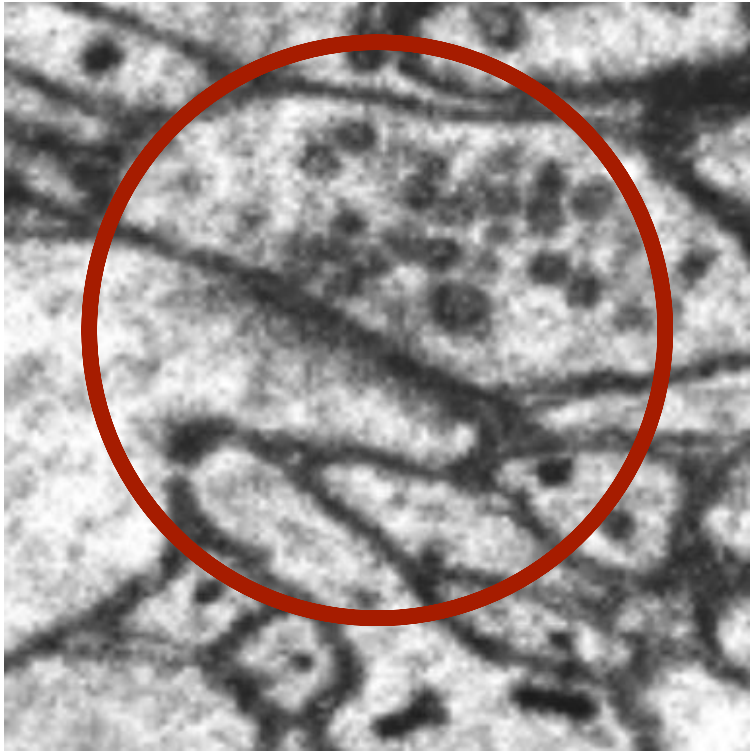

4-10 nanometer resolution

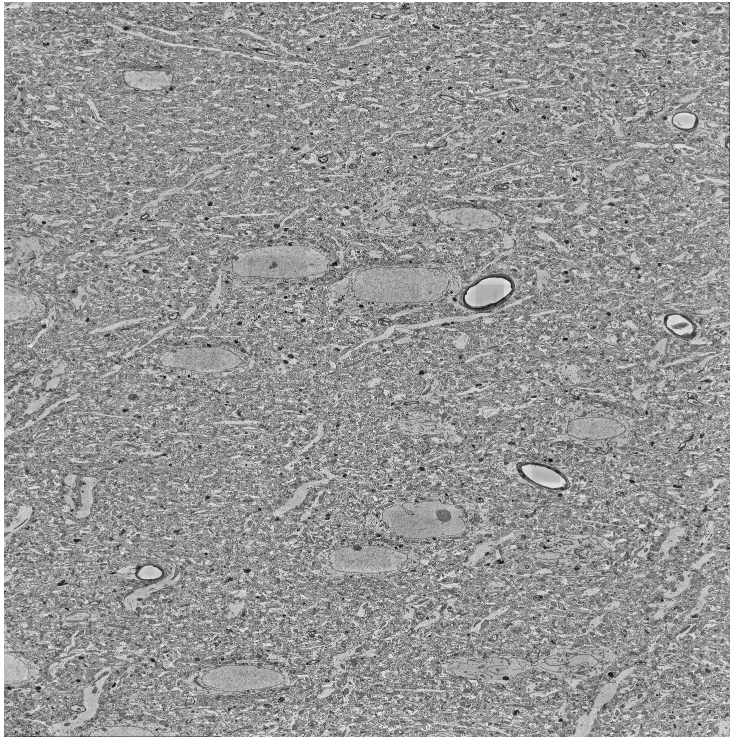

100 micrometers span

Four Orders of Magnitude Difference

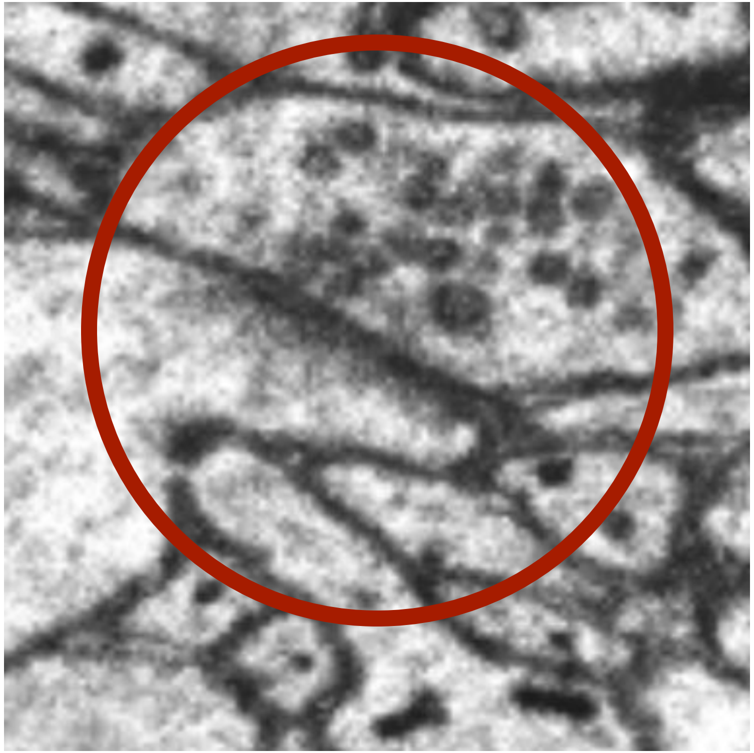

4-10 nanometer resolution

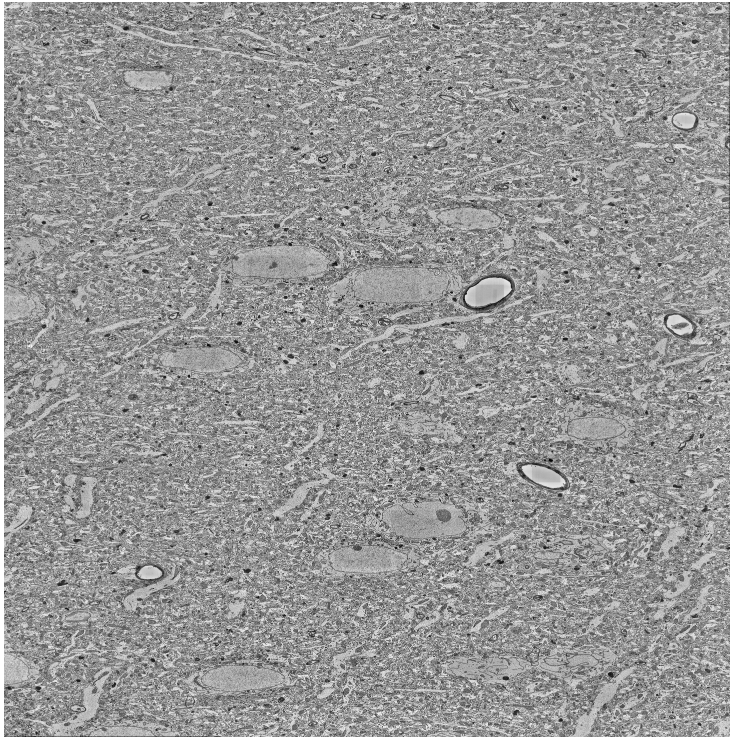

100 micrometers span

Scale Challenges of Connectomics

Scales compound with three dimensions

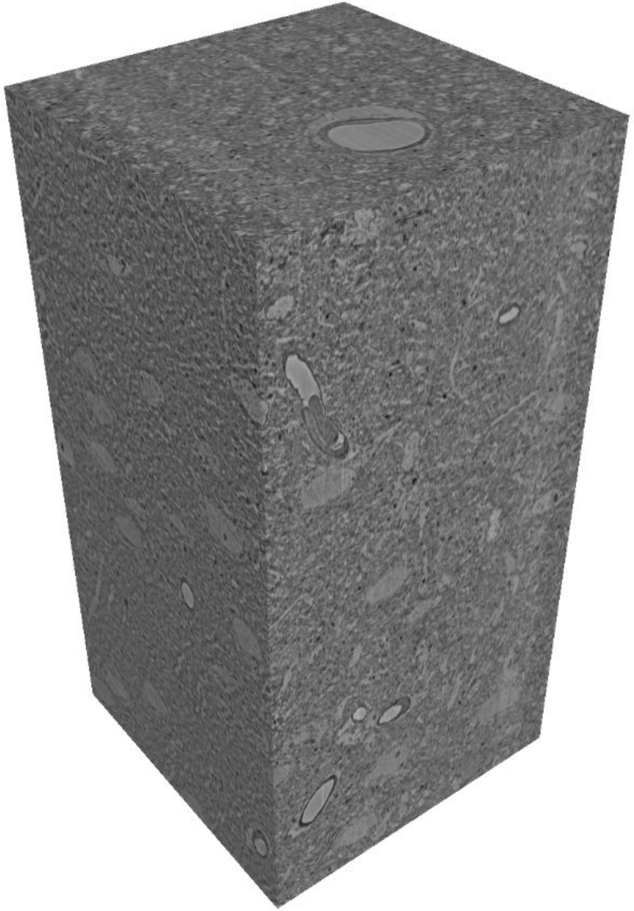

Scale Challenges of Connectomics

Scales compound with three dimensions

Small circuits with ~100-400 neurons require one trillion voxels

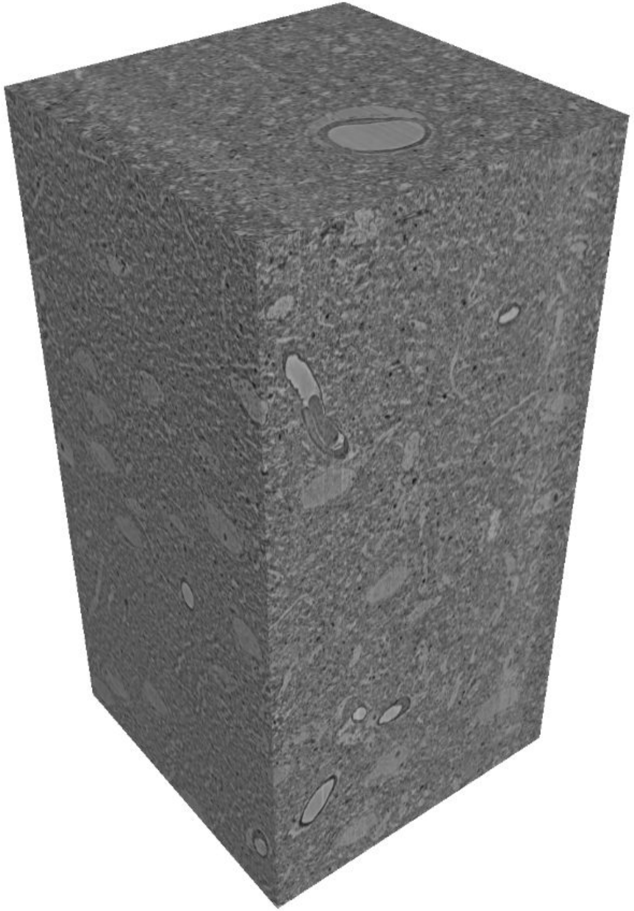

Scale Challenges of Connectomics

Scales compound with three dimensions

Small circuits with ~100-400 neurons require one trillion voxels

We require automatic solutions for reconstruction and analysis

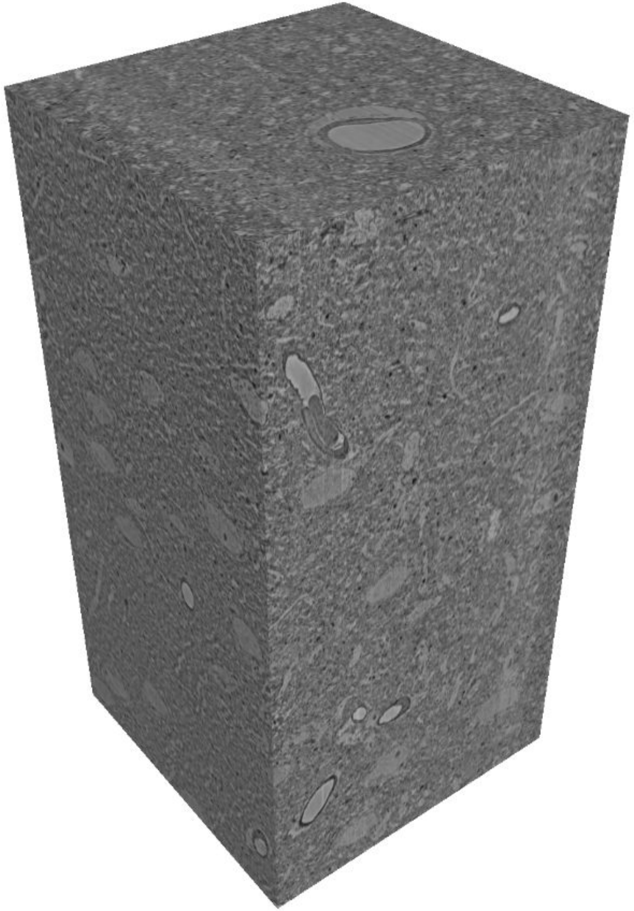

End-to-End Deep Learning

Increasingly, end-to-end trained deep learning models reconstruct the neurons

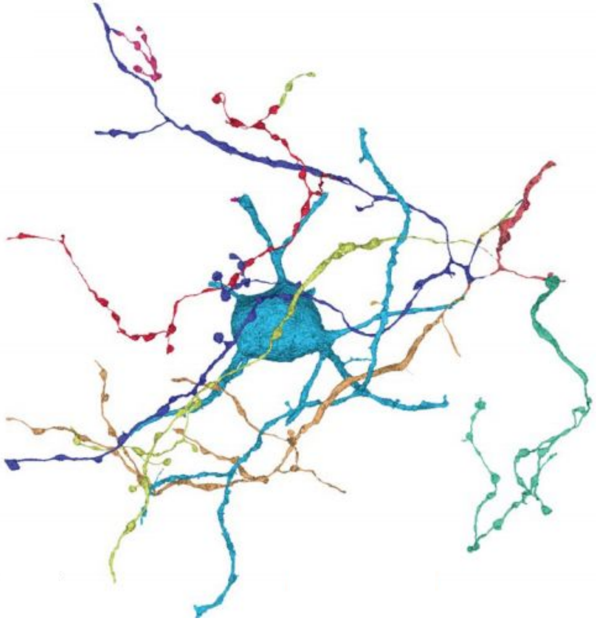

Januszewski *et al.*, High-Precision Automated Reconstruction of Neurons with Flood-Filling Networks, Nature Methods 2018

Errors with Automatic Methods

Despite incredible accuracies, these methods make mistakes at such large scales

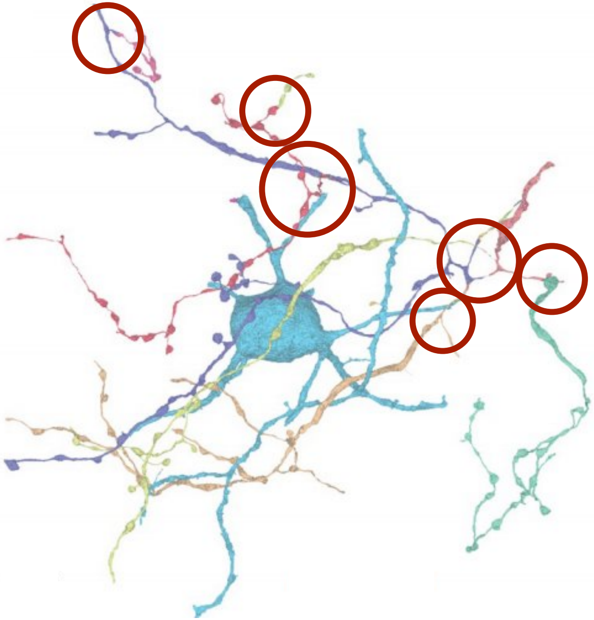

Januszewski *et al.*, High-Precision Automated Reconstruction of Neurons with Flood-Filling Networks, Nature Methods 2018

Dense Graphs

After reconstruction, the extracted wiring diagrams can be quite dense (20-100 connections per neuron)

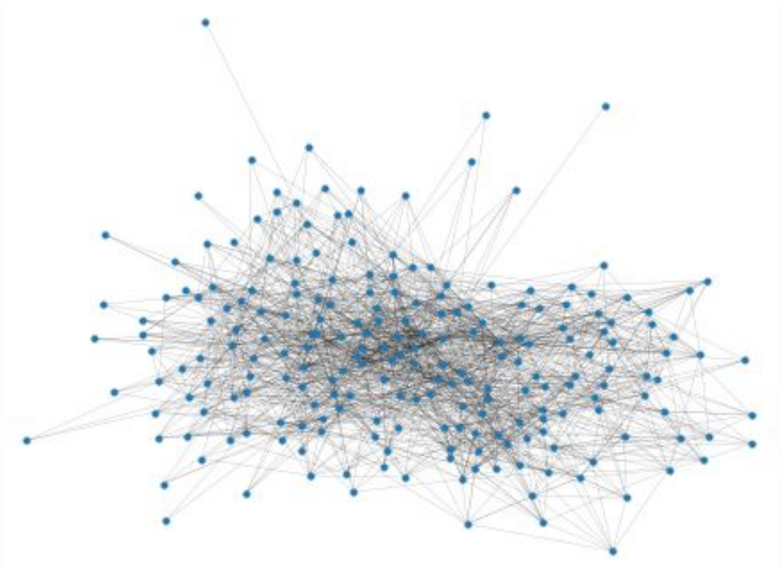

Dense Graphs with Biological Attributes

After reconstruction, the extracted wiring diagrams can be quite dense (20-100 connections per neuron)

The connections themselves have biological significance such as excitatory/inhibitory synapses

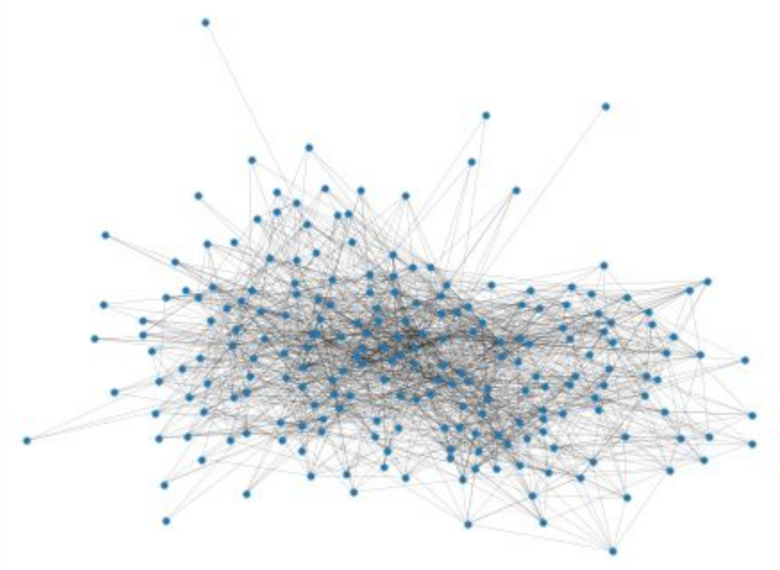

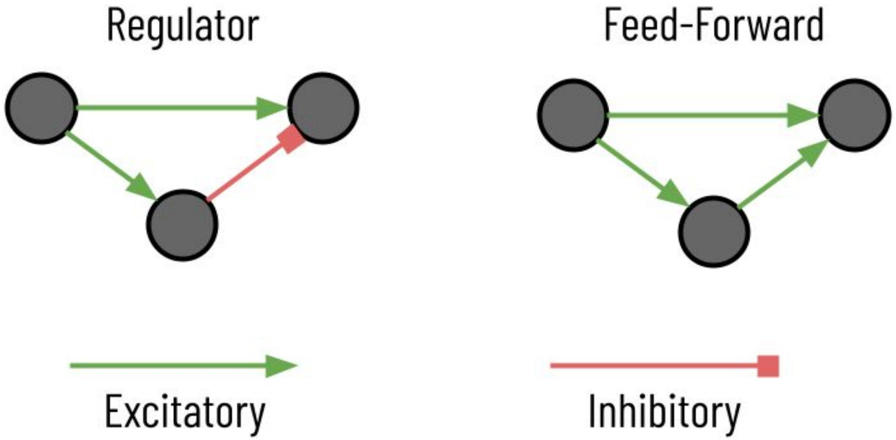

Biologically-Aware Algorithms Along the Connectomics Pipeline

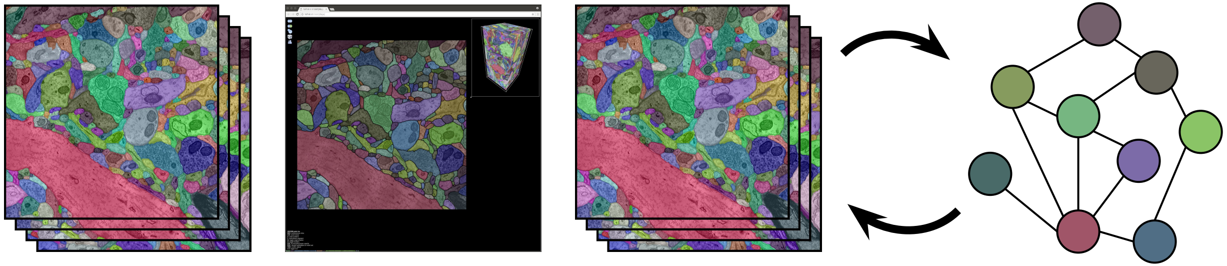

Segmentation

Proofreading

Network Analysis

Biologically-Aware Algorithms Along the Connectomics Pipeline

Compression

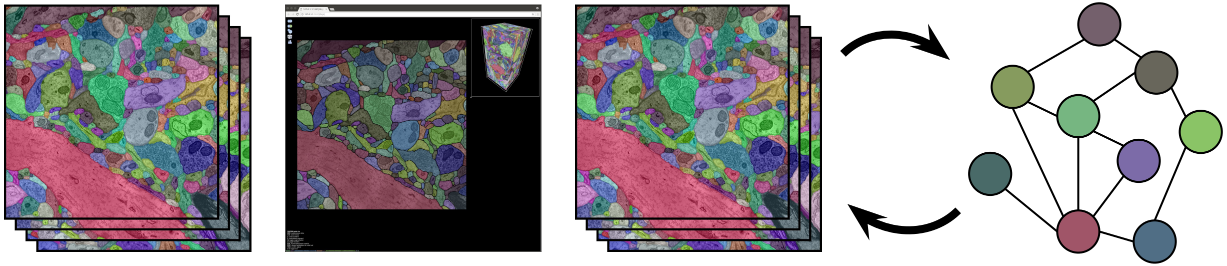

Segmentation

Proofreading

Network Analysis

Compresso: Efficient Compression of Segmentation Data for Connectomics

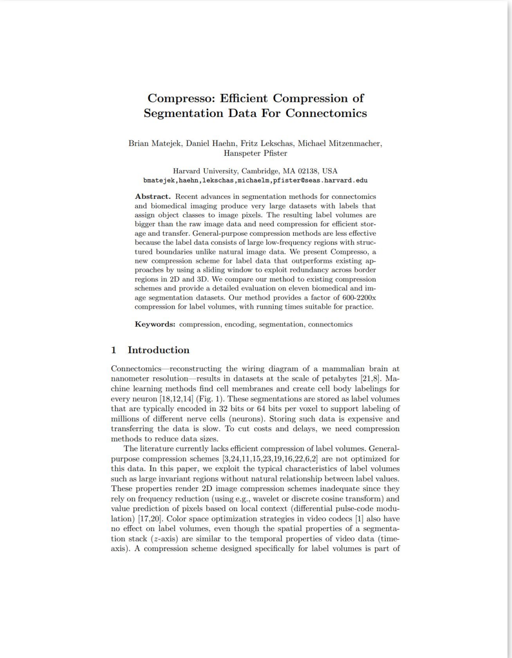

Compresso: Efficient Compression of Segmentation Data For Connectomics

Brian Matejek, Daniel Haehn, Fritz Lekschas, Michael Mitzenmacher,
Hanspeter Pfister

Harvard University, Cambridge, MA 02138, USA
`bmatejek,haehn,lekschas,michaelm,pfister@seas.harvard.edu`

Abstract. Recent advances in segmentation methods for connectomics and biomedical imaging produce very large datasets with labels that assign object classes to image pixels. The resulting label volumes are bigger than the raw image data and need compression for efficient storage and transfer. General-purpose compression methods are less effective because the label data consists of large low-frequency regions with structured boundaries unlike natural image data. We present Compresso, a new compression scheme for label data that outperforms existing approaches by using a sliding window to exploit redundancy across border regions in 2D and 3D. We compare our method to existing compression schemes and provide a detailed evaluation on eleven biomedical and image segmentation datasets. Our method provides a factor of 600-2200x compression for label volumes, with running times suitable for practice.

Keywords: compression, encoding, segmentation, connectomics

1 Introduction

Connectomics—reconstructing the wiring diagram of a mammalian brain at nanometer resolution—results in datasets at the scale of petabytes [21,8]. Machine learning methods find cell membranes and create cell body labelings for every neuron [18,12,14] (Fig. 1). These segmentations are stored as label volumes that are typically encoded in 32 bits or 64 bits per voxel to support labeling of millions of different nerve cells (neurons). Storing such data is expensive and transferring the data is slow. To cut costs and delays, we need compression methods to reduce data sizes.

The literature currently lacks efficient compression of label volumes. General-purpose compression schemes [3,24,11,15,23,19,16,22,6,2] are not optimized for this data. In this paper, we exploit the typical characteristics of label volumes such as large invariant regions without natural relationship between label values. These properties render 2D image compression schemes inadequate since they rely on frequency reduction (using e.g., wavelet or discrete cosine transform) and value prediction of pixels based on local context (differential pulse-code modulation) [17,20]. Color space optimization strategies in video codecs [1] also have no effect on label volumes, even though the spatial properties of a segmentation stack (z-axis) are similar to the temporal properties of video data (time-axis). A compression scheme designed specifically for label volumes is part of

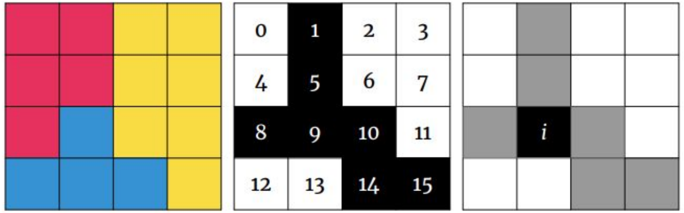

Brian Matejek, Daniel Haehn, Fritz Lekschas, Michael Mitzenmacher, and Hanspeter Pfister
MICCAI 2017

Biologically-Aware Algorithms Along the Connectomics Pipeline

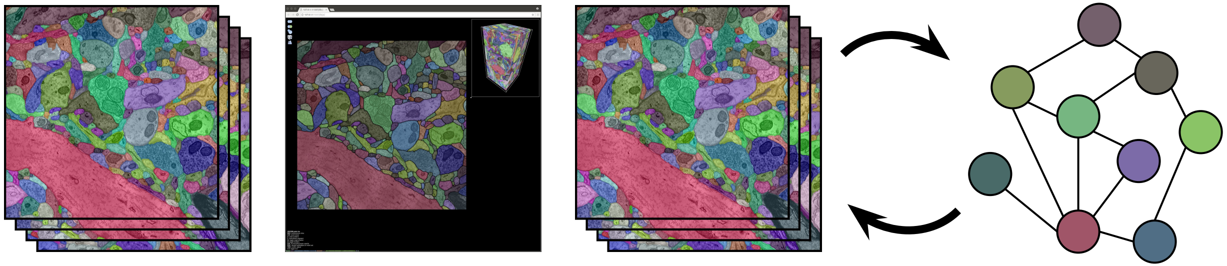

Compression

Error Correction

Segmentation

Proofreading

Network Analysis

Biologically-Constrained Graphs for Global Connectomics Reconstruction

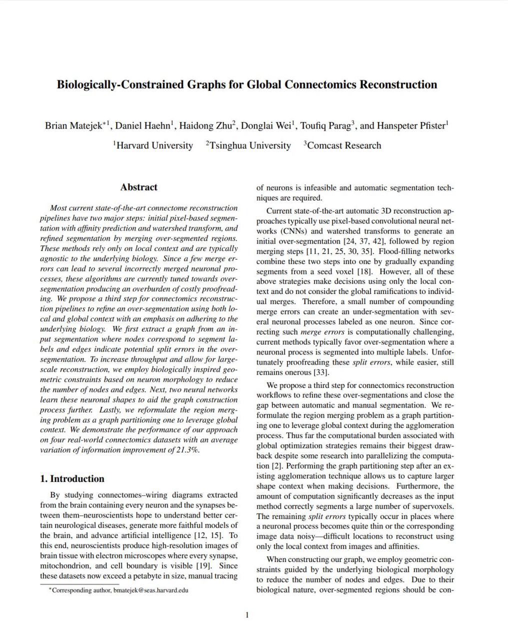

Biologically-Constrained Graphs for Global Connectomics Reconstruction

Brian Matejek*[1], Daniel Haehn[1], Haidong Zhu[2], Donglai Wei[1], Toufiq Parag[3], and Hanspeter Pfister[1]

[1]Harvard University [2]Tsinghua University [3]Comcast Research

Abstract

Most current state-of-the-art connectome reconstruction pipelines have two major steps: initial pixel-based segmentation with affinity prediction and watershed transform, and refined segmentation by merging over-segmented regions. These methods rely only on local context and are typically agnostic to the underlying biology. Since a few merge errors can lead to several incorrectly merged neuronal processes, these algorithms are currently tuned towards over-segmentation producing an overburden of costly proofreading. We propose a third step for connectomics reconstruction pipelines to refine an over-segmentation using both local and global context with an emphasis on adhering to the underlying biology. We first extract a graph from an input segmentation where nodes correspond to segment labels and edges indicate potential split errors in the over-segmentation. To increase throughput and allow for large-scale reconstruction, we employ biologically inspired geometric constraints based on neuron morphology to reduce the number of nodes and edges. Next, two neural networks learn these neuronal shapes to aid the graph construction process further. Lastly, we reformulate the region merging problem as a graph partitioning one to leverage global context. We demonstrate the performance of our approach on four real-world connectomics datasets with an average variation of information improvement of 21.3%.

1. Introduction

By studying connectomes–wiring diagrams extracted from the brain containing every neuron and the synapses between them–neuroscientists hope to understand better certain neurological diseases, generate more faithful models of the brain, and advance artificial intelligence [12, 15]. To this end, neuroscientists produce high-resolution images of brain tissue with electron microscopes where every synapse, mitochondrion, and cell boundary is visible [19]. Since these datasets now exceed a petabyte in size, manual tracing of neurons is infeasible and automatic segmentation techniques are required.

Current state-of-the-art automatic 3D reconstruction approaches typically use pixel-based convolutional neural networks (CNNs) and watershed transforms to generate an initial over-segmentation [24, 37, 42], followed by region merging steps [11, 21, 25, 30, 35]. Flood-filling networks combine these two steps into one by gradually expanding segments from a seed voxel [18]. However, all of these above strategies make decisions using only the local context and do not consider the global ramifications to individual merges. Therefore, a small number of compounding merge errors can create an under-segmentation with several neuronal processes labeled as one neuron. Since correcting such *merge errors* is computationally challenging, current methods typically favor over-segmentation where a neuronal process is segmented into multiple labels. Unfortunately proofreading these *split errors*, while easier, still remains onerous [33].

We propose a third step for connectomics reconstruction workflows to refine these over-segmentations and close the gap between automatic and manual segmentation. We reformulate the region merging problem as a graph partitioning one to leverage global context during the agglomeration process. Thus far the computational burden associated with global optimization strategies remains their biggest drawback despite some research into parallelizing the computation [2]. Performing the graph partitioning step after an existing agglomeration technique allows us to capture larger shape context when making decisions. Furthermore, the amount of computation significantly decreases as the input method correctly segments a large number of supervoxels. The remaining *split errors* typically occur in places where a neuronal process becomes quite thin or the corresponding image data noisy—difficult locations to reconstruct using only the local context from images and affinities.

When constructing our graph, we employ geometric constraints guided by the underlying biological morphology to reduce the number of nodes and edges. Due to their biological nature, over-segmented regions should be con-

---

*Corresponding author, bmatejek@seas.harvard.edu

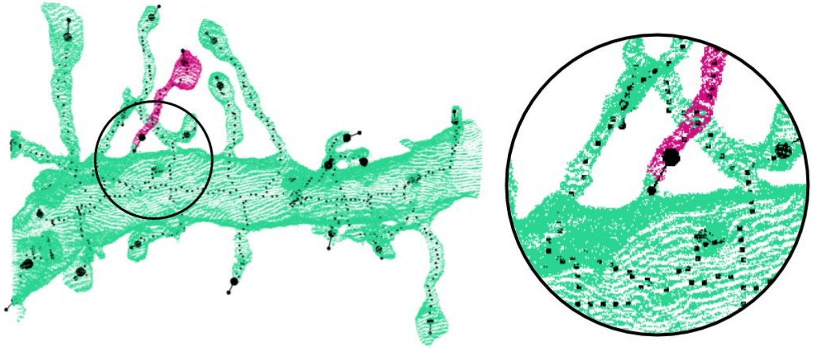

Brian Matejek, Daniel Haehn, Haidong Zhu, Daniel Haehn, Toufiq Parag, and Hanspeter Pfister

CVPR 2019

Biologically-Aware Algorithms Along the Connectomics Pipeline

Compression

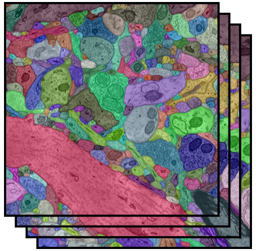

Segmentation

Error Correction

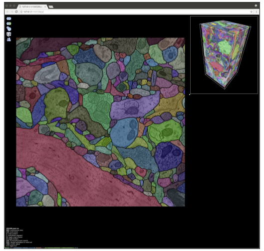

Proofreading

Subgraph Enumeration

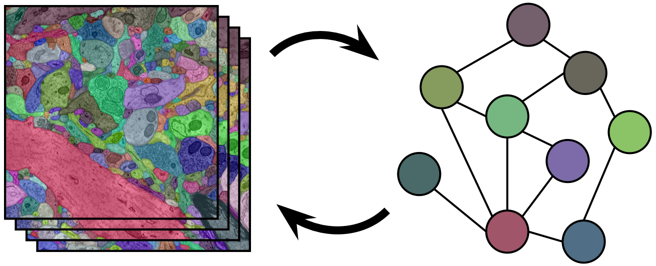

Network Analysis

Large-Scale Subgraph Enumeration on the Connectome

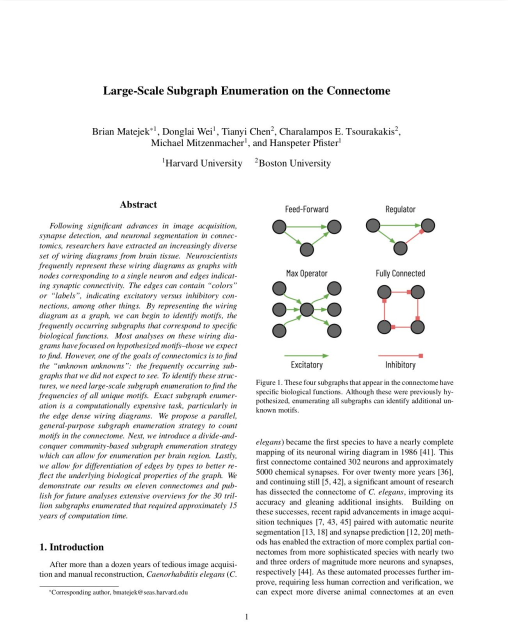

Large-Scale Subgraph Enumeration on the Connectome

Brian Matejek[*,1], Donglai Wei[1], Tianyi Chen[2], Charalampos E. Tsourakakis[2],
Michael Mitzenmacher[1], and Hanspeter Pfister[1]

[1]Harvard University [2]Boston University

Abstract

Following significant advances in image acquisition, synapse detection, and neuronal segmentation in connectomics, researchers have extracted an increasingly diverse set of wiring diagrams from brain tissue. Neuroscientists frequently represent these wiring diagrams as graphs with nodes corresponding to a single neuron and edges indicating synaptic connectivity. The edges can contain "colors" or "labels", indicating excitatory versus inhibitory connections, among other things. By representing the wiring diagram as a graph, we can begin to identify motifs, the frequently occurring subgraphs that correspond to specific biological functions. Most analyses on these wiring diagrams have focused on hypothesized motifs–those we expect to find. However, one of the goals of connectomics is to find the "unknown unknowns": the frequently occurring subgraphs that we did not expect to see. To identify these structures, we need large-scale subgraph enumeration to find the frequencies of all unique motifs. Exact subgraph enumeration is a computationally expensive task, particularly in the edge dense wiring diagrams. We propose a parallel, general-purpose subgraph enumeration strategy to count motifs in the connectome. Next, we introduce a divide-and-conquer community-based subgraph enumeration strategy which can allow for enumeration per brain region. Lastly, we allow for differentiation of edges by types to better reflect the underlying biological properties of the graph. We demonstrate our results on eleven connectomes and publish for future analyses extensive overviews for the 30 trillion subgraphs enumerated that required approximately 15 years of computation time.

1. Introduction

After more than a dozen years of tedious image acquisition and manual reconstruction, *Caenorhabditis elegans* (*C. elegans*) became the first species to have a nearly complete mapping of its neuronal wiring diagram in 1986 [41]. This first connectome contained 302 neurons and approximately 5000 chemical synapses. For over twenty more years [36], and continuing still [5, 42], a significant amount of research has dissected the connectome of *C. elegans*, improving its accuracy and gleaning additional insights. Building on these successes, recent rapid advancements in image acquisition techniques [7, 43, 45] paired with automatic neurite segmentation [13, 18] and synapse prediction [12, 20] methods has enabled the extraction of more complex partial connectomes from more sophisticated species with nearly two and three orders of magnitude more neurons and synapses, respectively [44]. As these automated processes further improve, requiring less human correction and verification, we can expect more diverse animal connectomes at an even

Figure 1. These four subgraphs that appear in the connectome have specific biological functions. Although these were previously hypothesized, enumerating all subgraphs can identify additional unknown motifs.

---

*Corresponding author, bmatejek@seas.harvard.edu

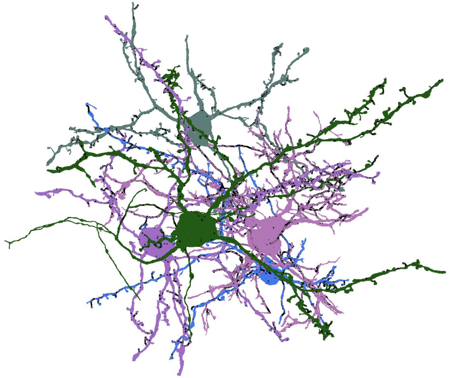

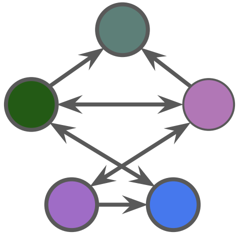

Brian Matejek, Donglai Wei, Tianyi Chen, Charalampos E. Tsourakakis, Michael Mitzenmacher, and Hanspeter Pfister

Preprint

Biologically-Aware Algorithms Along the Connectomics Pipeline

Skeleton Generation

Compression

Error Correction

Subgraph Enumeration

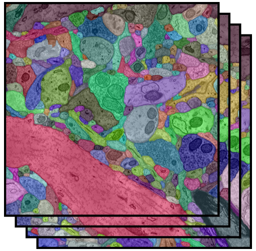

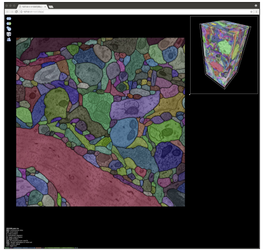

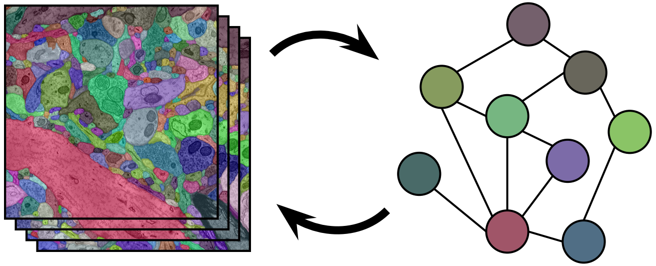

Segmentation

Proofreading

Network Analysis

Synapse-Aware Skeleton Generation for Neural Circuits

Synapse-Aware Skeleton Generation for Neural Circuits

Brian Matejek[1], Donglai Wei[1], Xueying Wang[2], Jinglin Zhao[2],
Kálmán Palágyi[3], and Hanspeter Pfister[1]

[1] John A. Paulson School of Engineering and Applied Sciences
Harvard University, Cambridge, MA, USA
[2] Center for Brain Science, Department of Molecular and Cellular Biology
Harvard University, Cambridge, MA, USA
[3] Department of Image Processing and Computer Graphics
University of Szeged, Szeged, Hungary
`bmatejek@seas.harvard.edu`

Abstract. Reconstructed terabyte and petabyte electron microscopy image volumes contain fully-segmented neurons at resolutions fine enough to identify every synaptic connection. After manual or automatic reconstruction, neuroscientists want to extract wiring diagrams and connectivity information to analyze the data at a higher level. Despite significant advances in image acquisition, neuron segmentation, and synapse detection techniques, the extracted wiring diagrams are still quite coarse, and often do not take into account the wealth of information in the densely reconstructed volumes. We propose a synapse-aware skeleton generation strategy to transform the reconstructed volumes into an information-rich yet abstract format on which neuroscientists can perform biological analysis and run simulations. Our method extends existing topological thinning strategies and guarantees a one-to-one correspondence between skeleton endpoints and synapses while simultaneously generating vital geometric statistics on the neuronal processes. We demonstrate our results on three large-scale connectomic datasets and compare against current state-of-the-art skeletonization algorithms.

Keywords: neural circuits · connectomics · skeleton generation.

1 Introduction

Acquisition techniques [17], automatic segmentation methods [5], and synapse detection strategies [3] in connectomics have all progressed rapidly in the last decade, yielding densely reconstructed volumes at nanometer resolution. These terabyte and petabyte volumes contain hundreds of thousands of interconnected neurons and millions of synaptic connections. Despite the rich detail in the reconstructed 3D volumes, most analysis of this data occurs at a very coarse level [4].

Little research has focused on generating accurate wiring diagrams from the raw reconstructions. Current approaches [5] directly use an off-the-shelf skeletonization method to reduce these volumes into a series of nodes (neurons) and

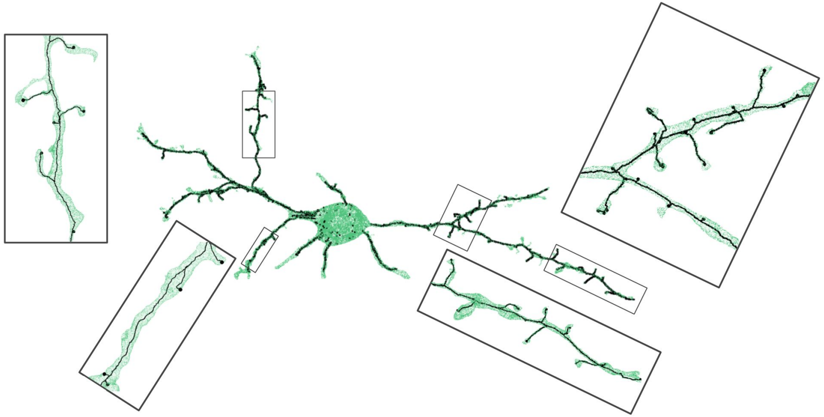

Brian Matejek, Donglai Wei, Xueying Wang, Jinglin Zhao, Kálmán Palágyi, and Hanspeter Pfister

MICCAI 2019

Scalable Biologically-Aware Skeleton Generation for Connectomic Volumes

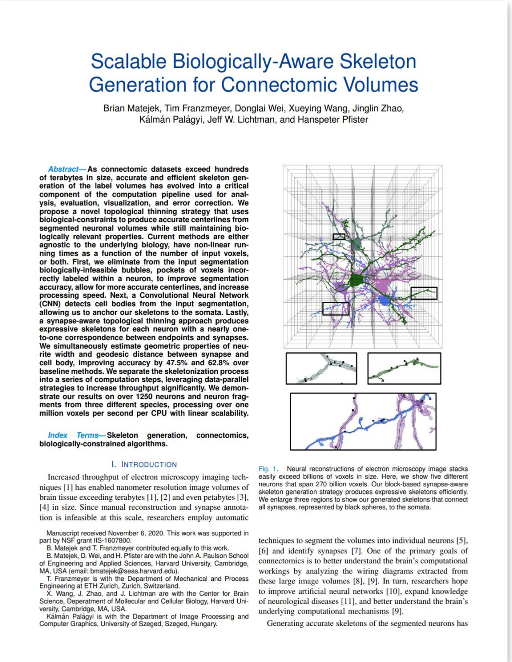

Scalable Biologically-Aware Skeleton Generation for Connectomic Volumes

Brian Matejek, Tim Franzmeyer, Donglai Wei, Xueying Wang, Jinglin Zhao,
Kálmán Palágyi, Jeff W. Lichtman, and Hanspeter Pfister

***Abstract*—As connectomic datasets exceed hundreds of terabytes in size, accurate and efficient skeleton generation of the label volumes has evolved into a critical component of the computation pipeline used for analysis, evaluation, visualization, and error correction. We propose a novel topological thinning strategy that uses biological-constraints to produce accurate centerlines from segmented neuronal volumes while still maintaining biologically relevant properties. Current methods are either agnostic to the underlying biology, have non-linear running times as a function of the number of input voxels, or both. First, we eliminate from the input segmentation biologically-infeasible bubbles, pockets of voxels incorrectly labeled within a neuron, to improve segmentation accuracy, allow for more accurate centerlines, and increase processing speed. Next, a Convolutional Neural Network (CNN) detects cell bodies from the input segmentation, allowing us to anchor our skeletons to the somata. Lastly, a synapse-aware topological thinning approach produces expressive skeletons for each neuron with a nearly one-to-one correspondence between endpoints and synapses. We simultaneously estimate geometric properties of neurite width and geodesic distance between synapse and cell body, improving accuracy by 47.5% and 62.8% over baseline methods. We separate the skeletonization process into a series of computation steps, leveraging data-parallel strategies to increase throughput significantly. We demonstrate our results on over 1250 neurons and neuron fragments from three different species, processing over one million voxels per second per CPU with linear scalability.**

***Index Terms*—Skeleton generation, connectomics, biologically-constrained algorithms.**

I. INTRODUCTION

Increased throughput of electron microscopy imaging techniques [1] has enabled nanometer resolution image volumes of brain tissue exceeding terabytes [1], [2] and even petabytes [3], [4] in size. Since manual reconstruction and synapse annotation is infeasible at this scale, researchers employ automatic techniques to segment the volumes into individual neurons [5], [6] and identify synapses [7]. One of the primary goals of connectomics is to better understand the brain's computational workings by analyzing the wiring diagrams extracted from these large image volumes [8], [9]. In turn, researchers hope to improve artificial neural networks [10], expand knowledge of neurological diseases [11], and better understand the brain's underlying computational mechanisms [9].

Generating accurate skeletons of the segmented neurons has

Fig. 1. Neural reconstructions of electron microscopy image stacks easily exceed billions of voxels in size. Here, we show five different neurons that span 270 billion voxels. Our block-based synapse-aware skeleton generation strategy produces expressive skeletons efficiently. We enlarge three regions to show our generated skeletons that connect all synapses, represented by black spheres, to the somata.

Manuscript received November 6, 2020. This work was supported in part by NSF grant IIS-1607800.

B. Matejek and T. Franzmeyer contributed equally to this work.

B. Matejek, D. Wei, and H. Pfister are with the John A. Paulson School of Engineering and Applied Sciences, Harvard University, Cambridge, MA, USA (email: bmatejek@seas.harvard.edu).

T. Franzmeyer is with the Department of Mechanical and Process Engineering at ETH Zurich, Zurich, Switzerland.

X. Wang, J. Zhao, and J. Lichtman are with the Center for Brain Science, Deperatment of Mollecular and Cellular Biology, Harvard University, Cambridge, MA, USA.

Kálmán Palágyi is with the Department of Image Processing and Computer Graphics, University of Szeged, Szeged, Hungary.

Brian Matejek†, Tim Franzmeyer†, Donglai Wei, Xueying Wang, Jinglin Zhao, Kálmán Palágyi, Jeff W. Lichtman, and Hanspeter Pfister
Under Review

Biologically-Aware Algorithms Along the Connectomics Pipeline

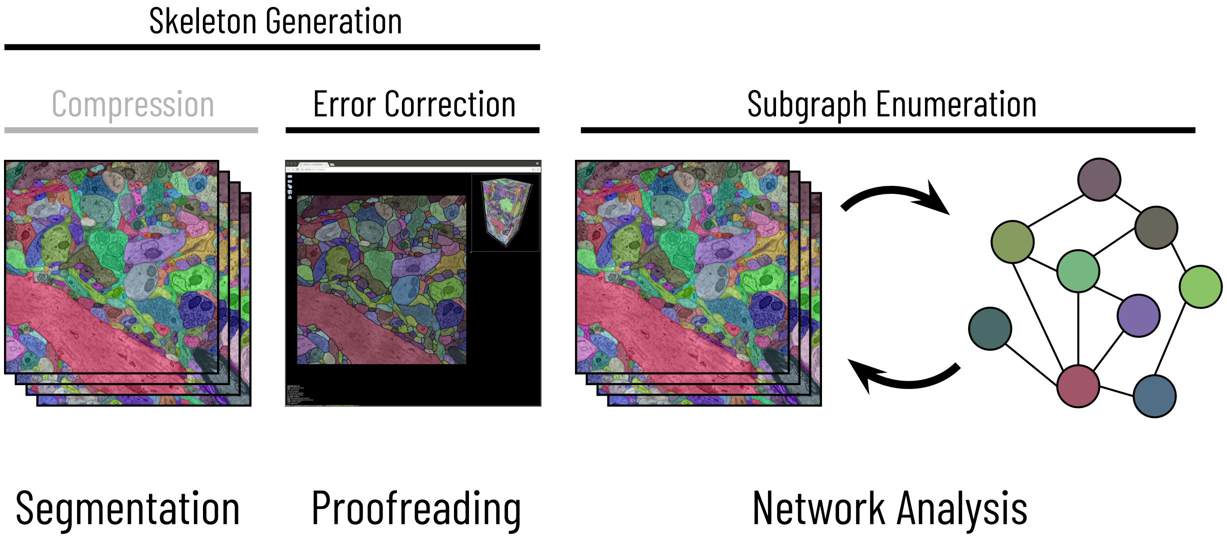

Skeleton Generation

Compression

Error Correction

Subgraph Enumeration

Segmentation

Proofreading

Network Analysis

Biologically-Aware Algorithms Along the Connectomics Pipeline

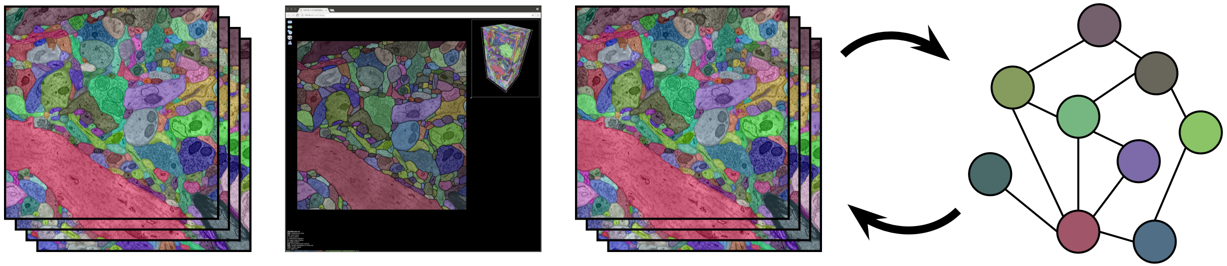

Skeleton Generation

Compression

Error Correction

Subgraph Enumeration

Segmentation

Proofreading

Network Analysis

Biologically-Constrained Graphs for Global Connectomics Reconstruction

Brian Matejek, Daniel Haehn, Haidong Zhu,
Donglai Wei, Toufiq Parag, and Hanspeter Pfister

IEEE Conference on Computer Vision and Pattern Recognition, 2019

Affinity Generation

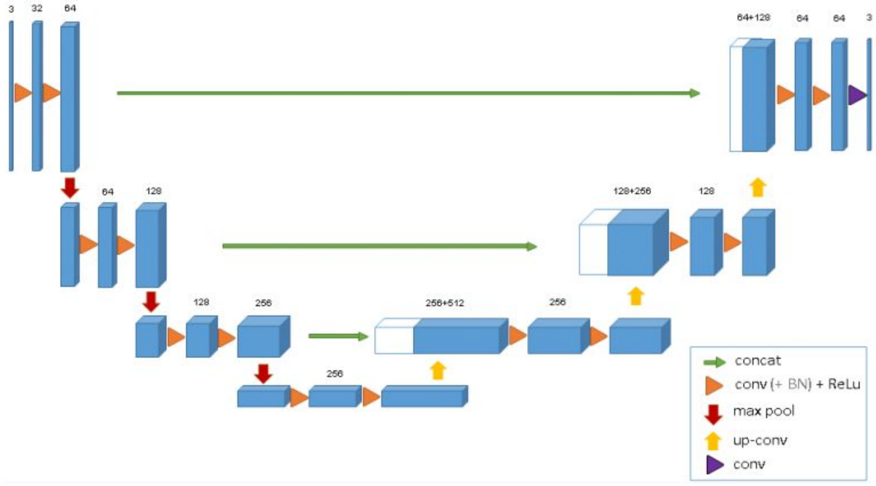

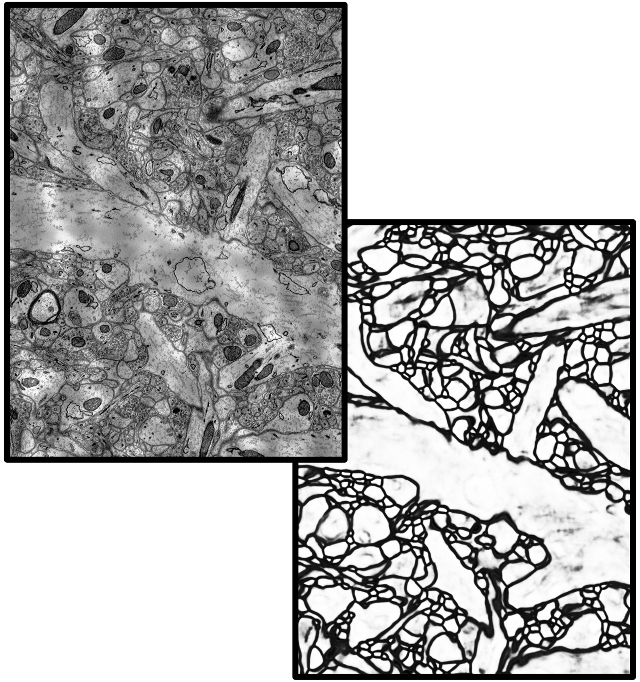

Ronneberger *et al.*, U-Net: Convolutional Networks for Biomedical Image Segmentation, MICCAI 2015
Cicek *et al.*, 3D U-Net: Learning Dense Volumetric Segmentation from Sparse Annotation, MICCAI 2016

3D Watershed on Affinities

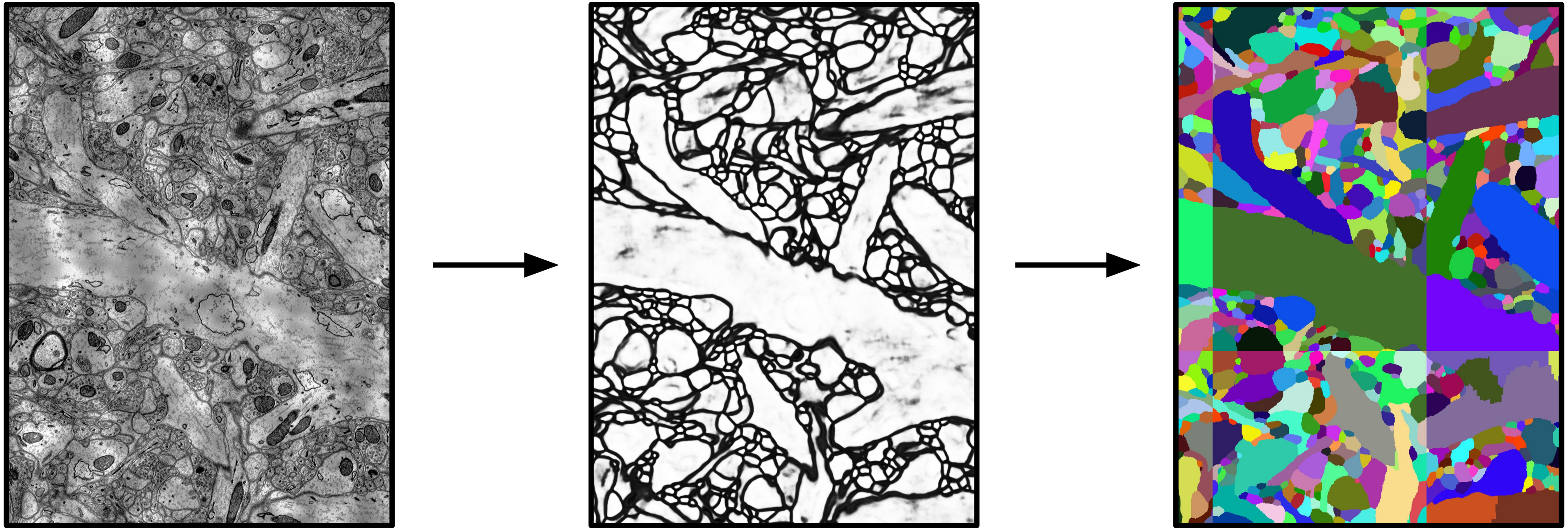

Zlateski *et al.*, Image Segmentation by Size-Dependent Single Linkage Clustering of a Watershed Basin Graph, 2015
Funke *et al.*, A Deep Structured Learning Approach Towards Automating Connectome Reconstruction from 3D Electron Micrographs, 2017
Zeng *et al.*, DeepEM3D: Approaching Human-Level Performance on 3D Anisotropic EM Image Segmentation, Bioinformatics 2017

Agglomeration

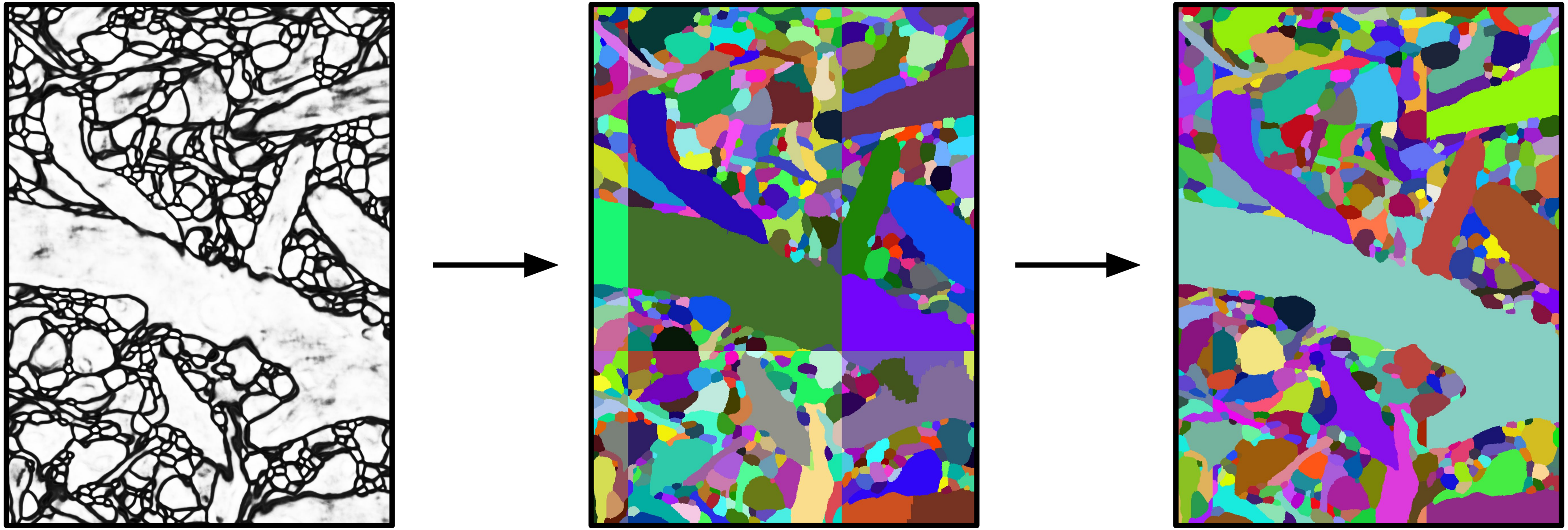

Nunez-Iglesias *et al.*, Machine Learning of Hierarchical Clustering to Segment 2D and 3D Images, PLoS ONE, 2013
Parag *et al.*, A Context-Aware Delayed Agglomeration Framework for Electron Microscopy Segmentation, PLoS ONE 2015
Funke *et al.*, A Deep Structured Learning Approach Towards Automating Connectome Reconstruction from 3D Electron Micrographs, 2017

Lifted Multicuts

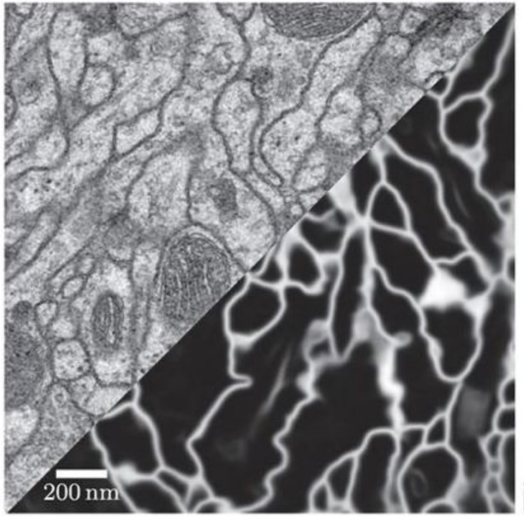

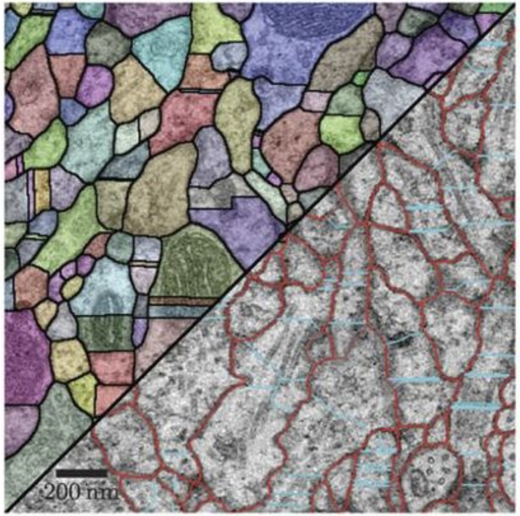

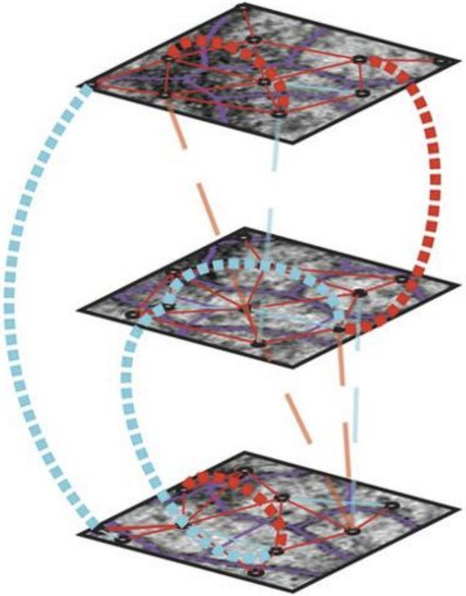

Beier *et al.*, Multicut Brings Automated Neurite Segmentation Closer to Human Performance, Nature 2017

Errors

Automatic Segmentation

Ground Truth

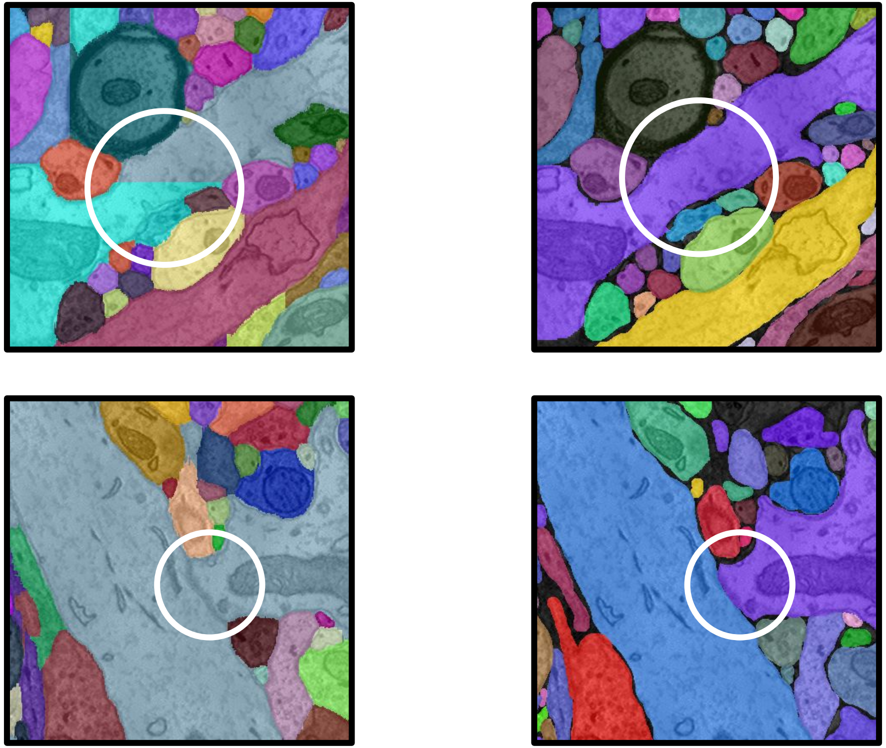

Guided Proofreading

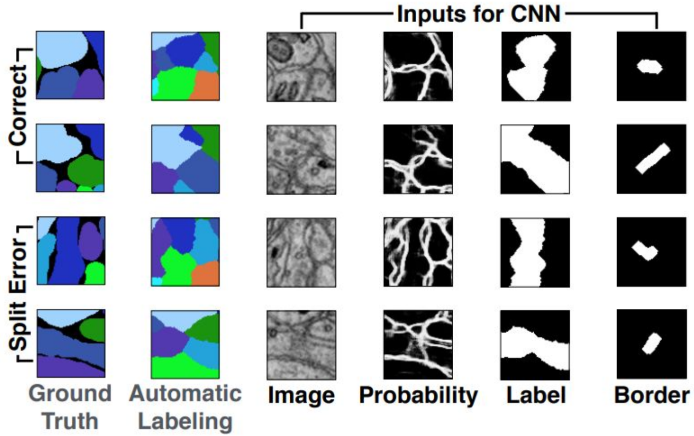

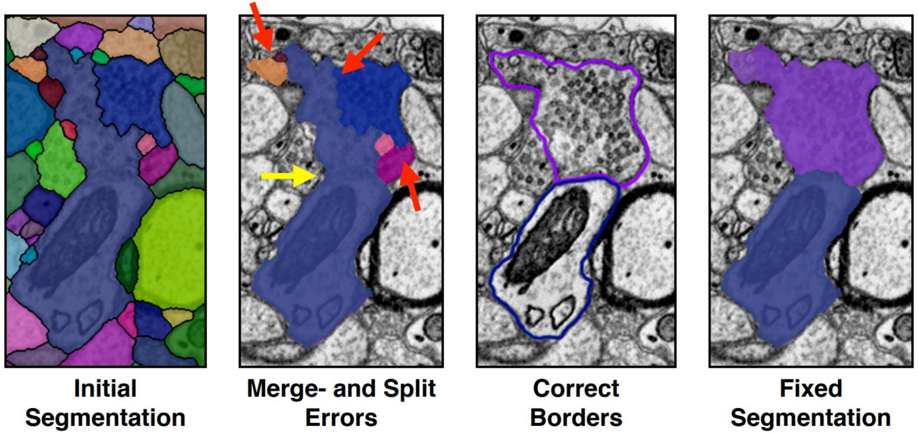

Haehn *et al.*, Guided Proofreading of Automatic Segmentations for Connectomics, CVPR 2018

Automatic Proofreading

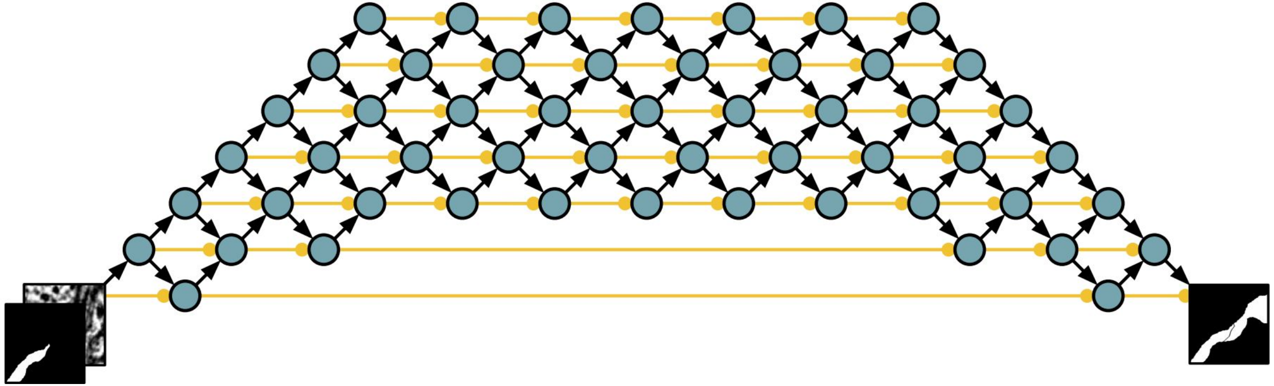

Zung *et al.*, An Error Detection and Correction Framework for Connectomics, NIPS 2017

Proposed Automatic Error Correction

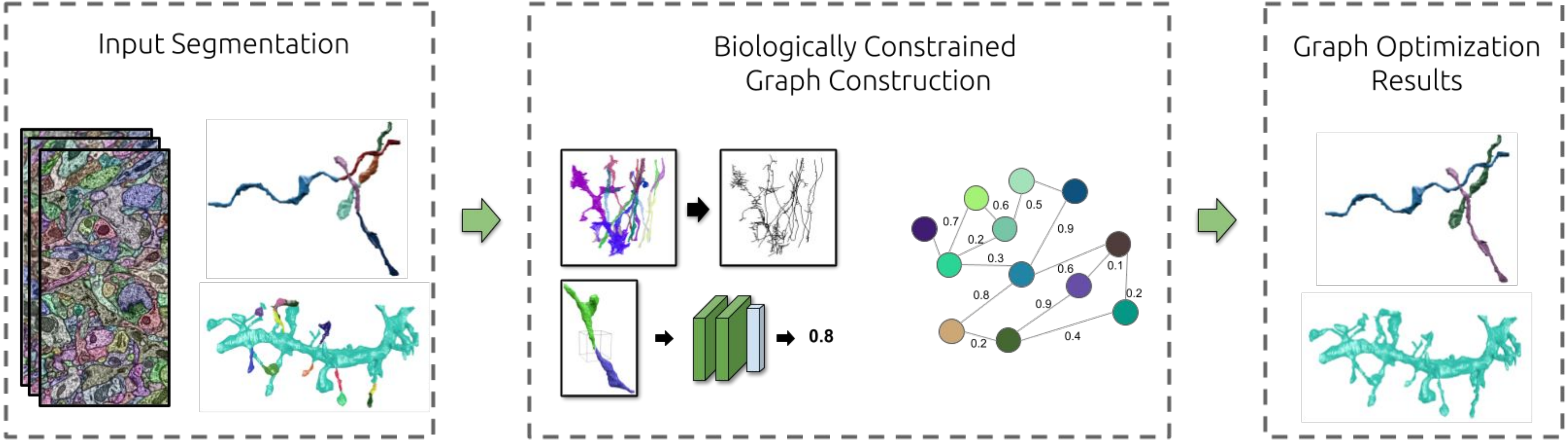

Input Segmentation

Biologically Constrained Graph Construction

Graph Optimization Results

Input

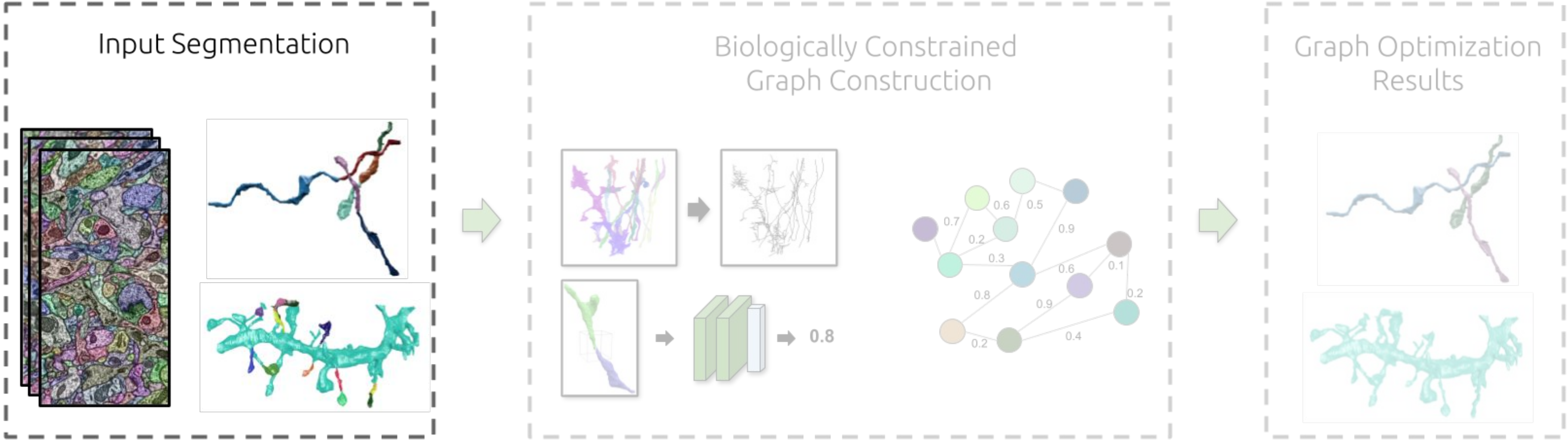

Input Segmentation

Biologically Constrained Graph Construction

Graph Optimization Results

Traditional Two-Stage Frameworks

Existing segmentation strategies typically produce over-segmentations

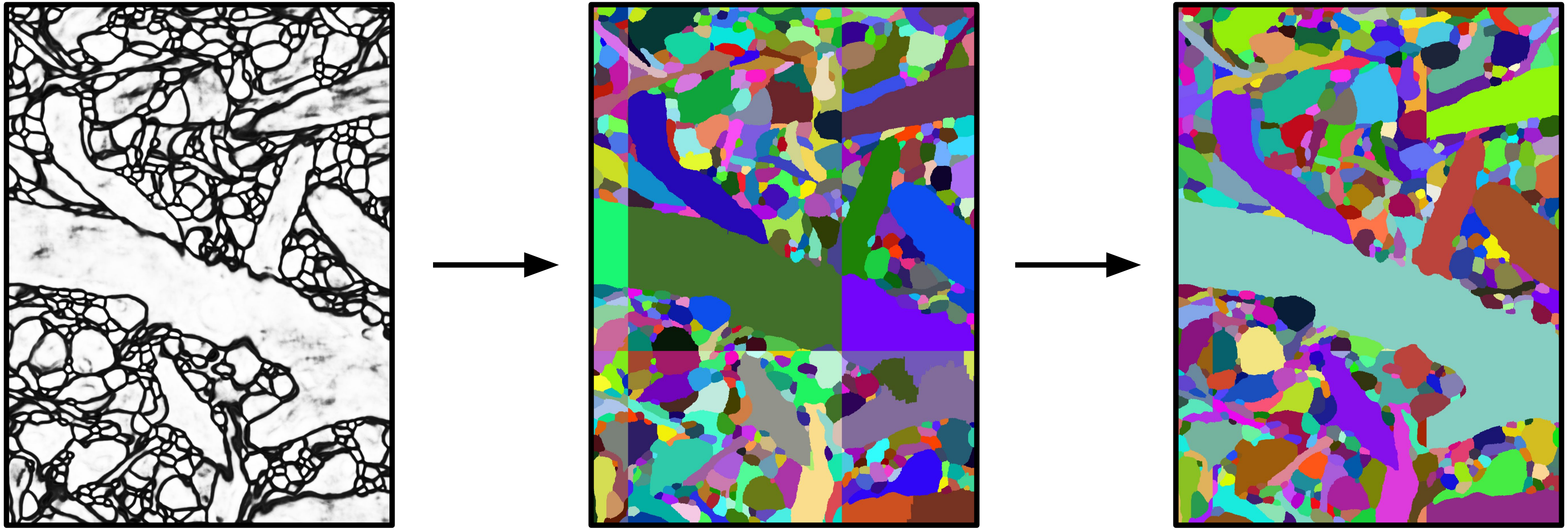

Affinity Generation

Watershed Transform

Agglomeration

Traditional Two-Stage Frameworks

Existing segmentation strategies typically produce over-segmentations

We use the result from an existing strategy as our input

Traditional Two-Stage Frameworks

Existing segmentation strategies typically produce over-segmentations

We use the result from an existing strategy as our input

- Allows us to leverage larger local context when forming our graph

Goal: Construct a graph with as few nodes and edges as possible

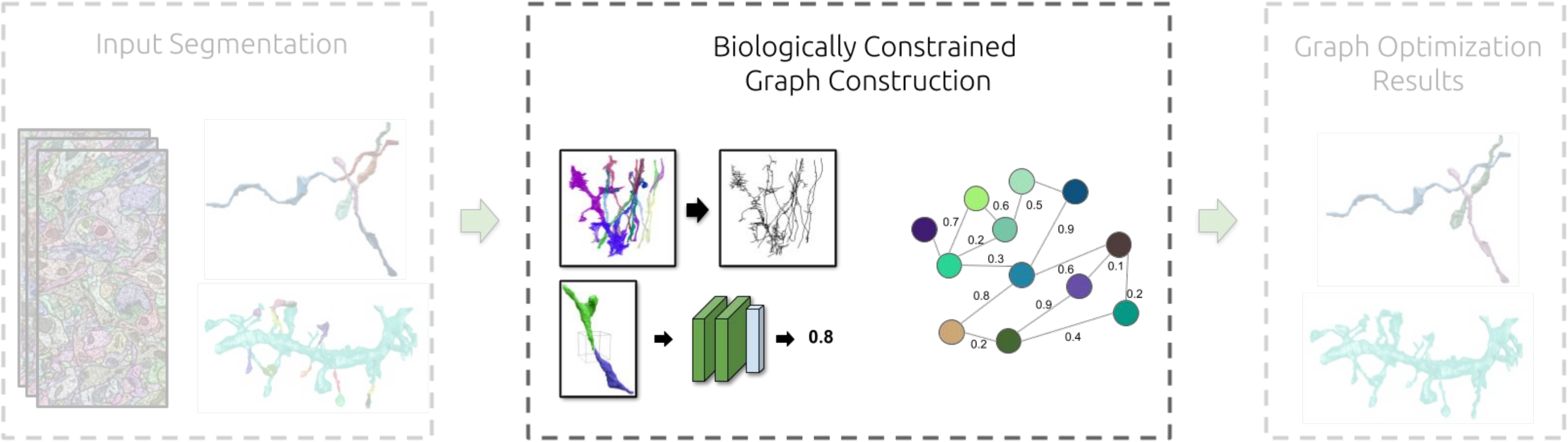

Input Segmentation

Biologically Constrained
Graph Construction

Graph Optimization
Results

Graph Construction with Biological Constraints

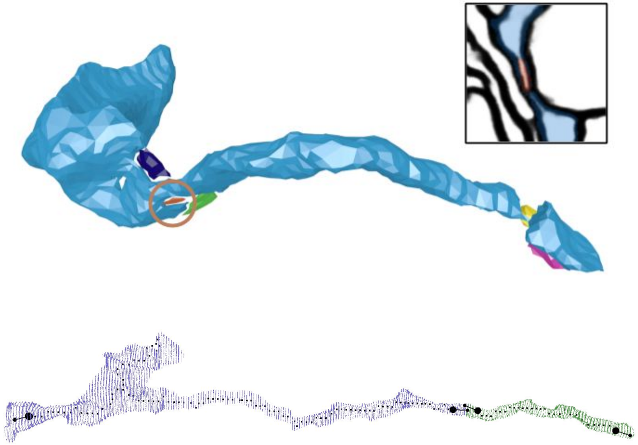

Hand-Designed
Geometric Constraints

Graph Construction with Biological Constraints

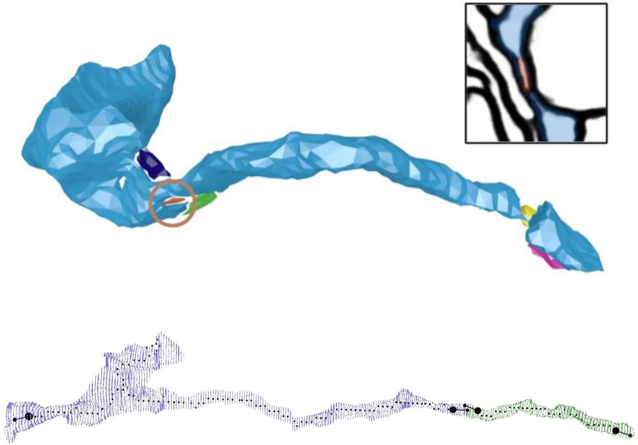

Hand-Designed
Geometric Constraints

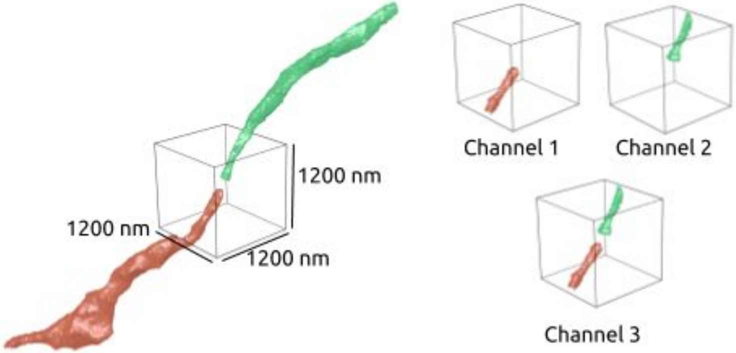

Machine-Learned
Morphologies

Node Generation

Existing segmentation strategies produce a large number of small segments

Node Generation

Existing segmentation strategies produce a large number of small segments

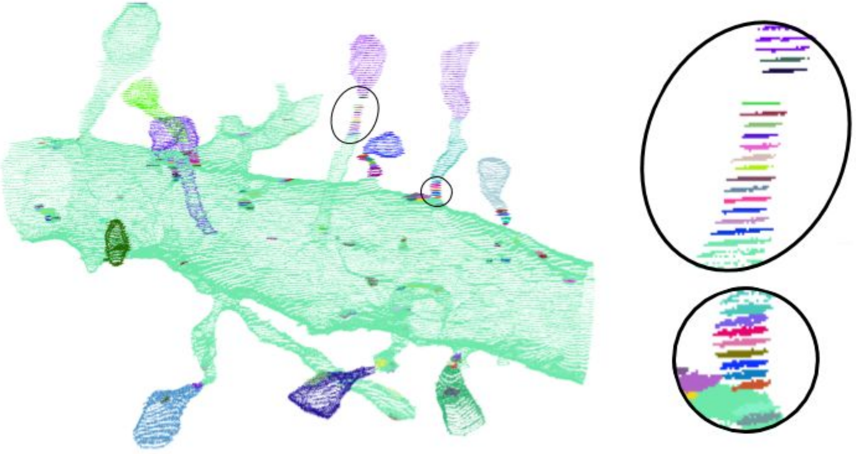

Singleton Slices

Node Generation

Existing segmentation strategies produce a large number of small segments

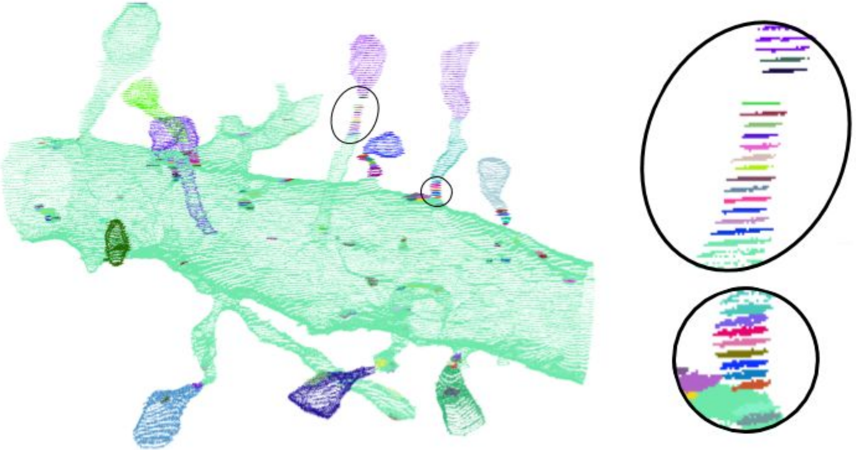

Singleton Slices

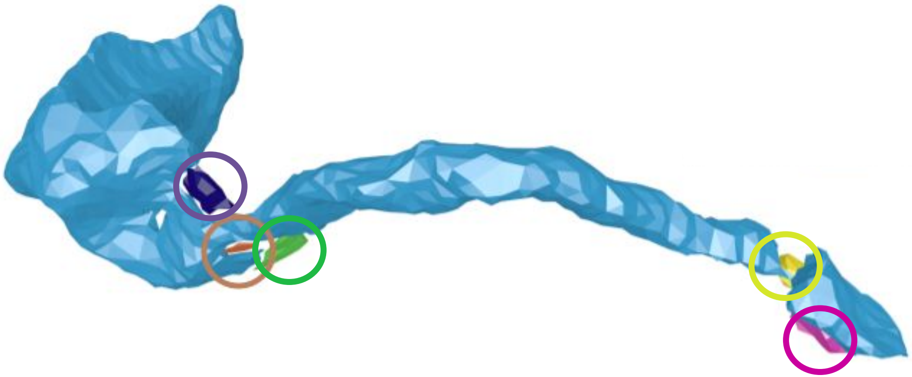

5 Small Segments

Singleton Removal

Merge adjacent singleton slices that have an Intersection-over-Union above 0.30

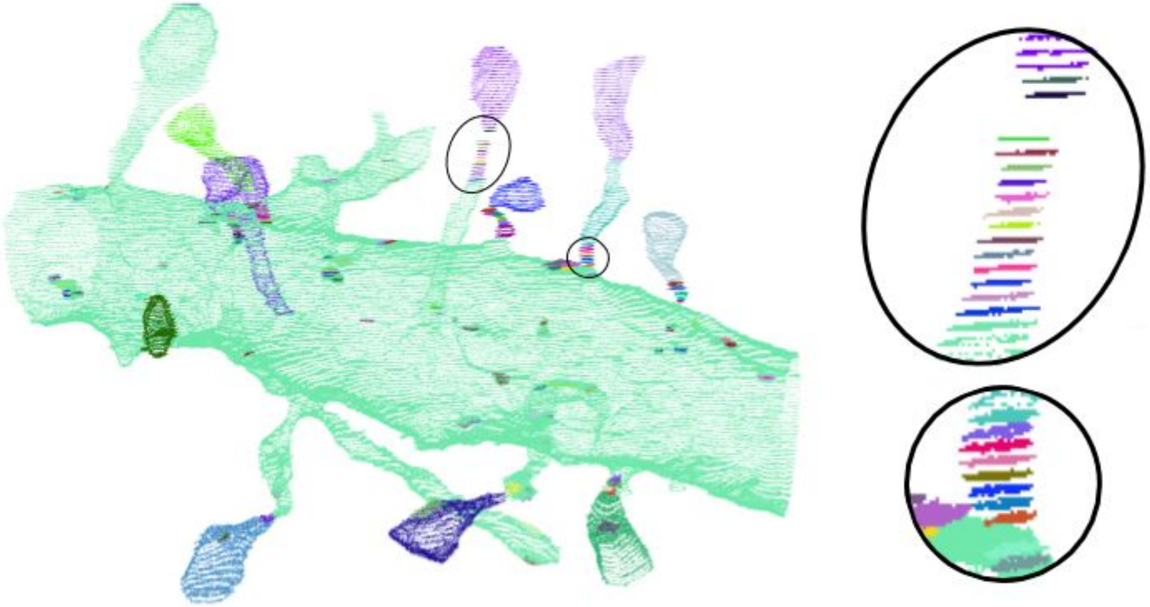

Merging Other Small Segments

Up to 80% of remaining segments are very small with little shape information

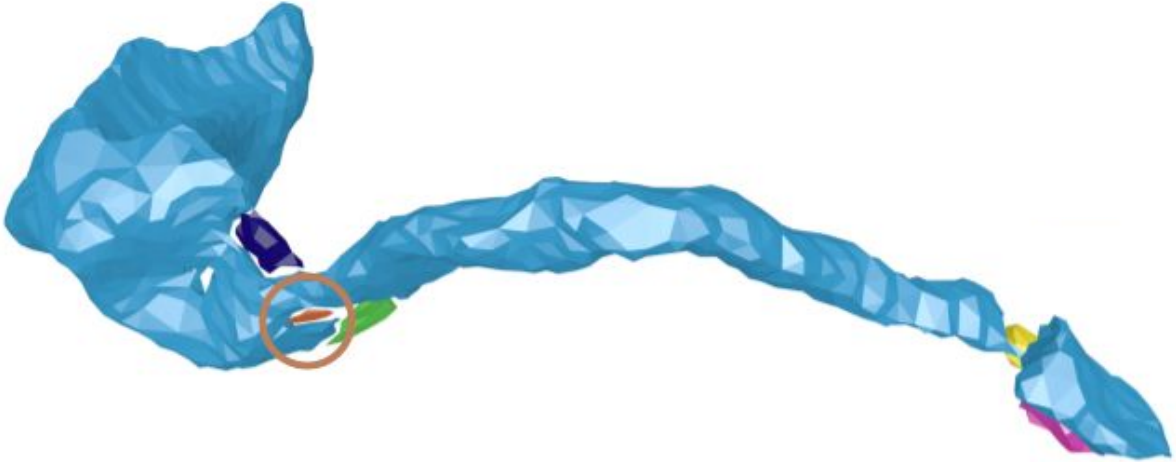

Merging Other Small Segments

Up to 80% of remaining segments are very small with little shape information

These small segments often occur at narrow locations with noisy affinities

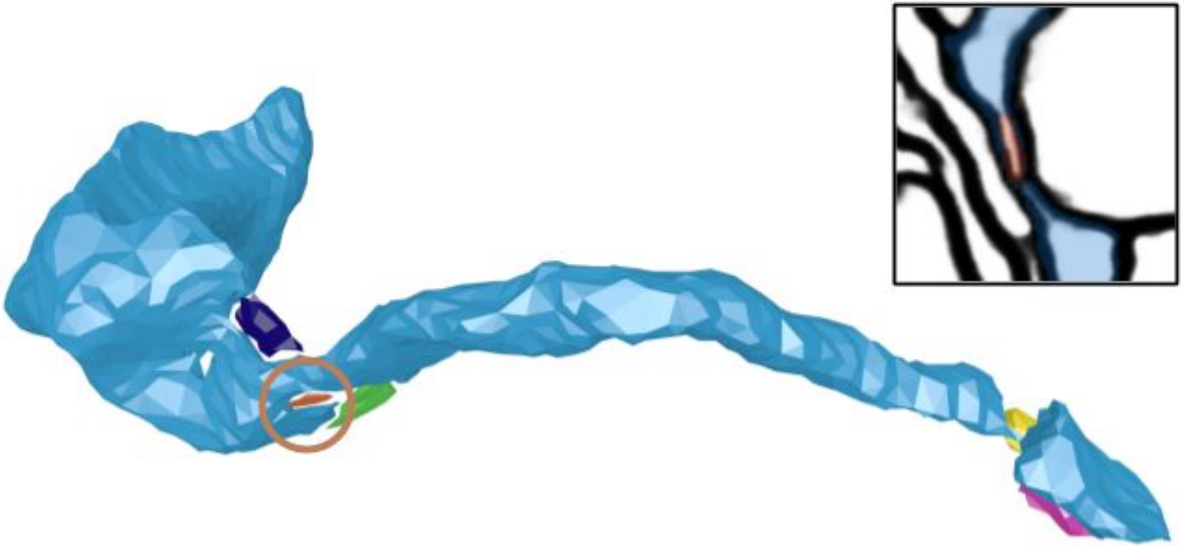

Small Segment Merging

Each small segment is merged with a nearby large segment

Small Segment Merging

Each small segment is merged with a nearby large segment

A 3D CNN predicts the most likely neighbor to belong to the same neuronal process

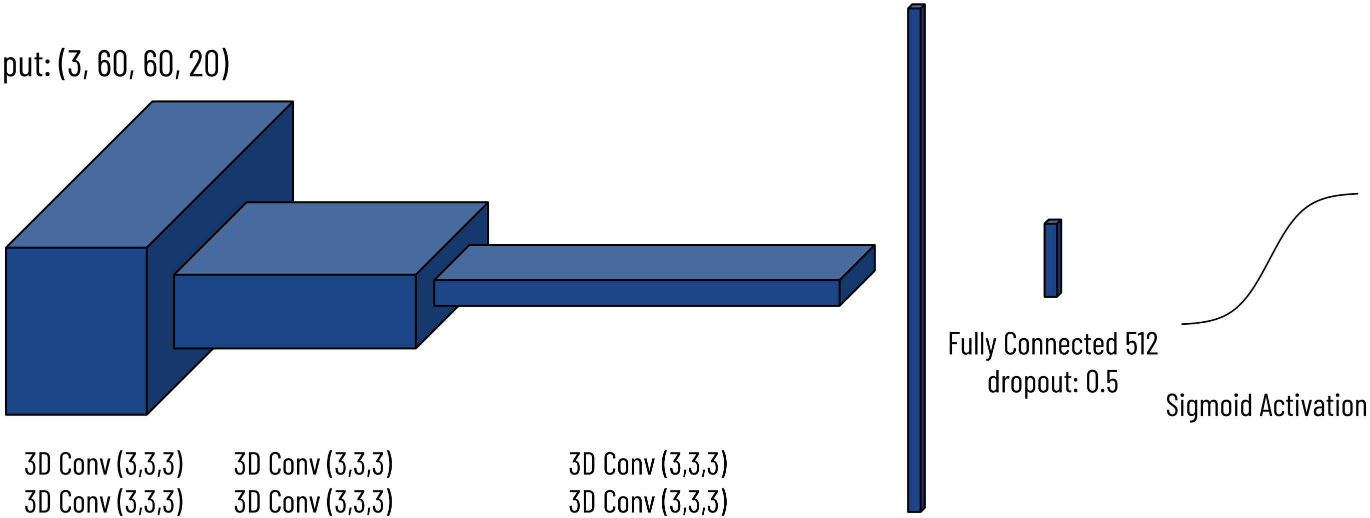

Input: (3, 60, 60, 20)

3D Conv (3,3,3)
3D Conv (3,3,3)
3D Pool (2,2,1)
16 filters
dropout: 0.2

3D Conv (3,3,3)
3D Conv (3,3,3)
3D Pool (2,2,1)
32 filters
dropout: 0.2

3D Conv (3,3,3)
3D Conv (3,3,3)
3D Pool (2,2,2)
64 filters
dropout: 0.2

Flatten
4,096

Fully Connected 512
dropout: 0.5

Sigmoid Activation

Edge Generation

Each segment has too many adjacent neighbors to use the adjacency matrix

Edge Generation

Each segment has too many adjacent neighbors to use the adjacency matrix

Typical Segment

Edge Generation

Each segment has too many adjacent neighbors to use the adjacency matrix

Typical Segment

103 Adjacent Neighbors

Handcrafted Geometric Constraints

Use directional information to identify potential split error locations

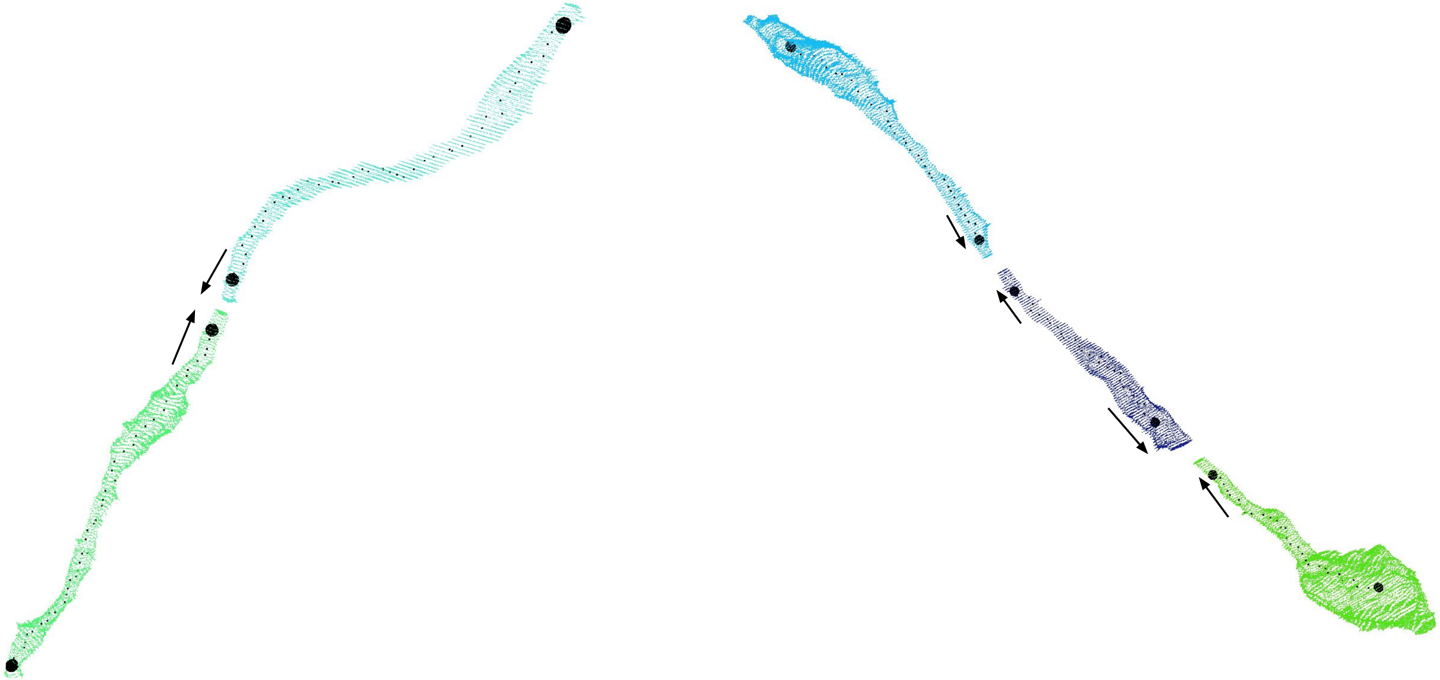

Skeleton Generation

Approximate volume shapes with 1D skeletons and identify potential split errors based on skeletal geometry around the endpoints

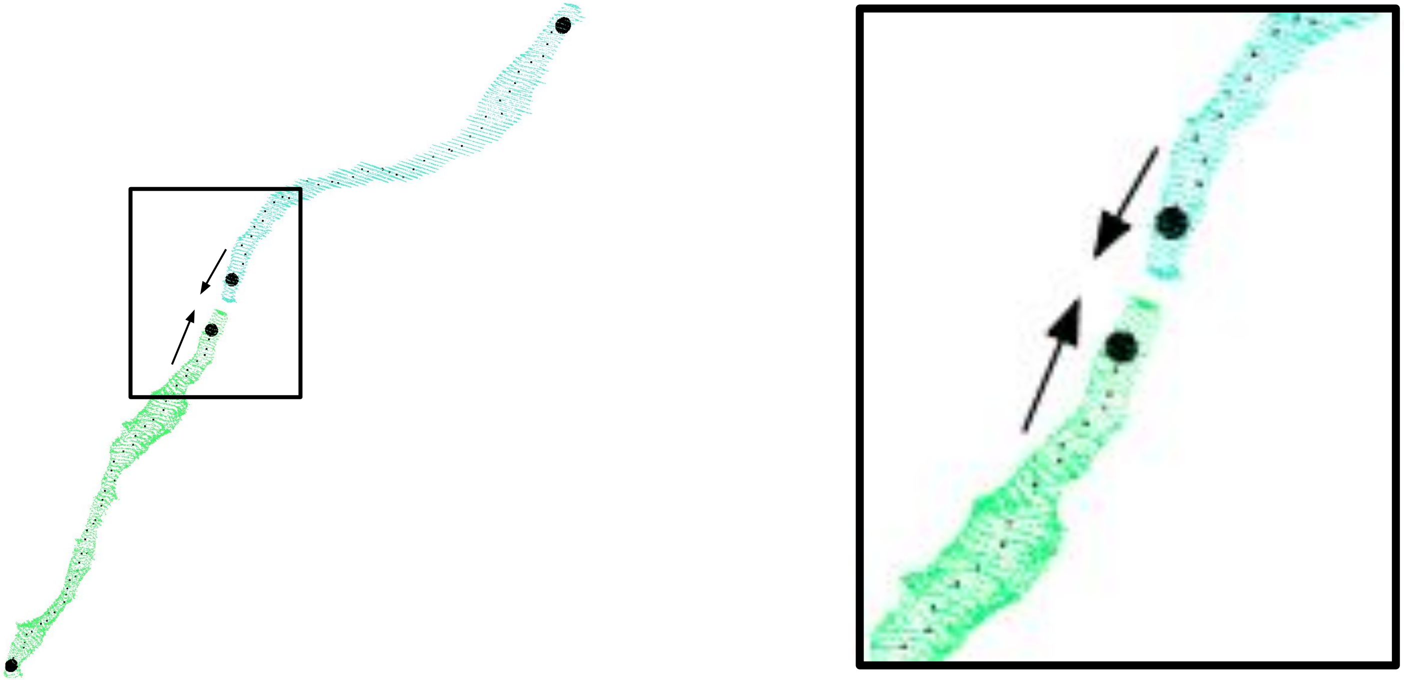

Edge Generation

Two nodes receive an edge in the graph if one of the corresponding skeletons has an endpoint vector towards the other segment

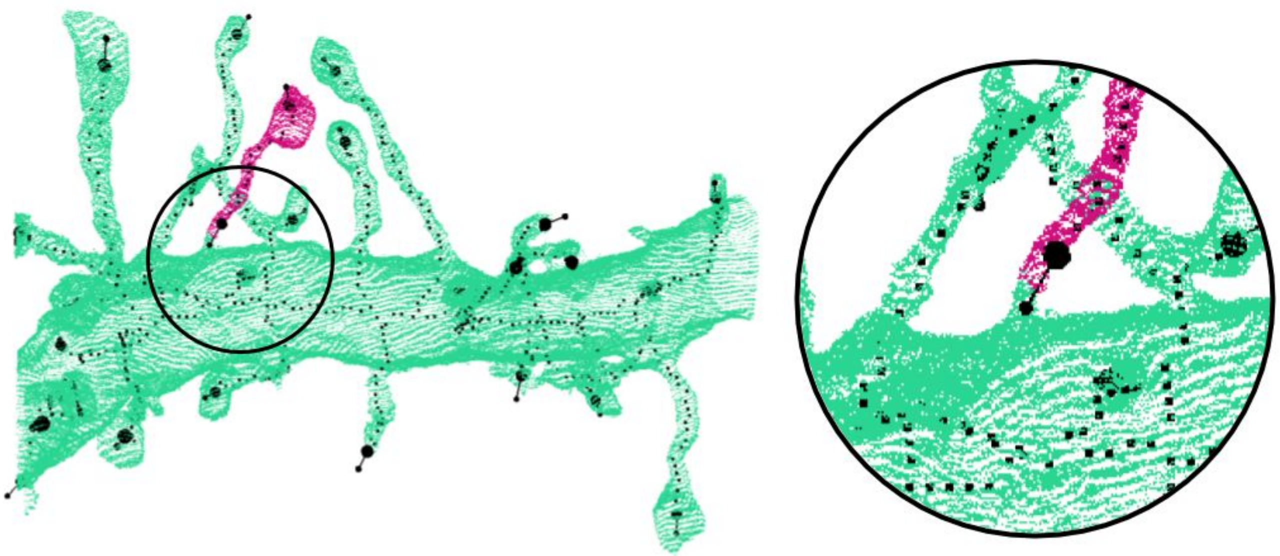

Generating Edge Weights with Machine-learned Morphologies

We train a convolutional neural network to predict if two segments belong to the same neuronal process

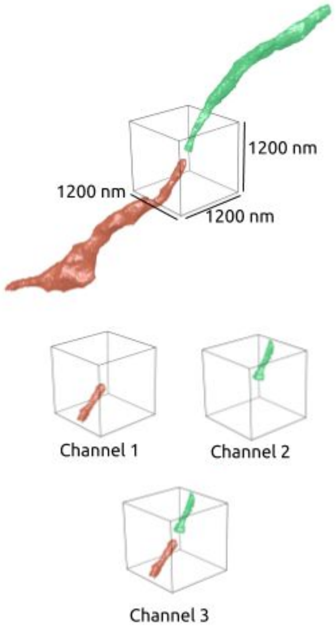

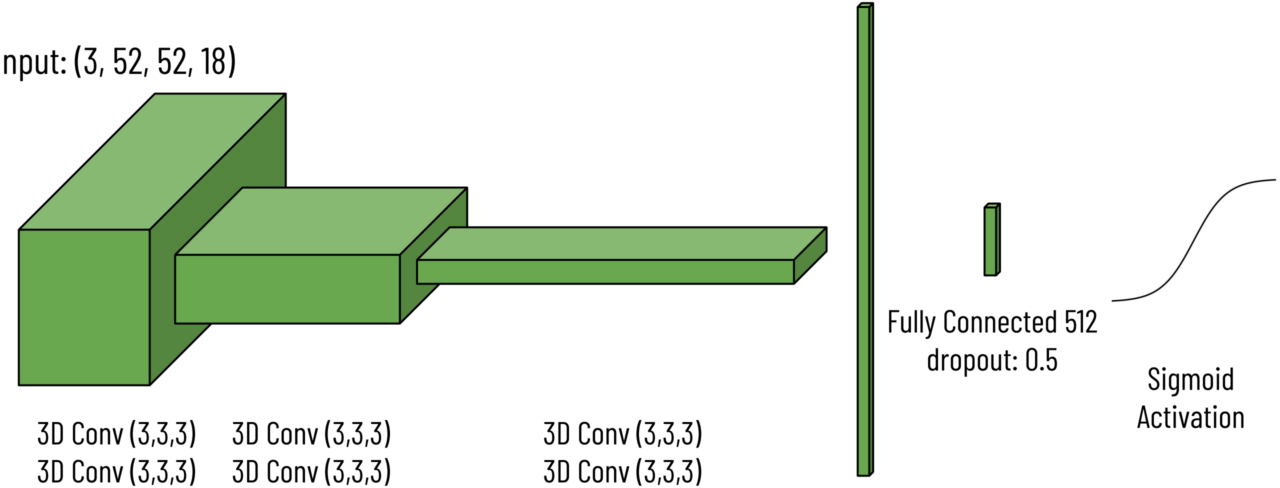

Input: (3, 52, 52, 18)

3D Conv (3,3,3)
3D Conv (3,3,3)
3D Pool (2,2,1)
16 filters
dropout: 0.2

3D Conv (3,3,3)
3D Conv (3,3,3)
3D Pool (2,2,1)
32 filters
dropout: 0.2

3D Conv (3,3,3)
3D Conv (3,3,3)
3D Pool (2,2,2)
64 filters
dropout: 0.2

Flatten
1,728

Fully Connected 512
dropout: 0.5

Sigmoid
Activation

Input Examples

Should Merge

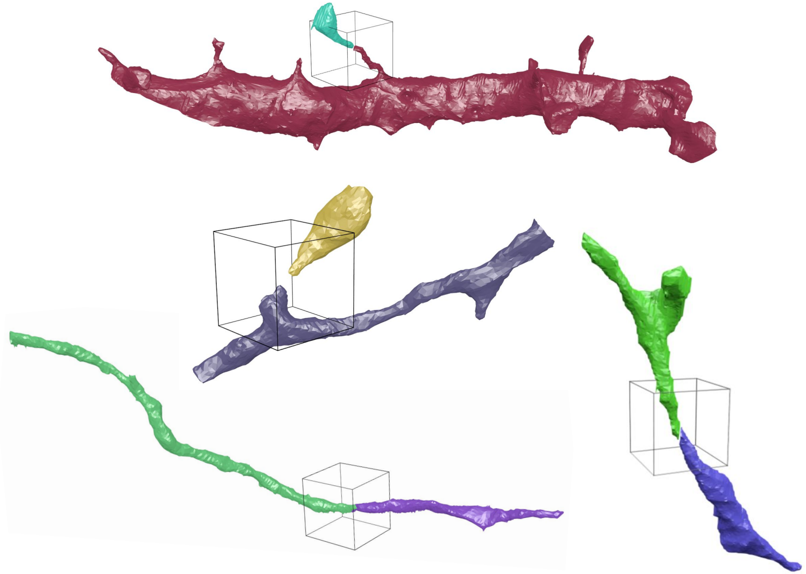

Input Examples

Should Merge

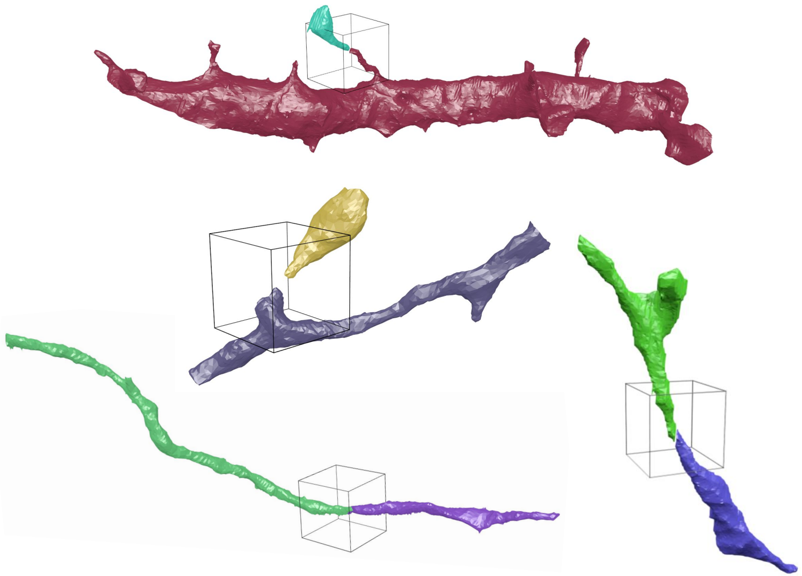

Should Not Merge

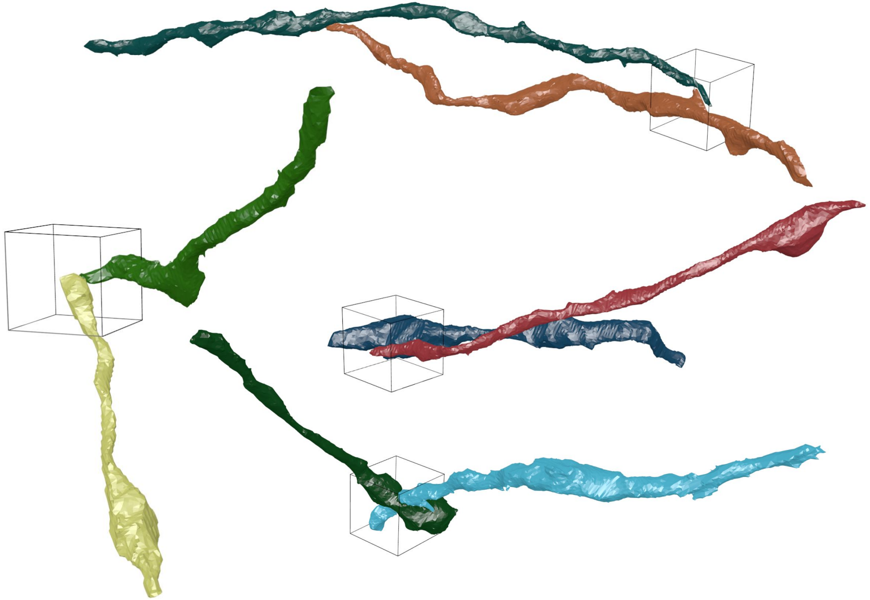

Goal: Partition graph into neuronal processes

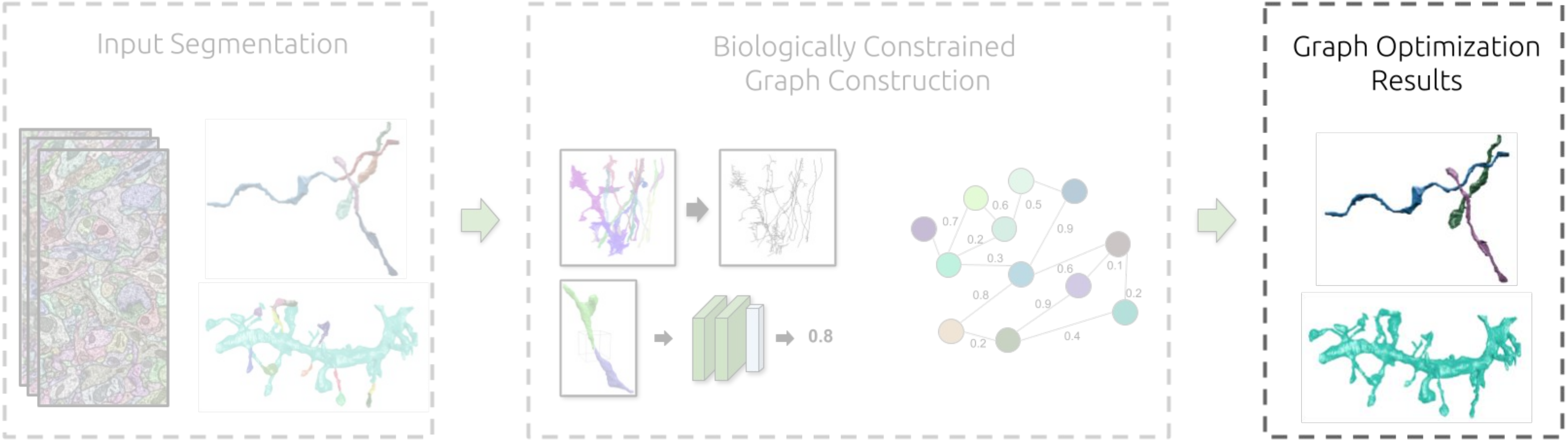

Input Segmentation

Biologically Constrained Graph Construction

Graph Optimization Results

Multicut

Reformulate the segmentation problem as a multicut graph partitioning one

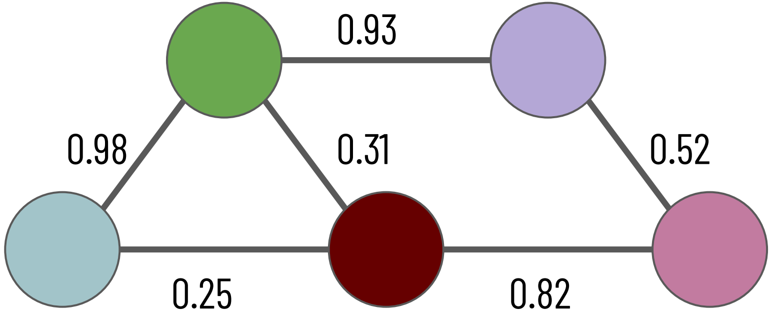

Multicut

Reformulate the segmentation problem as a multicut graph partitioning one

- The final number of segments is not predetermined

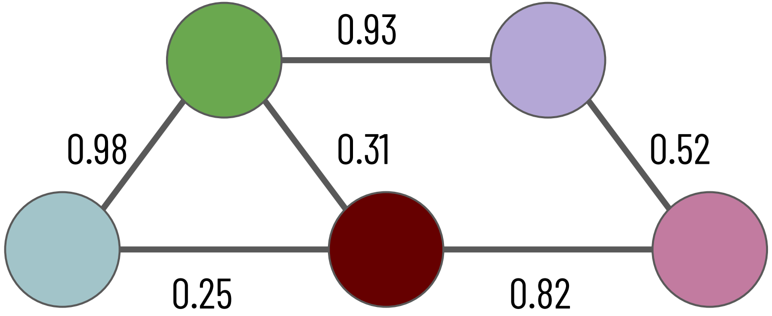

Multicut

Reformulate the segmentation problem as a multicut graph partitioning one

- The final number of segments is not predetermined
- Guarantees a globally consistent solution

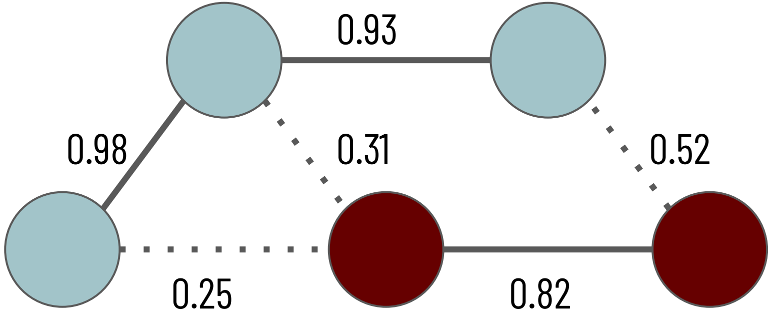

Datasets

Kasthuri

Princeton Neuroscience Institute

SNEMI3D

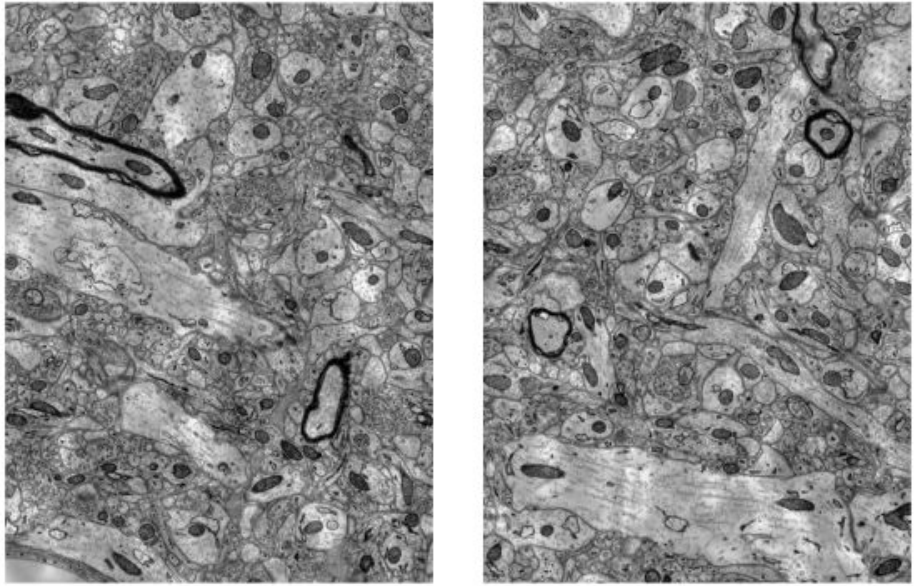

2 Volumes

6 x 6 x 30 nm^3 / vx

1335 x 1809 x 338 vx

8.01 x 10.85 x 10.14 μm^3

Datasets

Kasthuri

Princeton Neuroscience Institute

SNEMI3D

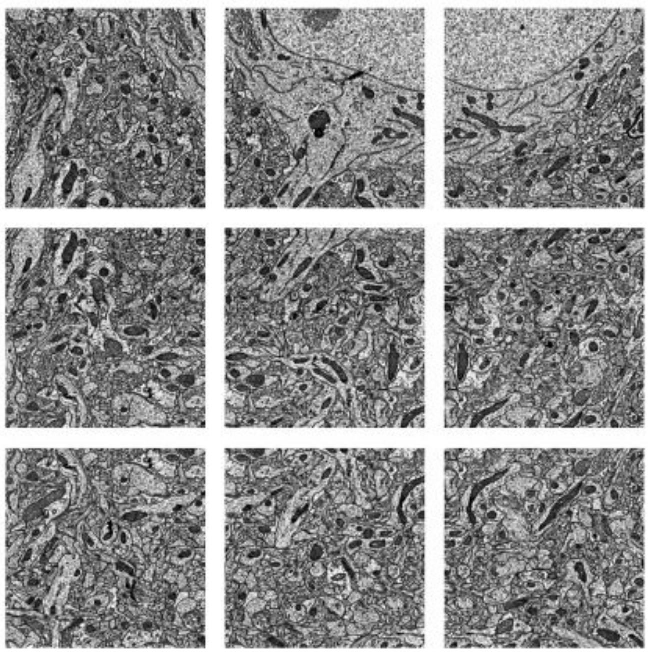

9 Volumes

$3.6 \times 3.6 \times 40\ nm^3$ / vx

2048 x 2048 x 256 vx

$7.37 \times 7.37 \times 10.24\ \mu m^3$

Datasets

Kasthuri

Princeton Neuroscience Institute

SNEMI3D

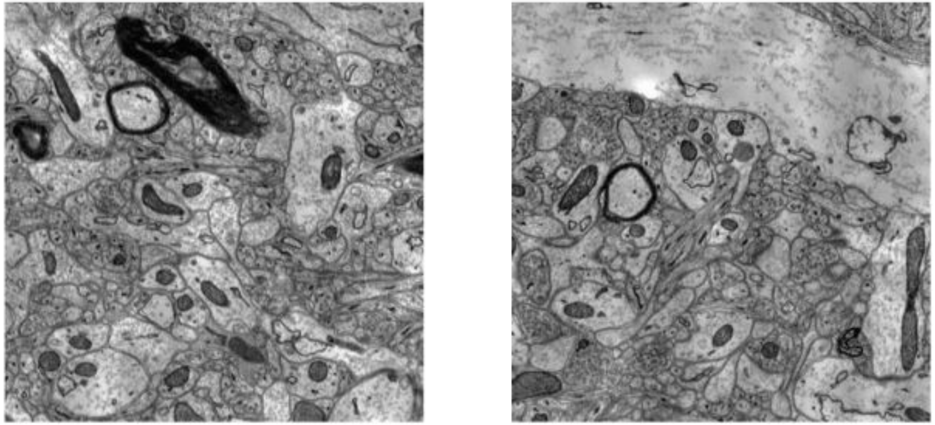

2 Volumes

3 x 3 x 30 nm^3 / vx

1024 x 1024 x 100 vx

3.07 x 3.07 x 3 μm^3

Input Segmentations

For the two PNI Test datasets, we use zwatershed and mean agglomeration

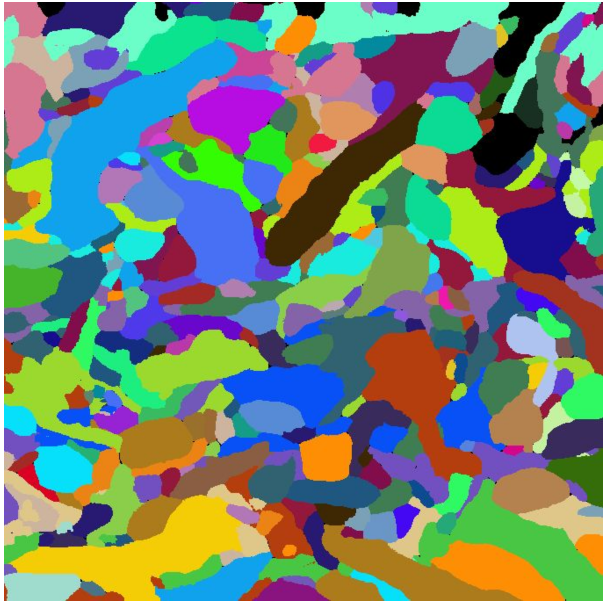

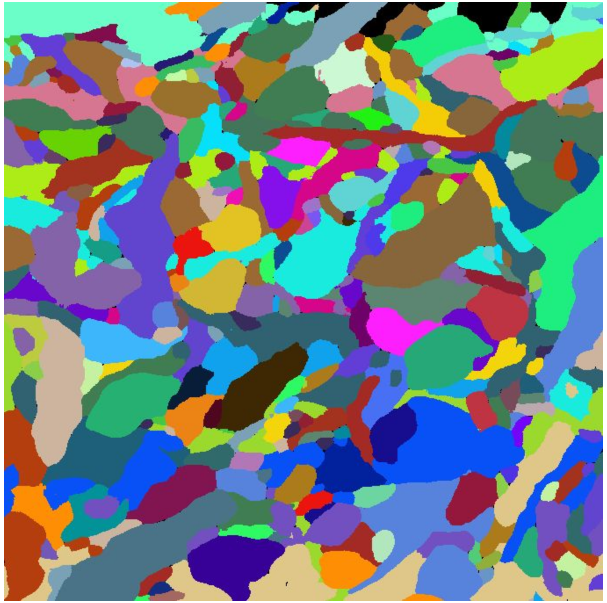

Input Segmentations

For the Kasthuri and SNEMI3D datasets, we use the waterz agglomeration strategy

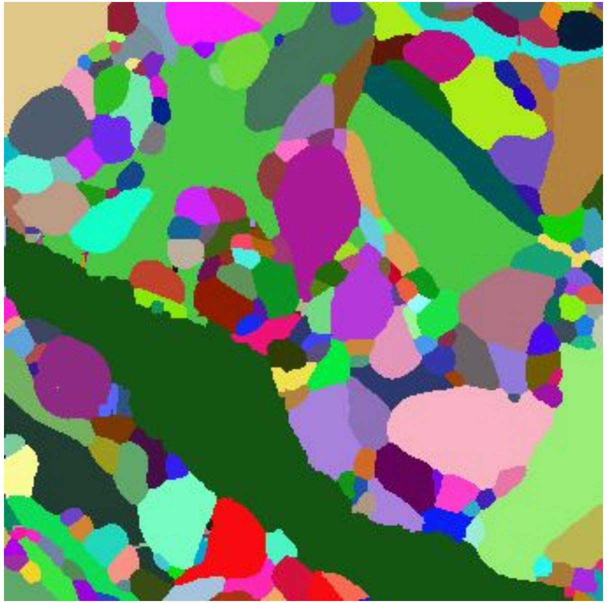

Split Variation of Information

Measure of entropy between segmentation and ground truth

Split Variation of Information

Measure of entropy between segmentation and ground truth

- VI Split: Increases if two voxels from the same neuron have different labels

Split Variation of Information

Measure of entropy between segmentation and ground truth

VI Split: Increases if two voxels from the same neuron have different labels

VI Merge: Increases if two voxels from different neurons have the same label

Split Variation of Information

Measure of entropy between segmentation and ground truth

VI Split: Increases if two voxels from the same neuron have different labels

Segmentation

Ground Truth

VI Merge: Increases if two voxels from different neurons have the same label

Segmentation

Ground Truth

Total Variation of Information = VI Split + VI Merge

Variation of Information

Dataset	**Baseline (↓)**	**Proposed (↓)**	**Decrease (↑)**
PNI Test One	0.491	0.388	-20.9%
PNI Test Two	0.416	0.297	-28.7%
Kasthuri Test	0.965	0.815	-15.6%
SNEMI3D	0.807	0.647	-19.8%

Variation of Information

Dataset	**Baseline (↓)**	**Proposed (↓)**	**Decrease (↑)**
PNI Test One	0.491	0.388	-20.9%
PNI Test Two	0.416	0.297	-28.7%
Kasthuri Test	0.965	0.815	-15.6%
SNEMI3D	0.807	0.647	-19.8%

Average decrease of Variation of Information by 21.3% over the four datasets

Qualitative Results

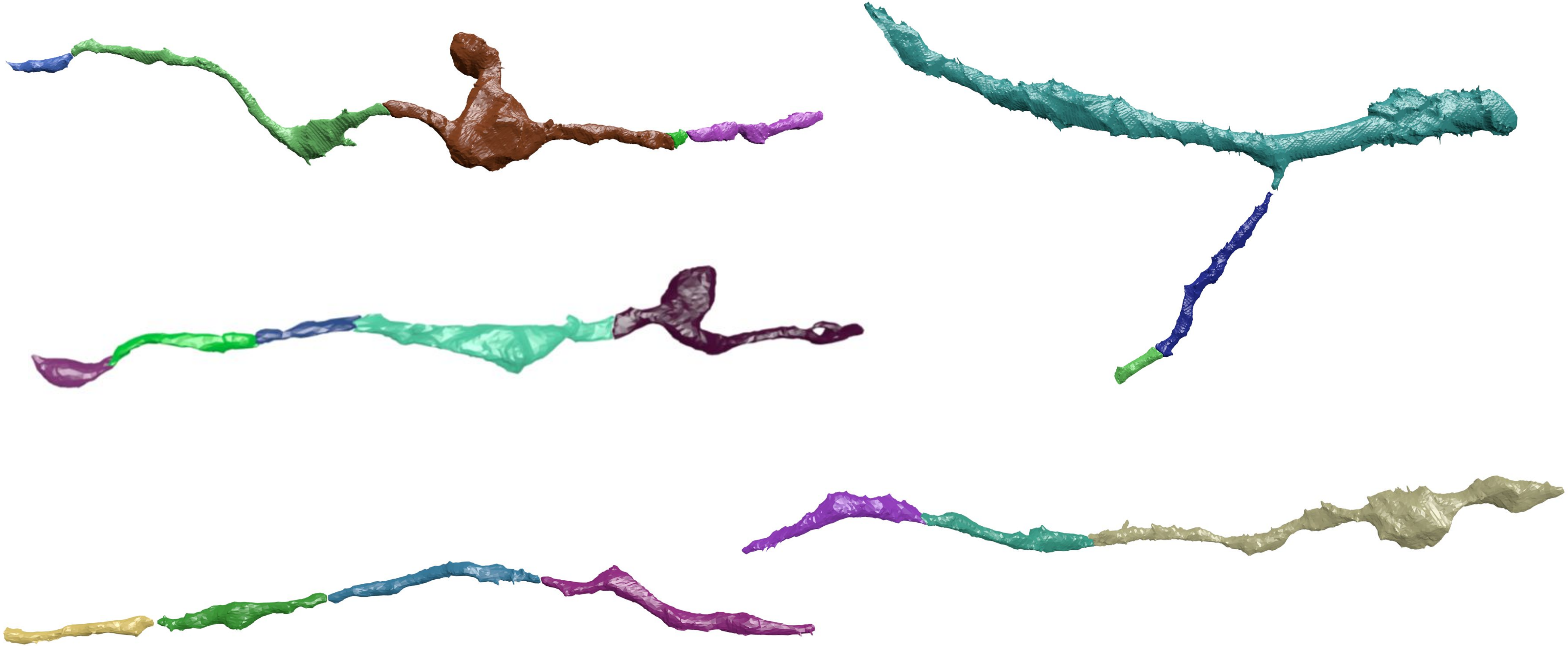

Qualitative Results

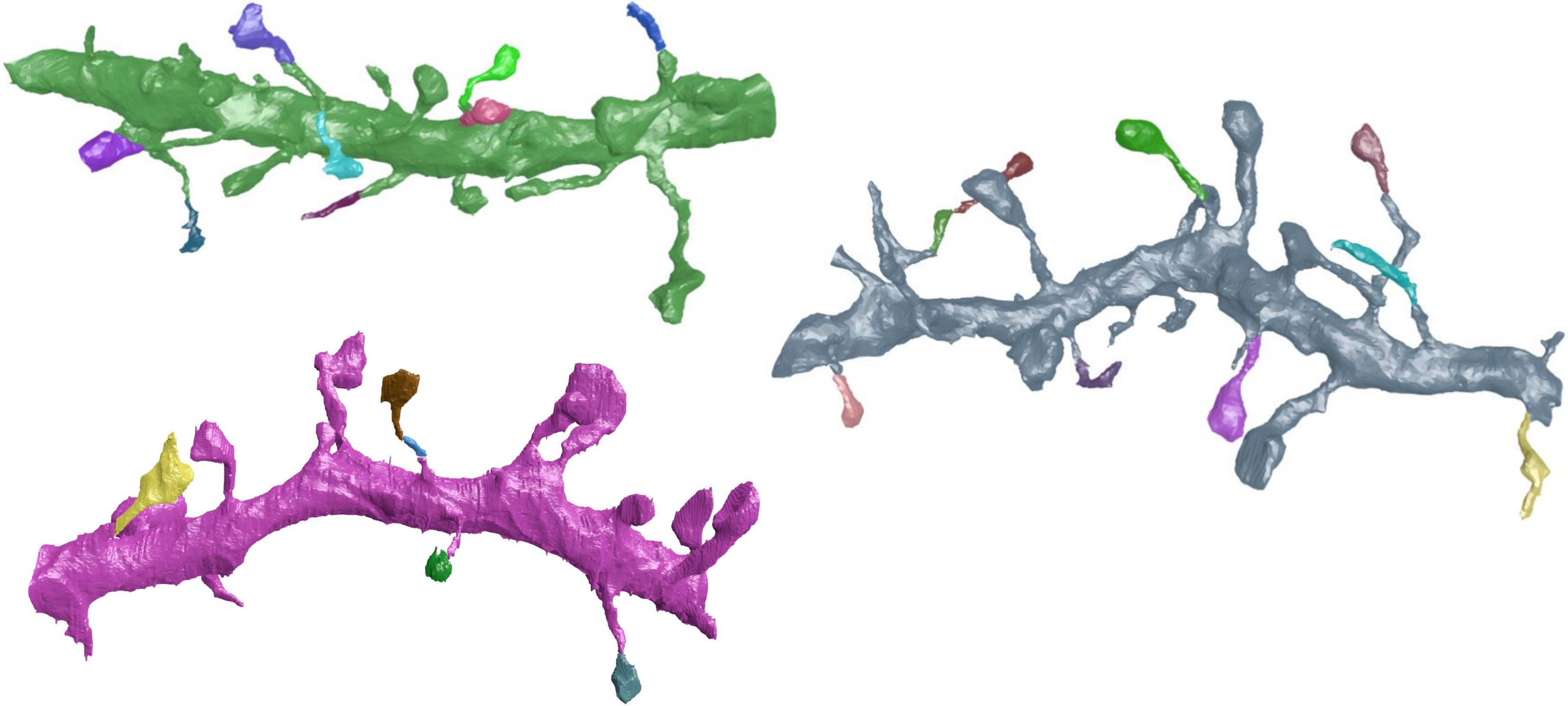

Failure Cases

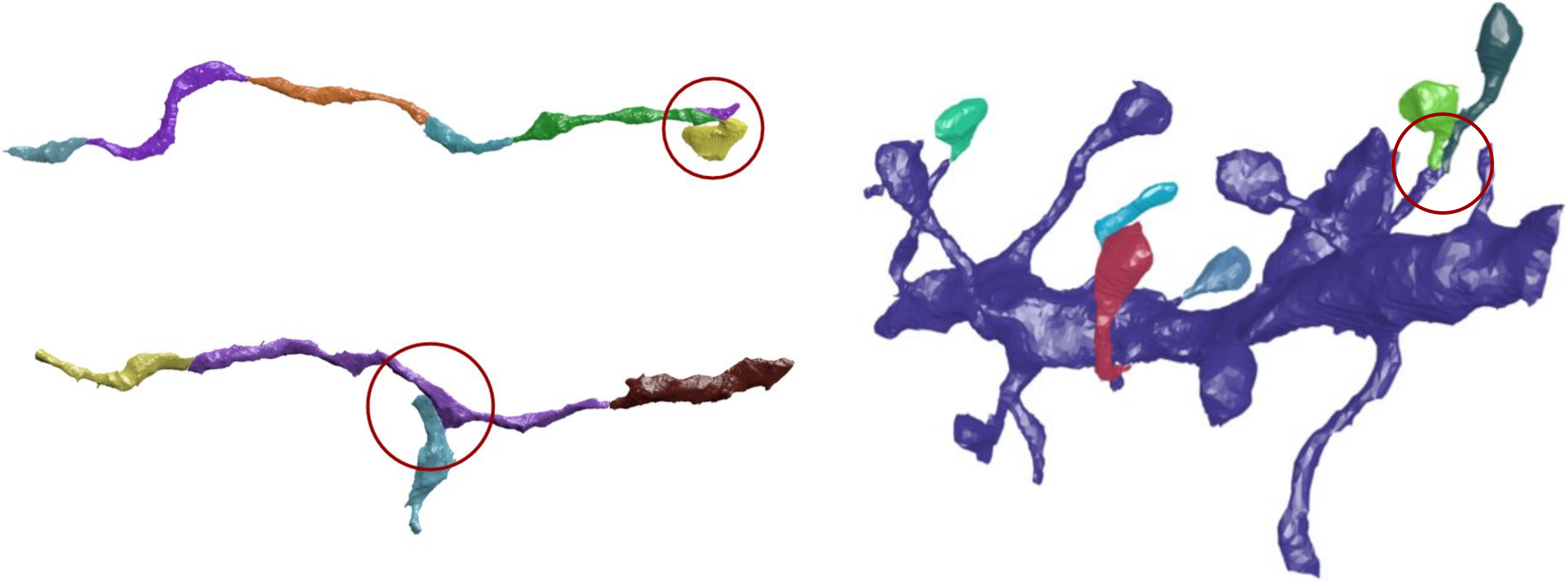

Failure Cases

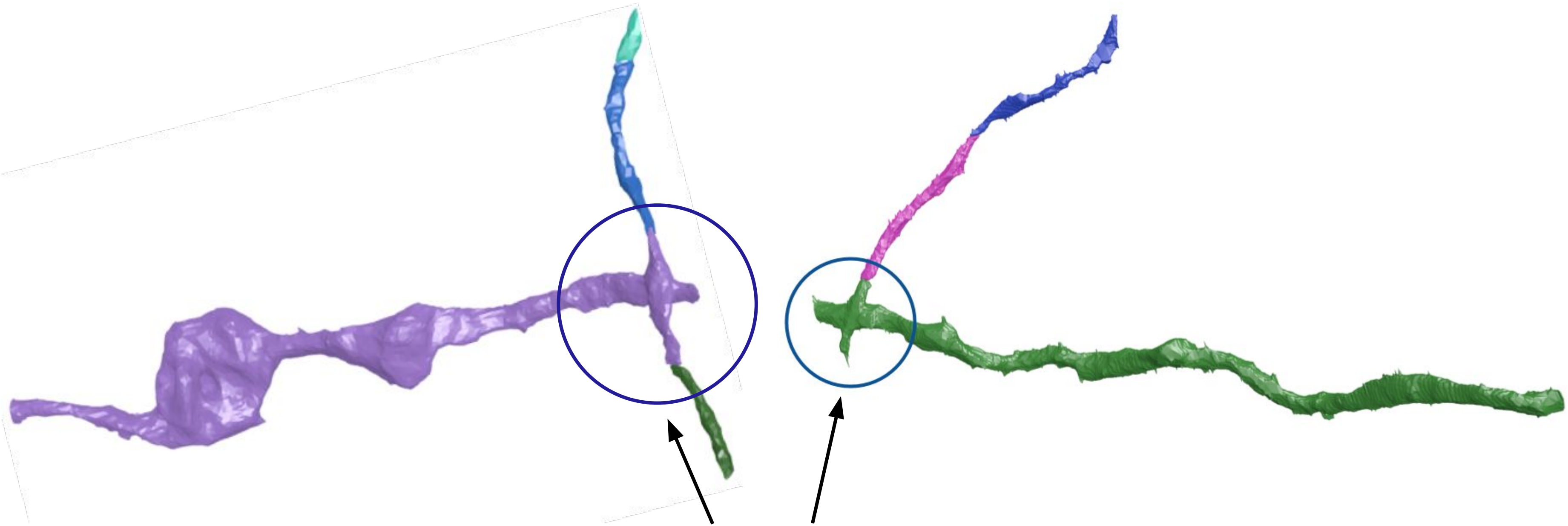

Errors in Input Segmentation

Ablation Studies: Node Generation

Goal: Merge all small segments with a nearby larger segment from the same neuronal process

Ablation Studies: Node Generation

Goal: Merge all small segments with a nearby larger segment from the same neuronal process

Baseline: How many small segments belong to the same neuron as the high affinity large neighbor?

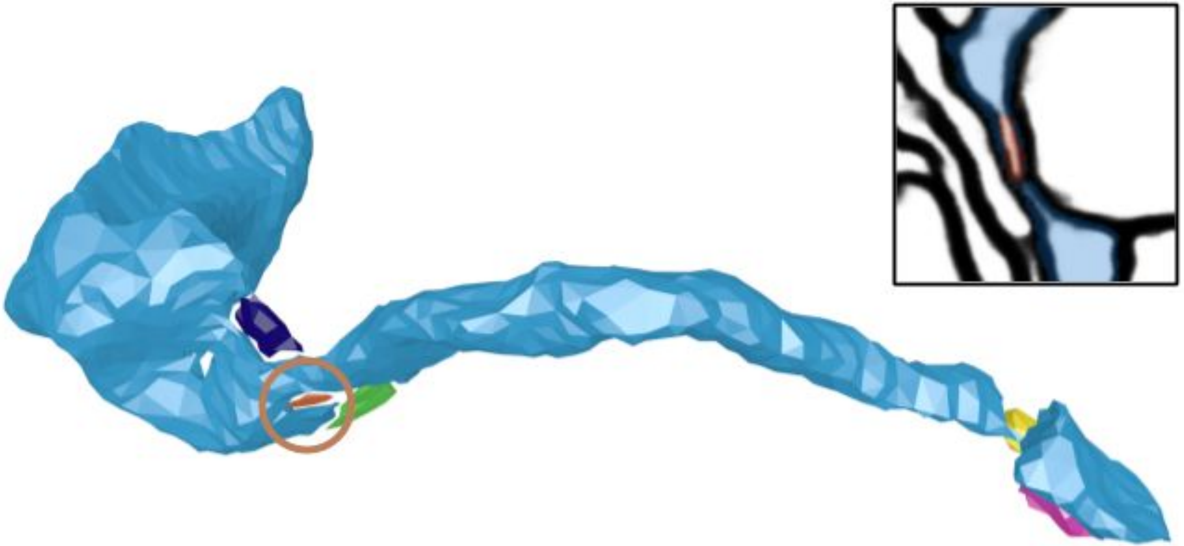

Ablation Studies: Node Generation

Goal: Merge all small segments with a nearby larger segment from the same neuronal process

Baseline: How many small segments belong to the same neuron as the high affinity large neighbor?

Dataset	**Baseline** (↑)	**Proposed** (↑)
PNI Test One	305/521 (36.9%)	686/129 (80.2%)
PNI Test Two	185/281 (39.7%)	444/75 (85.5%)
Kasthuri Test	4,514/8,604 (52.5%)	6,623/2,020 (76.6%)

The number of correctly merged small segments versus the number of incorrectly merged segments

Ablation Studies: Edge Generation

Goal: Identify all split errors while minimizing the number of total edges in the graph

Ablation Studies: Edge Generation

Goal: Identify all split errors while minimizing the number of total edges in the graph

Baseline: How many total edges are there in the adjacency graph?

Dataset	**Baseline**	**Proposed**	**Edge Recall** (↑/↓)
PNI Test One	528 / 25,619	417 / 10,074	79.0% / 39.3%
PNI Test Two	460 / 30,388	370 / 11,869	80.4% / 39.1%
Kasthuri Test	1,193 / 43,951	936 / 18,168	78.5% / 41.3%

The number of edges in the graph that correspond to split errors, the total number of edges, and the recall

Ablation Studies: Edge Generation

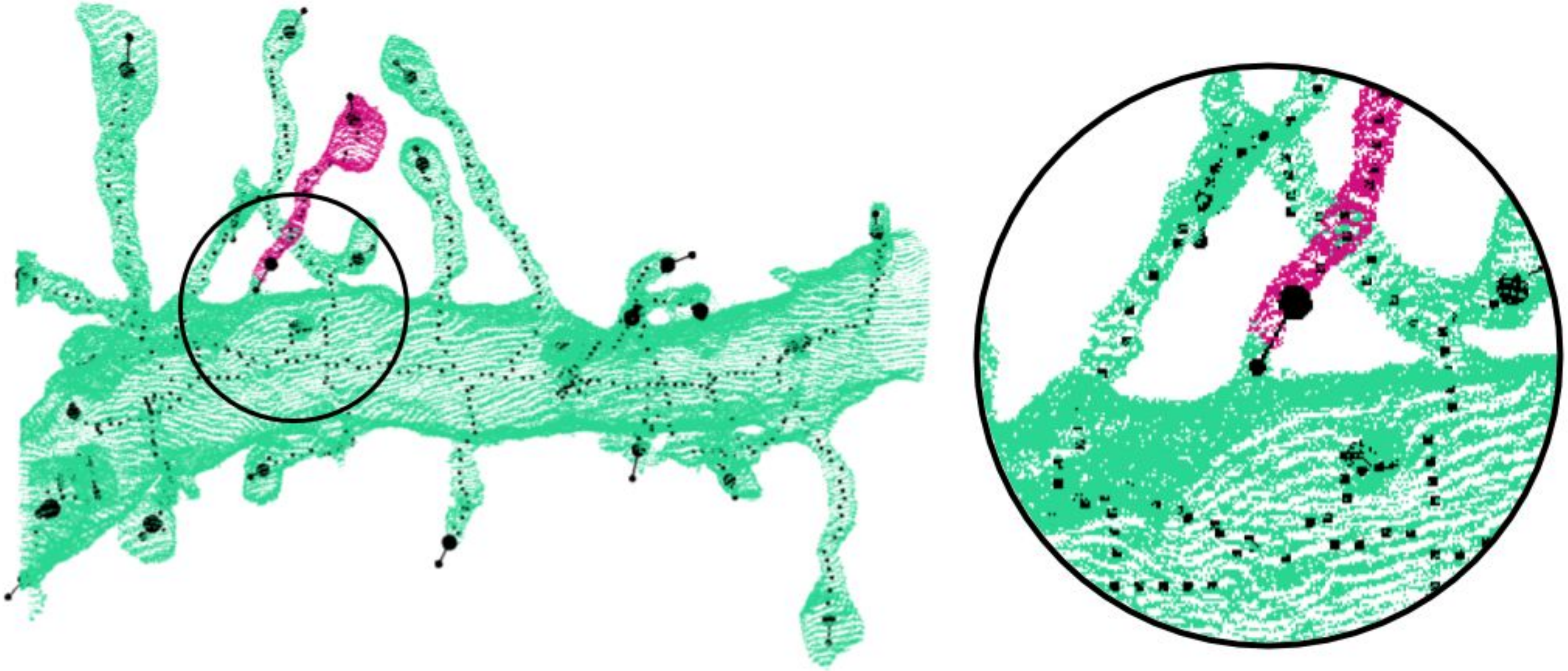

Ablation Studies: Edge Generation

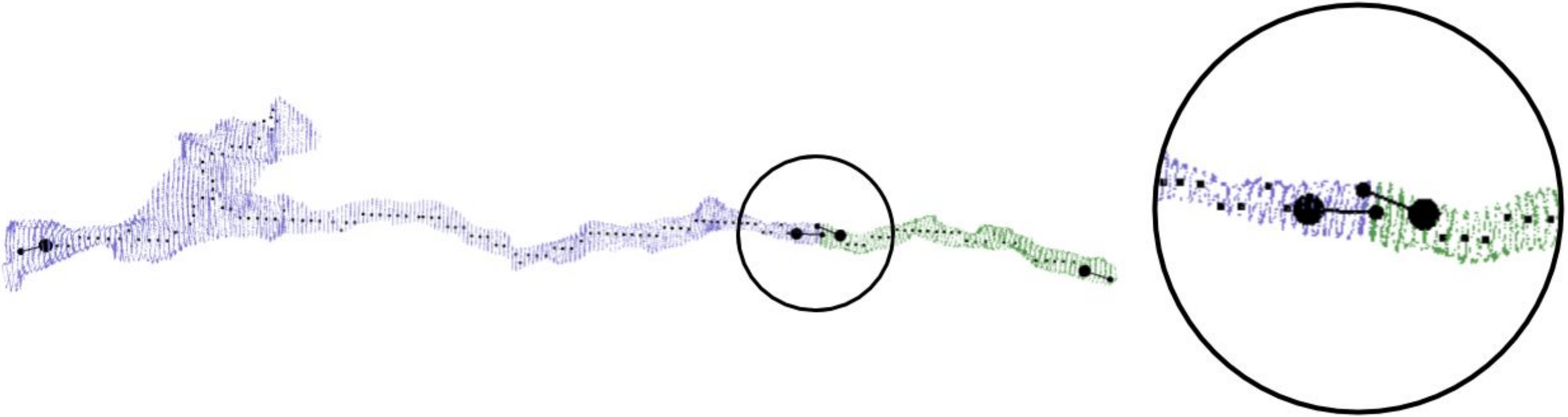

Edge Generation Failure Cases

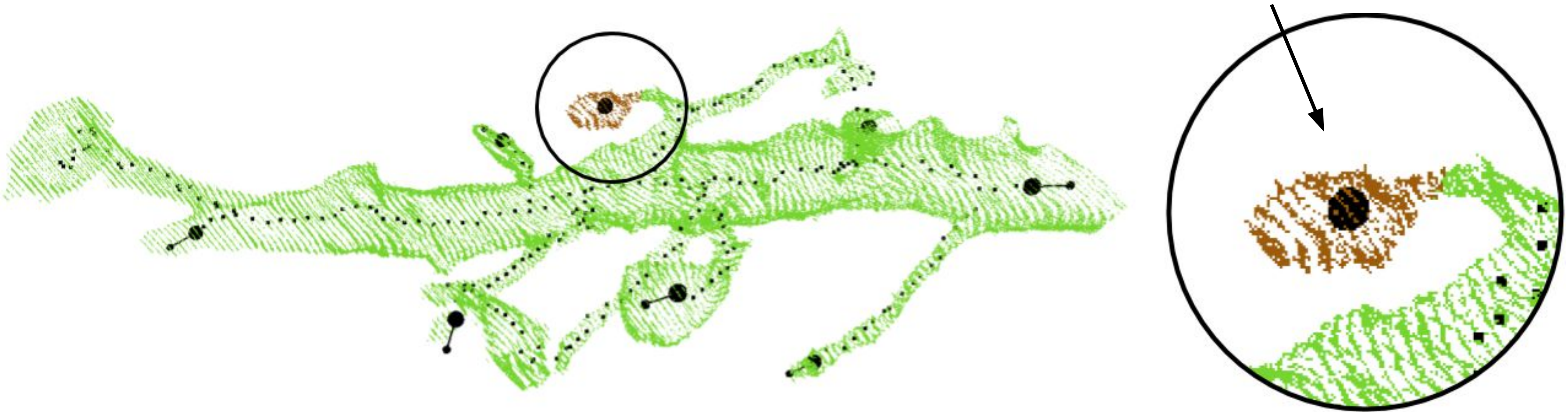

Trivial Skeleton

Edge Generation Failure Cases

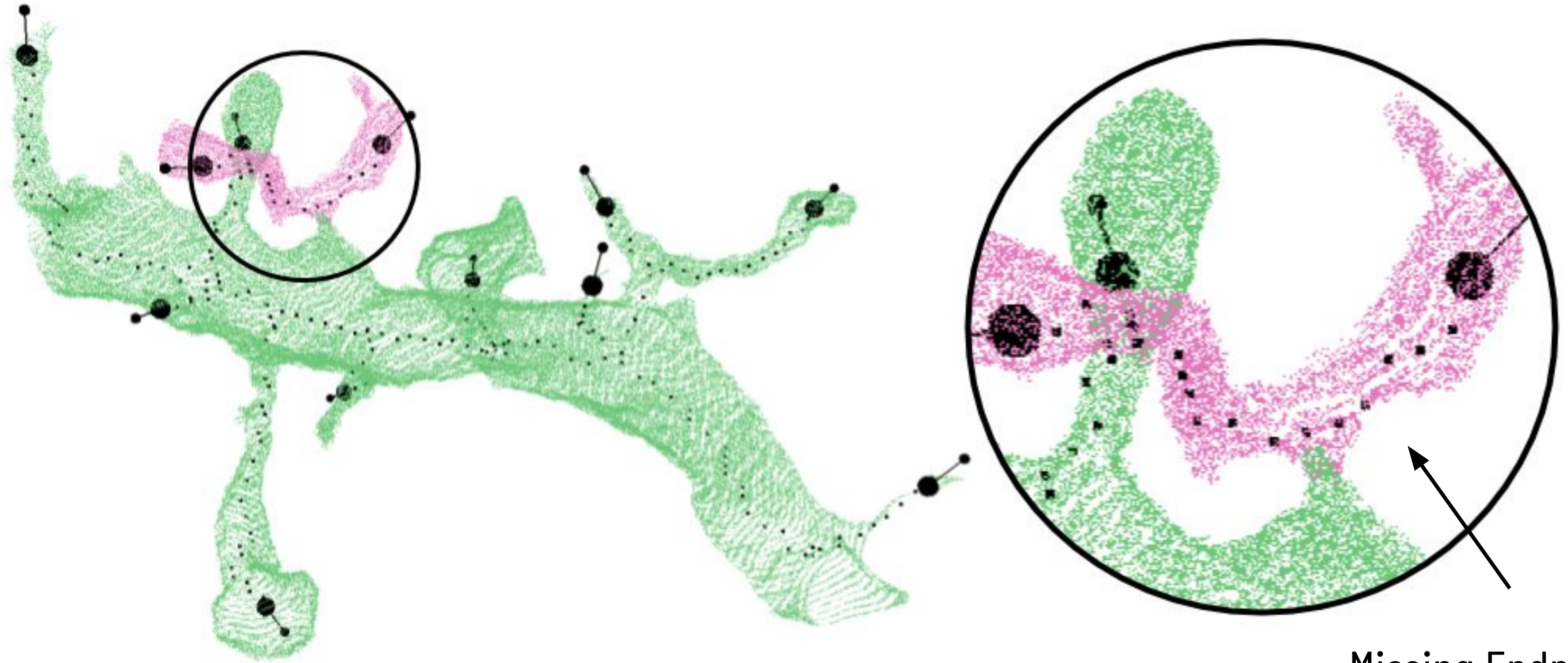

Missing Endpoint

Ablation Studies: Edge Weight Assignment

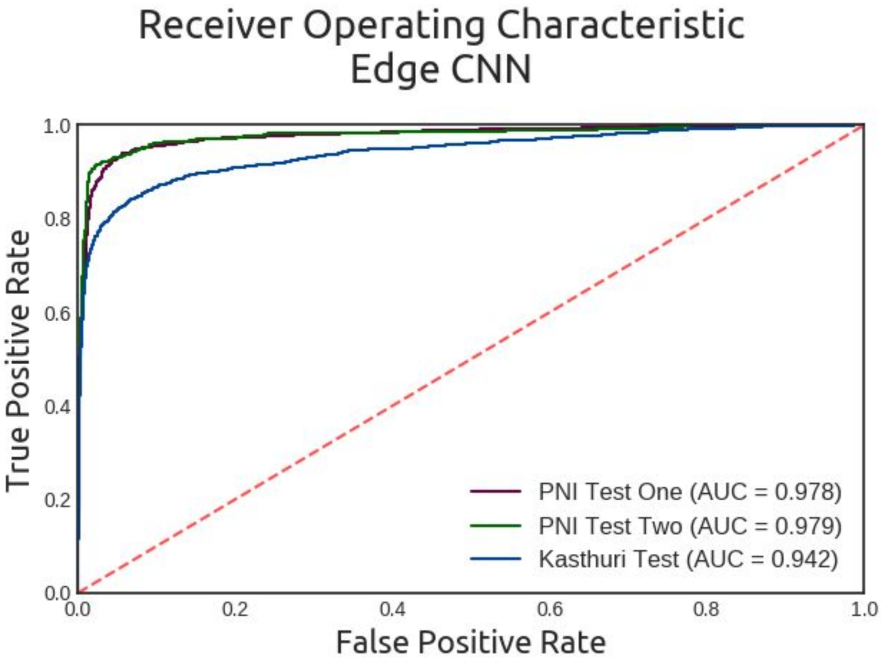

Accuracies:

PNI Test One: 96.4%
PNI Test Two: 97.2%
Kasthuri: 93.4%

Running Times

Time to process a gigavoxel dataset

Step	**Running Time**
Node Generation	281 seconds
Edge Generation	351 seconds
Lifted Multicut	13 seconds
Total	10.75 minutes

Biologically-Aware Algorithms Along the Connectomics Pipeline

Skeleton Generation

Compression

Error Correction

Subgraph Enumeration

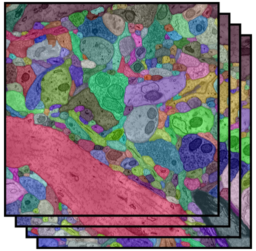

Segmentation

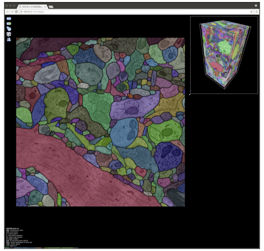

Proofreading

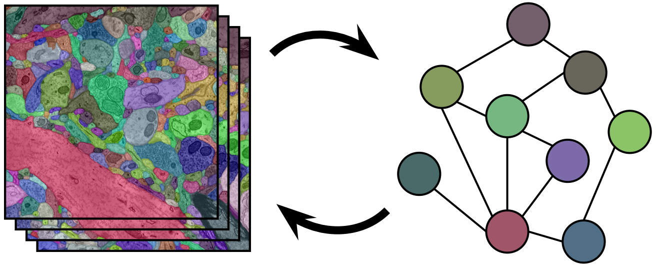

Network Analysis

Biologically Constrained Graph Construction

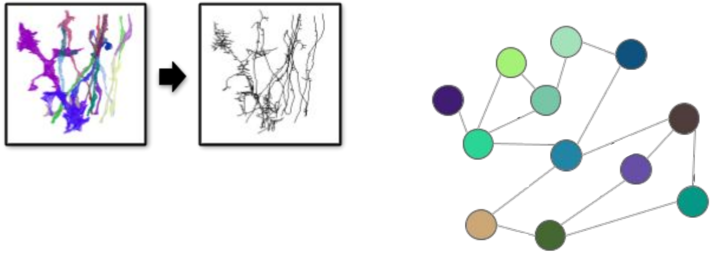

Biologically Constrained Graph Construction

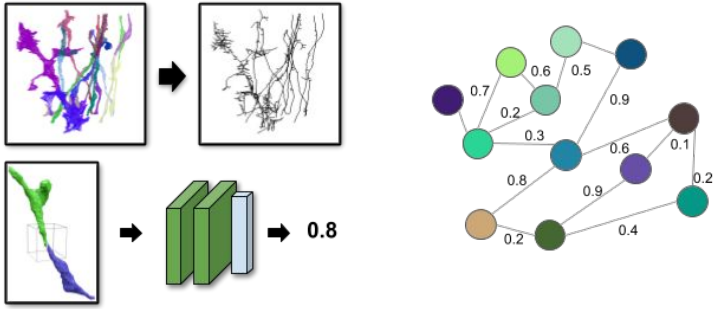

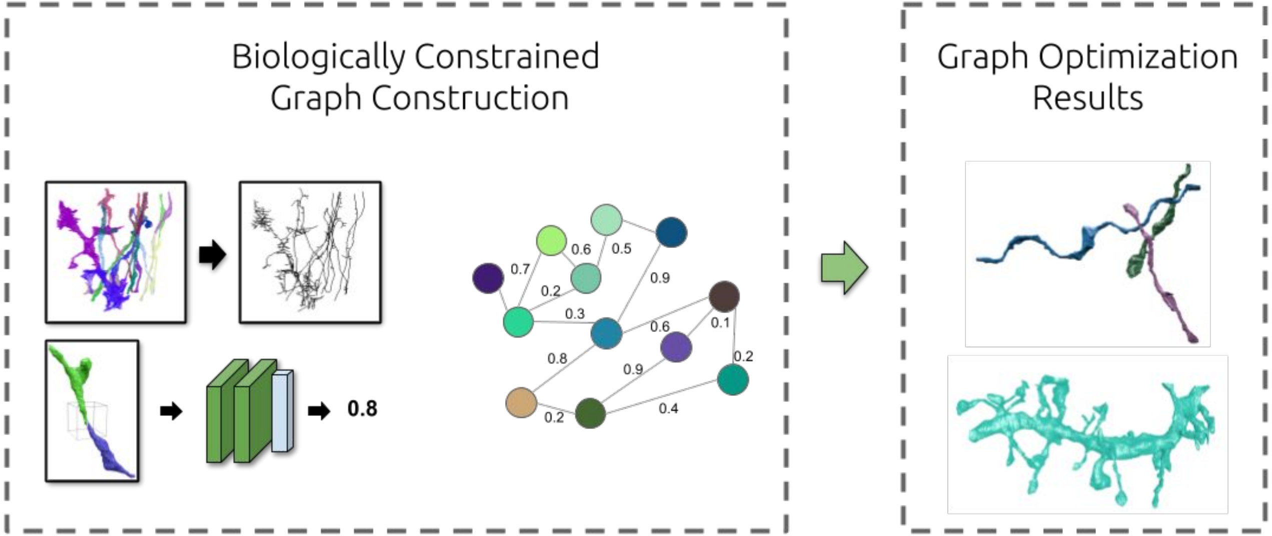

Biologically Constrained Graph Construction

Graph Optimization Results

Biologically-Aware Algorithms Along the Connectomics Pipeline

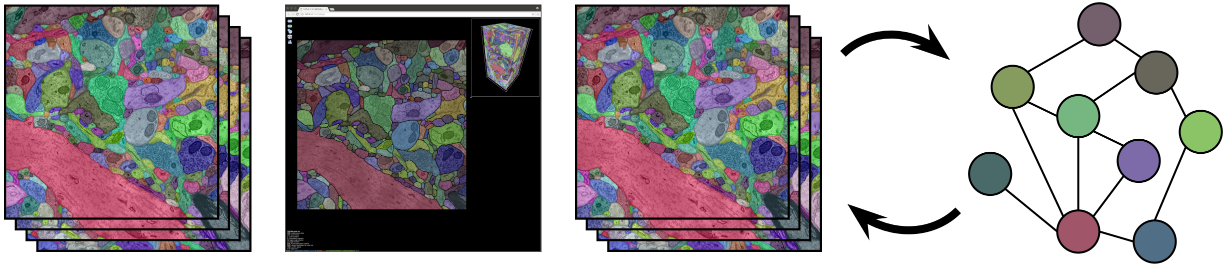

Skeleton Generation

Compression

Error Correction

Subgraph Enumeration

Segmentation

Proofreading

Network Analysis

Large-Scale Subgraph Enumeration on the Connectome

Brian Matejek, Donglai Wei, Tianyi Chen, Charalampos E. Tsourakakis,
Michael Mitzenmacher, and Hanspeter Pfister

Preprint, 2021

Extracting the Entire Wiring Diagram

C. elegans, the first nearly complete connectome

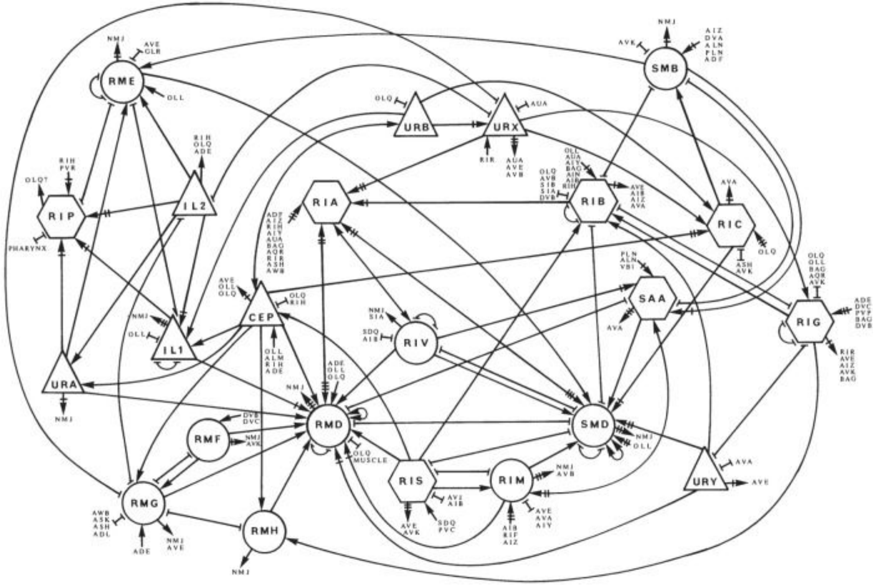

Emmons S.W., The Beginning of Connectomics: A Commentary on White et al. (1986) ‘The Structure of the Nervous System of the Nematode Caenorhabditis elegans.’ Philosophical Transactions of the Royal Society of London 2015.
Copyright © The Royal Society

Rapid Expansions in Large-Scale Wiring Diagrams

Improvements in the automatic processes allow for larger and more diverse connectomes

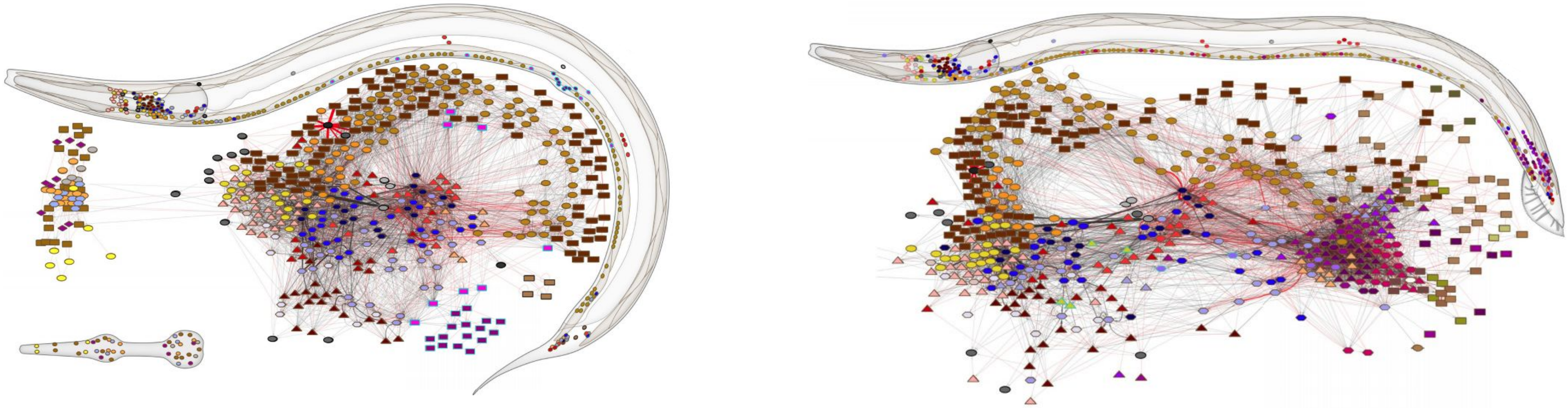

Cook *et al.*, Whole-animal Connectomes of Both *Caenorhabditis elegans sexes*, Nature 2019

Rapid Expansions in Large-Scale Wiring Diagrams

Improvements in the automatic processes allow for larger and more diverse connectomes

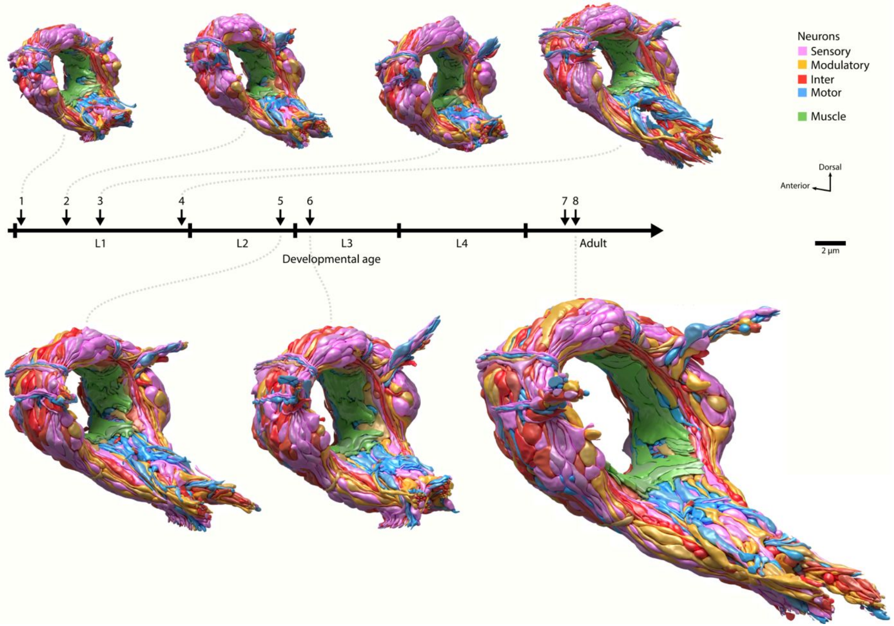

Witvliet *et al.*, Connectomes Across Development Reveal Principles of Brain Maturation in *C. elegans*, biorxiv 2020.

Rapid Expansions in Large-Scale Wiring Diagrams

Improvements in the automatic processes allow for larger and more diverse connectomes

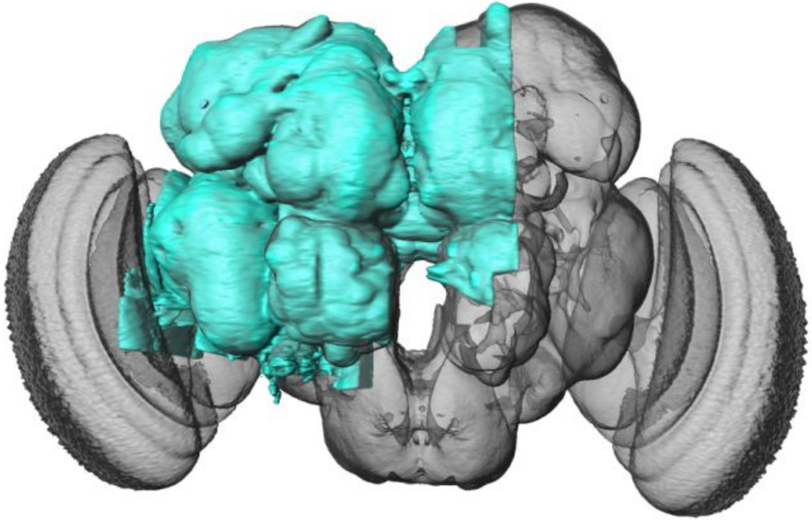

Xu *et al.*, A Connectome of the Adult *Drosophila* Central Brain, biorxiv 2020

Motif Discovery

Some subgraphs, or motifs, in the wiring diagram correspond to specific computational functions

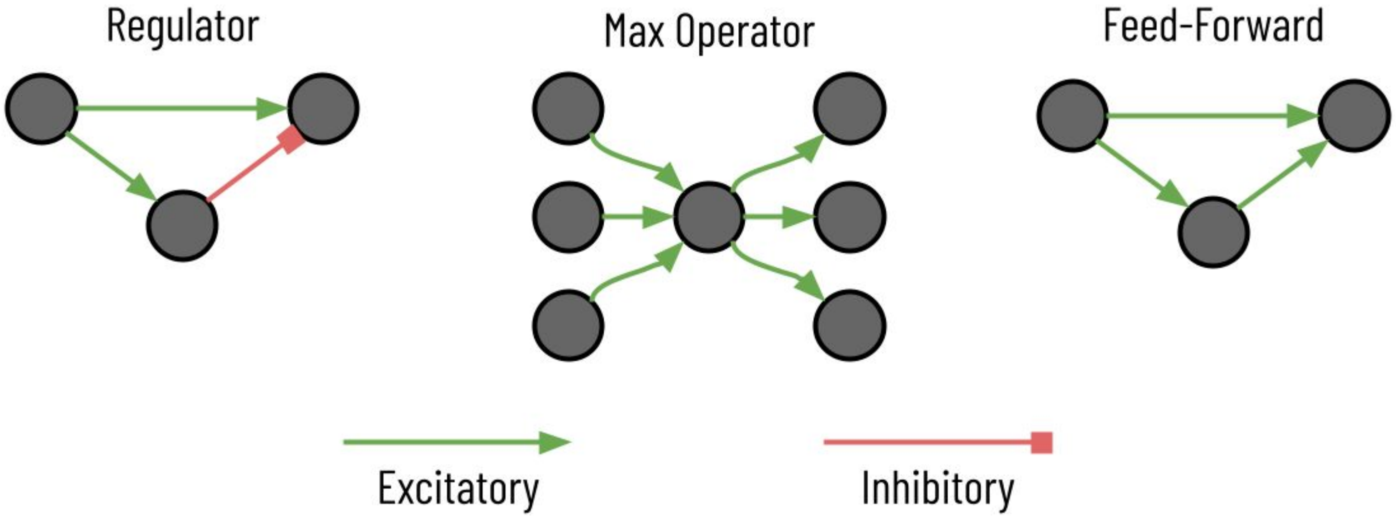

Motif-Centric Subgraph Enumeration

Most current motif analysis on these connectomes looks only for currently expected motifs

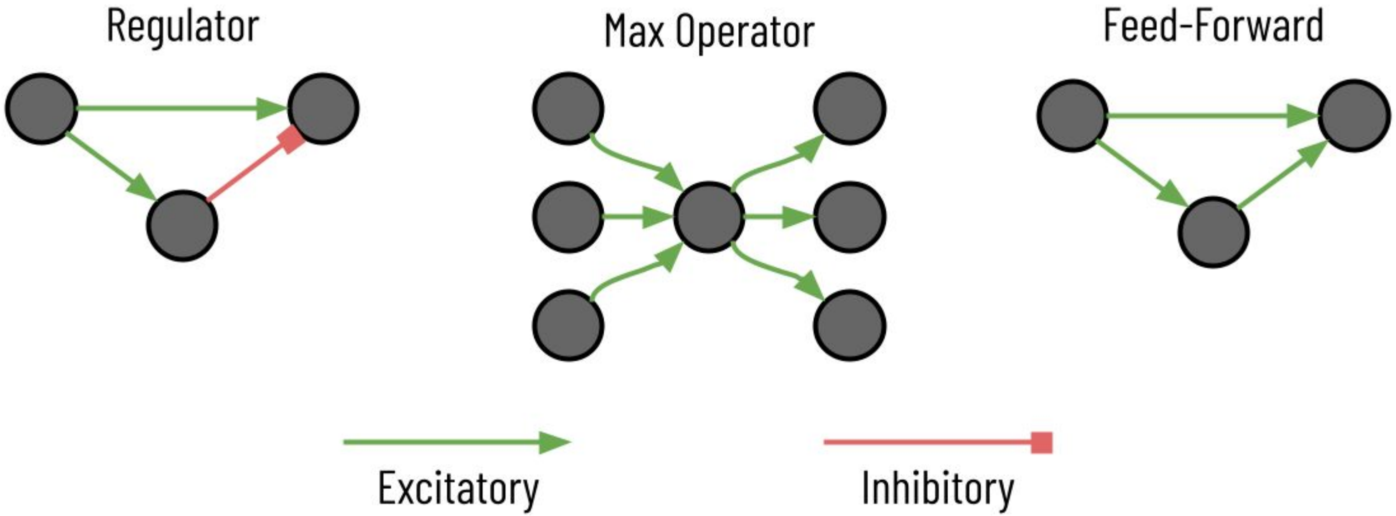

Motif-Centric Subgraph Enumeration

Most current motif analysis on these connectomes looks only for currently expected motifs

However, these strategies cannot identify “unknown unknowns”

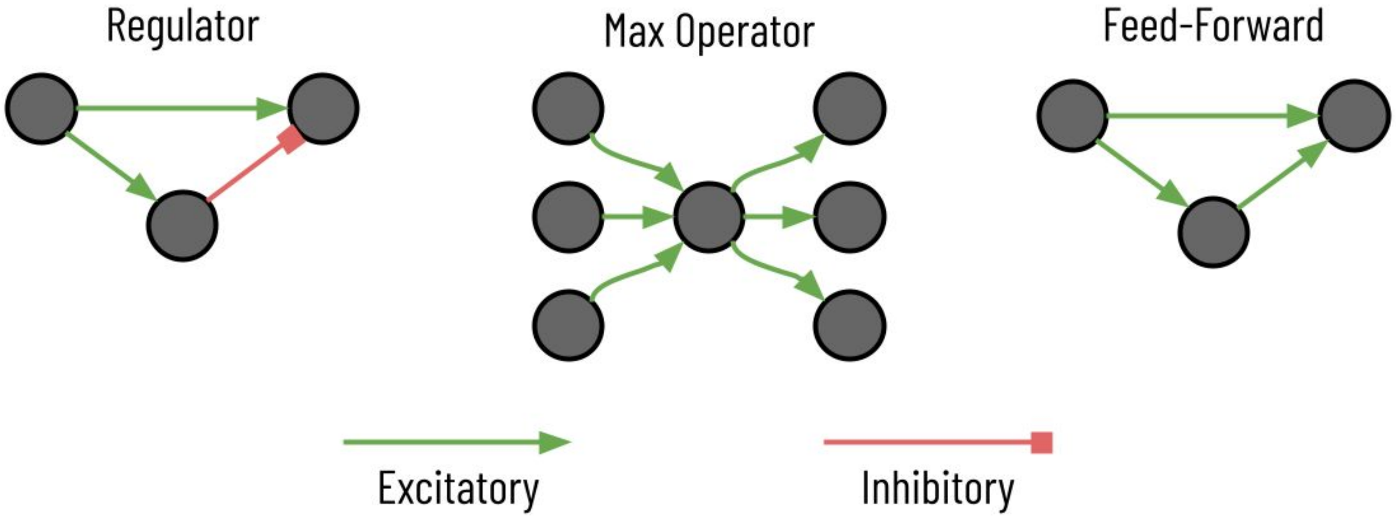

Network-Centric Subgraph Enumeration

Analyses that consider all viable subgraphs of size *k* in a connectome typically restrict *k* to 2 or 3

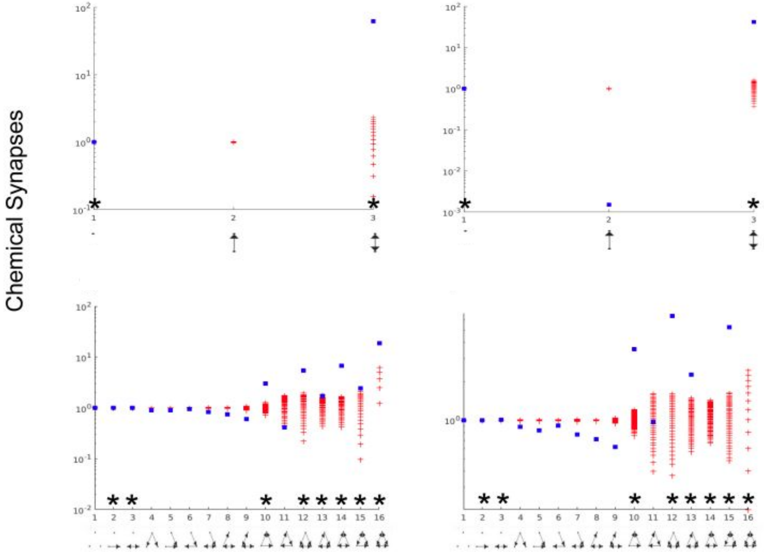

Cook *et al.*, Whole-animal Connectomes of Both *Caenorhabditis elegans sexes*, Nature 2019

Computational Issues

The number of subgraphs to enumerate grows quickly as *k* increases

Subgraph Size (k)	No. Subgraphs
3	125,601
4	3,809,067
5	126,545,565
6	4,286,896,477
7	143,807,877,796

Results from one connectome with 598 neurons/muscles/end-organs and 7,725 edges

Computational Issues

The number of subgraphs to enumerate grows quickly as *k* increases

Subgraph Size (k)	**No. Subgraphs**
3	125,601
4	3,809,067
5	126,545,565
6	4,286,896,477
7	143,807,877,796

30 x

33 x

34 x

34 x

Results from one connectome with 585 neurons/muscles/end-organs and 7,415 edges

Computational Issues

The number of subgraphs to enumerate grows quickly as *k* increases

The complexity to correctly classify a single subgraph increases exponentially with *k*

Subgraph Size (k)	**Subgraphs per second**
4	285,136
5	221,352
6	161,812
7	119,991
8	95,244

Averaged over eight connectomes with 225 neurons each (variable edges)

Computational Issues

Subgraph Size (k)	No. Subgraphs	Computation Time
3	126,610,248	9.44 min
4	36,041,949,778	2.15 d
5	12,522,283,314,604	2.77 yr

Results from one connectome with 21,739 neurons and 841,720 edges

Kavosh Subgraph Enumeration

We extend on the Kavosh algorithm, an existing fast method for network-centric enumeration

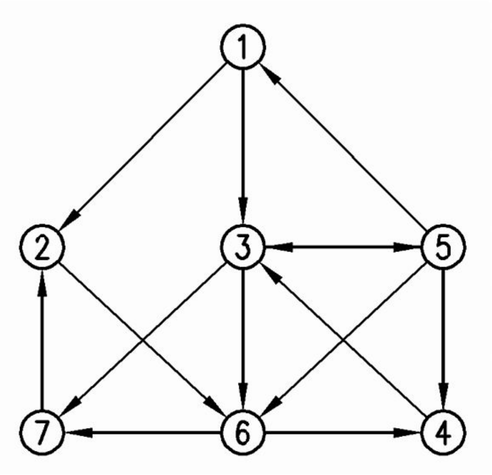

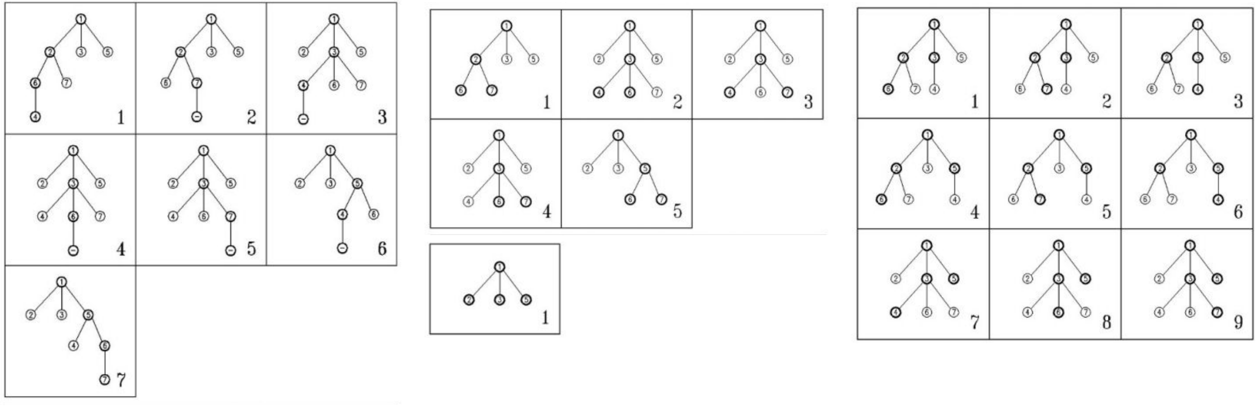

Kashani *et al.*, Kavosh: A New Algorithm for Finding Network Motifs, BMC Bioinformatics 2009

Kavosh Subgraph Enumeration

We extend on the Kavosh algorithm, an existing fast method for subgraph enumeration

To avoid subgraph duplication, the algorithm considers all subgraphs rooted at a given vertex

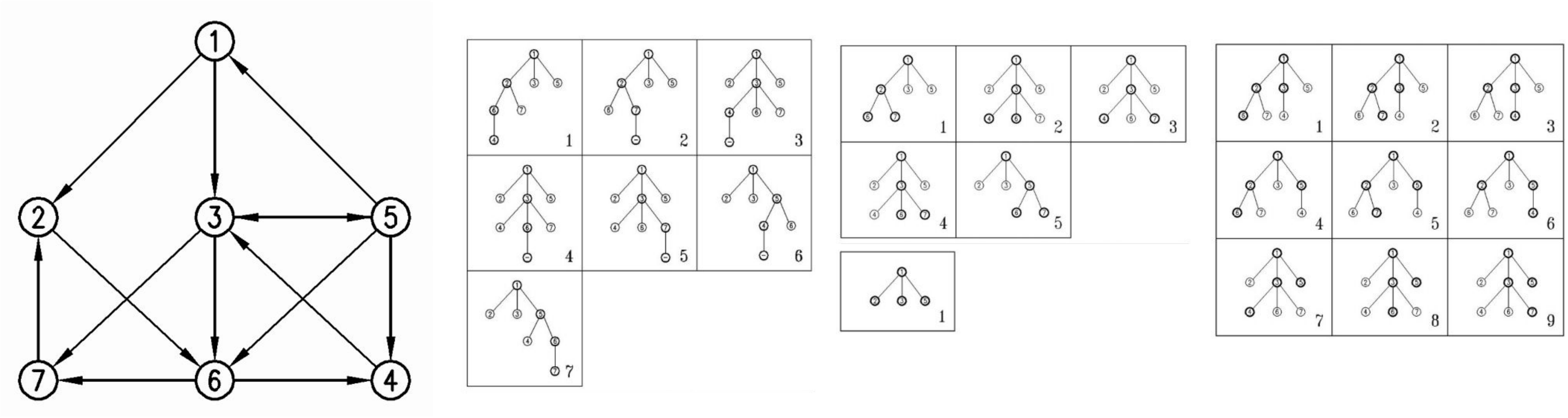

Kashani *et al.*, Kavosh: A New Algorithm for Finding Network Motifs, BMC Bioinformatics 2009

Proposed Large-Scale Subgraph Enumeration

Parallel Enumeration

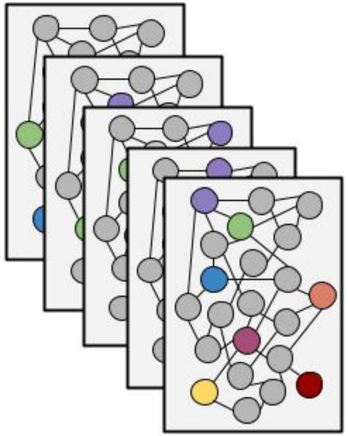

Community-Based Motif Discovery

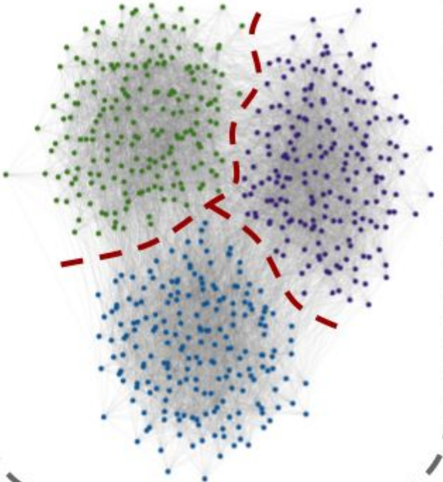

Edge Coloring

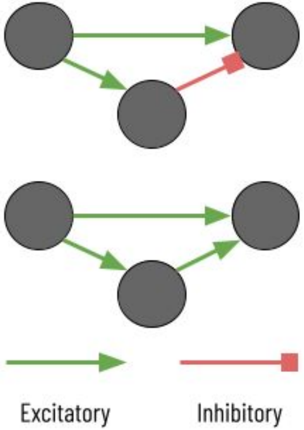

Goal: Distribute Enumeration over a Compute Cluster

Parallel Enumeration

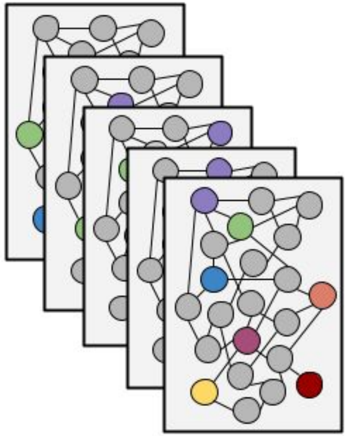

Community-Based Motif Discovery

Edge Coloring

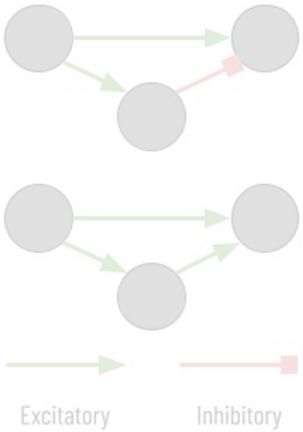

Parallelizing Kavosh

The algorithm itself is easy to parallelize—enumerate the subgraphs rooted at each vertex in parallel

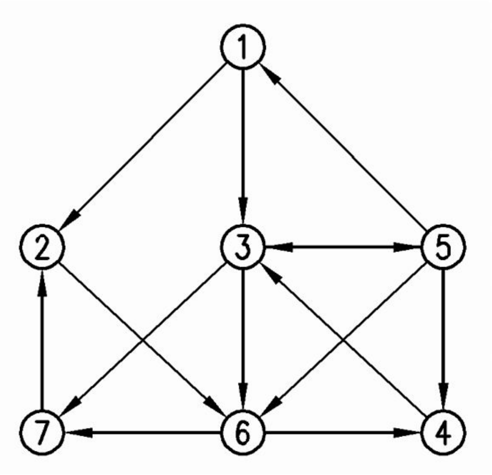

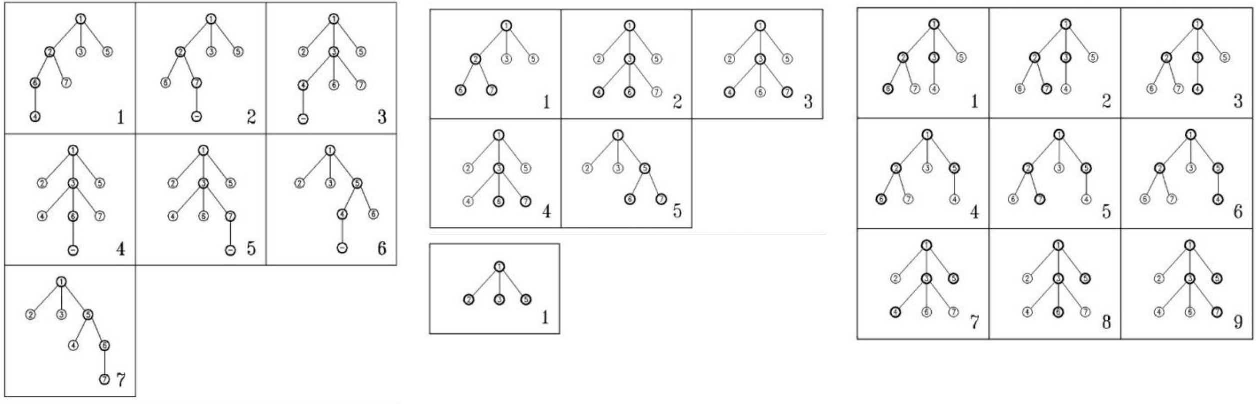

Kashani *et al.*, Kavosh: A New Algorithm for Finding Network Motifs, BMC Bioinformatics 2009

Better Parallelization

There are significant disparities in the number of subgraphs rooted at a given vertex

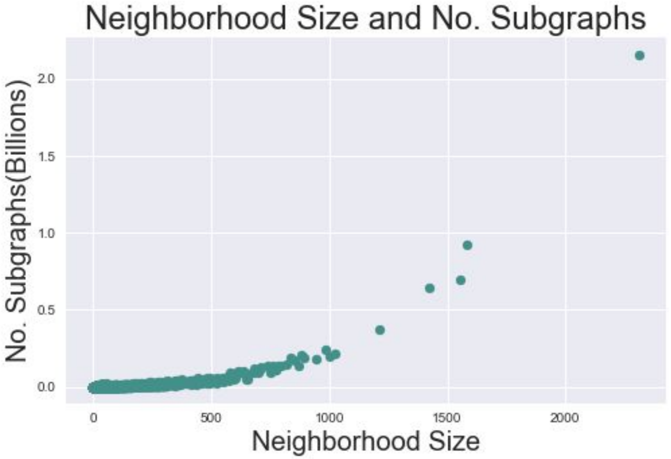

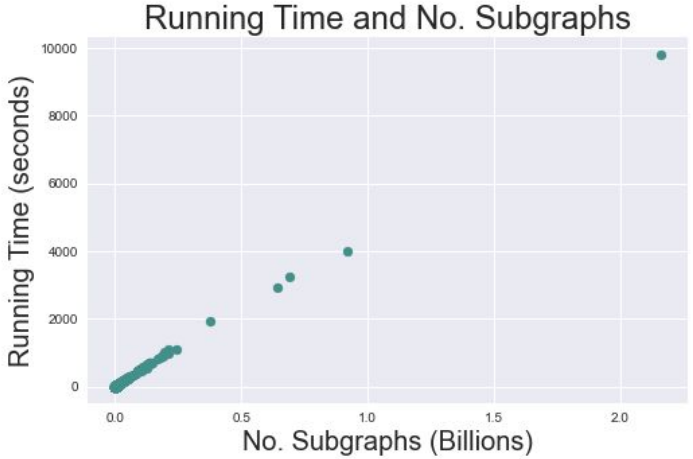

Better Parallelization

There are significant disparities in the number of subgraphs rooted at a given vertex

The many large cliques in connectomics can produce vertices with thousands of times more subgraphs

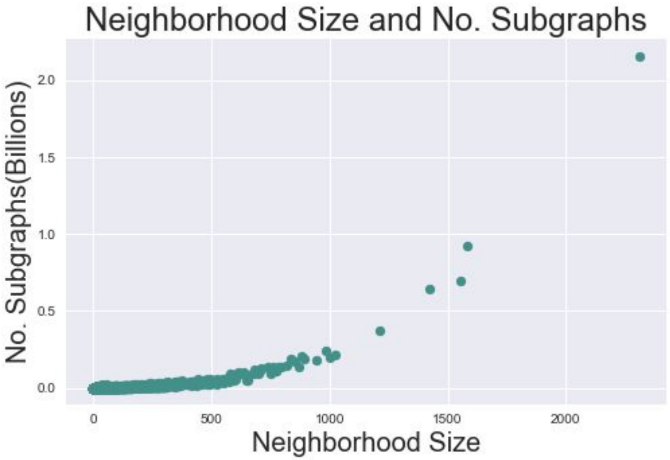

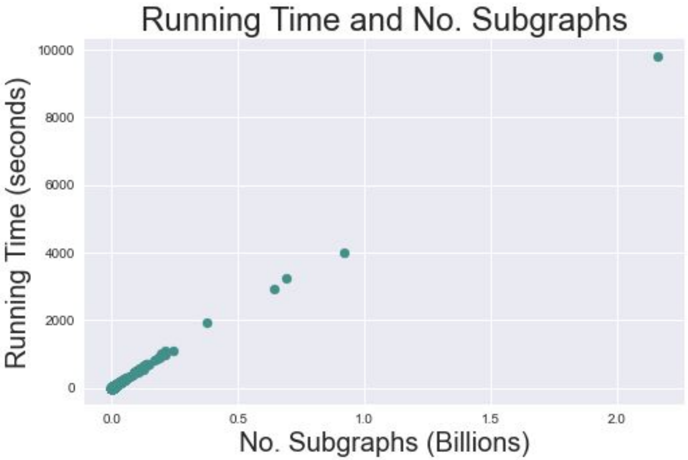

Readjusting the Enumeration Order

We relabel the vertices to minimize the influence of these cliques and reduce the idle CPU time

	Standard Order	**Readjusted Order**
Mean Time	8.21 sec	8.54 sec
Median Time	0.92 sec	5.80 sec
Maximum Time	9,820.40 sec	74.12 sec
Wall Time	175.20 min	15.78 min
Idle CPU Time	680.44 hr	14.18 hr

Results for $k = 4$ from one connectome with 21,739 neurons and 841,720 synaptic connections

Readjusting the Enumeration Order

We relabel the vertices to minimize the influence of these cliques and reduce the idle CPU time

	Standard Order	**Readjusted Order**
Mean Time	8.21 sec	8.54 sec
Median Time	0.92 sec	5.80 sec
Maximum Time	9,820.40 sec	74.12 sec
Wall Time	175.20 min	15.78 min
Idle CPU Time	680.44 hr	14.18 hr

Results for *k* = 4 from one connectome with 21,739 neurons and 841,720 synaptic connections

Goal: Divide and Conquer Enumeration for Very Large Datasets

Parallel Enumeration

Community-Based Motif Discovery

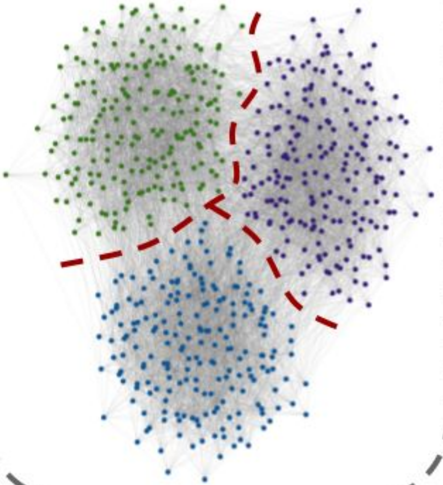

Edge Coloring

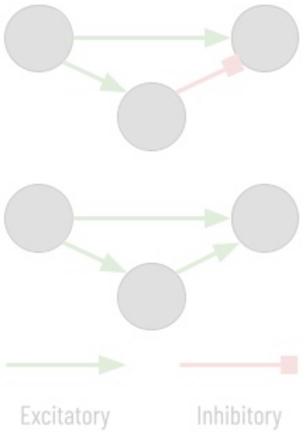

Clustering Before Enumeration

For very large connectomes, parallelization will not be enough as the number of subgraphs grows quickly

Clustering Before Enumeration

For very large connectomes, parallelization will not be enough as the number of subgraphs grows quickly

We use the METIS algorithm to create similarly sized clusters and enumerate subgraphs within clusters

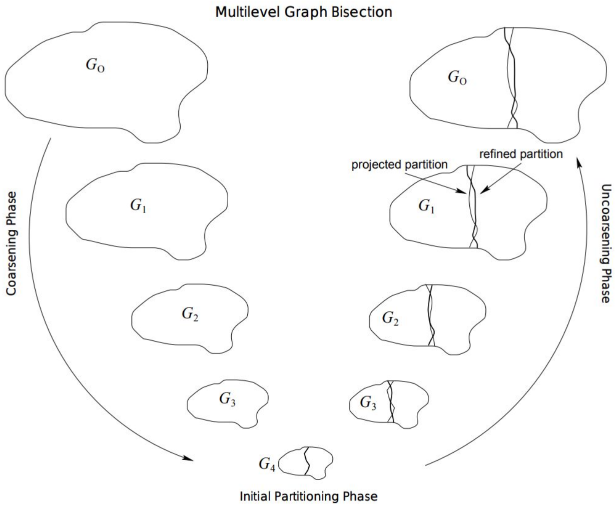

Karypis *et al.*, A Fast and Highly Quality Multilevel Scheme for Partitioning Irregular Graphs, SIAM Journal on Scientific Computing 1999

Clustering Before Enumeration

For very large connectomes, parallelization will not be enough as the number of subgraphs grows quickly

We use the METIS algorithm to create similarly sized clusters and enumerate subgraphs within clusters

These clusters could similarly be determined by domain-knowledge of the brain regions

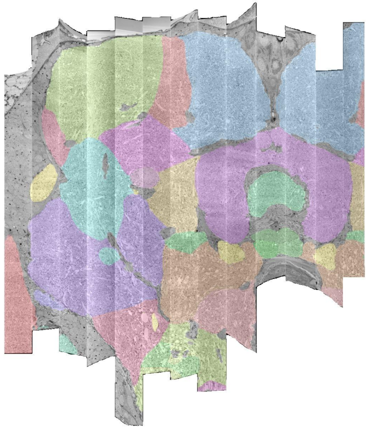

Xu *et al.*, A Connectome of the Adult *Drosophila* Central Brain, biorxiv 2020

Goal: Augment Graphs with Biologically Relevant Features

Parallel Enumeration

Community-Based Motif Discovery

Edge Coloring

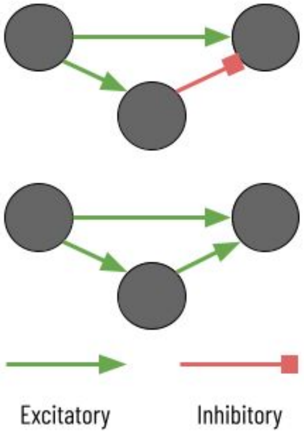

Creating Graphs that Better Resemble the Biology

Similar motifs can have variable functionalities depending on the connections

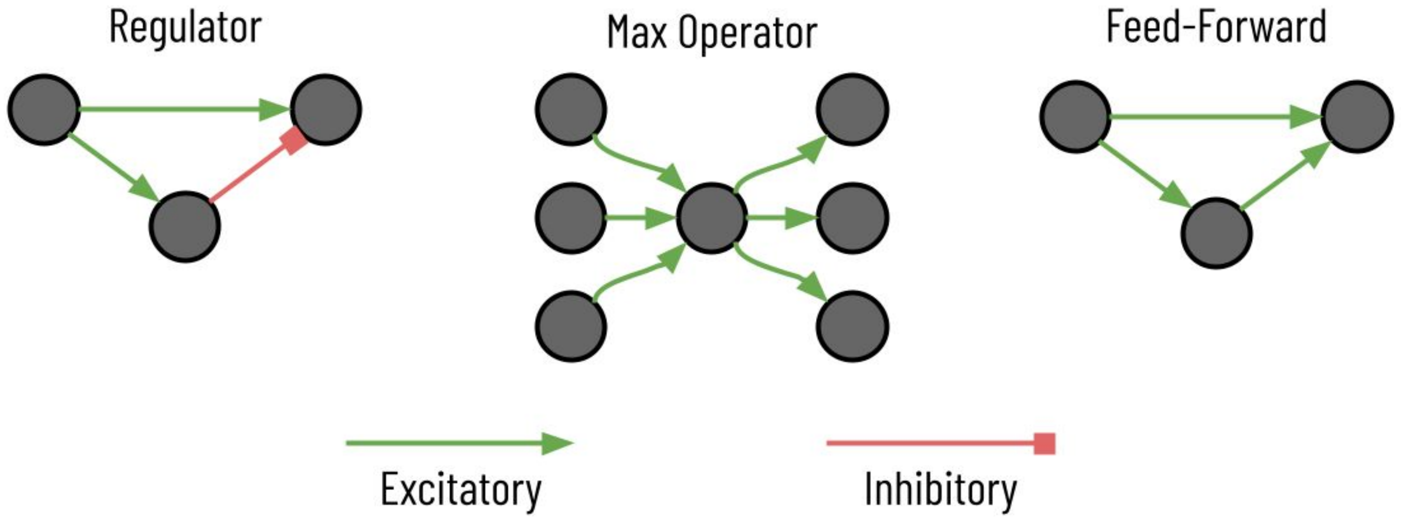

Creating Graphs that Better Resemble the Biology

Similar motifs can have variable functionalities depending on the connections

Edges can be excitatory/inhibitory, or even represent chemical/electrical synapse connections

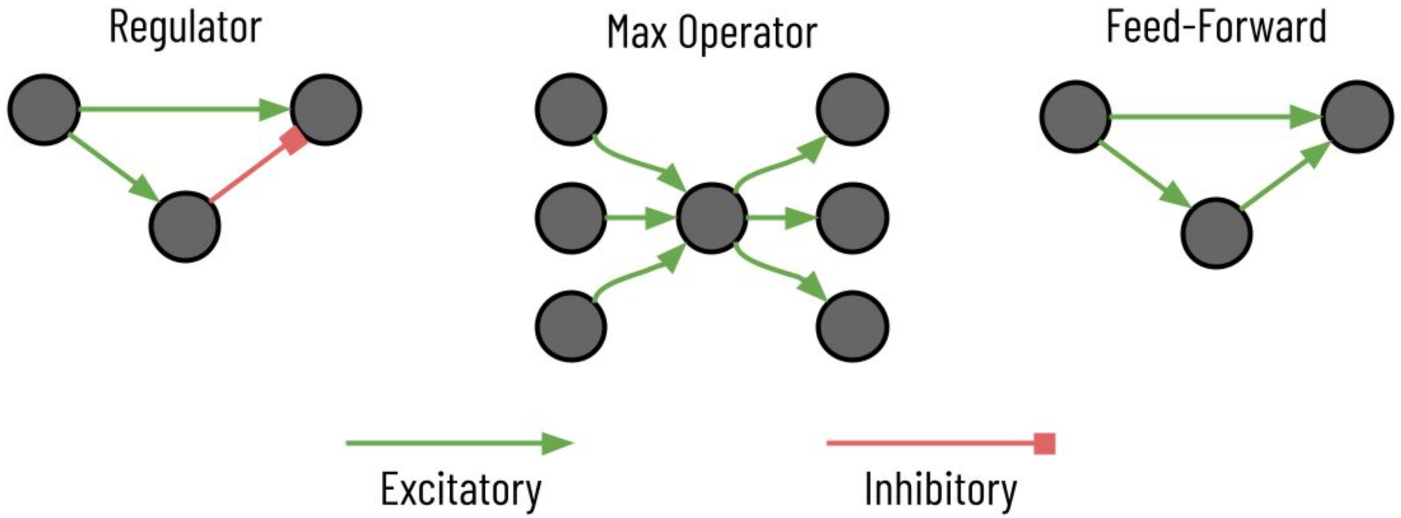

Datasets

Drosophila

Age	Sex	Neurons	Edges	Edge Types
Adult	Female	21,739	841,720	Moderate/Strong

C. elegans Development

C. elegans Sexes

Xu *et al.*, A Connectome of the Adult *Drosophila* Central Brain, biorxiv 2020

Datasets

Drosophila

***C. elegans* Development**

C. elegans Sexes

Age	Sex	Neurons	Edges	Edge Types
0 hr	Hermaphrodite	225	775	N/A
5 hr	Hermaphrodite	225	986	N/A
8 hr	Hermaphrodite	225	1,006	N/A
16 hr	Hermaphrodite	225	1,101	N/A
23 hr	Hermaphrodite	225	1,504	N/A
27 hr	Hermaphrodite	225	1,524	N/A
Adult (50 hr)	Hermaphrodite	225	2,193	N/A
Adult (50 hr)	Hermaphrodite	225	2,189	N/A

Witvliet *et al.*, Connectomes Across Development Reveal Principles of Brain Maturation in *C. elegans*, biorxiv 2020.

Datasets

Drosophila

C. elegans Development

***C. elegans* Sexes**

Age	**Sex**	**Neurons**	**Edges**	**Edge Types**
Adult	Hermaphrodite	473	6,897	Chem/Elec/Both
Adult	Male	598	7,725	Chem/Elec/Both

Cook *et al.*, Whole-animal Connectomes of Both *Caenorhabditis elegans sexes*, Nature 2019

Common Subgraphs in *Drosophila*

The four most common motifs of size 5 accounts for over 27.5% of all subgraphs

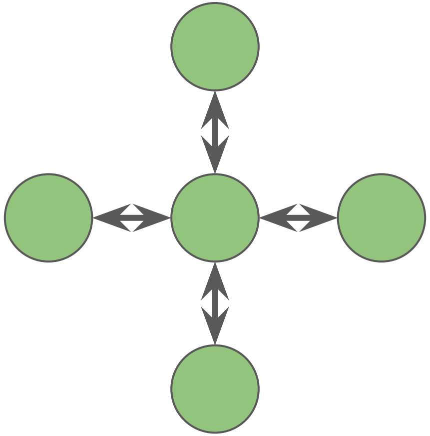

13.87%

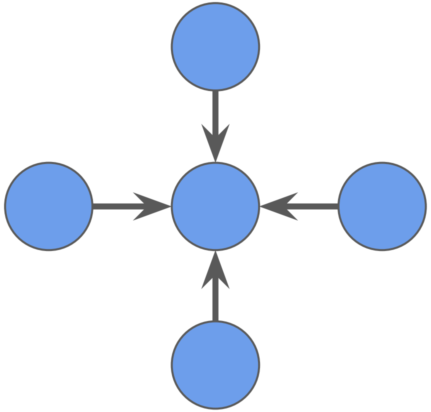

6.55%

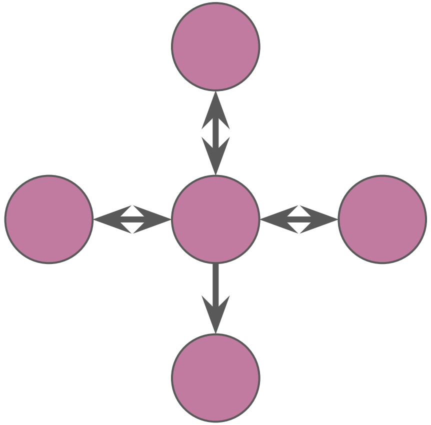

3.67%

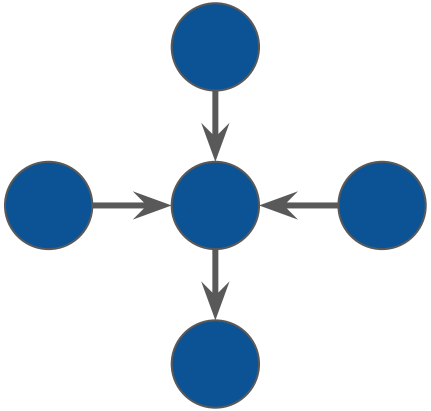

3.45%

Common Subgraphs in *Drosophila*

The four most common motifs of size 5 accounts for over 27.5% of all subgraphs

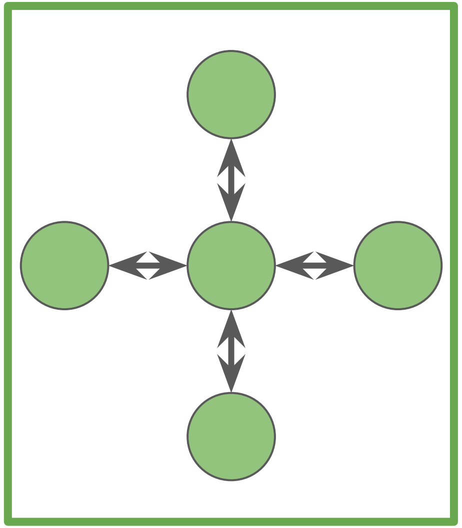

13.87%

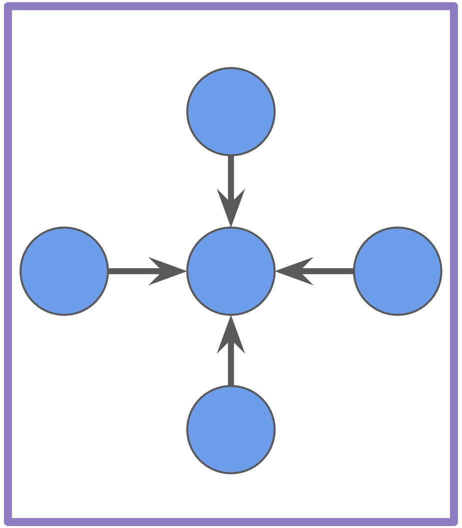

6.55%

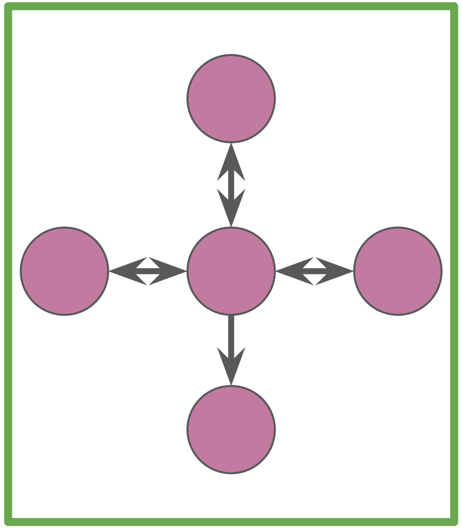

3.67%

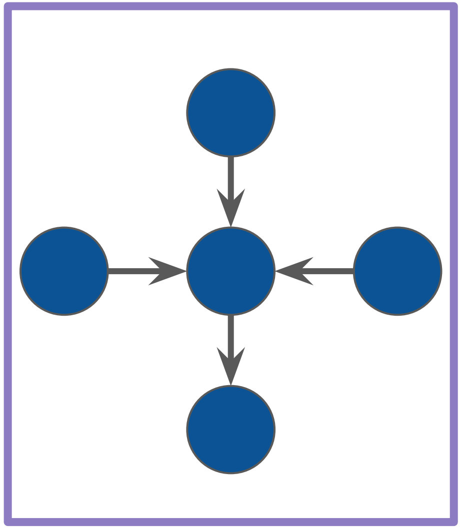

3.45%

Developmental Growth of *C. elegans*

Amazingly, the relative proportions of specific subgraphs of size 3 and 4 does not differ significantly across the *C. elegans* development

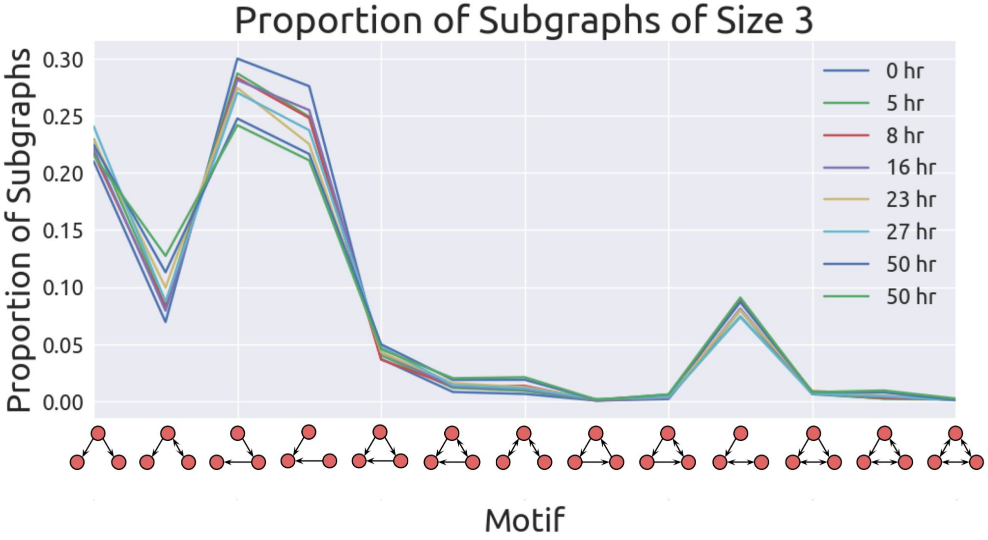

Developmental Growth of *C. elegans*

Amazingly, the relative proportions of specific subgraphs of size 3 and 4 does not differ significantly across the *C. elegans* development

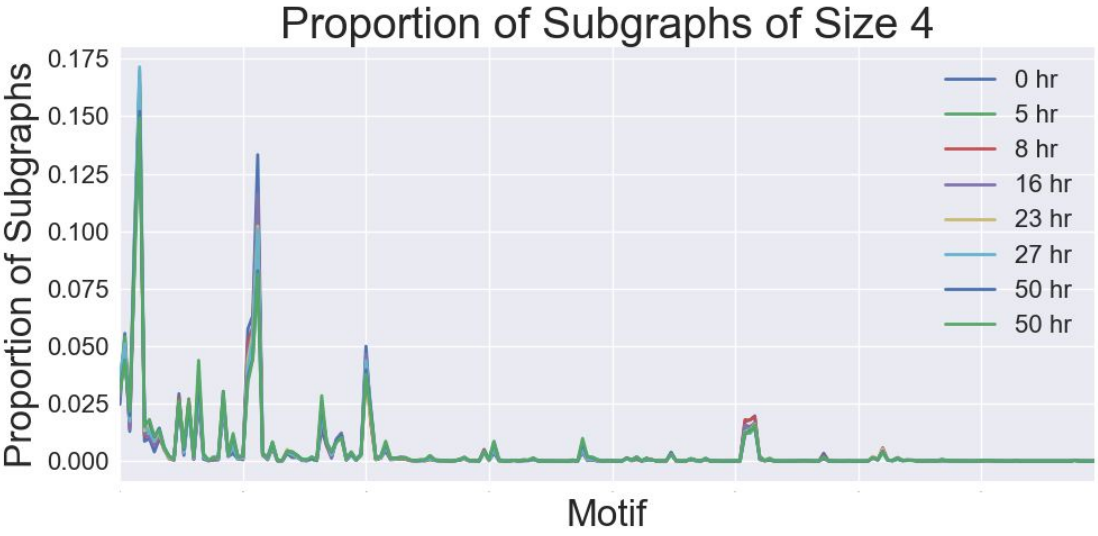

Comparison Between the Two *C. Elegans* Sexes

Both the adult sexes of the *C. elegans* samples compared had very similar motif counts for *k* = 3 and 4

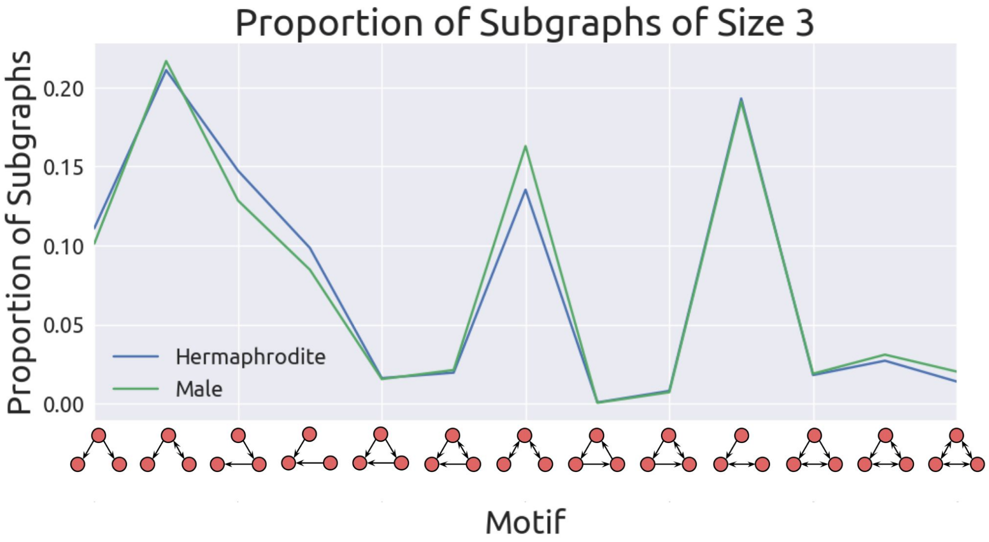

These *C. elegans* datasets are not directly comparable to the previous set since they contain end-organs, muscles, and gap junctions

Comparison Between the Two *C. Elegans* Sexes

Both the adult sexes of the *C. elegans* samples compared had very similar motif counts for *k* = 3 and 4

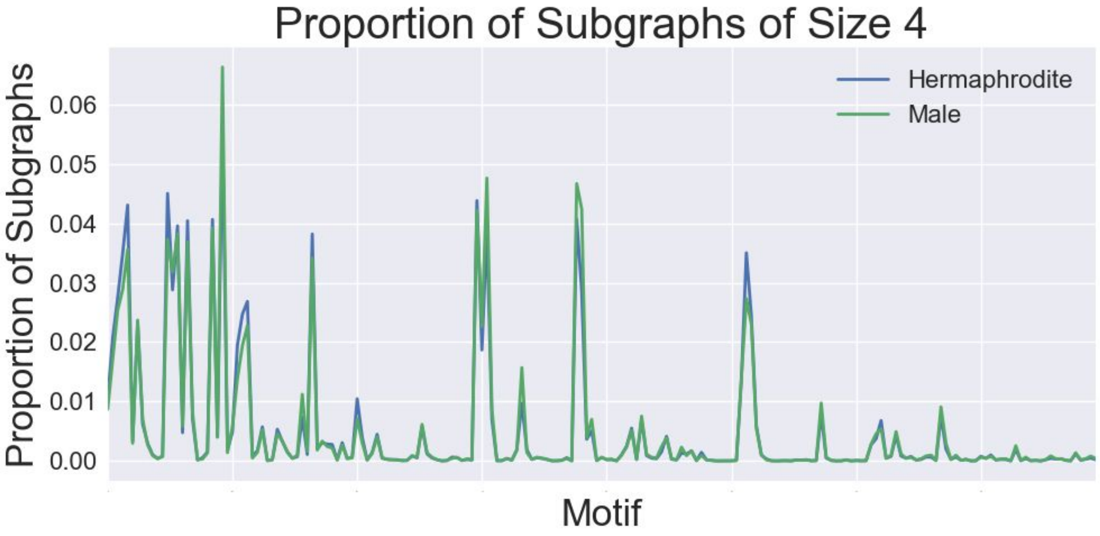

These *C. elegans* datasets are not directly comparable to the previous set since they contain end-organs, muscles, and gap junctions

Ablation Studies: Community-Based Motif Discovery

No. Communities	No. Subgraphs (k = 5)	Computation Time
1	12,522,283,314,604	2.77 yr
5	3,645,456,758,599	0.82 yr
10	2,130,560,777,611	0.48 yr
15	1,458,545,460,827	0.31 yr
20	1,014,016,146,436	0.22 yr
25	607,287,828,074	0.13 yr
30	456,303,664,640	0.098 yr

Ablation Studies: Edge Coloring

Dataset	**No Edge/Edge Color Computation Times**			
	3	**4**	**5**	**6**
Drosophila	566.63 / 1053.48 s	2.15 / 4.39 d	2.77 / 6.12 yr	N/A
C. elegans Herm.	0.37 / 0.77 s	14.75 / 31.78 s	727.96 / 1607.75 s	9.53 / 21.76 hr
C. elegans Male	0.38 / 0.72 s	13.18 / 29.61 s	593.57 / 1296.49 s	7.13 / 16.38 hr

Dataset Publication

We publish summaries of all enumerated subgraphs from the twelve connectomes to enable further analysis from the community

Graph Type	No. Subgraphs	Computation Time
Standard	13,153,746,555,370	2.92 yr
Edge Colored	12,568,788,861,035	6.13 yr
Community-Based	9,362,073,052,898	2.08 yr

Dataset Publication

We publish summaries of all enumerated subgraphs from the eleven connectomes to enable further analysis from the community

Graph Type	No. Subgraphs	Computation Time
Standard	13,153,746,555,370	2.92 yr
Edge Colored	12,568,788,861,035	6.13 yr
Community-Based	9,362,073,052,898	2.08 yr

35 trillion enumerated subgraphs

Dataset Publication

We publish summaries of all enumerated subgraphs from the eleven connectomes to enable further analysis from the community

Graph Type	No. Subgraphs	Computation Time
Standard	13,153,746,555,370	2.92 yr
Edge Colored	12,568,788,861,035	6.13 yr
Community-Based	9,362,073,052,898	2.08 yr

35 trillion enumerated subgraphs over 11.13 years of computation time

Biologically-Aware Algorithms Along the Connectomics Pipeline

Skeleton Generation

Compression

Error Correction

Subgraph Enumeration

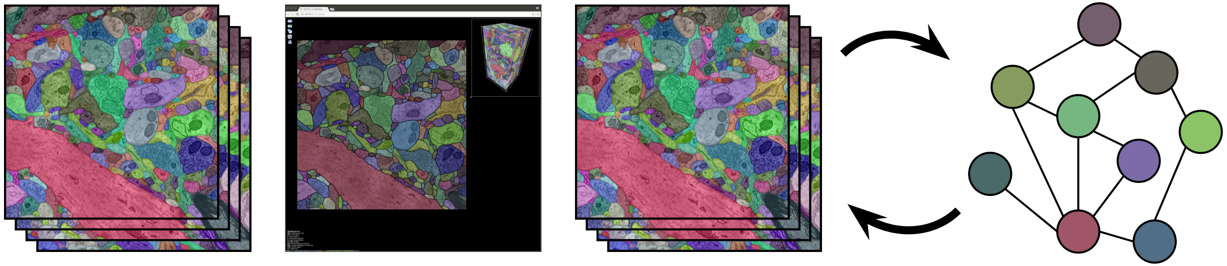

Segmentation

Proofreading

Network Analysis

Biologically-Aware Algorithms Along the Connectomics Pipeline

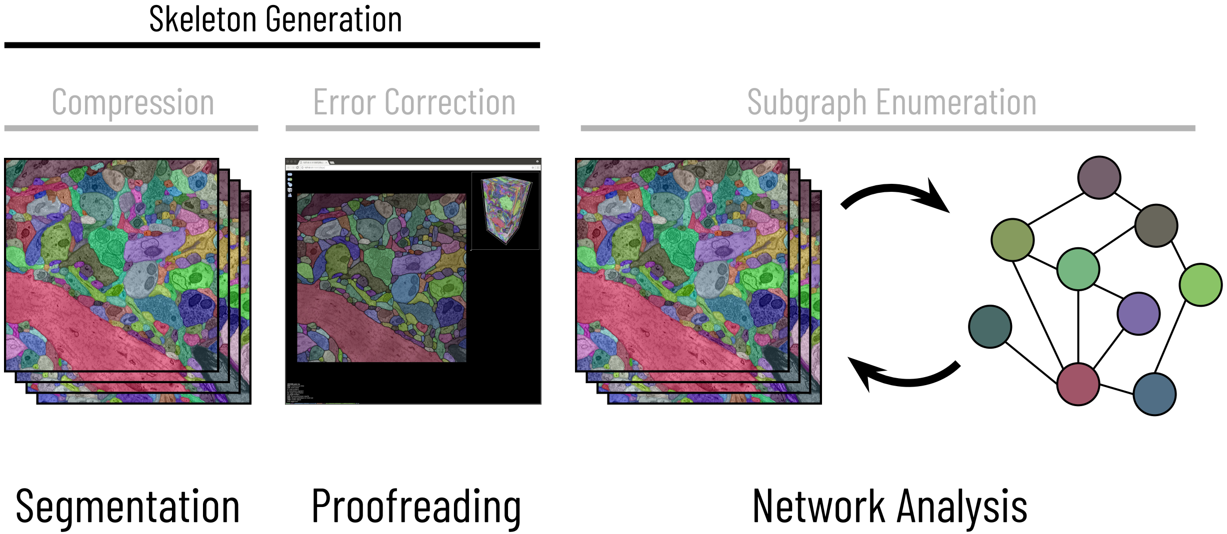

Skeleton Generation

Compression

Error Correction

Subgraph Enumeration

Segmentation

Proofreading

Network Analysis

Biologically-Aware Algorithms Along the Connectomics Pipeline

Skeleton Generation

Compression

Error Correction

Subgraph Enumeration

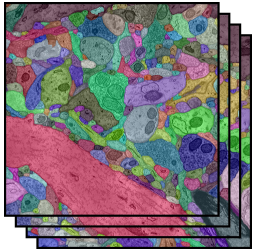

Segmentation

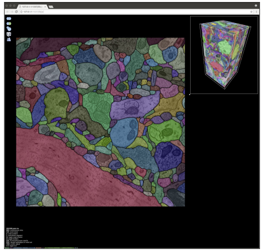

Proofreading

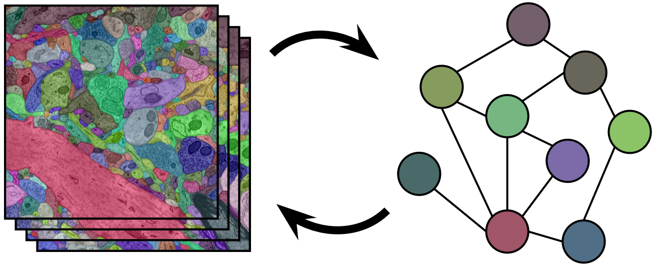

Network Analysis

Scalable Biologically-Aware Skeleton Generation for Connectomic Volumes

Brian Matejek, Tim Franzmeyer, Donglai Wei, Xueying Wang, Jinglin Zhao,
Kálmán Palágyi, Jeff W. Lichtman, and Hanspeter Pfister

International Conference on Medical Image Computing and Computer Assisted Intervention, 2019
Under Review, 2021

Skeletonized Representations of Label Volumes

Across the connectomics pipeline, skeletonized representations of the label volumes are incredibly useful

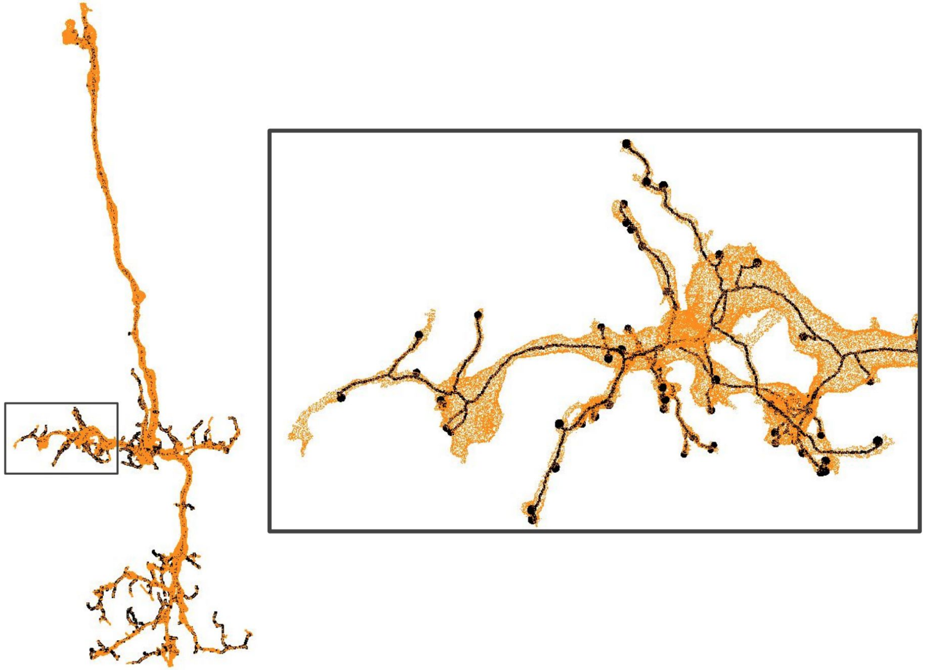

Skeletonization for Analysis

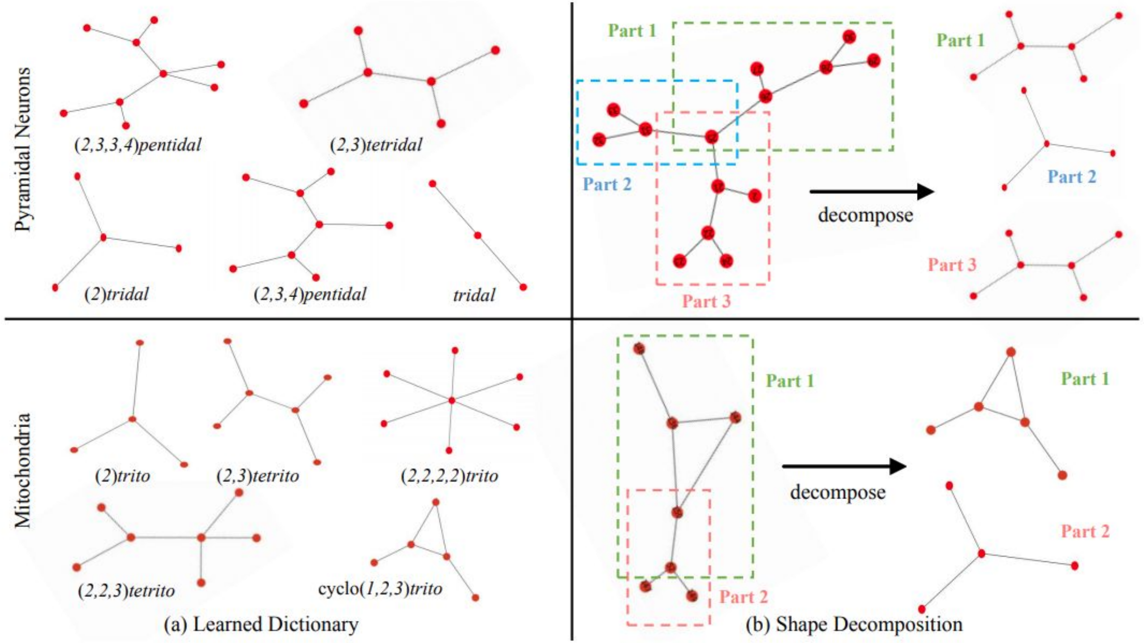

(a) Learned Dictionary (b) Shape Decomposition

Xu *et al.*, A Connectome of the Adult *Drosophila* Central Brain, biorxiv 2020
Talwar *et al.*, A Topological Nomenclature for 3D Shape Analysis in Connectomics, CVPR Workshops 2020

Skeletonization for Segmentation Evaluation

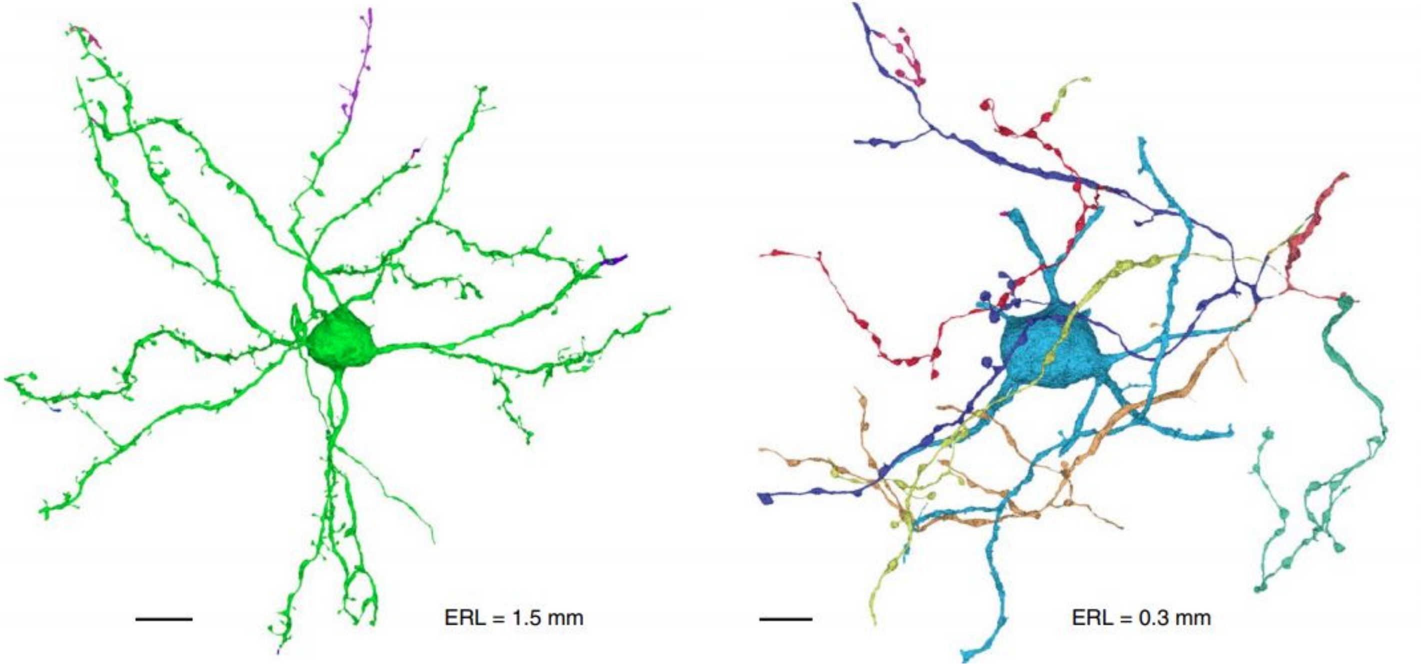

Januszewski *et al.*, High-Precision Automated Reconstruction of Neurons with Flood-Filling Networks, Nature Methods 2018

Skeletonization for Visualization

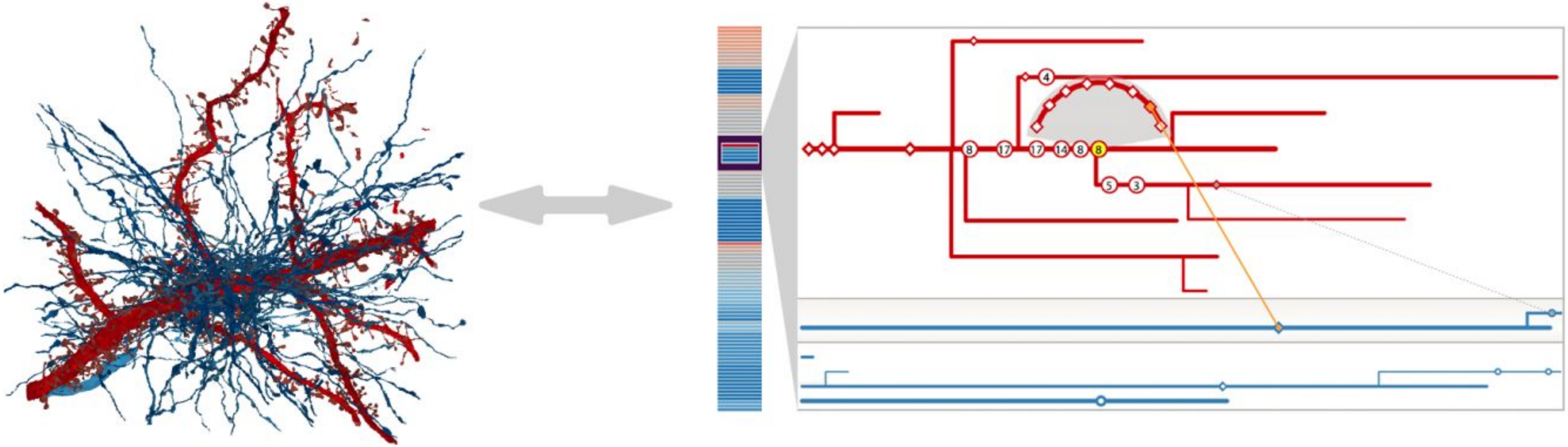

Mohammed *et al.*, Abstractocyte: A Visual Tool for Exploring Nanoscale Astroglial Cells, IEEE VIS 2017

Skeletonization for Error Correction

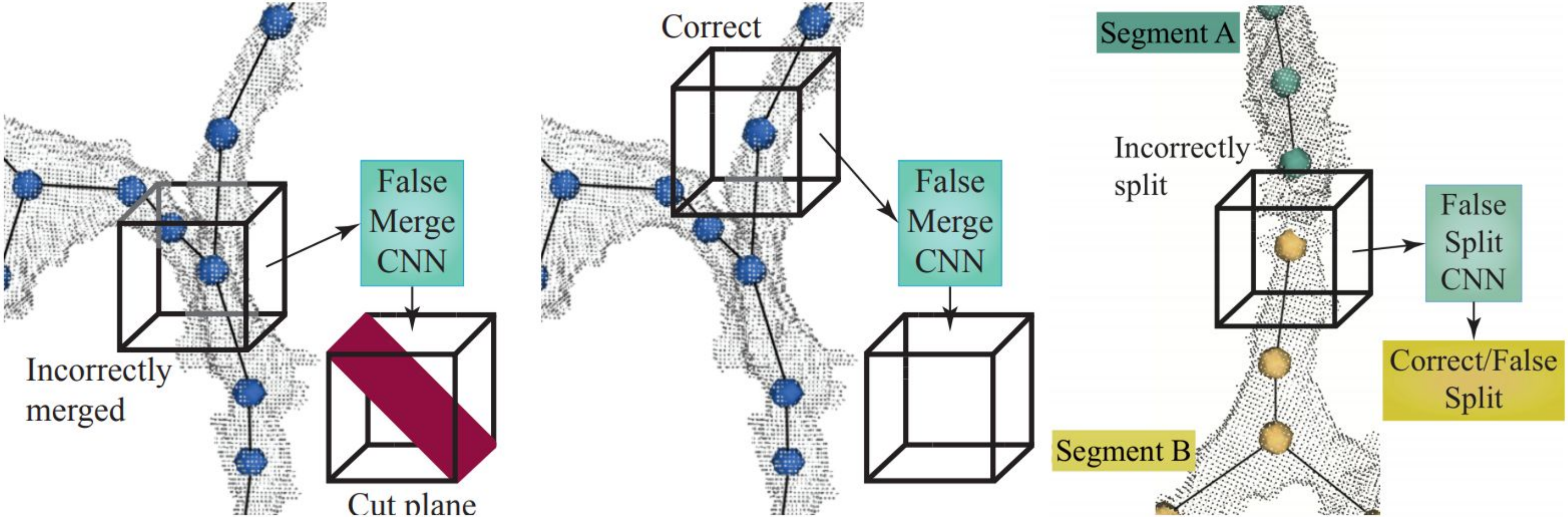

Berning *et al.*, SegEM: Efficient Image Analysis for High-Resolution Connectomes, Neuron 2015
Dmitriev *et al.*, Efficient Correction for EM Connectomics with Skeletal Representation, BMVC 2018
Matejek *et al.*, Biologically-Constrained Graphs for Global Connectomics Reconstruction, CVPR 2018

Improving Wiring Diagrams with Skeletons

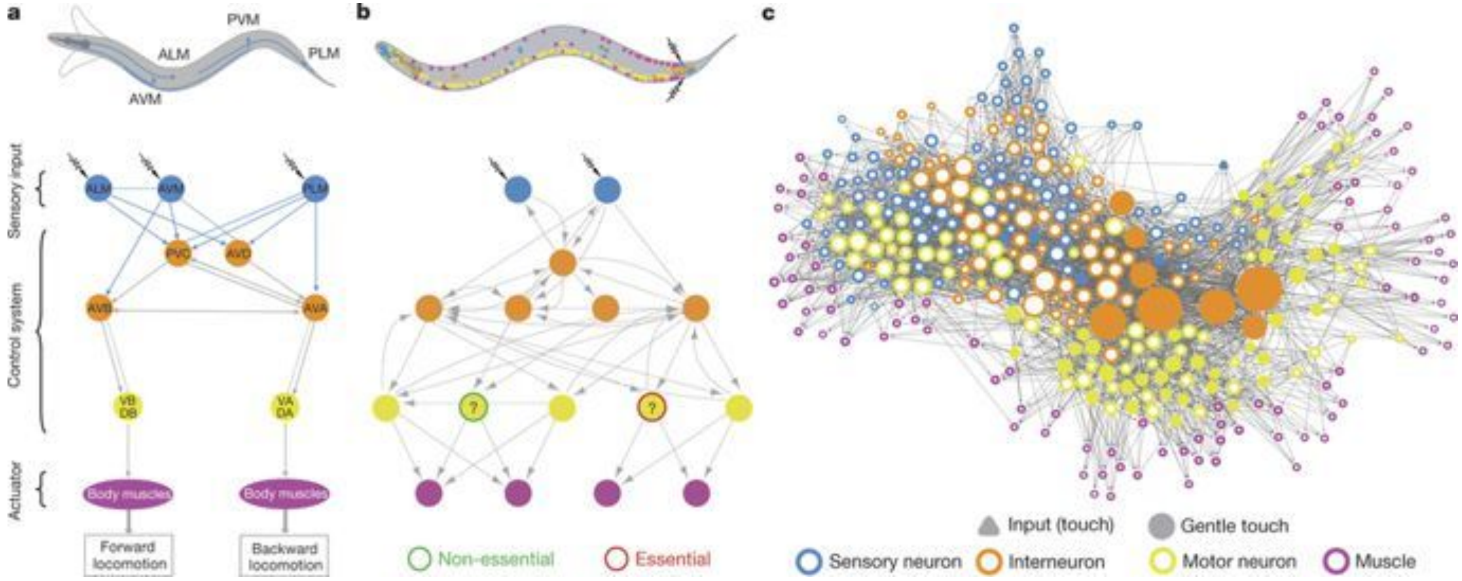

Yan *et al.*, Network Control Principles Predict Neuron Functions in the Caenorhabditis elegans Connectome, Nature 2017

Current Graph-Based Wiring Diagram Methodology

Each node represents one neuron

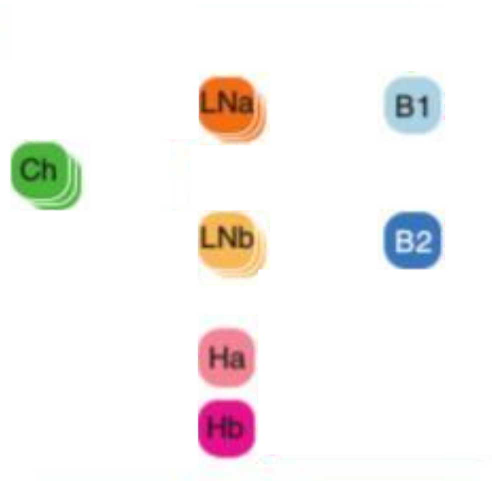

Jovanic *et al.*, Competitive Disinhibition Mediates Behavioral Choice and Sequences in Drosophila, Cell 2016

Current Graph-Based Wiring Diagram Methodology

Each node represents one neuron

Weighted edges indicate number of synapses between two neurons

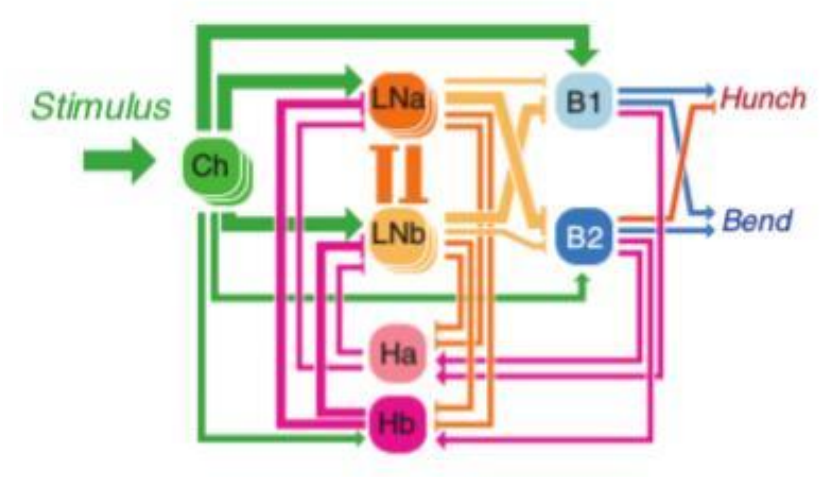

Jovanic *et al.*, Competitive Disinhibition Mediates Behavioral Choice and Sequences in Drosophila, Cell 2016

Information Lost in the Graph

Synapses that are closer to the cell body provide stronger signal

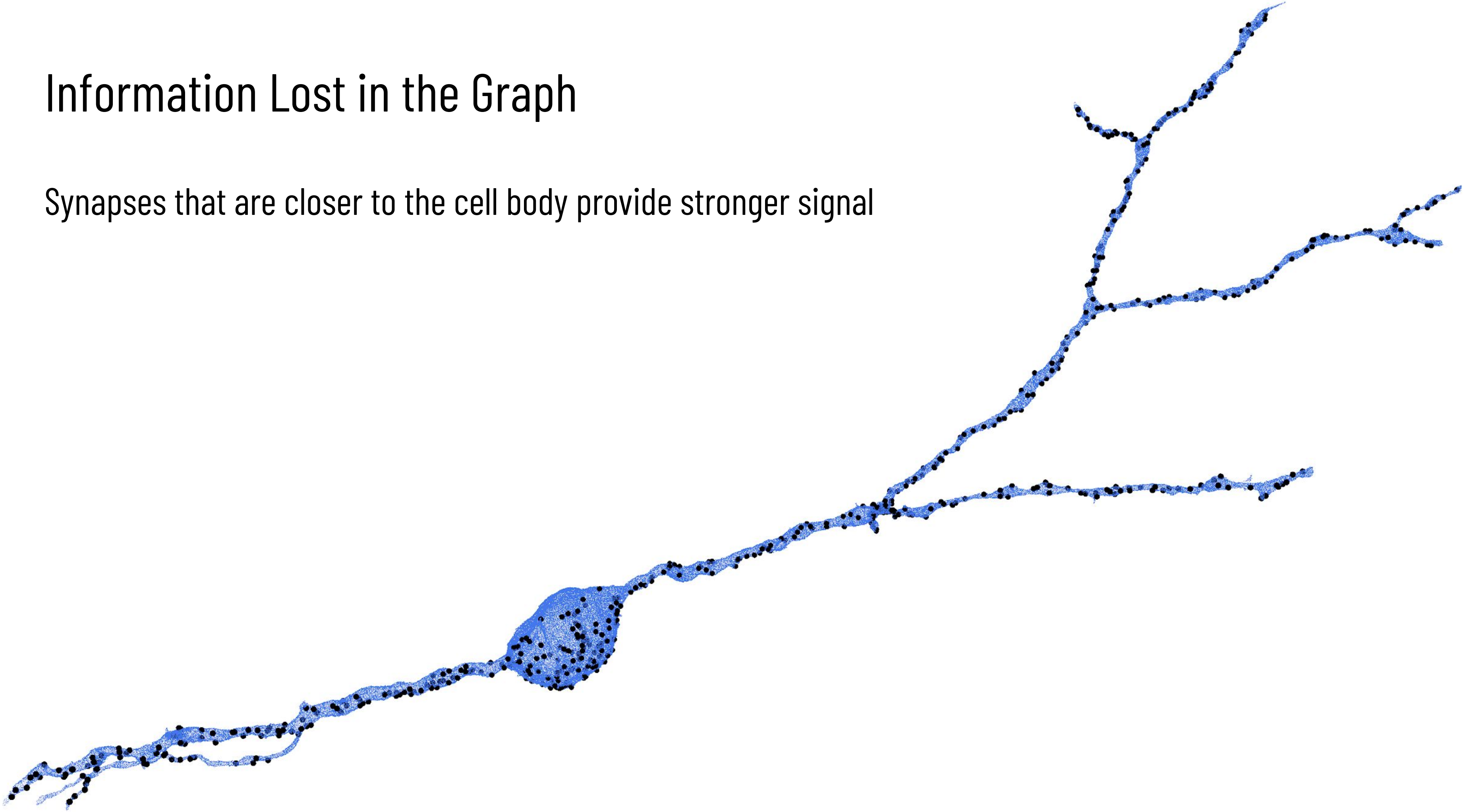

Information Lost in the Graph

Synapses that are closer to the cell body provide stronger signal

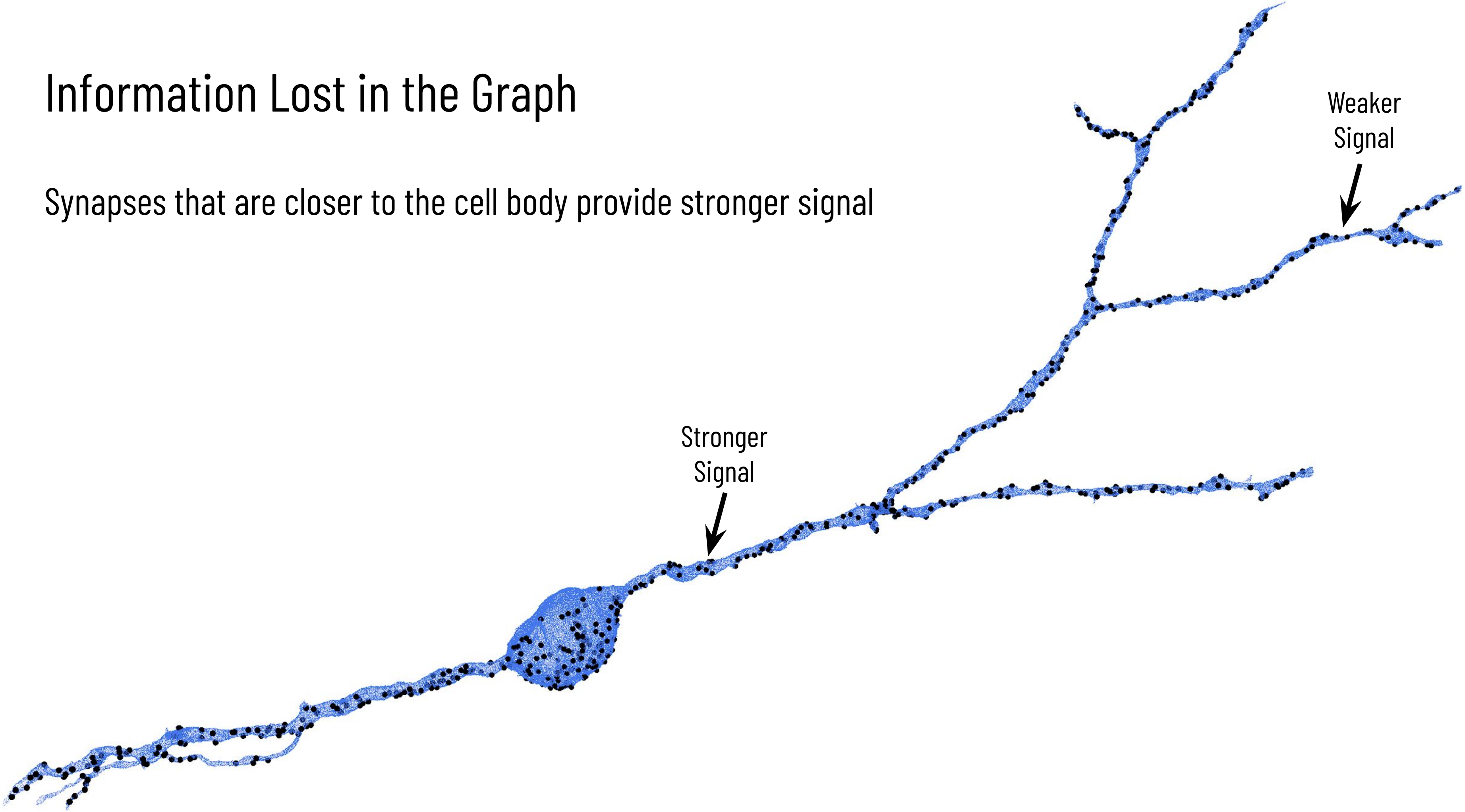

Information Lost in the Graph

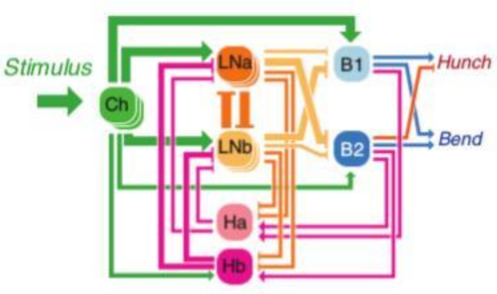

Can't rely only on number of connections alone

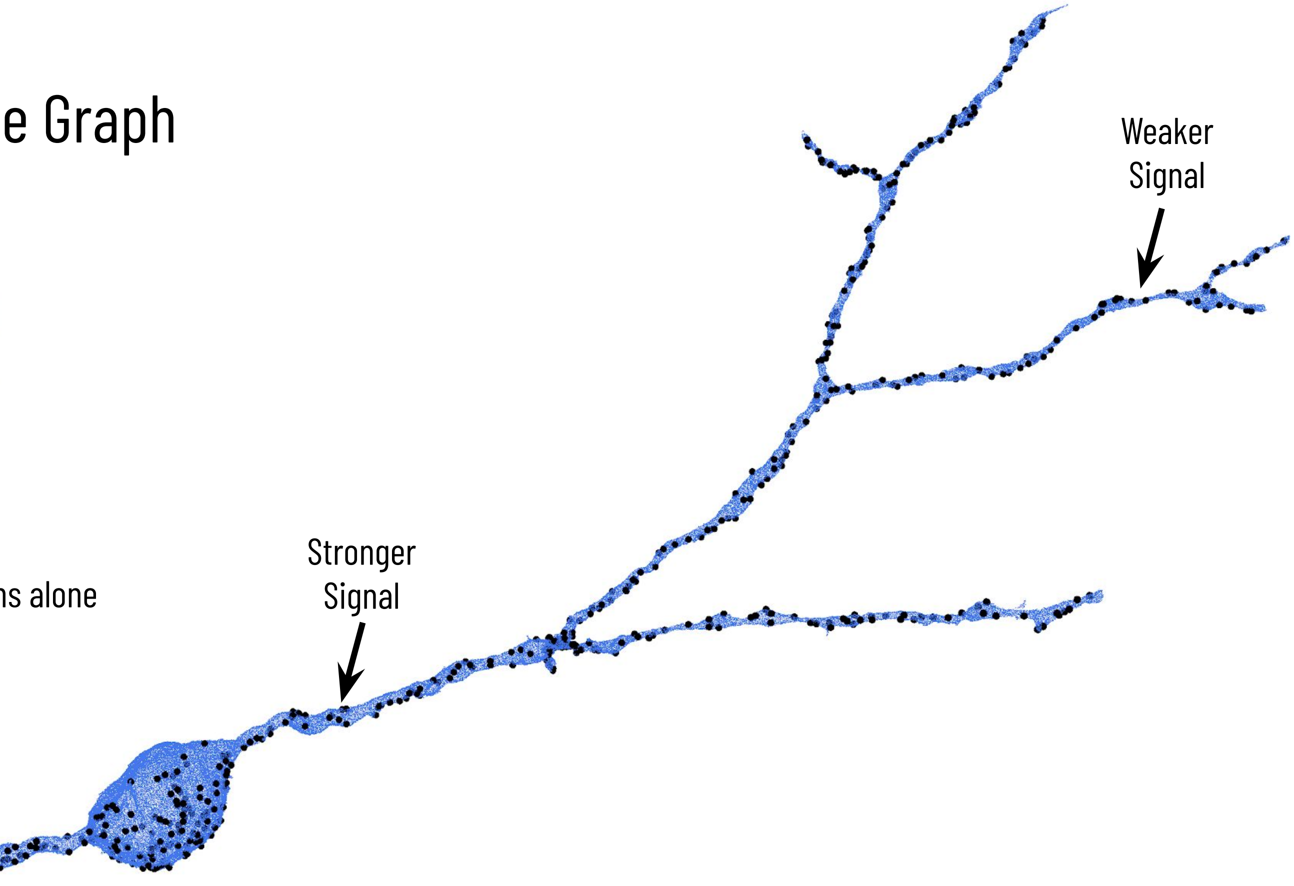

Information Lost in the Graph

Width of neuron along path from synapse to cell body

Information Lost in the Graph

Width of neuron along path from synapse to cell body

Cable Theory:

$$\frac{1}{r_l}\frac{\partial^2 V}{\partial x^2} = c_m \frac{\partial V}{\partial t} + \frac{V}{r_m}$$

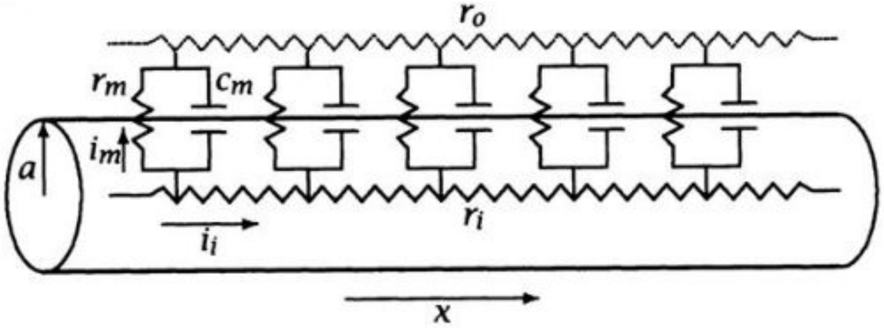

Johnston and Wu, Foundations of Cellular Neurophysiology, MIT Press 1995

Information Lost in the Graph

Width of neuron along path from synapse to cell body

Cable Theory:

$$\frac{1}{\boxed{r_l}}\frac{\partial^2 V}{\partial x^2} = \boxed{c_m}\frac{\partial V}{\partial t} + \frac{V}{\boxed{r_m}}$$

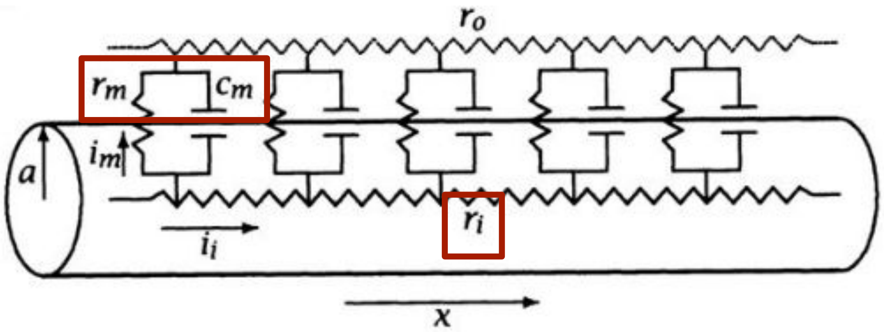

r_l, c_m, r_m are functions of the neurite diameter

Johnston and Wu, Foundations of Cellular Neurophysiology, MIT Press 1995

Biologically-Aware Skeleton Generation

Generate skeletons that connect all synapses to the cell body

Biologically-Aware Skeleton Generation

Generate skeletons that connect all synapses to the cell body

Calculate vital geometric statistics needed for evaluating the perceived synaptic strength like geodesic distance from the synapse to the cell body and the width along each neurite

Block-Based Processing

Connectome label volumes now regularly exceed hundreds of gigabytes

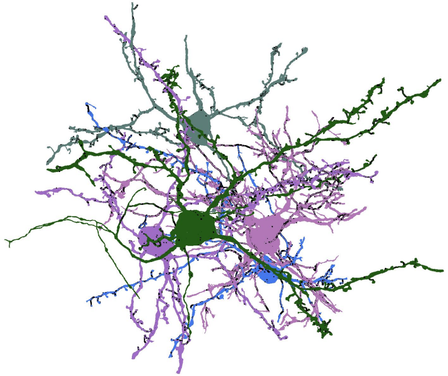

Block-Based Processing

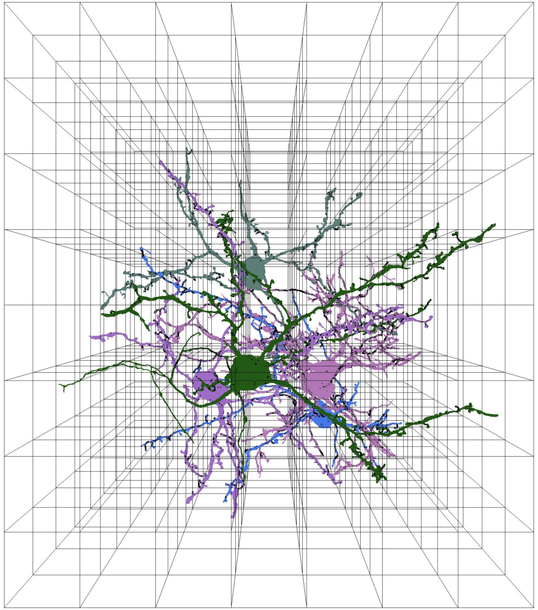

Connectome label volumes now regularly exceed hundreds of gigabytes

Processing needs to be mostly block-based for widespread adoption

Block-Based Processing

Connectome label volumes now regularly exceed hundreds of gigabytes

Processing needs to be mostly block-based for widespread adoption

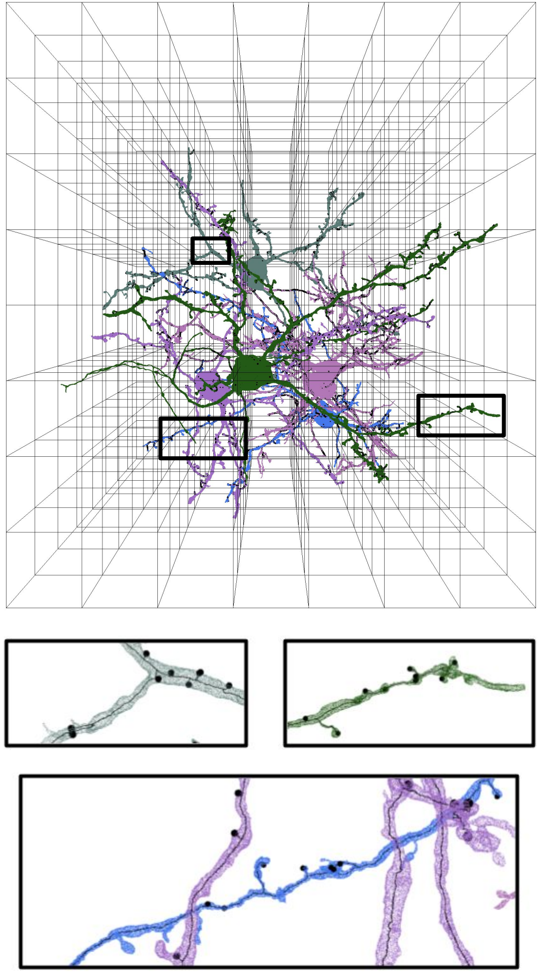

Tree-structure Extraction Algorithm for Accurate and Robust Skeletons

TEASER is the predominantly used skeleton generation technique for connectomics

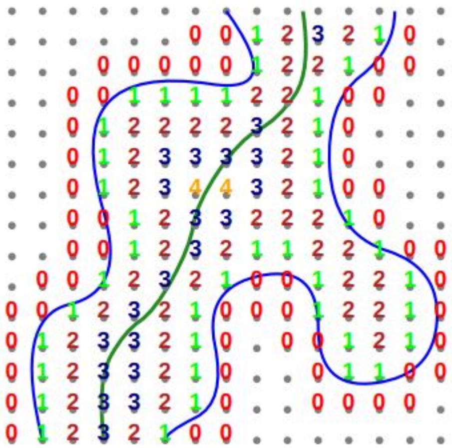

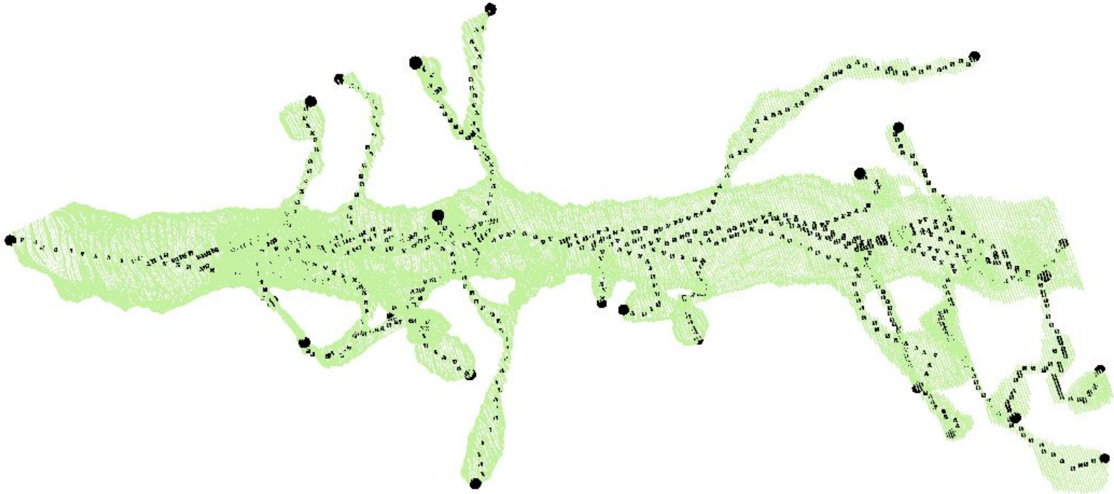

Sato *et al.*,TEASER: Tree-structure Extraction Algorithm for Accurate and Robust Skeletons, PCCGA 2000
Zhao *et al.*, NeuTu: Software for Collaborative, Large-Scale, Segmentation-Based Connectome Reconstruction, Frontiers in Neural Circuits 2018

Tree-structure Extraction Algorithm for Accurate and Robust Skeletons

TEASER is the predominantly used skeleton generation technique for connectomics

The algorithm continually identifies distant voxels to attach to a root voxel using Dijkstra's algorithm

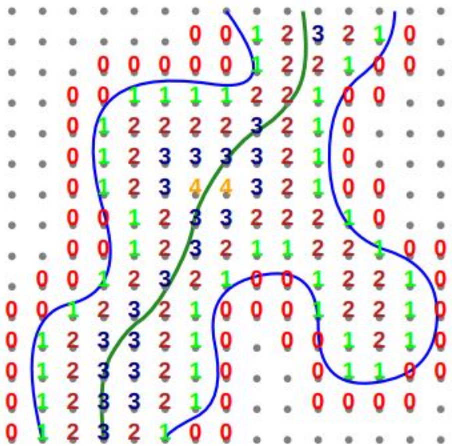

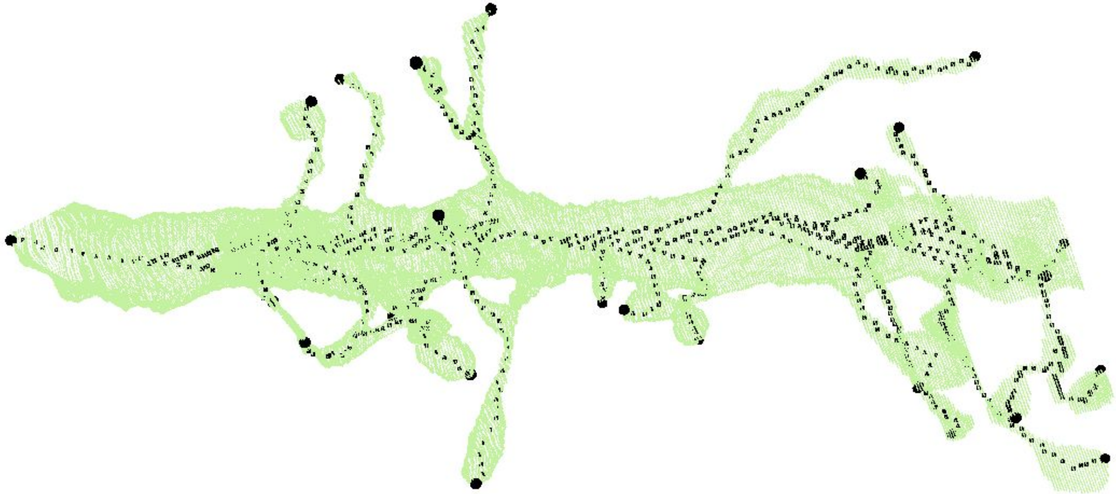

Sato *et al.*,TEASER: Tree-structure Extraction Algorithm for Accurate and Robust Skeletons, PCCGA 2000
Zhao *et al.*, NeuTu: Software for Collaborative, Large-Scale, Segmentation-Based Connectome Reconstruction, Frontiers in Neural Circuits 2018

Tree-structure Extraction Algorithm for Accurate and Robust Skeletons

Silversmith *et al.*, have implemented a block-based version of the algorithm for larger connectome volumes

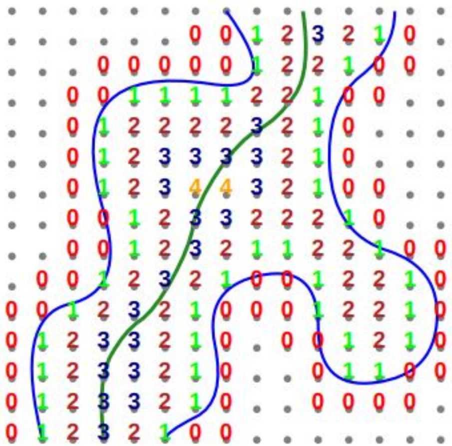

•	•	•	•	•	•	•	•	•	•	•	•	•	•	•
•	•	•	•	•	•	0	0	1	2	3	2	1	0	•
•	•	•	0	0	0	0	0	1	2	2	1	0	0	•
•	•	0	0	1	1	1	1	2	2	1	0	0	•	•
•	•	0	1	2	2	2	2	3	2	1	0	•	•	•
•	•	0	1	2	3	3	3	3	2	1	0	•	•	•
•	•	0	1	2	3	4	4	3	2	1	0	0	•	•
•	•	0	0	1	2	3	3	2	2	2	1	0	•	•
•	•	0	0	1	2	3	2	1	1	2	2	1	0	0
•	0	0	1	2	3	2	1	0	0	1	2	2	1	0
0	0	1	2	3	2	1	0	0	0	1	2	2	1	0
0	1	2	3	3	2	1	0	•	0	0	1	2	1	0
0	1	2	3	3	2	1	0	•	•	0	1	1	0	0
0	1	2	3	3	2	1	0	•	•	0	0	0	0	•
0	1	2	3	2	1	0	0	•	•	•	•	•	•	•

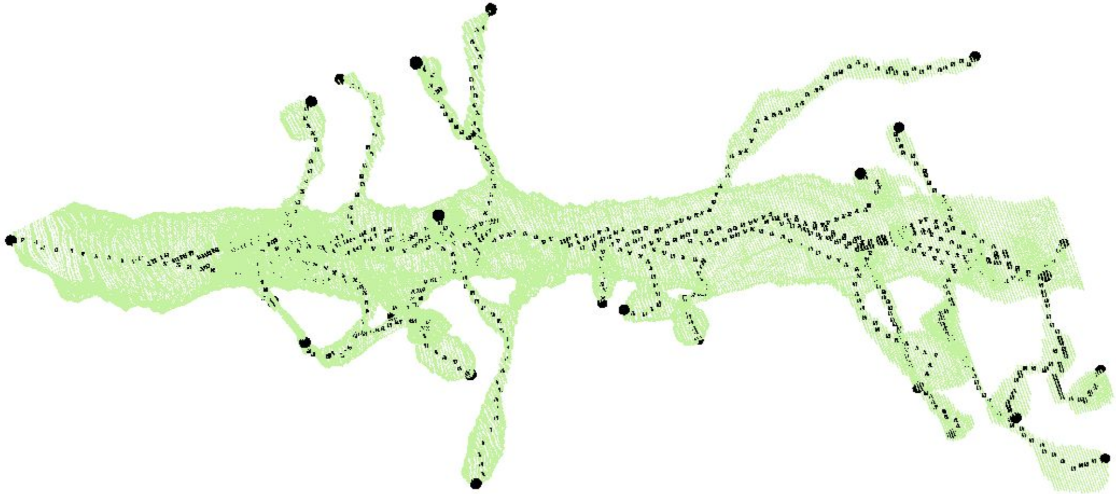

Silversmith *et al.*, Kimimaro: Skeletonize Densely Labeled 3D Image Segmentations, https://github.com/seung-lab/kimimaro

Topological Thinning

Topological thinning algorithms gradually erode the surface of a volume to a centerline

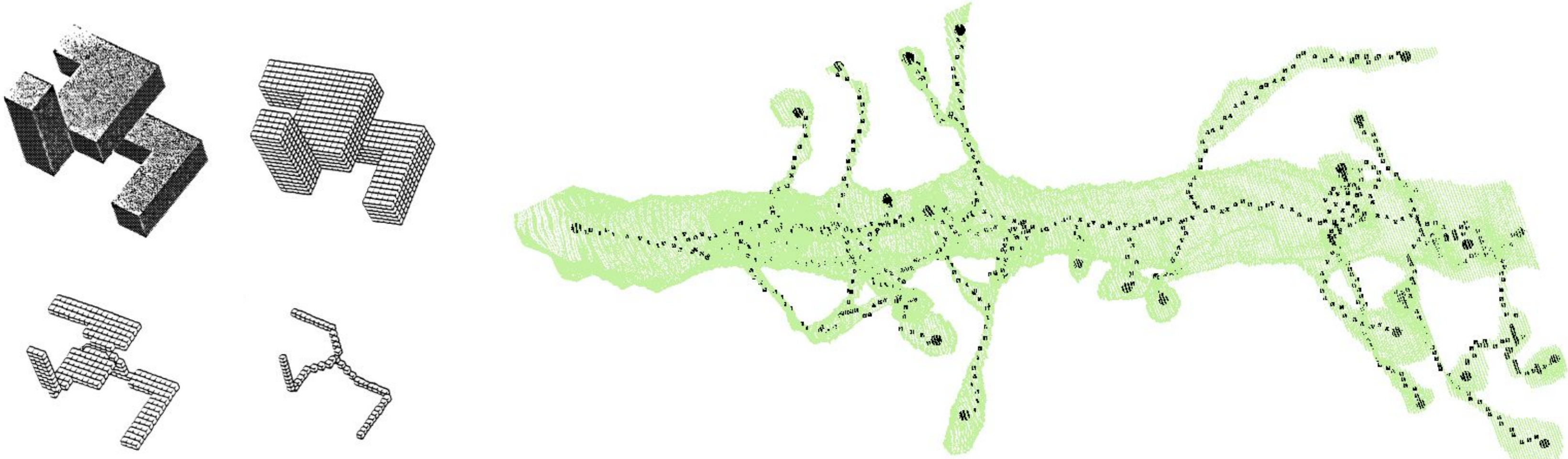

Lee *et al.*, Building Skeleton Models via 3-D Medial Surface Axis Thinning Algorithms, CVGIP 1994

Topological Thinning

Topological thinning algorithms erode the surface of a volume to a centerline while preserving topology

These algorithms rely only on the immediate local neighborhood around a voxel to determine deletion

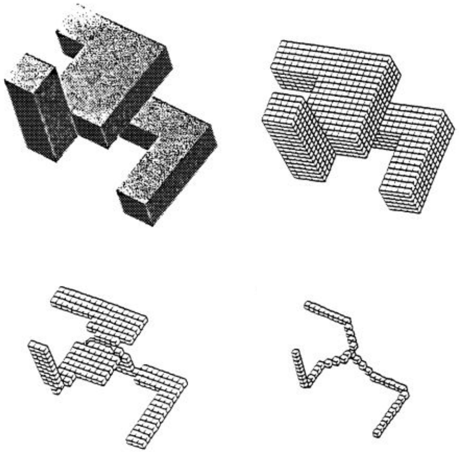

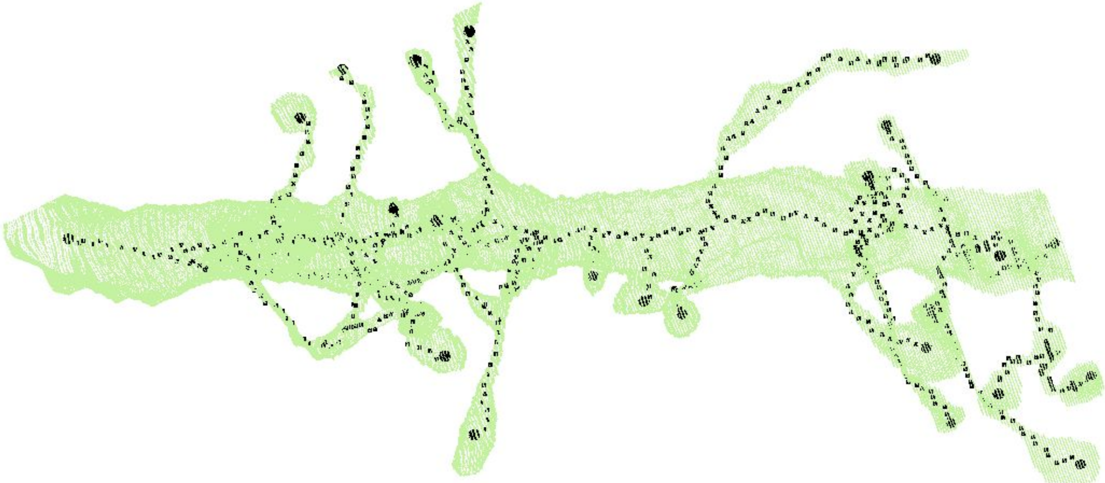

Lee *et al.*, Building Skeleton Models via 3-D Medial Surface Axis Thinning Algorithms, CVGIP 1994

Topological Thinning

Topological thinning algorithms iteratively consider all voxels on the boundary of a volume for deletion

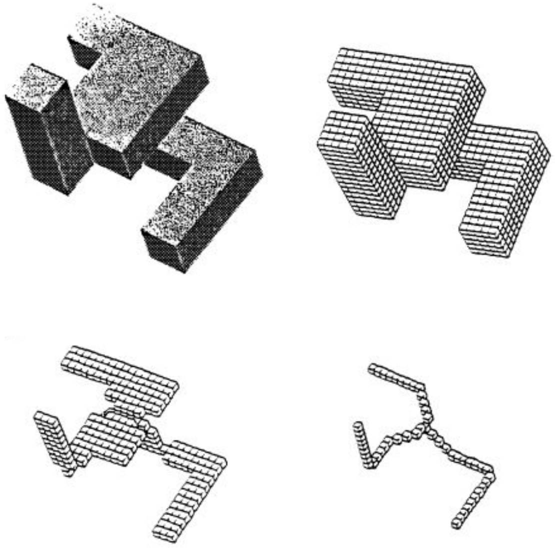

Lee *et al.*, Building Skeleton Models via 3-D Medial Surface Axis Thinning Algorithms, CVGIP 1994

Topological Thinning

Topological thinning algorithms iteratively consider all voxels on the boundary of a volume for deletion

Points that are considered “Simple” are deleted, i.e., those that do not change the topology of the object

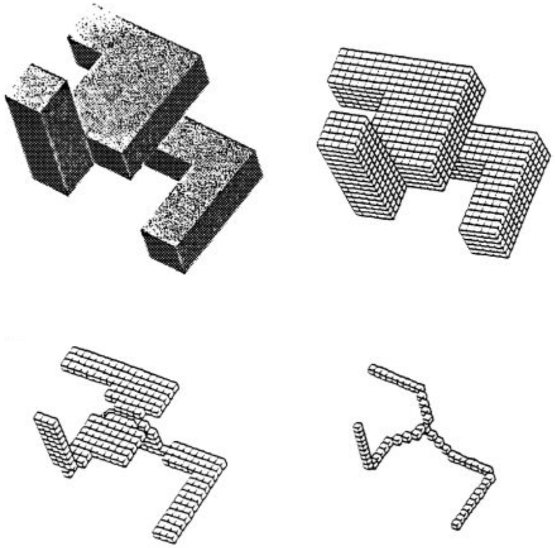

Lee *et al.*, Building Skeleton Models via 3-D Medial Surface Axis Thinning Algorithms, CVGIP 1994

Topological Thinning

However, certain points (e.g., endpoints) are preserved despite being simple

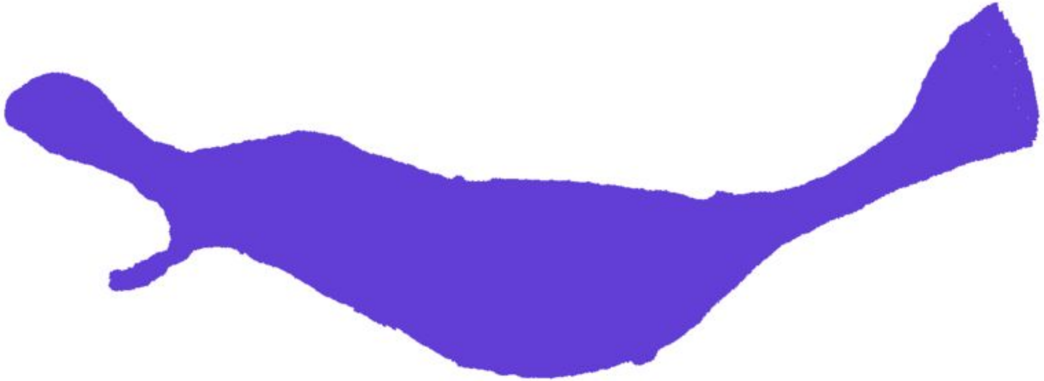

Isthmus Thinning

Other extensions on topological thinning define classes of voxels (e.g., isthmuses) that cannot be deleted to both preserve topology and create more expressive skeletons

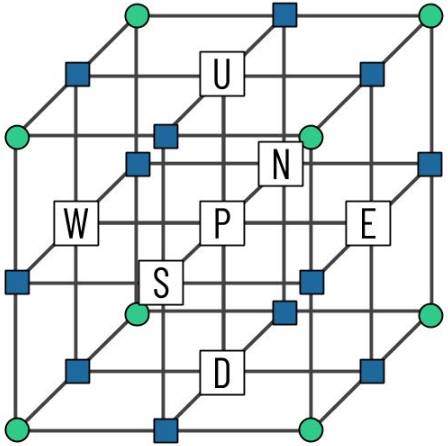

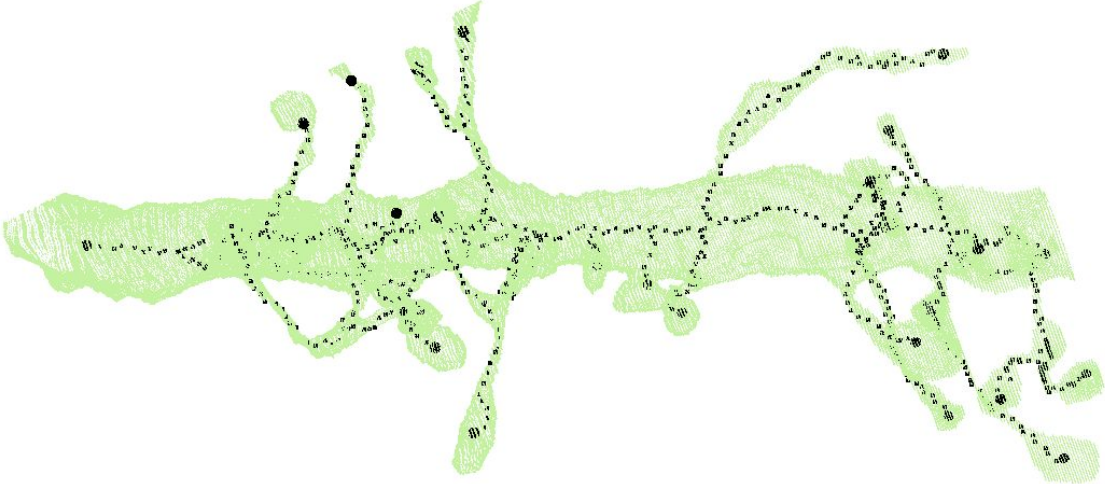

Palagyi, K., A Sequential 3D Curve-Thinning Algorithm Based on Isthmuses, International Symposium on Visual Computing 2014.

Proposed Skeleton Generation

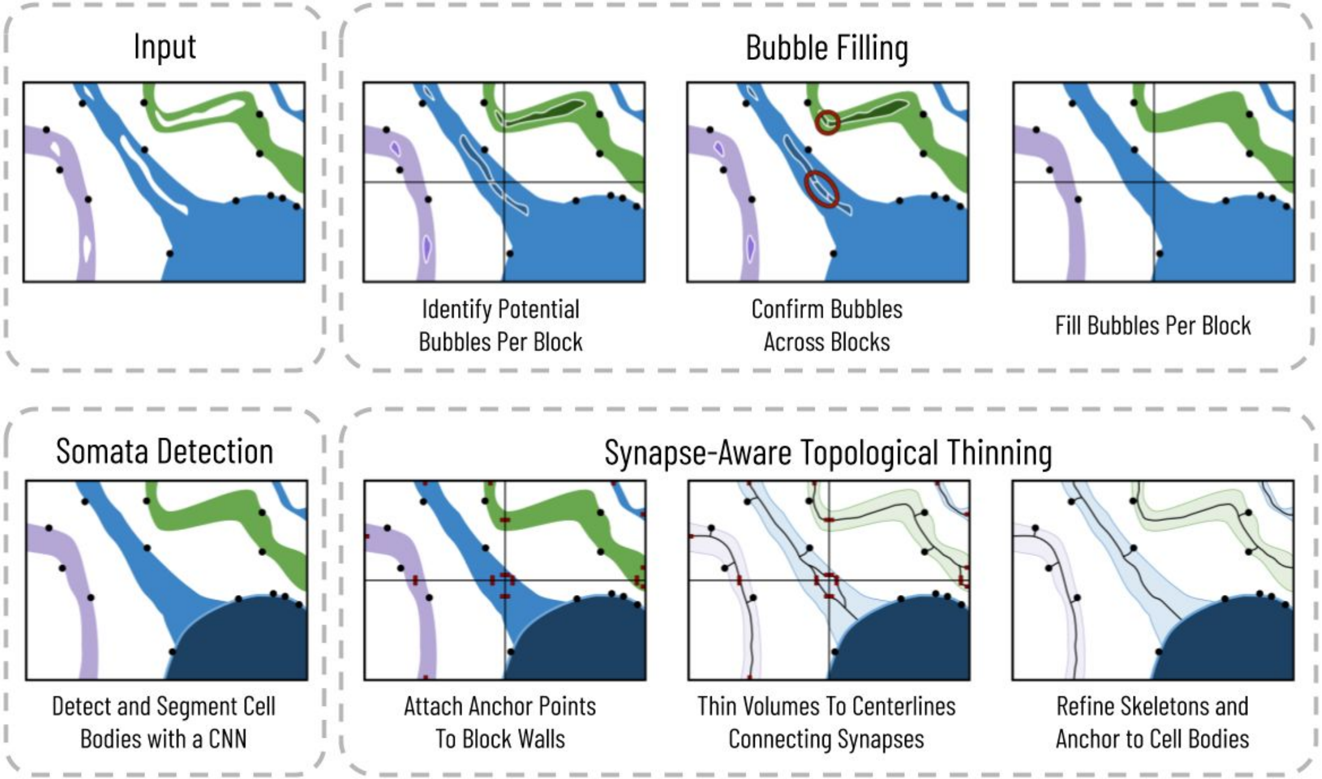

Input

Bubble Filling

Identify Potential Bubbles Per Block

Confirm Bubbles Across Blocks

Fill Bubbles Per Block

Somata Detection

Detect and Segment Cell Bodies with a CNN

Synapse-Aware Topological Thinning

Attach Anchor Points To Block Walls

Thin Volumes To Centerlines Connecting Synapses

Refine Skeletons and Anchor to Cell Bodies

Input

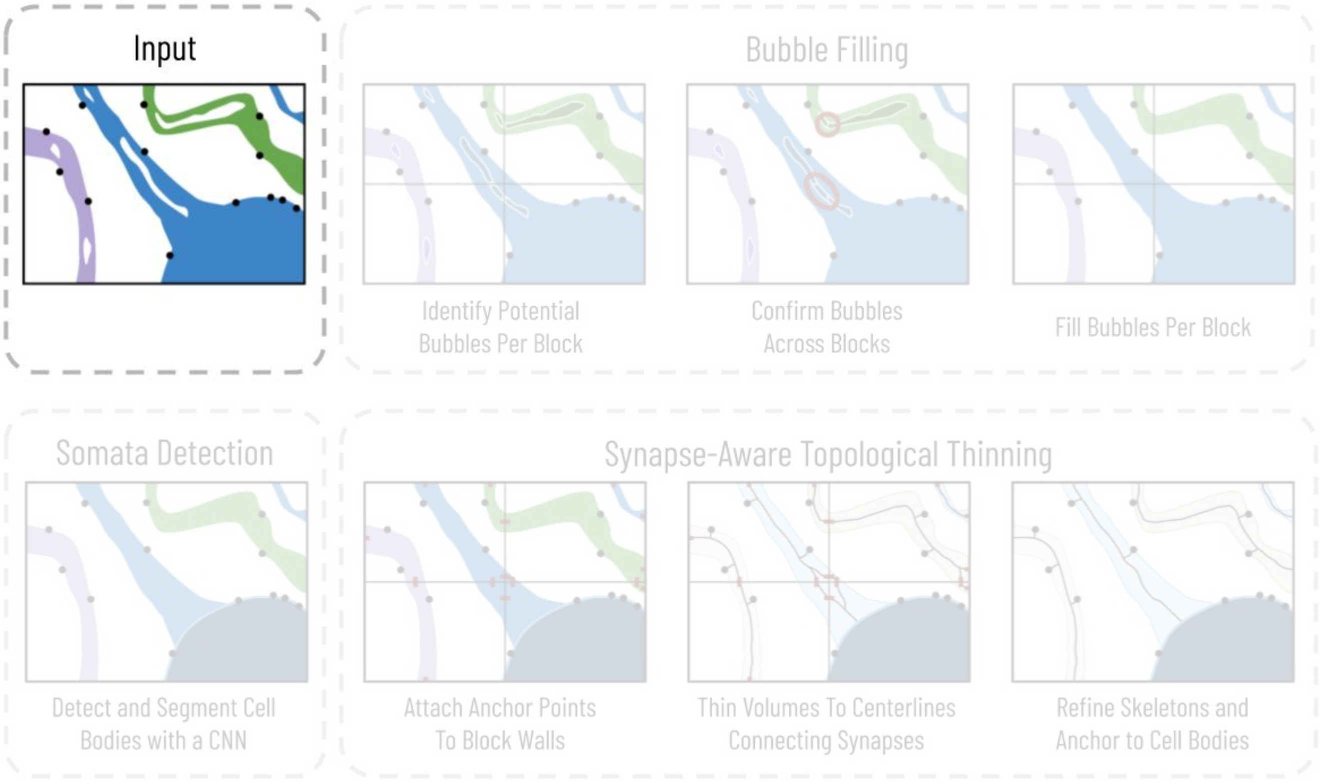

Input

Bubble Filling

Identify Potential Bubbles Per Block

Confirm Bubbles Across Blocks

Fill Bubbles Per Block

Somata Detection

Detect and Segment Cell Bodies with a CNN

Synapse-Aware Topological Thinning

Attach Anchor Points To Block Walls

Thin Volumes To Centerlines Connecting Synapses

Refine Skeletons and Anchor to Cell Bodies

Input Segmentations and Synapses

Our method takes as input a label volume and a corresponding set of synapse locations

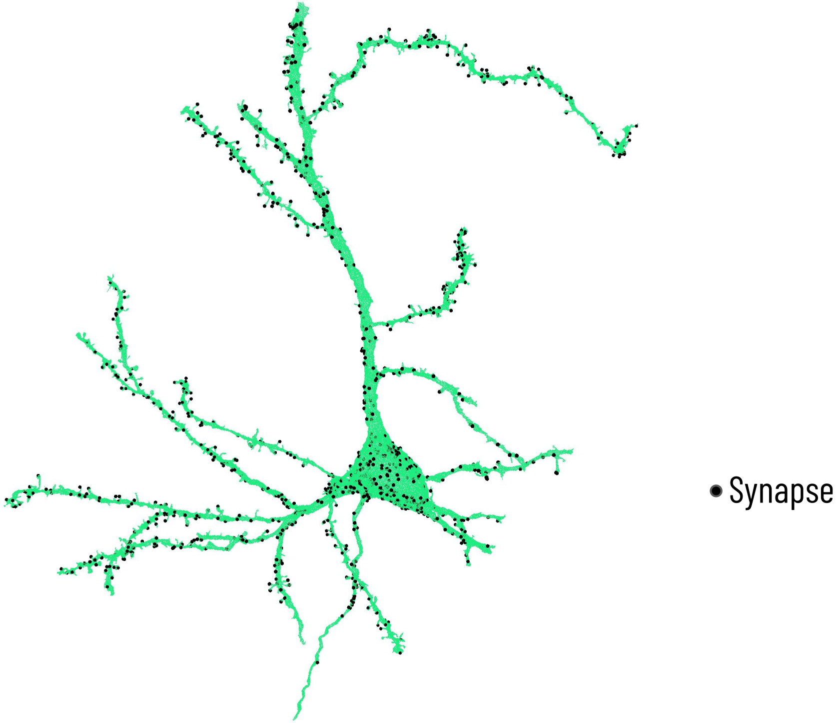

Bubbles in Input Segmentation

Segmentations can contain millions of bubbles

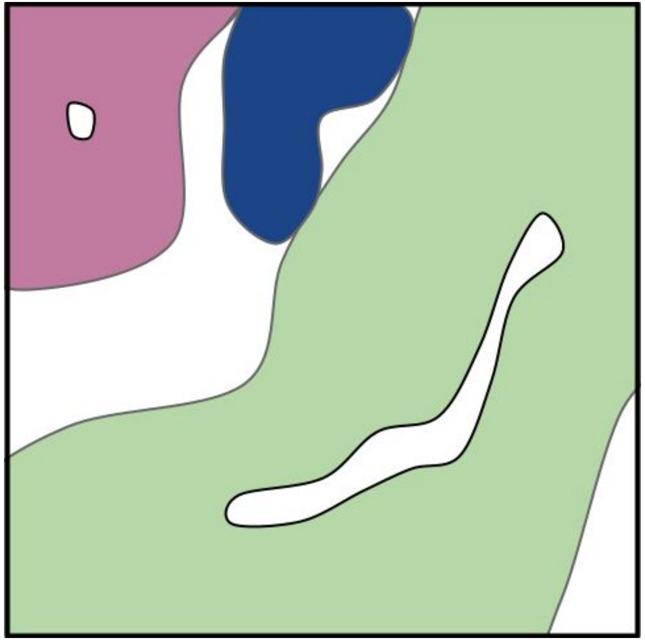

Bubbles in Input Segmentation

Segmentations can contain millions of bubbles, i.e., pockets of mislabeled voxels contained within a label

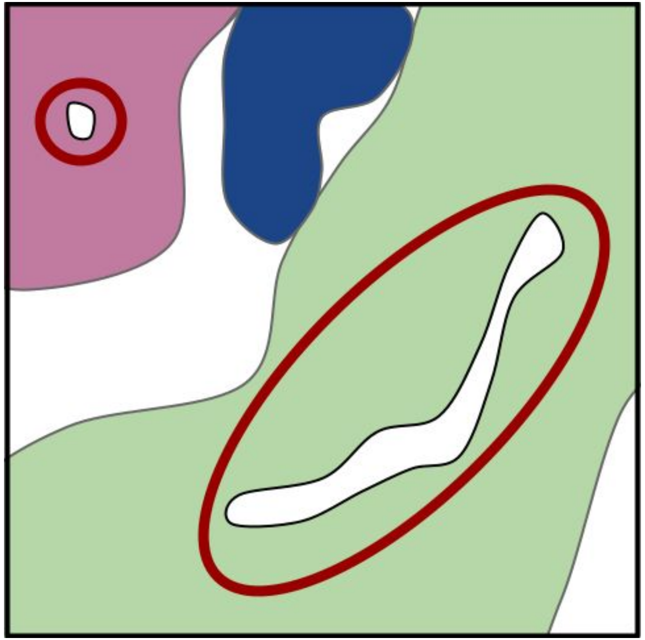

Bubbles in Input Segmentation

These bubbles can span across multiple blocks and therefore we need to consider global information

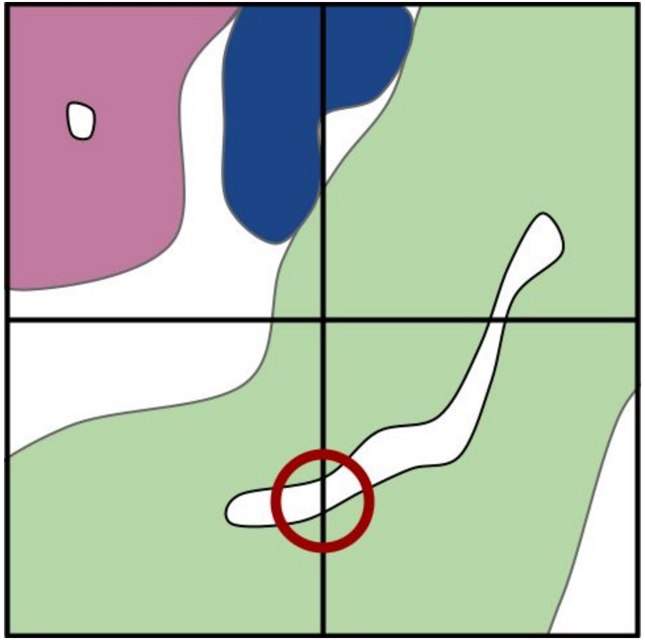

Bubbles in Input Segmentation

These biologically-infeasible bubbles increase thinning runtime and cause errors in width estimation

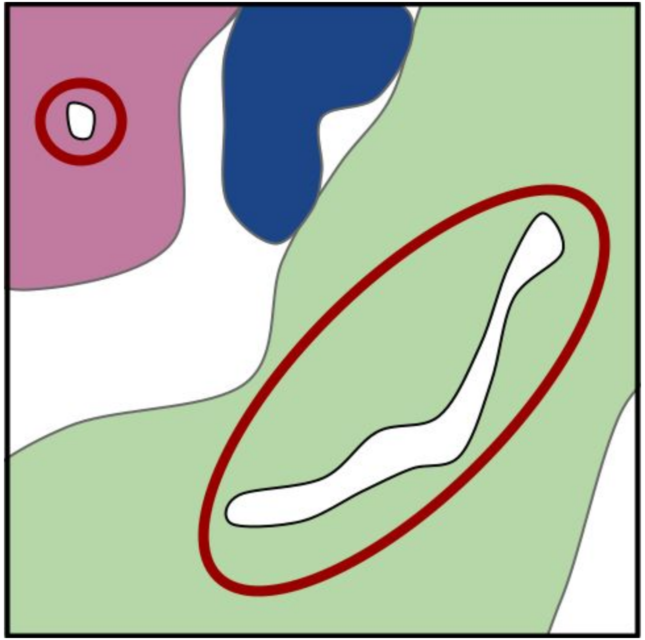

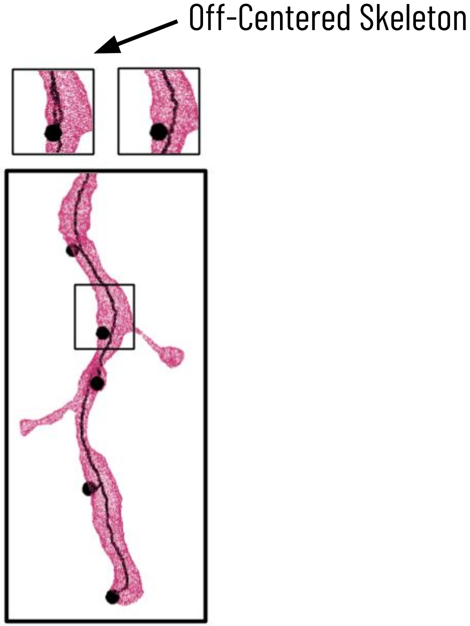

Goal: Fill bubbles in the input segmentation

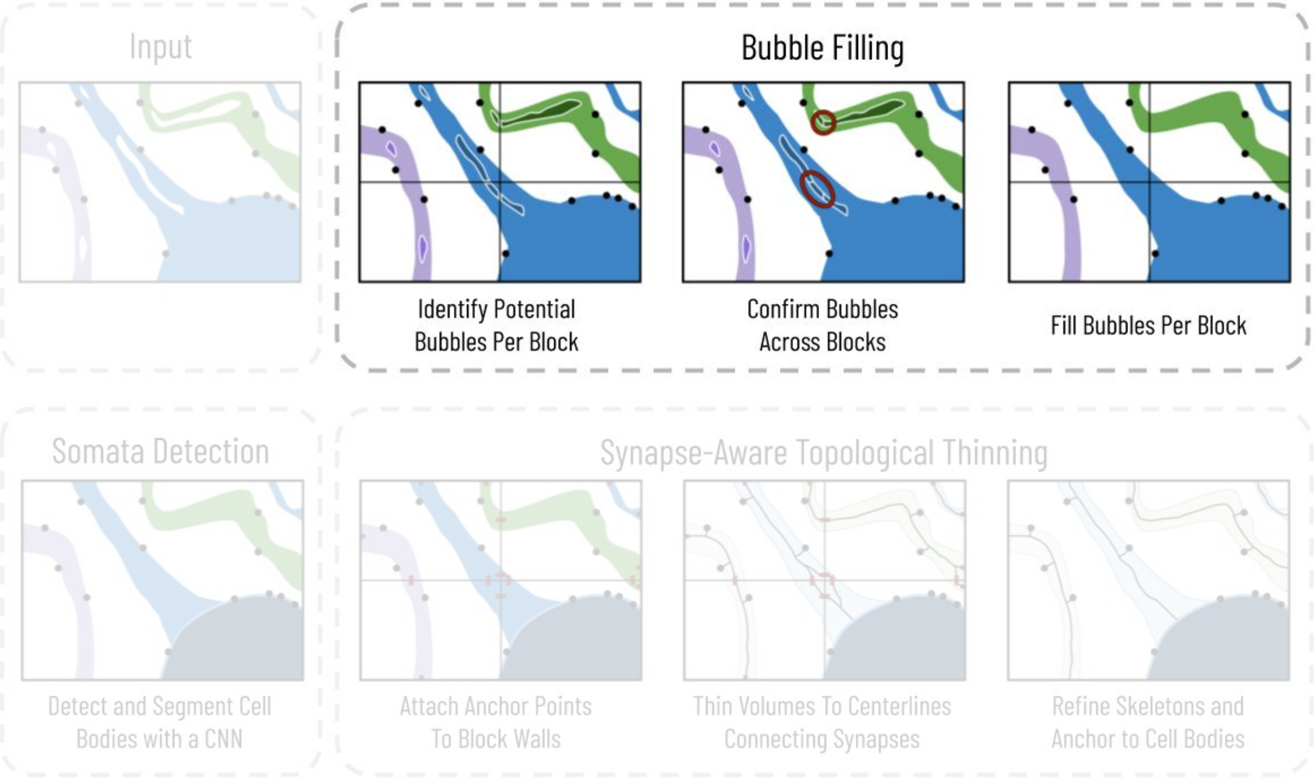

Parallelizable Bubble Filling

We divide the bubble filling process into two computationally expensive but parallelizable operations and one computationally cheap step that requires global scope

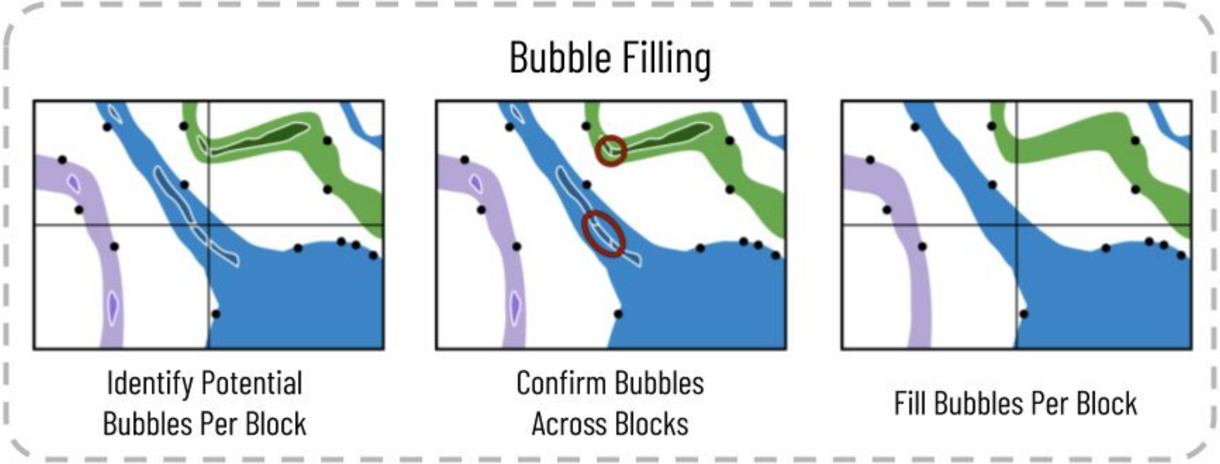

Identify Potential Bubbles Per Block

Our method identifies bubbles per block

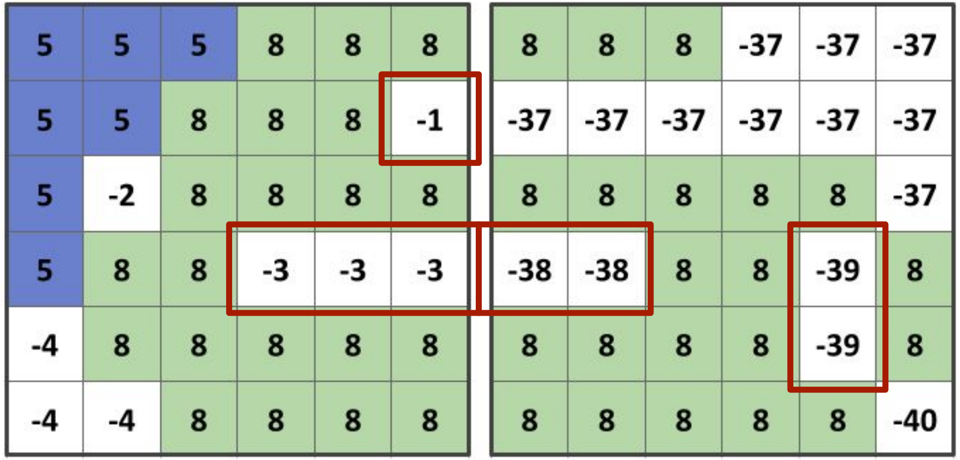

5	5	5	8	8	8
5	5	8	8	8	-1
5	-2	8	8	8	8
5	8	8	-3	-3	-3
-4	8	8	8	8	8
-4	-4	8	8	8	8

8	8	8	-37	-37	-37
-37	-37	-37	-37	-37	-37
8	8	8	8	8	-37
-38	-38	8	8	-39	8
8	8	8	8	-39	8
8	8	8	8	8	-40

Identify Potential Bubbles Per Block

Our method identifies bubbles per block, links bubbles across blocks

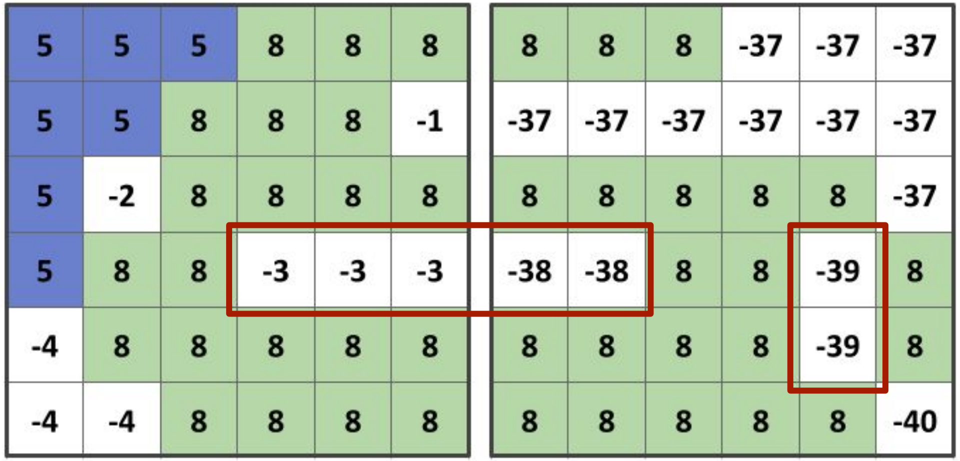

5	5	5	8	8	8
5	5	8	8	8	-1
5	-2	8	8	8	8
5	8	8	-3	-3	-3
-4	8	8	8	8	8
-4	-4	8	8	8	8

8	8	8	-37	-37	-37
-37	-37	-37	-37	-37	-37
8	8	8	8	8	-37
-38	-38	8	8	-39	8
8	8	8	8	-39	8
8	8	8	8	8	-40

Identify Potential Bubbles Per Block

Our method identifies bubbles per block, links bubbles across blocks, and then fills in the bubbles creating dense neurons

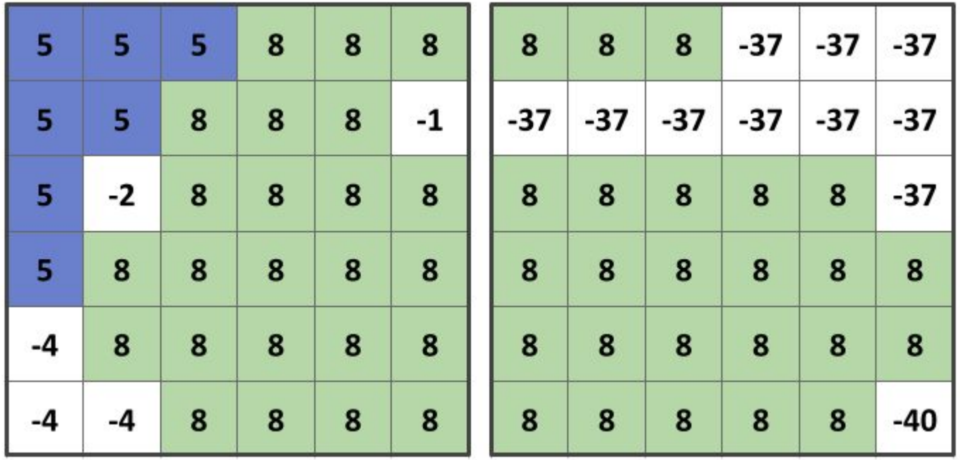

5	5	5	8	8	8
5	5	8	8	8	-1
5	-2	8	8	8	8
5	8	8	8	8	8
-4	8	8	8	8	8
-4	-4	8	8	8	8

8	8	8	-37	-37	-37
-37	-37	-37	-37	-37	-37
8	8	8	8	8	-37
8	8	8	8	8	8
8	8	8	8	8	8
8	8	8	8	8	-40

Goal: Detect somata to anchor skeletons onto the cell body

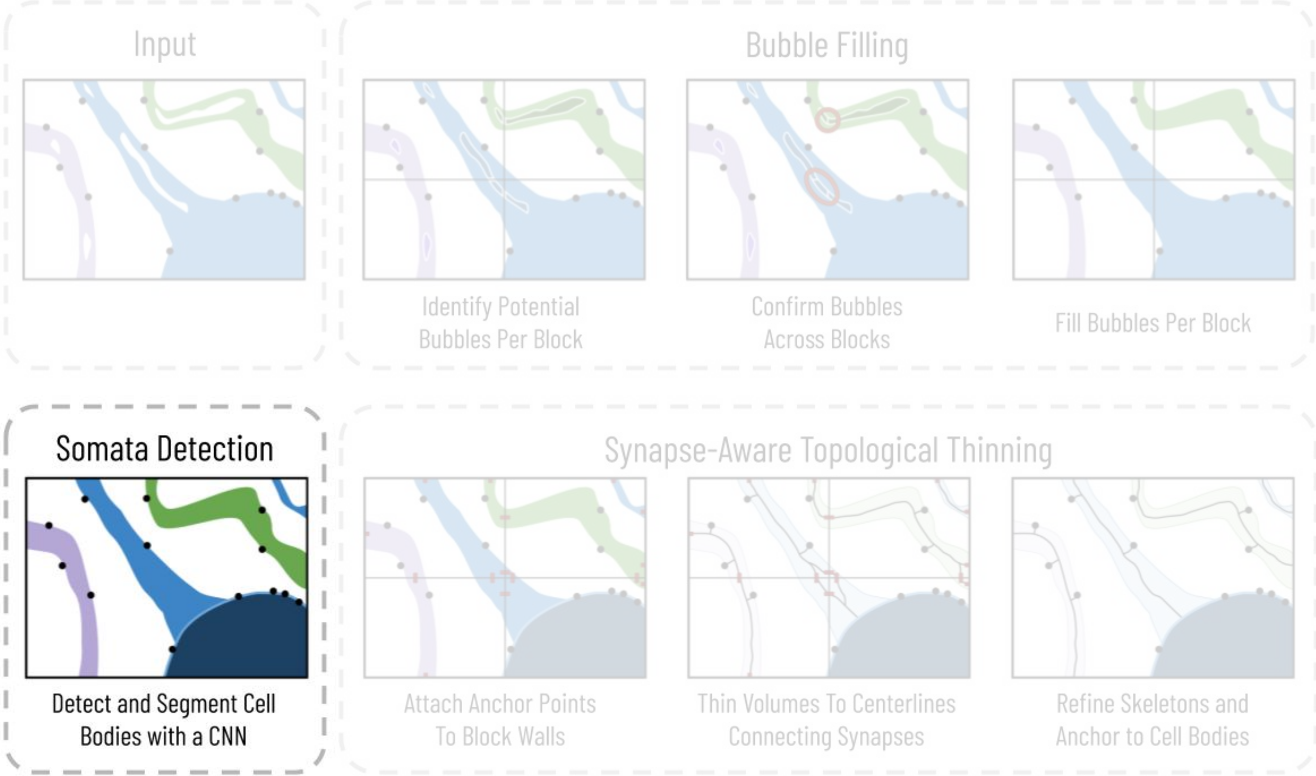

Cell Bodies

We can significantly reduce the total runtime by masking out the cell bodies before thinning

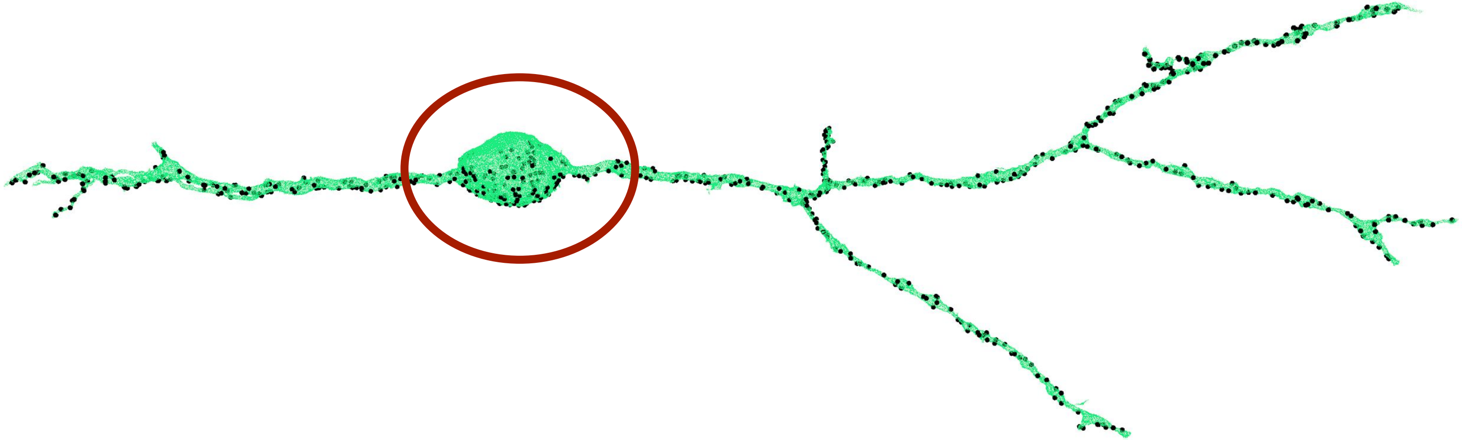

Cell Bodies

We can significantly reduce the total runtime by masking out the cell bodies before thinning

In some volumes, cell bodies represent up to 65% of the total volume

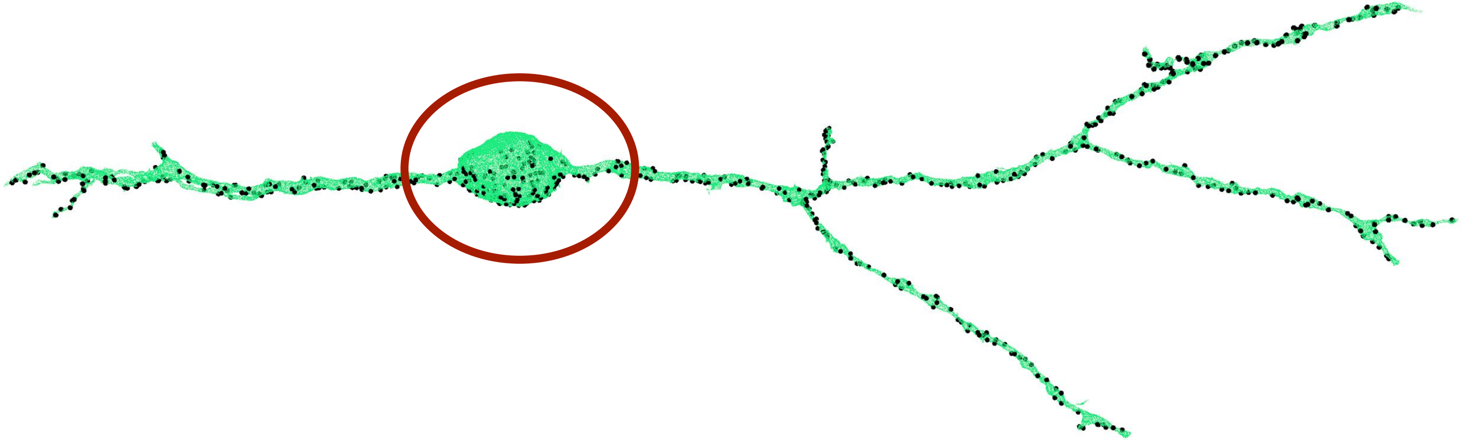

Cell Bodies

We can significantly reduce the total runtime by masking out the cell bodies before thinning

In some volumes, cell bodies represent up to 65% of the total volume

This also enables us to anchor the skeletons on the cell body

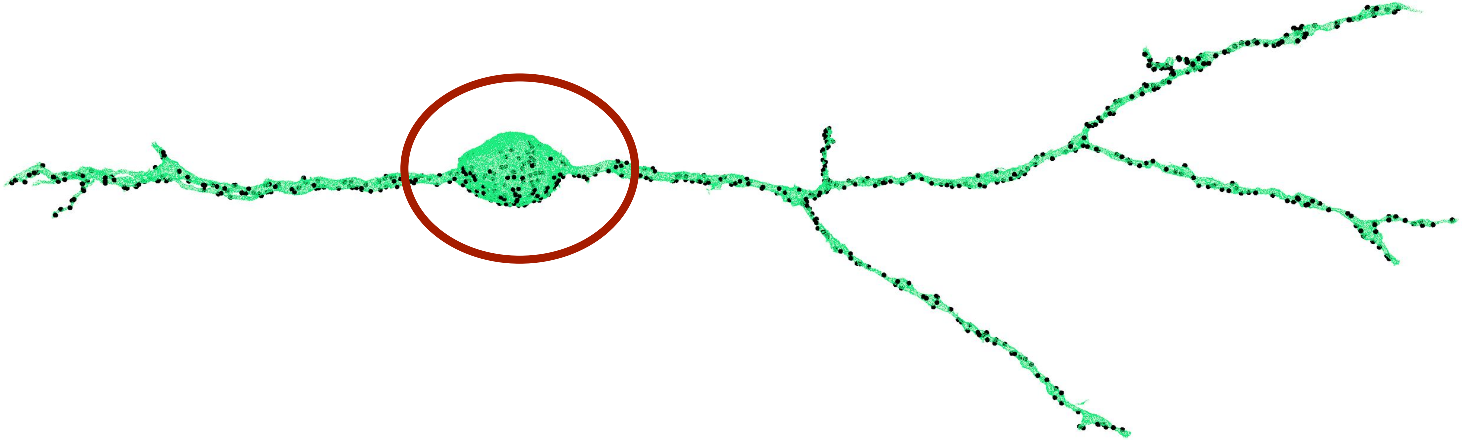

Cell Body Detection

We train a U-Net to identify individual cell bodies in each slice of the label volume

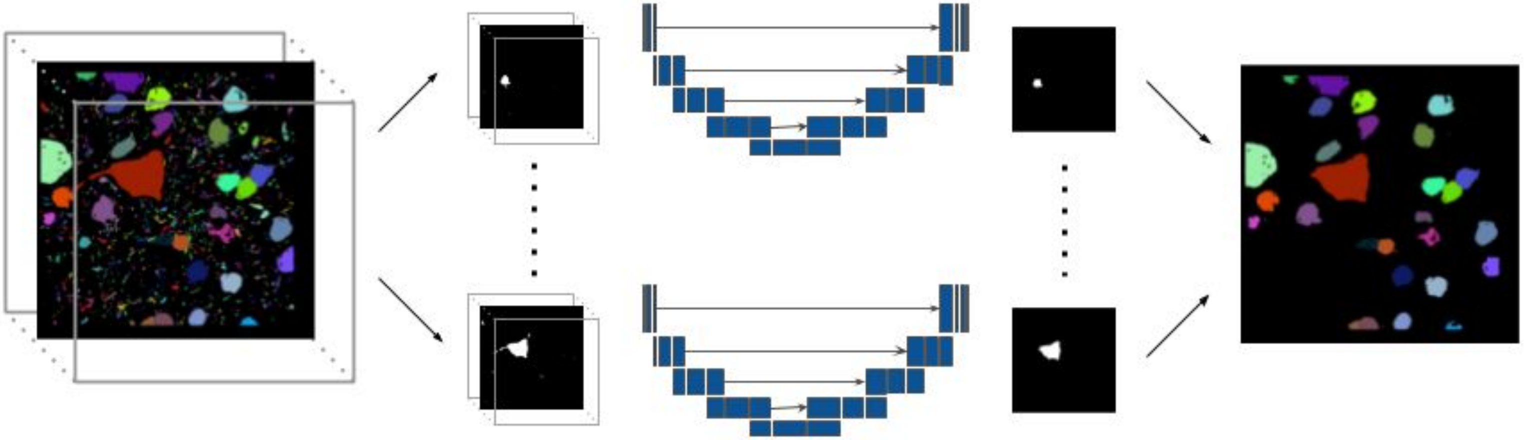

Cell Body Detection

We train a U-Net to identify individual cell bodies in each slice of the label volume

We find that U-Nets trained on one dataset transfer well to others

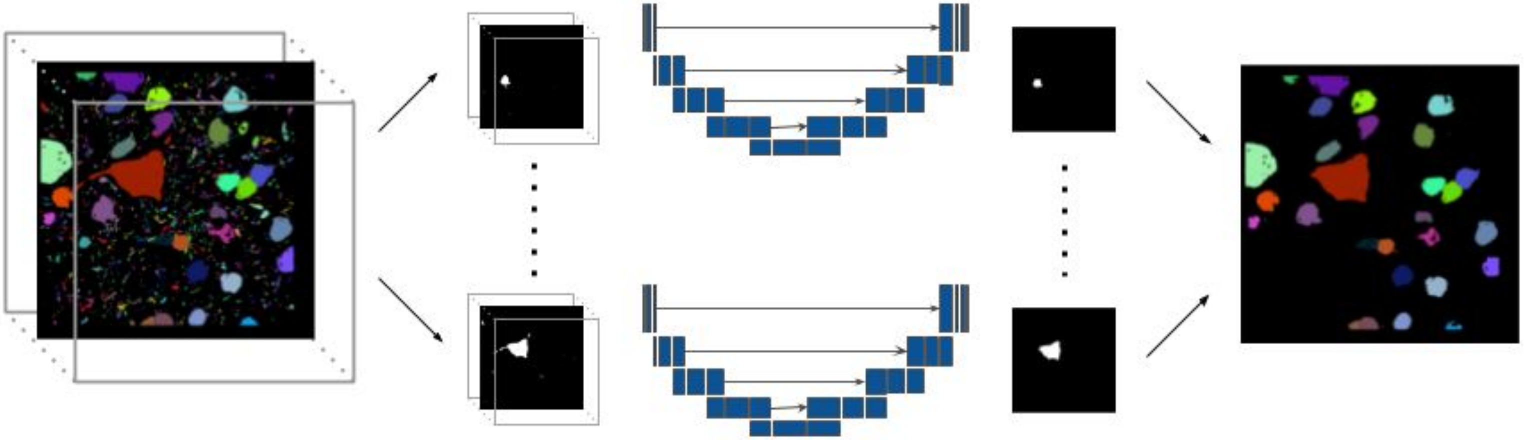

Goal: Extract accurate skeletons that connect all synapses to the cell body

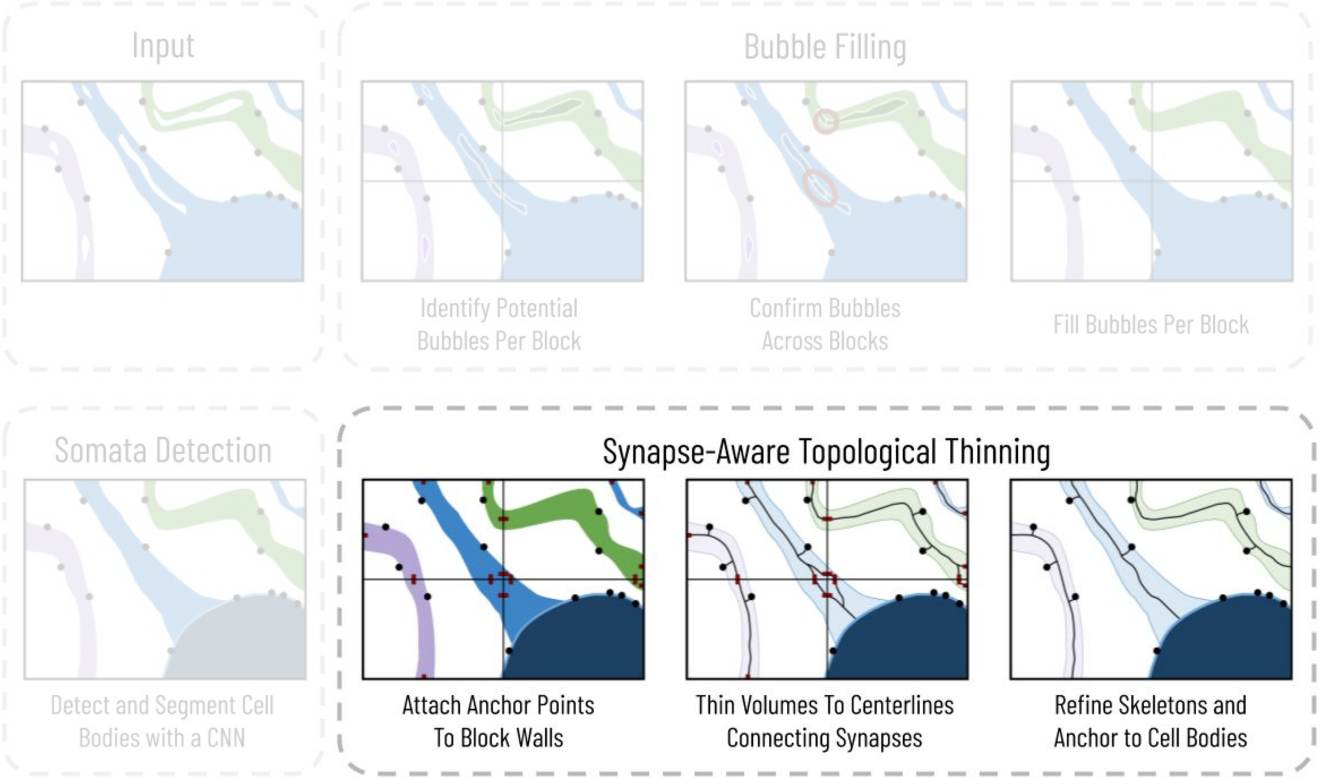

Input

Bubble Filling

Identify Potential Bubbles Per Block

Confirm Bubbles Across Blocks

Fill Bubbles Per Block

Somata Detection

Detect and Segment Cell Bodies with a CNN

Synapse-Aware Topological Thinning

Attach Anchor Points To Block Walls

Thin Volumes To Centerlines Connecting Synapses

Refine Skeletons and Anchor to Cell Bodies

Synapse-Aware Topological Thinning

We do not allow the deletion of synapses from the skeleton

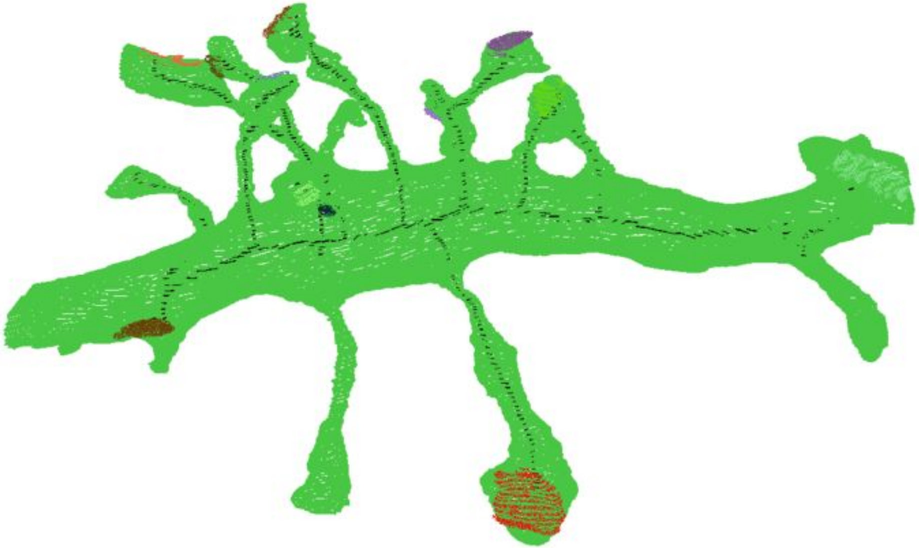

Synapse-Aware Topological Thinning

We do not allow the deletion of synapses from the skeleton

This guarantees that every synapse will remain connected in the skeletons

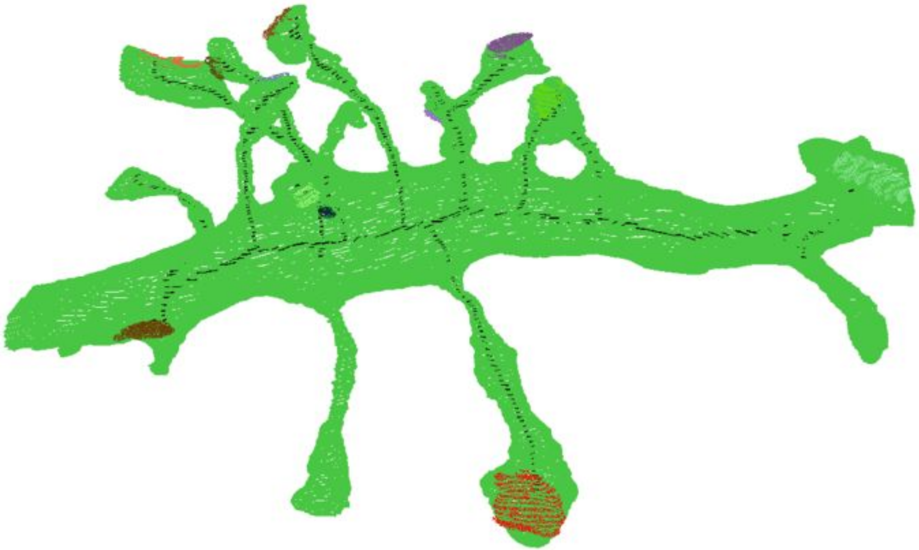

Attach Anchor Points to Block Walls

We need to guarantee that the skeletons generated in each block connect to those in neighboring blocks

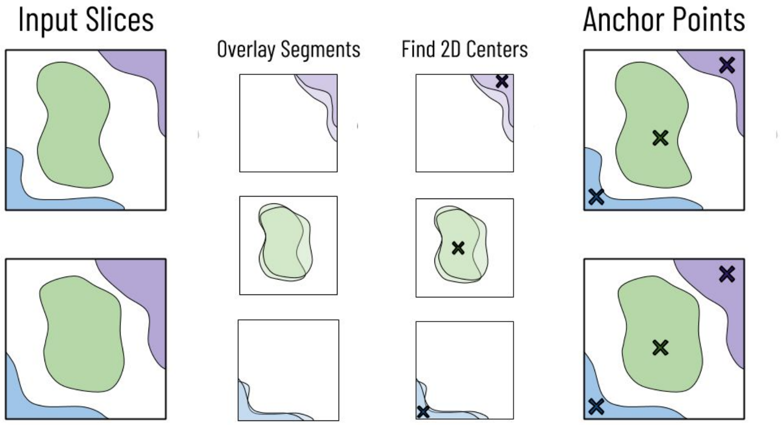

Attach Anchor Points to Block Walls

We need to guarantee that the skeletons generated in each block connect to those in neighboring blocks

For each pair of neighboring blocks, we look at the intersections of the adjacent block surfaces

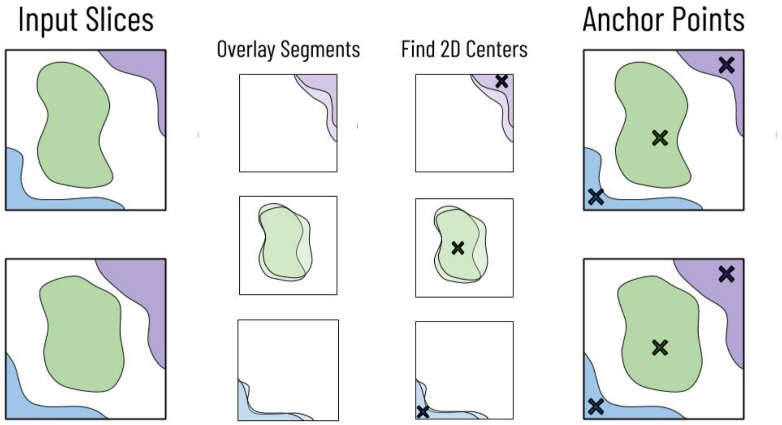

Thin Volumes to Centerlines Connecting Synapses

After determining anchor points, we can thin each segmentation per block

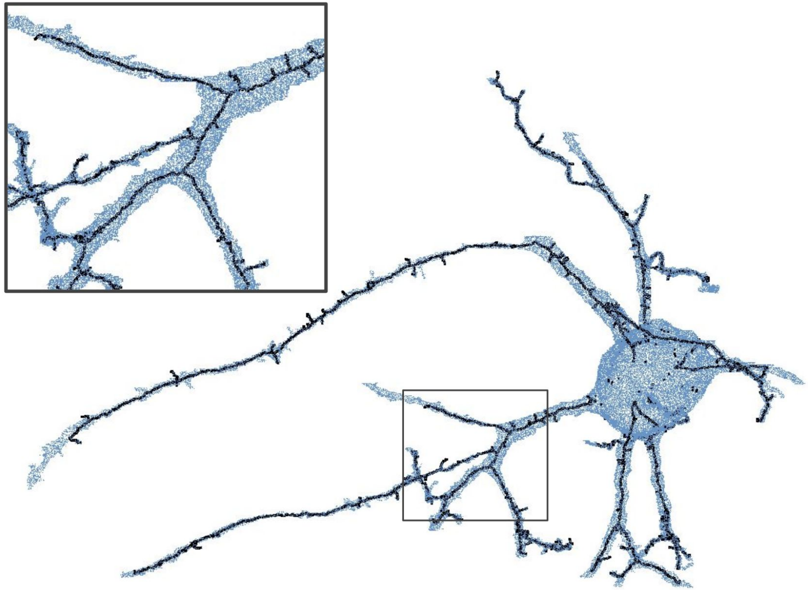

Estimating Neurite Width

During topological thinning, we estimate the nearest distance from a thinned point to the cell boundary

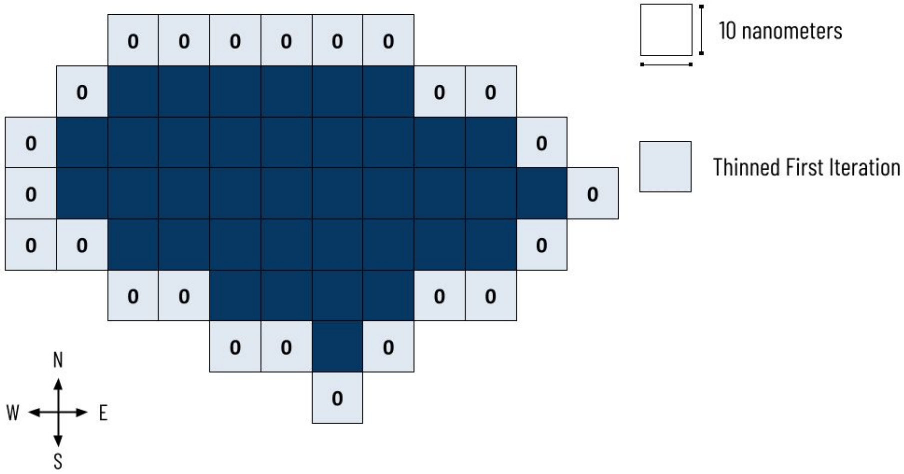

Estimating Neurite Width

During topological thinning, we estimate the nearest distance from a thinned point to the cell boundary

Voxels on the cell boundary are initialized at a distance of 0

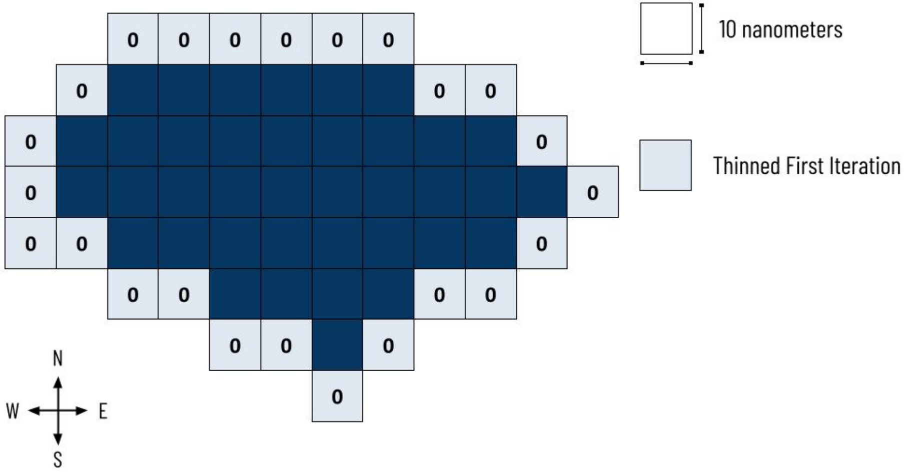

Estimating Neurite Width

During topological thinning, we estimate the nearest distance from a thinned point to the cell boundary

Voxels on the cell boundary are initialized at a distance of 0

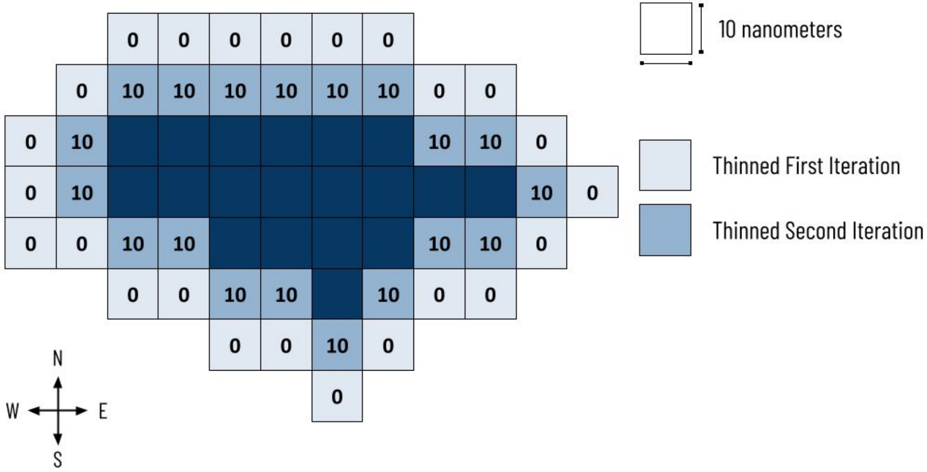

		0	0	0	0	0	0				
	0	10	10	10	10	10	10	0	0		
0	10							10	10	0	
0	10									10	0
0	0	10	10					10	10	0	
		0	0	10	10		10	0	0		
				0	0	10	0				
						0					

Estimating Neurite Width

During topological thinning, we estimate the nearest distance from a thinned point to the cell boundary

Voxels on the cell boundary are initialized at a distance of 0

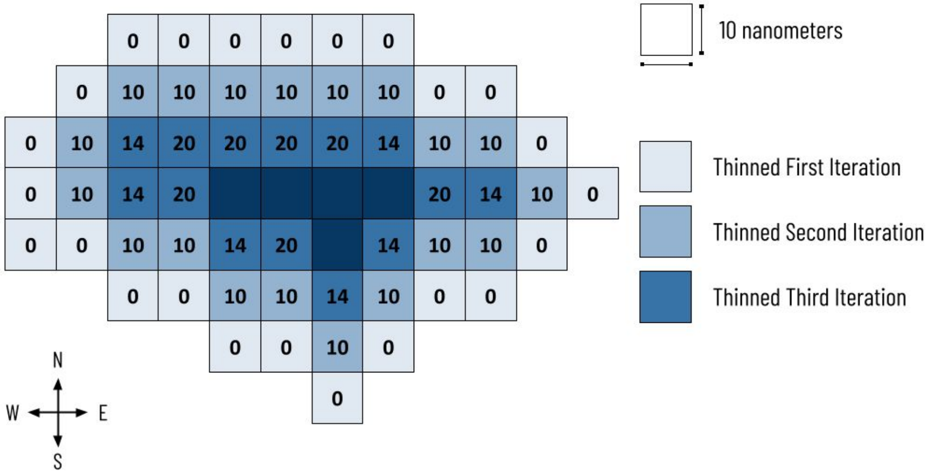

		0	0	0	0	0	0				
	0	10	10	10	10	10	10	0	0		
0	10	14	20	20	20	20	14	10	10	0	
0	10	14	20					20	14	10	0
0	0	10	10	14	20		14	10	10	0	
		0	0	10	10	14	10	0	0		
				0	0	10	0				
						0					

Estimating Neurite Width

During topological thinning, we estimate the nearest distance from a thinned point to the cell boundary

Voxels on the cell boundary are initialized at a distance of 0

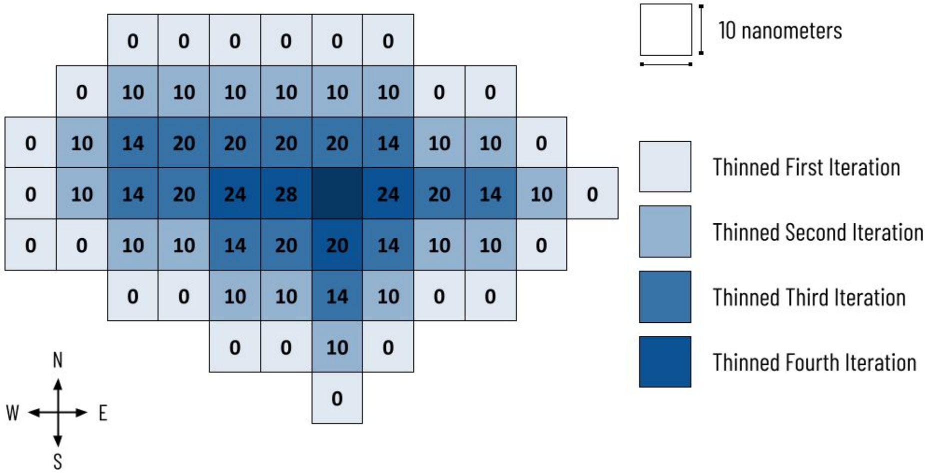

		0	0	0	0	0	0				
	0	10	10	10	10	10	10	0	0		
0	10	14	20	20	20	20	14	10	10	0	
0	10	14	20	24	28		24	20	14	10	0
0	0	10	10	14	20	20	14	10	10	0	
		0	0	10	10	14	10	0	0		
				0	0	10	0				
						0					

Estimating Neurite Width

During topological thinning, we estimate the nearest distance from a thinned point to the cell boundary

Voxels on the cell boundary are initialized at a distance of 0

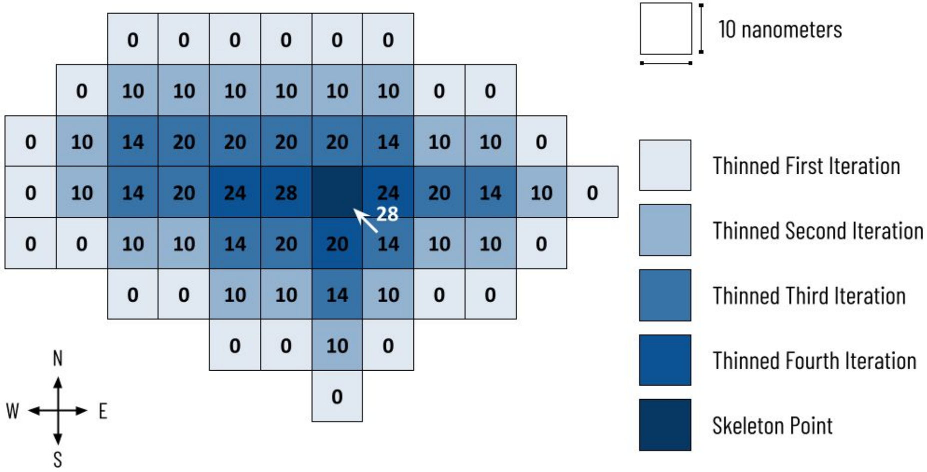

		0	0	0	0	0	0				
	0	10	10	10	10	10	10	0	0		
0	10	14	20	20	20	20	14	10	10	0	
0	10	14	20	24	28	28	24	20	14	10	0
0	0	10	10	14	20	20	14	10	10	0	
		0	0	10	10	14	10	0	0		
				0	0	10	0				
						0					

Refine Skeletons and Anchor to Cell Bodies

Tunnels through the label volumes can cause loops in the skeletons

Before

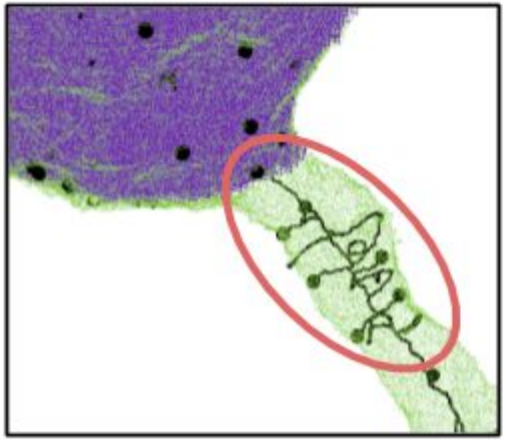

Refine Skeletons and Anchor to Cell Bodies

Tunnels through the label volumes can cause loops in the skeletons

We simultaneously remove these loops and calculate the geodesic distance from each synapse to the soma

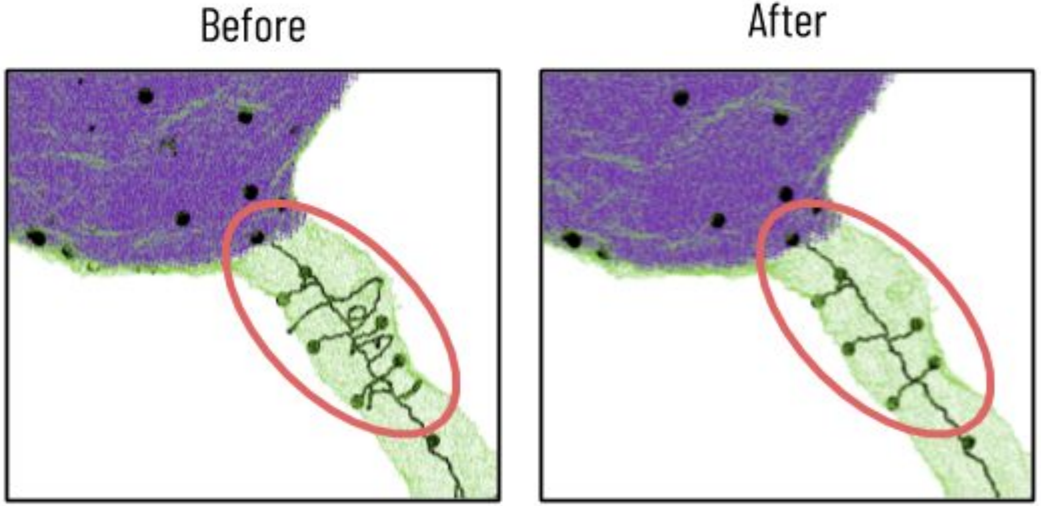

Refine Skeletons and Anchor to Cell Bodies

Tunnels through the label volumes can cause loops in the skeletons

We simultaneously remove these loops and calculate the geodesic distance from each synapse to the soma

Although this step requires global scope, it is incredibly quick since it requires only the skeletons

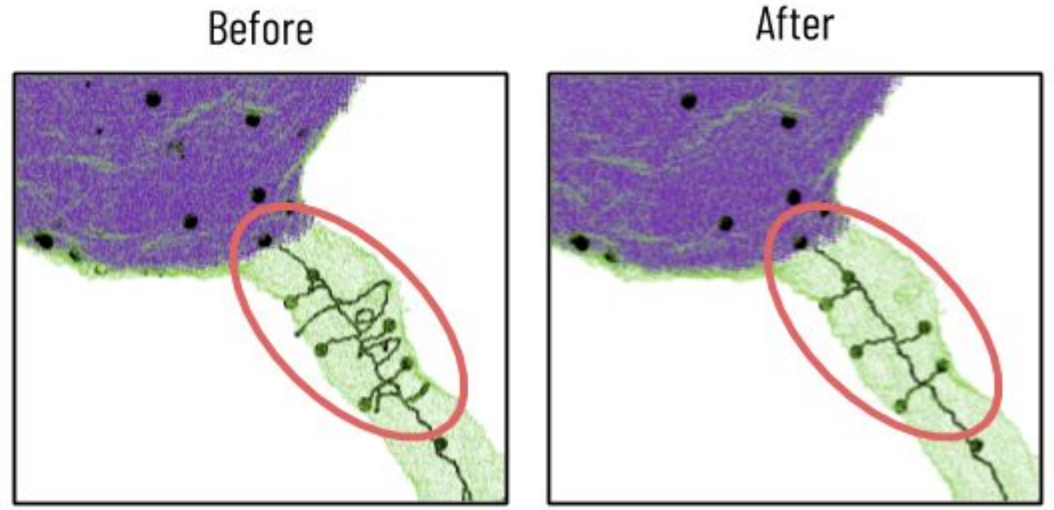

Datasets

JWR

FIB-25

J0126

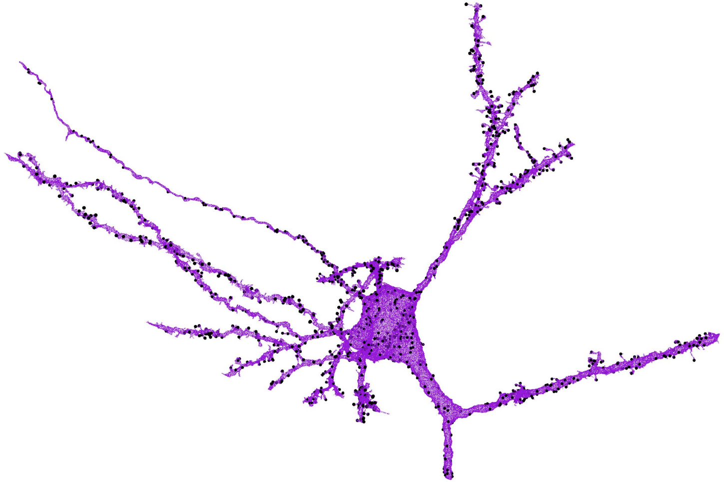

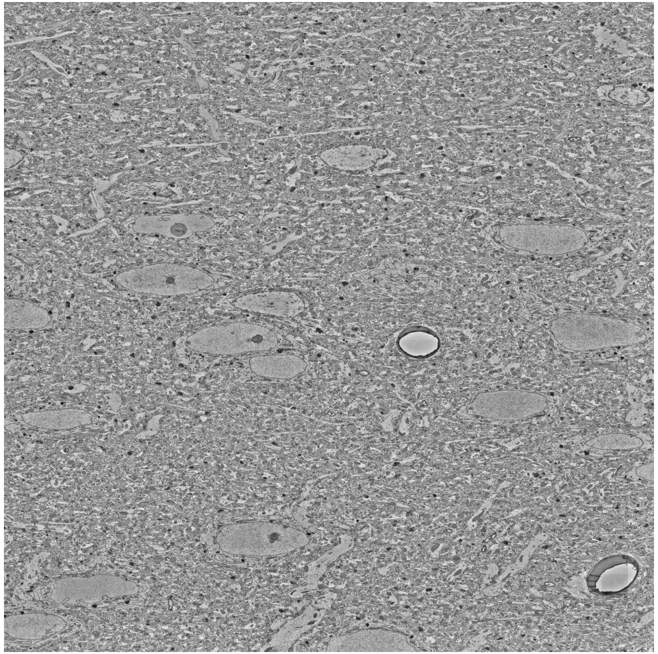

106 x 106 x 93 μm^3

32 x 64 x 30 nm^3 / vx

85 Neurons

50,334 Synapses

Datasets

JWR

FIB-25

J0126

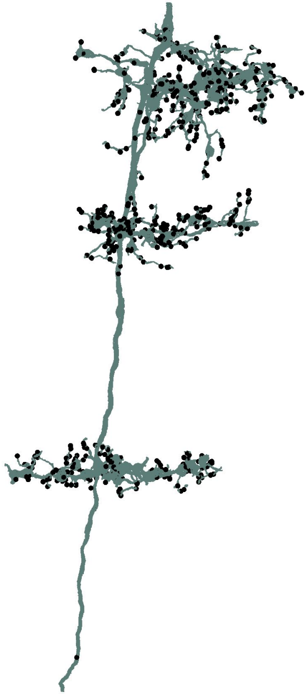

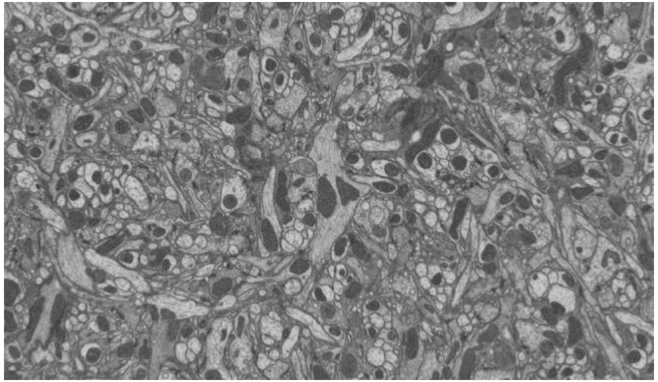

36 x 29 x 69 μm^3

10 x 10 x 10 nm^3 / vx

763 Neurons

84,157 Synapses

Datasets

JWR

FIB-25

J0126

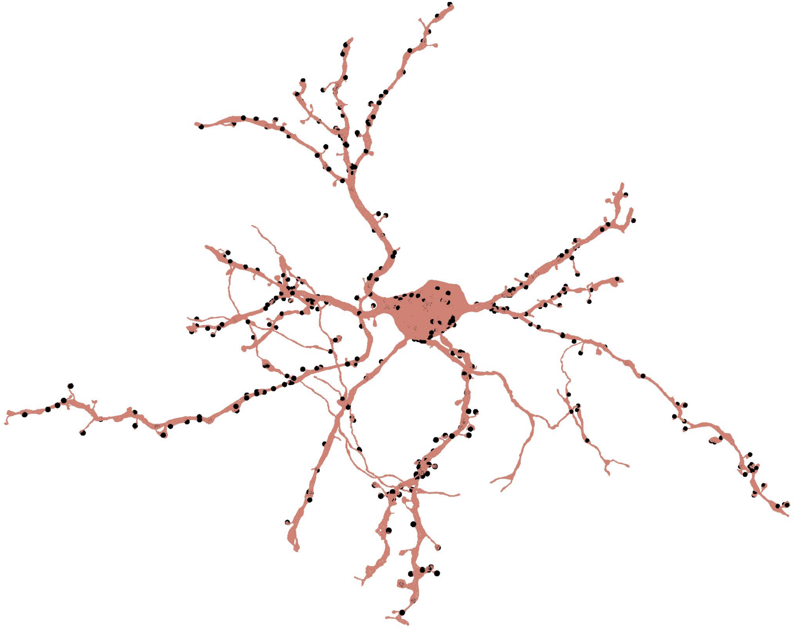

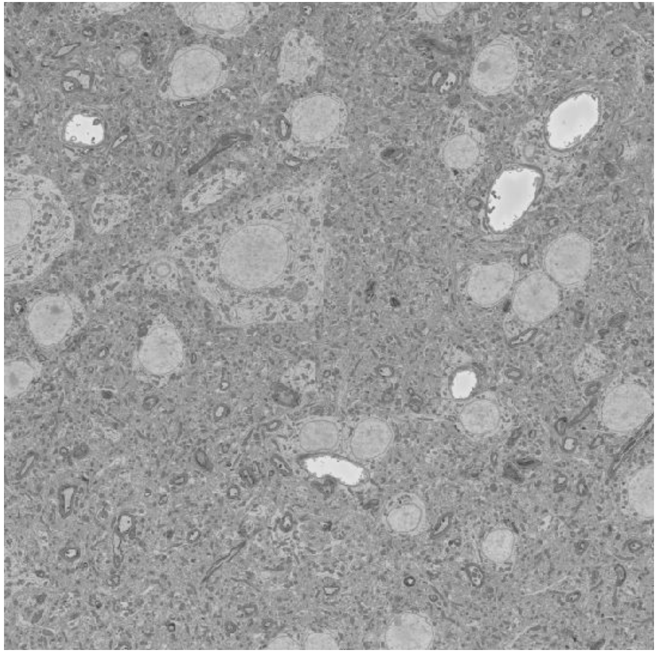

96 x 98 x 114 μm^3

18 x 18 x 20 nm^3 / vx

407 Neurons

91, 465 Synapses

Neural Reconstruction Integrity (NRI)

The NRI score measures how well a method preserves the intracellular pathways between synapses

Neural Reconstruction Integrity (NRI)

The NRI score measures how well a method preserves the intracellular pathways between synapses

We adapt the method to measure the correspondence between synapses and endpoints

Neural Reconstruction Integrity (NRI)

The NRI score measures how well a method preserves the intracellular pathways between synapses

We adapt the method to measure the correspondence between synapses and endpoints

For the baselines, we consider a synapse mapped to an endpoint if they are within 1600 nanometers

Width Estimation

For each point along the skeleton path, we calculate the largest sphere that we could center at that point without leaving the volume

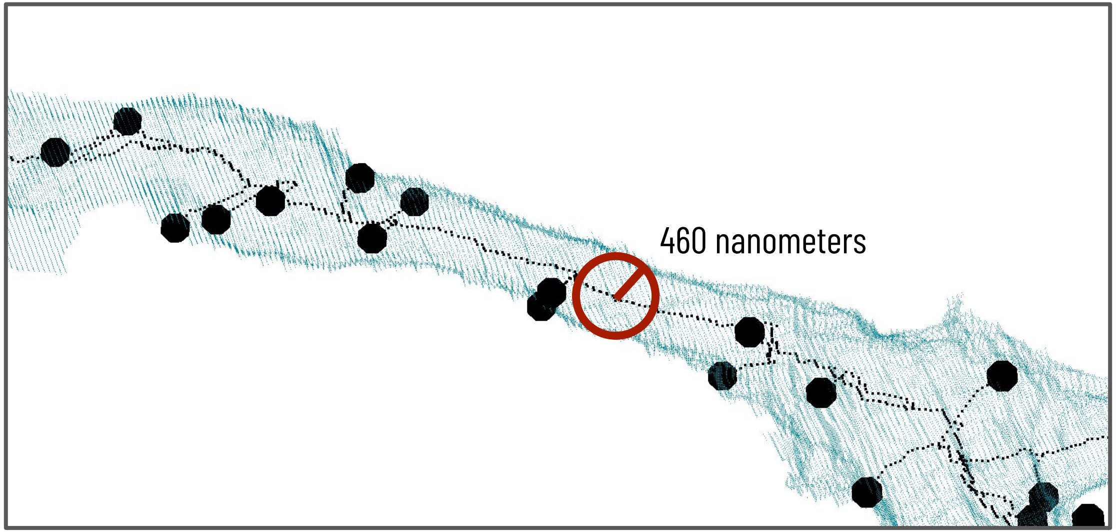

Width Estimation

For each point along the skeleton path, we calculate the largest sphere that we could center at that point without leaving the volume

We use this as an estimate for the cross-sectional width of the neurite at a given location

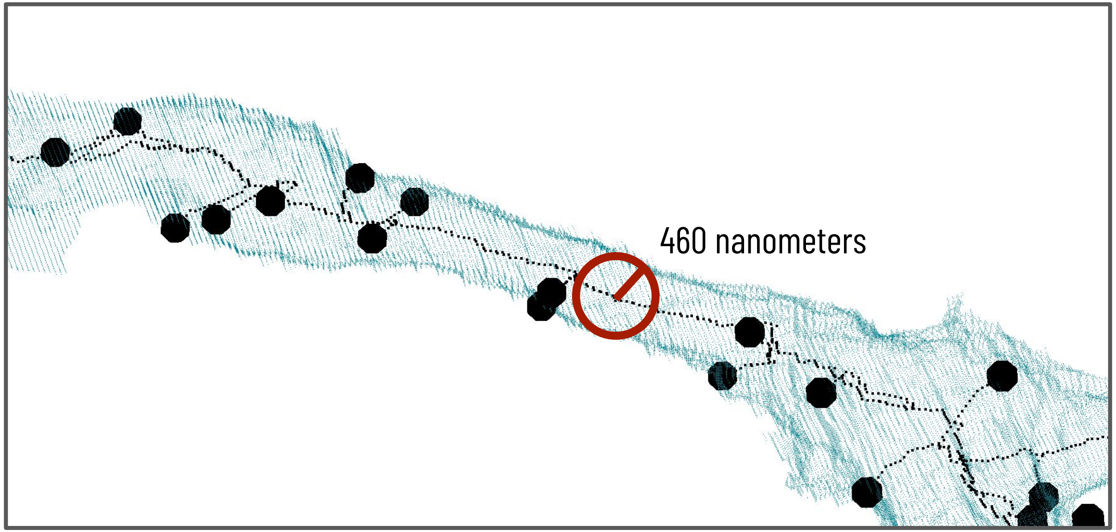

Skeleton Simplicity

Our final evaluation metric considers skeleton simplicity—the number of points in the skeleton

Skeleton Simplicity

Our final evaluation metric considers skeleton simplicity—the number of points in the skeleton

All else equal, fewer points is better

Quantitative Results

Method	**JWR**			**FIB-25**			**J0126**		
	NRI (↑)	**Width (↓)**	**Points (↓)**	**NRI (↑)**	**Width (↓)**	**Points (↓)**	**NRI (↑)**	**Width (↓)**	**Points (↓)**
Proposed	**0.9988**	**40.03 nm**	26,752	**0.9952**	**14.42 nm**	11,755	**0.9997**	**25.55 nm**	**25,562**
TEASER	0.1011	120.69 nm	**18,250**	0.2477	19.78 nm	**10,216**	0.1729	171.33 nm	33,022
Isthmus Thinning	0.2574	N/A	1,645,966	0.3158	N/A	39,873	0.2454	N/A	1,089,923

Quantitative Results

Method	JWR			FIB-25			J0126		
	NRI (↑)	**Width (↓)**	**Points (↓)**	**NRI (↑)**	**Width (↓)**	**Points (↓)**	**NRI (↑)**	**Width (↓)**	**Points (↓)**
Proposed	**0.9988**	**40.03 nm**	26,752	**0.9952**	**14.42 nm**	11,755	**0.9997**	**25.55 nm**	**25,562**
TEASER	0.1011	120.69 nm	**18,250**	0.2477	19.78 nm	**10,216**	0.1729	171.33 nm	33,022
Isthmus Thinning	0.2574	N/A	1,645,966	0.3158	N/A	39,873	0.2454	N/A	1,089,923

We improve on NRI score by 288%, 215%, and 307% over the next best method

Quantitative Results

Method		**JWR**			**FIB-25**			**J0126**	
	NRI (↑)	**Width (↓)**	**Points (↓)**	**NRI (↑)**	**Width (↓)**	**Points (↓)**	**NRI (↑)**	**Width (↓)**	**Points (↓)**
Proposed	**0.9988**	**40.03 nm**	26,752	**0.9952**	**14.42 nm**	11,755	**0.9997**	**25.55 nm**	**25,562**
TEASER	0.1011	120.69 nm	**18,250**	0.2477	19.78 nm	**10,216**	0.1729	171.33 nm	33,022
Isthmus Thinning	0.2574	N/A	1,645,966	0.3158	N/A	39,873	0.2454	N/A	1,089,923

We improve on the width estimates by 67%, 27%, and 85% over the next best method

Quantitative Results

Method	**JWR**			**FIB-25**			**J0126**		
	NRI (↑)	**Width (↓)**	**Points (↓)**	**NRI (↑)**	**Width (↓)**	**Points (↓)**	**NRI (↑)**	**Width (↓)**	**Points (↓)**
Proposed	**0.9988**	**40.03 nm**	26,752	**0.9952**	**14.42 nm**	11,755	**0.9997**	**25.55 nm**	**25,562**
TEASER	0.1011	120.69 nm	**18,250**	0.2477	19.78 nm	**10,216**	0.1729	171.33 nm	33,022
Isthmus Thinning	0.2574	N/A	1,645,966	0.3158	N/A	39,873	0.2454	N/A	1,089,923

TEASER has fewer points on two of the three datasets

Qualitative Results

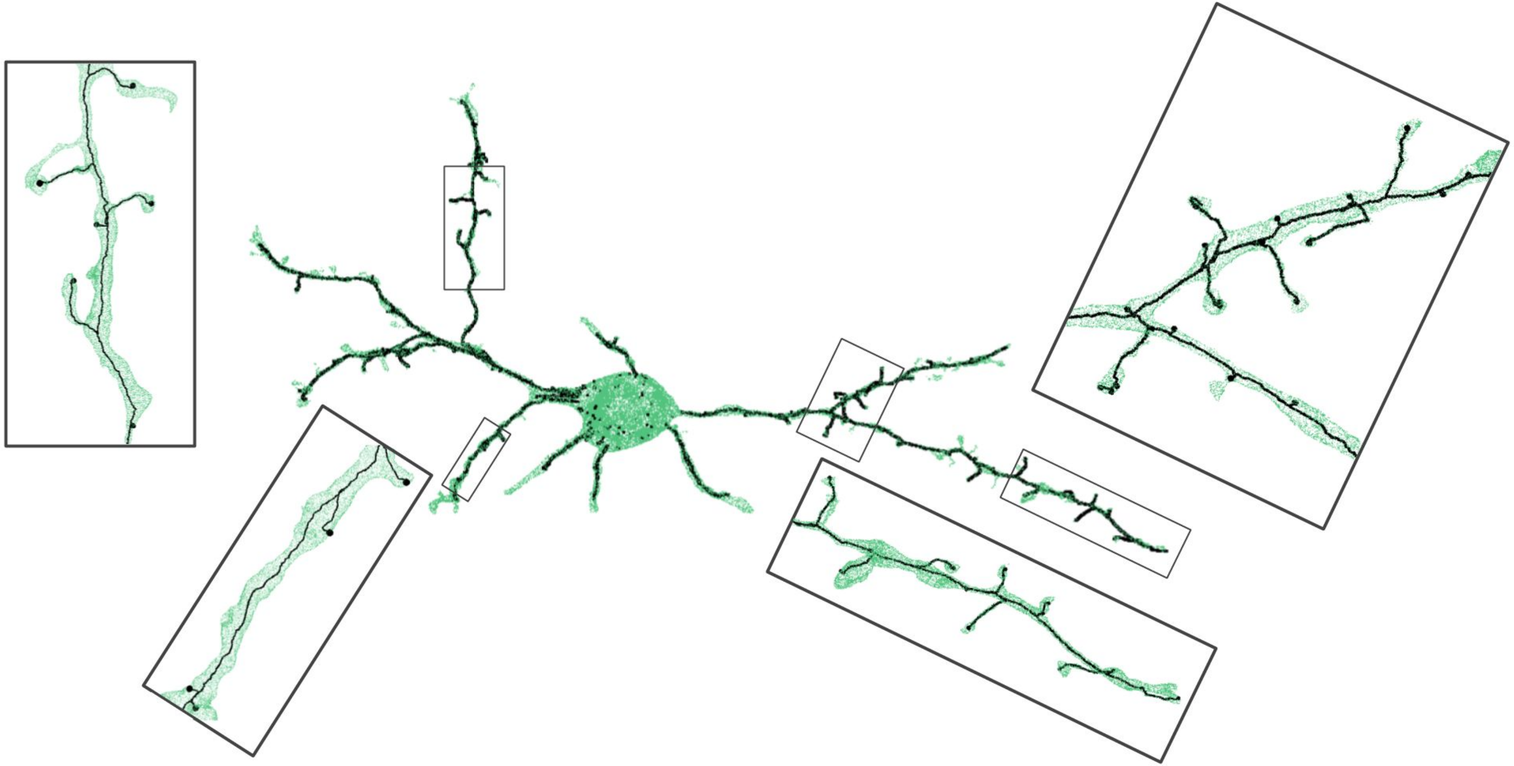

Qualitative Results

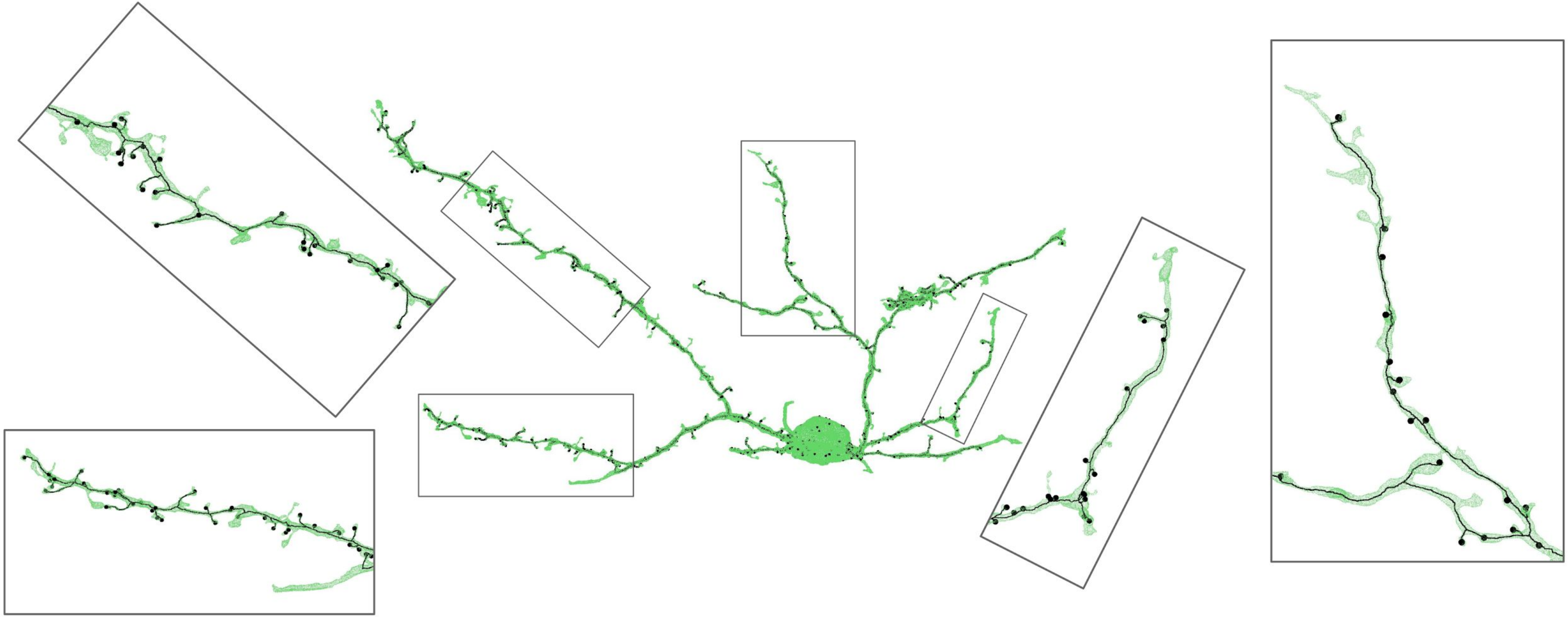

Ablation Studies: Bubble Filling

The J0126 reconstruction (automatic with Flood-Filling Networks), had over 24 million bubbles, corresponding to 0.80% of the total volume

Ablation Studies: Bubble Filling

The J0126 reconstruction (automatic with Flood-Filling Networks), had over 24 million bubbles, corresponding to 0.80% of the total volume

Removing these bubbles reduced topological thinning time by 57.16%

Ablation Studies: Soma Detection

We predict which voxels belong to cell bodies with 99.28% accuracy (TPR: 99.77%, FPR: 0.76%)

Masking out the cell bodies reduces the running time of topological thinning by 49.95% and 60.21% on the JWR and J0126 datasets, respectively

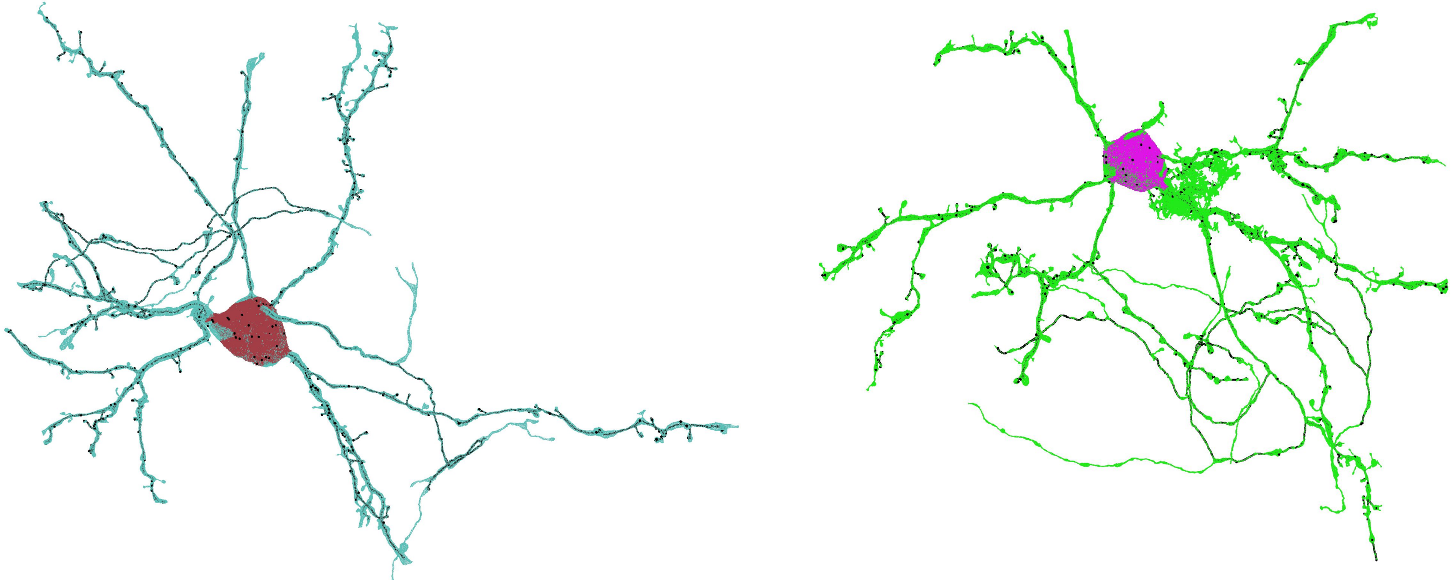

Ablation Studies: Synapse-Aware Topological Thinning

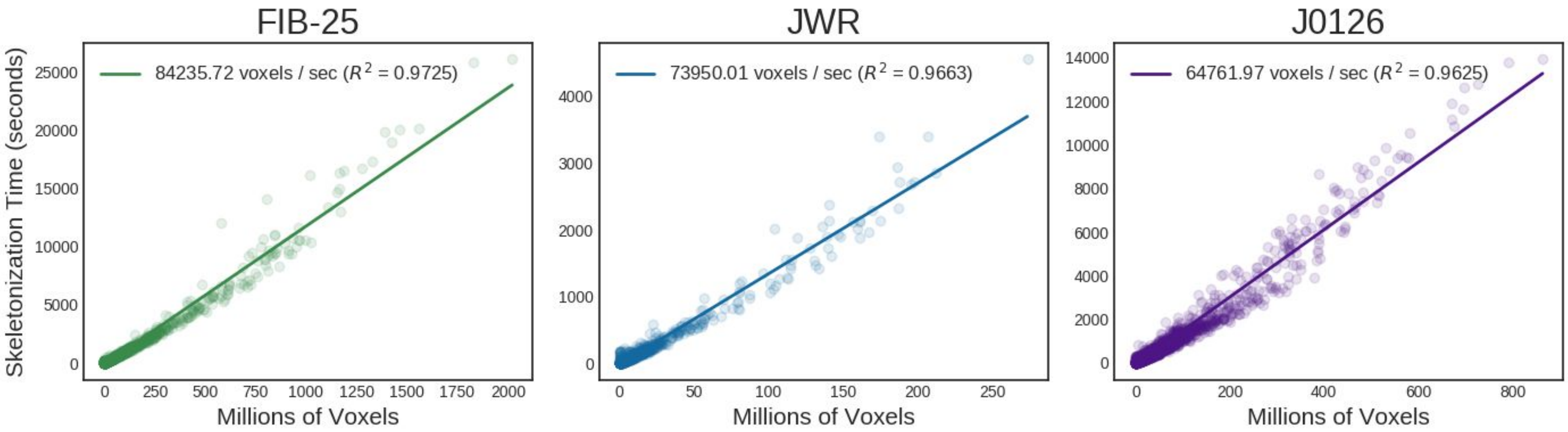

Ablation Studies: Computational Complexity

Method	JWR	FIB-25	J0126
Entire Pipeline	5.19 hr	N/A	45.29 hr
No Bubble Filling	4.03 hr	N/A	78.85 hr
No Soma Detection	10.37 hr	33.54 hr	113.82 hr
Only Thinning	20.56 hr	30.72 hr	479.19 hr

Ablation Studies: Computational Complexity

Method	**JWR**	**FIB-25**	**J0126**
Entire Pipeline	5.19 hr	N/A	45.29 hr
No Bubble Filling	4.03 hr	N/A	78.85 hr
No Soma Detection	10.37 hr	33.54 hr	113.82 hr
Only Thinning	20.56 hr	30.72 hr	479.19 hr

Biologically-Aware Algorithms for Connectomics

Skeleton Generation

Compression

Error Correction

Subgraph Enumeration

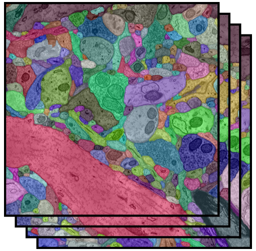

Segmentation

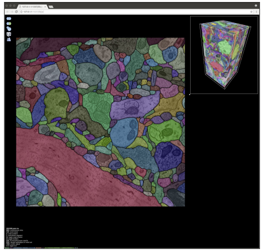

Proofreading

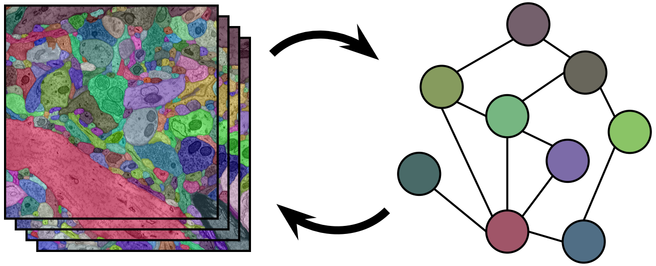

Network Analysis

Bubble Filling

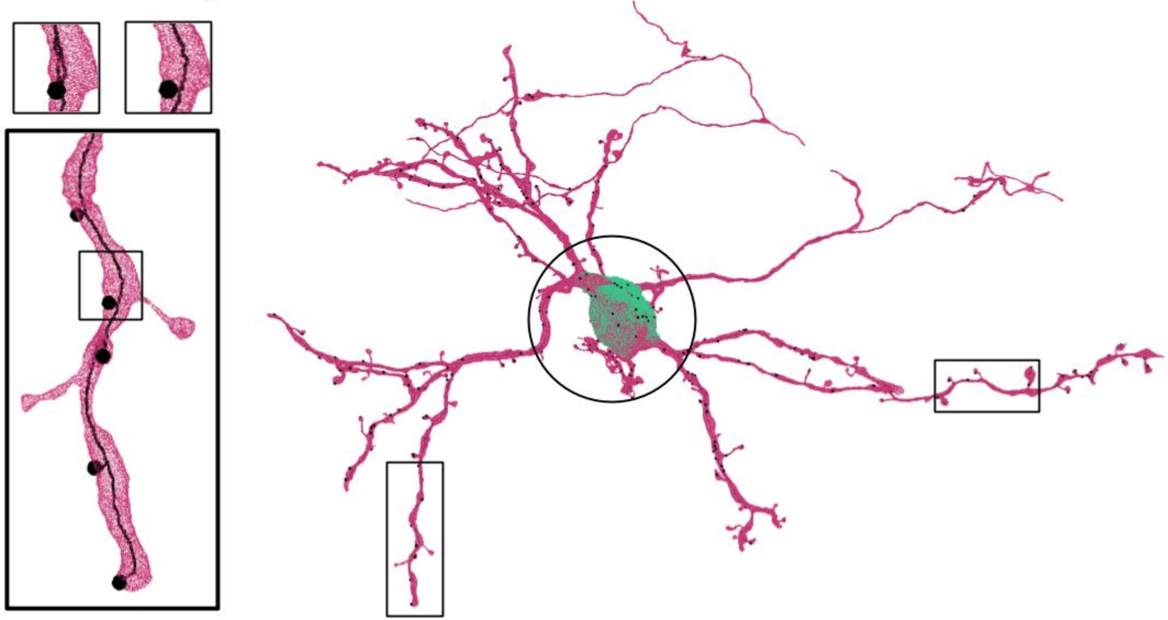


Bubble Filling
Soma Detection


Bubble Filling
Soma Detection
Synapse Connectivity

Future Directions

Different Biological-Constraints for Error Correction

Biological-constraints should differ between species as morphologies can look wildly different

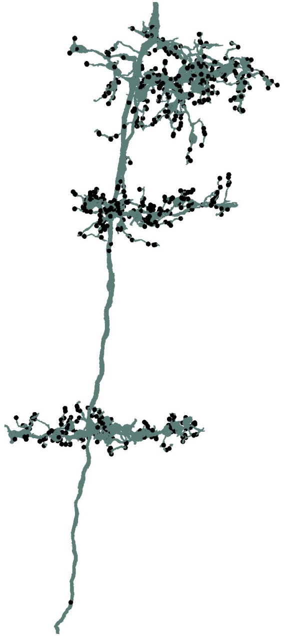

Fruit Fly

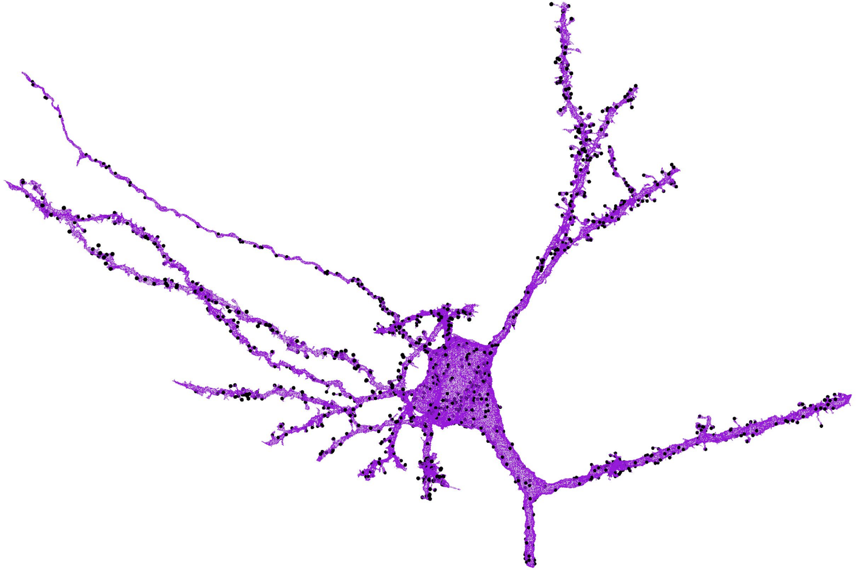

Rat

Random Graph Generation for Motif Discovery

Random graphs allow us to identify subgraphs that appear more frequently than expected

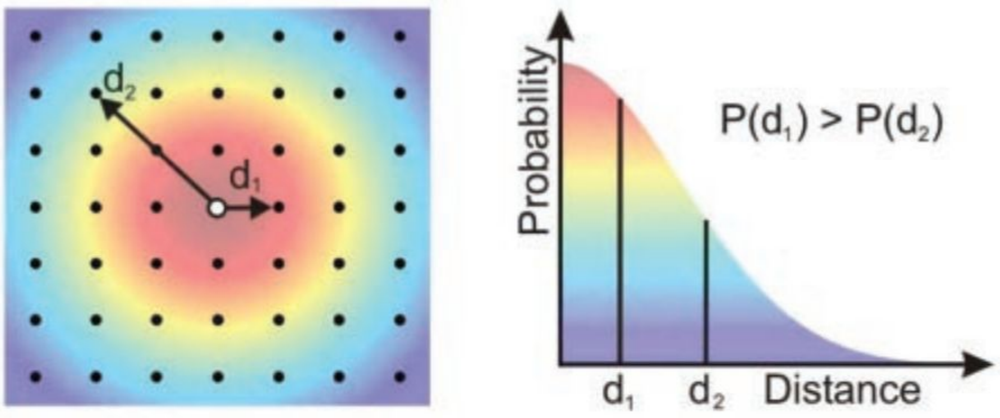

Artzy-Randrup, Comment on “Network Motifs: Simple Building”, Science 2004

Random Graph Generation for Motif Discovery

Random graphs allow us to identify subgraphs that appear more frequently than expected

Without using biological priors on our random graphs, we can mistakenly identify "important motifs"

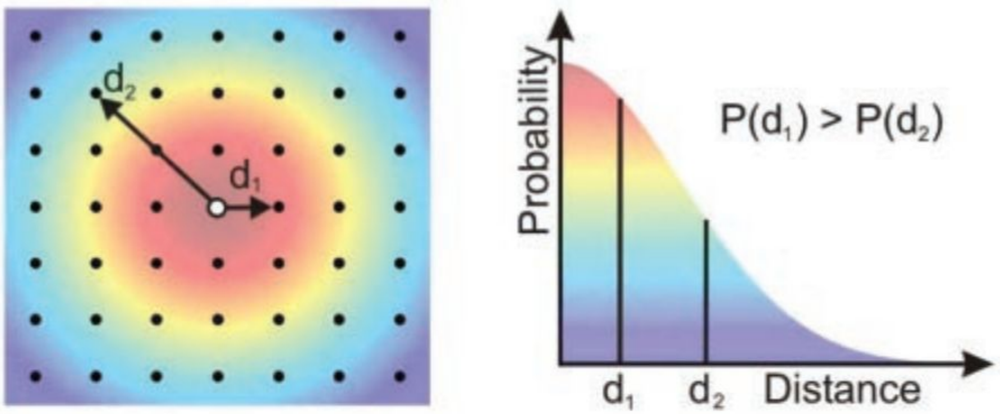

Artzy-Randrup, Comment on "Network Motifs: Simple Building", Science 2004

Augmenting the Wiring Diagram with Skeletonization

Current wiring diagrams ignore any interplay between neurites

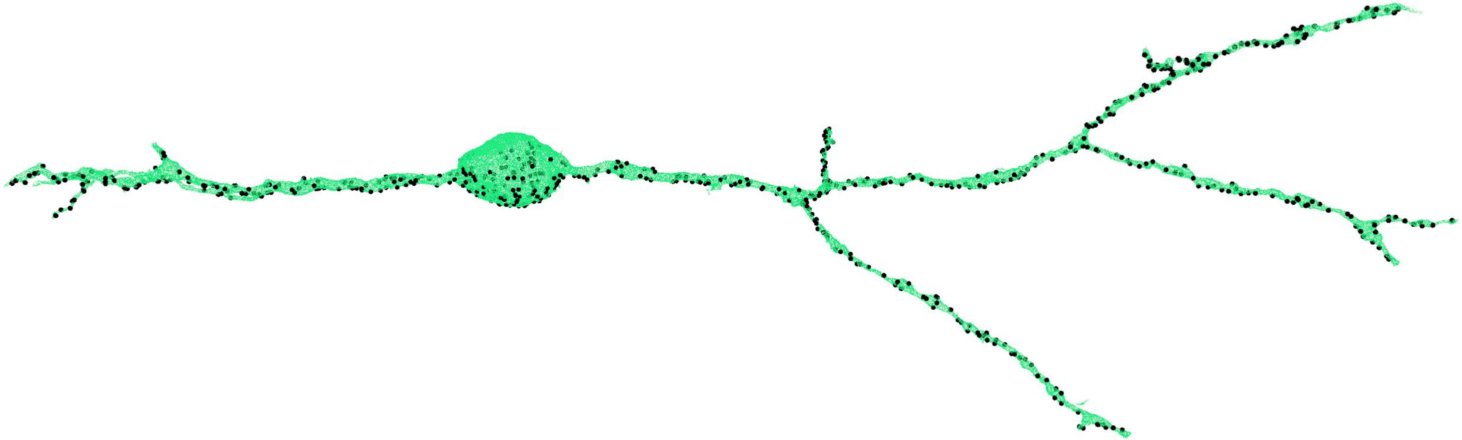

Augmenting the Wiring Diagram with Skeletonization

Neurites themselves can each become nodes in a wiring diagram where neurons become multiple nodes

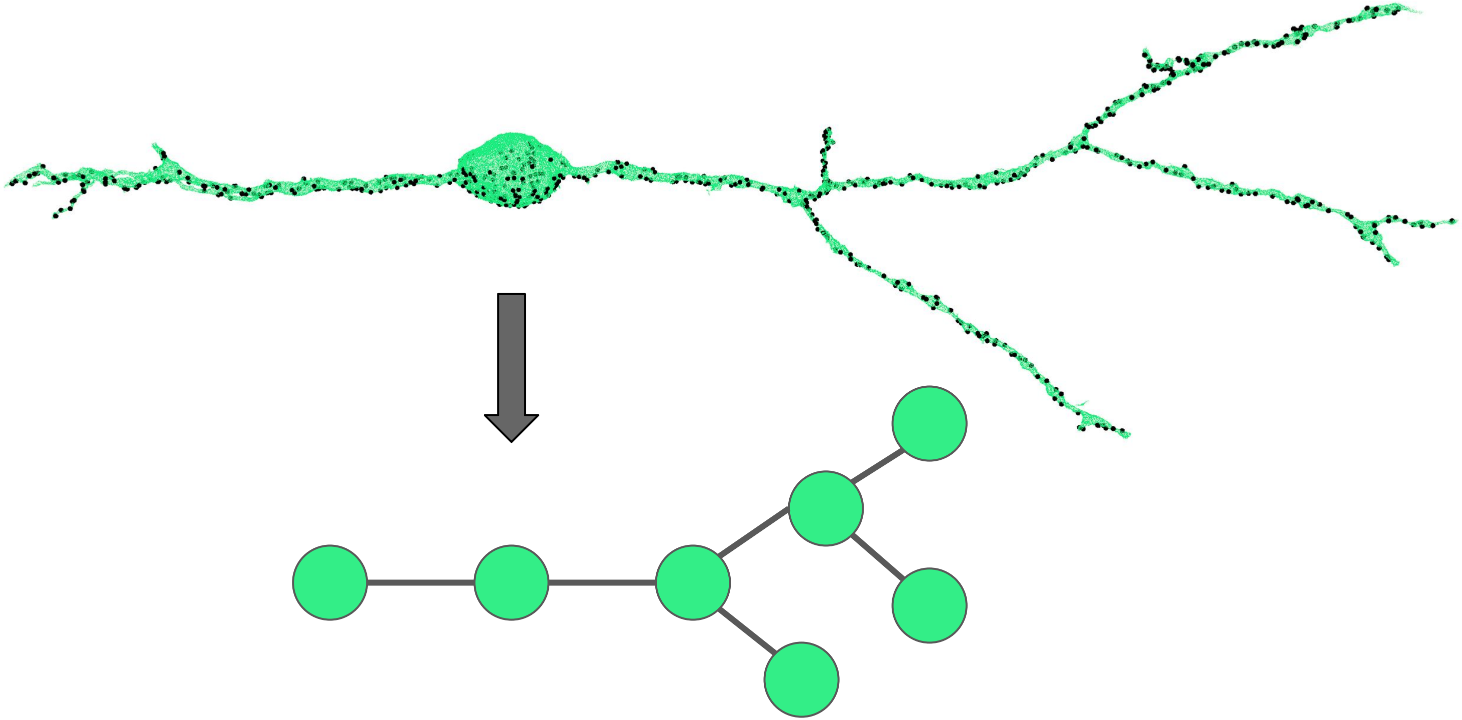

Acknowledgements

Hanspeter Pfister

Acknowledgements

Todd Zickler

Michael Mitzenmacher

Acknowledgements

Tianyi Chen

Tim Franzmeyer

Daniel Haehn

Fritz Lekschas

Jeff W. Lichtman

Michael Mitzenmacher

Kálmán Palágyi

Toufiq Parag

Hanspeter Pfister

Babis Tsourakakis

Snow Wang

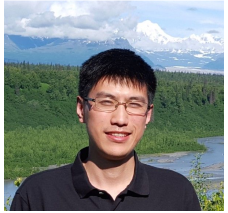

Donglai Wei

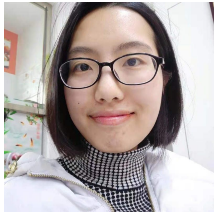

Jinglin Zhao

Haidong Zhu

Visual Computing Group

Thank you!

Questions?